PHOTOCATALYTIC REACTIONS OF METAL DIPHTHALOCYANINE COMPLEXES

THESIS

Submitted to

Rhodes University

in fulfilment of the requirements for the degree of

DOCTOR OF PHILOSOPHY

by

NGUDIANKAMA NENSALA

November 1999

Department of Chemistry

Rhodes University

Grahamstown

ACKNOWLEDGEMENTS

I would like to thank my supervisor Prof. T. Nyokong for her guidance and valuable teaching throughout the duration of this research project. Indeed, it was an excellent learning experience to work under her supervision.

I would also like to thank:

- Deutscher Akademiscer Austauschdienst (DAAD) for a graduate scholarship.
- Foundation for Research and Development (FRD) for a study bursary in 1998.
- Rev. Jean-Marie Nkonge for his encouragement and computer skills which contributed in the preparation of this manuscript.
- Staff of chemistry department at Rhodes University for their assistance in different ways.
- My fellow students for their cooperation in different ways and for making our department a pleasant work place.
- My parents Manuel Lula and Isabel Luwengo and friends for their moral support. I am grateful to my uncles Nginamau António and Nzengele Edouard for their valuable support. Mr Ndimba David is thanked for his constant support.

Finally, I would like to give my very special thanks to my wife, Teresa Bernardo Nensala for the encouragement and the moral support she has provided throughout the course of this project.

ABSTRACT

Photocatalytic reactions of tin diphthalocyanine, $Sn^{IV}Pc_2$ and anionic form of Nd^{III}, Dy^{III}, Eu^{III}, Tm^{III} and Lu^{III} diphthalocyanine complexes ($[Pc(-2)Nd^{III}Pc(-2)]^-$, $[Pc(-2)Dy^{III}Pc(-2)]^-$, $[Pc(-2)Eu^{III}Pc(-2)]^-$, $[Pc(-2)Tm^{III}Pc(-2)]^-$ and $[Pc(-2)Lu^{III}Pc(-2)]^-$, respectively) in the presence of CH_2Cl_2, SO_2, pentachlorophenol (PCP), 4-chlorophenol (4-Cp) and thionyl chloride have been studied. Photoreactions involving lanthanide diphthalocyanines, filtered and unfiltered radiations were employed, whereas for photoreactions involving tin diphthalocyanine, only unfiltered radiation was employed. For lanthanide diphthalocyanine complexes, $LnPc_2^-$, the photosensitization power increases with the decrease of the lanthanide ionic radii, implying that the photocatalytic activity of $LnPc_2^-$ complexes is associated with the π-π interaction between both phthalocyanine rings. Thus, $LuPc_2^-$ is a better photocatalyst than other lanthanide diphthalocyanine complexes.

Photolysis of $SnPc_2$ in an acetonitrile/dichloromethane solvent mixture, using unfiltered radiation from a tungsten lamp, results in the one-electron oxidation of this species to $[Pc(-2)Sn(IV)Pc(-1)]^-$. The relative quantum yields for the disappearance of $SnPc_2$ are in the order of 10^{-4}. The photoreaction of $SnPc_2$ is preceded by excitation to $n\pi^*$ excited states, before been quenched by CH_2Cl_2. The one-electron oxidation species, $[Pc(-2)Sn(IV)Pc(-1)]^-$ was also formed during the photolysis of $SnPc_2$ in dichloromethane containing SO_2, and with quantum yields of order of 10^{-3}.

Visible photolysis of $[Pc(-2)Nd^{III}Pc(-2)]^-$, $[Pc(-2)Dy^{III}Pc(-2)]^-$ and $[Pc(-2)Lu^{III}Pc(-2)]^-$ in N,N, dimethylformamide (DMF)/dichloromethane solvent mixture containing SO_2 results in the

formation of the one-electron oxidation species, Pc(-2)Nd^{III}Pc(-1), Pc(-2) Dy^{III}Pc(-1) and Pc(-2)Lu^{III}Pc(-1), respectively. The relative quantum yields are in the order of 10^{-2}. The photoreactions are preceded by population of the excited triplet state, $^3\pi$-π^* [$LnPc_2$] $^-$ complex, before exchanging an electron with SO_2. The one-electron oxidation species of Dy^{III} and Lu^{III} diphthalocyanine complexes have also been formed from visible photolysis of [Pc(-2)Dy^{III}Pc(-2)] $^-$ and [Pc(-2)Lu^{III}Pc(-2)] $^-$ in acetonitrile containing PCP. The PCP is reductively dechlorinated to tetra- and trichlorophenols. The quantum yields for the photosensitization reactions are in the order of 10^{-4}.

Photolysis, using visible radiation from 220 W Quartzline lamp, of an aqueous solution of 4-Cp, saturated with oxygen and containing a suspension of solid [Pc(-2)Nd^{III}Pc(-2)] $^-$, results in the formation of benzoquinone, hydroquinone and 4-chlorocatechol. The quantum yields for the degradation of 4-Cp are in the order of 10^{-4}. Langmuir-Hinshelwood kinetic model shows the adsorption of 4-chlorophenol onto solid [Pc(-2)Nd^{III}Pc(-2)] $^-$.

Lanthanide diphthalocyanine complexes ([Pc (-2)Nd^{III}Pc(-2)] $^-$, [Pc(-2)Eu^{III}Pc(-2)] $^-$, [Pc(-2)Tm^{III}Pc(-2)] $^-$ and [Pc(-2)Lu^{III}Pc(-2)] $^-$) undergo one or two-electron oxidation in the presence of thionyl chloride. At low concentrations of $SOCl_2$ ($< 10^{-4}$ mol dm^{-3}), the visible photolysis of [Pc(-2)LnPc(-2)] $^-$ complexes result in the one-electron oxidation, giving neutral lanthanide diphthalocyanine species, Pc(-2)Ln^{III}Pc(-1). The Pc(-2)LnPc(-1) species undergoes one-electron photooxidation to [Pc(-1)LnPc(-1)] $^-$ in dichloromethane and in the presence of $SOCl_2$. At large concentrations of $SOCl_2$ ($> 10^{-2}$ mol dm^{-3}), direct two-electron oxidation of the [Pc(-2)LnPc (-2)] $^-$ species to [Pc(-1)LnPc(-1)] $^-$ occurs.

Spectroelectrochemical behaviours of $Sn^{IV}Pc_2$ have been also studied. The cyclic voltammetry of $SnPc_2$ in CH_2Cl_2/TBAP show two reduction couples at -0.56 V and -0.89 V versus saturated calomel electrode (SCE) and one oxidation couple at 0.35 V versus SCE. In DMF/TEAP system, the reduction couples are observed at -0.44 V and -0.81 V versus SCE whereas the oxidation couple occurred at 0.43 V versus SCE. The oxidation couple corresponds to $[Pc(-2)Sn^{IV}Pc(-2)]/[Pc(-2)SnIVPc(-1)]^-$ and the reduction couples to $[Pc(-2)Sn^{IV}Pc(-2)]/[Pc(-2)Sn^{IV}Pc(-3)]^-$ and $[Pc(-2)Sn^{IV}Pc(-3)]^-/[Pc(-3)Sn^{IV}Pc(-3)]^{2-}$, respectively. The electronic absorption spectra of these reduced and oxidized species are reported.

TABLE OF CONTENTS

LIST OF ABBREVIATIONS

BAS	= Bio-Analytical Systems
BM	= Bohr Magneton
BQ	= Benzoquinone
CV	= Cyclic Voltammetry
DCB	= Dichlorobenzene
DMF	= N,N-dimethyl formamide
DMSO	= Dimethyl sulfoxide
DPV	= Differential Pulse Voltammetry
EPR	= Electron Paramagnetic Resonance
ESR	= Electron Spin Resonance
Fig.	= Figure
GC	= Gas chromatography
HOMO	= Highest Occupied Molecular Orbital
HQ	= Hydroquinone
HPLC	= High Performance Liquid Chromatography
IR	= Infrared
Ic	= Internal conversion
Isc	= Intersystem crossing
LOs	= Localized Orbitals
LUMO	= Lowest Unoccupied Molecular Orbital
$LnPc_2$	= Neutral lanthanide diphthalocyanine complexes.

$LnPc_2^-$ = Anionic lanthanide diphthalocyanine complexes

$Ln(OEP)_2$ = Lanthanide bis (octaethyl porphyrinates)

L-H = Langmuir-Hinshelwood

MPc = Metallophthalocyanine

MPc_2 = Metallodiphthalocyanine

MOs = Molecular Orbitals

Nc = Naphthalocyanine

NIR = Near Infrared

NMR = Nuclear Magnetic Resonance

OCDD = O-Chlorophenol Dibenzo Dioxin

Pc = Phthalocyanine

PCP = Pentachlorophenol

PCDD = Polychlorinated dibenzo dioxin

PCDF = Polychlorinated dibenzo furan

Ph = Phenol

POM = Polyoxometalate

TBAP = Tetrabutylammonium perchlorate

TCBP = Tetrachlorobiphenyl

TCBQ = Tetrachlorobenzoquinone

TCDD = Tetrachlorodibenzo dioxin

TCE = Tetrachloroethane

TCP = Trichlorophenol

TEAP = Tetraethylammonium perchlorate

TEOA = Triethanolamine

THF	= Tetrahydrofuran
SCE	= Saturated Calomel Electrode
SOMO	= Semi-occupied molecular orbital
UV	= Ultra-Violet
VEH	= Valence Electron Halmitonian
Vis	= Visible
4-CC	= 4-Chlorocatechol
4-Cp	= 4-Chlorophenol
4-CR	= 4-Chlororesorcinol

LIST OF SYMBOLS

A	= Constant of activation
A_t	= Absorbance at time t
A_∞	= Absorbance at infinity
ΔA	= Difference of absorbance
C_o	= Concentration of a given compound
Co	= Concentration of oxidised species
Cr	= Concentration of reduced species
E	= Cell potential
E^o	= Standard potential
E_p	= difference of potential between anodic and cathodic potentials
E_{pa}	= Anodic potential
E_{pc}	= Cathodic potential
ΔE	= Separation between anodic and cathodic peak potential.
$\Delta E''_{1\,2}$	= Difference between the half-wave potential of the first oxidation couple and first reduction couple.
F	= Faraday 's constant
g	= Isotropic factor
hv	= Light energy
$i_d{}^a$	= Anodic diffusion current
$i_d{}^c$	= Cathodic diffusion current
I_o	= Intensity of light incident
k	= Rate constant

K	= Adsorption coefficient
k'	= Apparent first-order constant
k_a	= Apparent reaction rate constant
k_d	= Rate constant of decay
k_f	= Rate constant of forward reaction
k_{ic}	= Rate constant of internal conversion system
k_{isc}	= Rate constant of intercrossing system
k_{obs}	= Observed rate constant
k_p	= Rate constant of phosphorescence
k_r	= Rate constant of reverse reaction
Mm	= Molecular mass
n	= number of electrons
O_1	= First oxidation couple
O_2	= Second oxidation couple
Q	= Electrical charge
R	= Gas constant
r	= Radius of lanthanide ion
R_1	= First reduction couple
R_2	= Second reduction couple
S	= Spin number
S o	= Ground state
S_1	= Singlet excited state
T	= Temperature (Kelvin)
T_1	= Triplet excited state

V	= Volume
v	= Scan rate
W_x	= Weight of sample
W_s	= Weight of standard compound
ΔW_x	= Difference of weights between the sample and air
ΔW_s	= Difference of weights between the standard and air
ε	= Extinction coefficient
λ	= Wavelength
ν	= Stretching vibrations (IR)
π	= P_i
Φ	= Quantum yield
Φ^o	= Limit quantum yield
τ	= Lifetime

LIST OF FIGURES

LIST OF TABLES

LIST OF SCHEMES

1. INTRODUCTION

1.1 General remarks

Phthalocyanine (Pc) (Fig. 1.1), is a synthetic macrocyclic compound which was first reported in 1907 [1]. Phthalocyanines are blue and green dyestuffs which are important industrial materials with a production of 45,000 tons in 1987 [2]. The basic structural feature of a phthalocyanine complex consists of tetra (aza)-macrocycle complexing a central atom. These compounds are used primarily in ink (especially ballpoint pens), colouring for plastics and metal surfaces, and as dyestuffs for jeans and other clothing [2]. More recently, they have been used in different areas such as sensing elements in chemical sensors, electrochromic devices, in cancer therapy (photodynamic therapy) and other medical applications, as well as for many other applications [1,2].

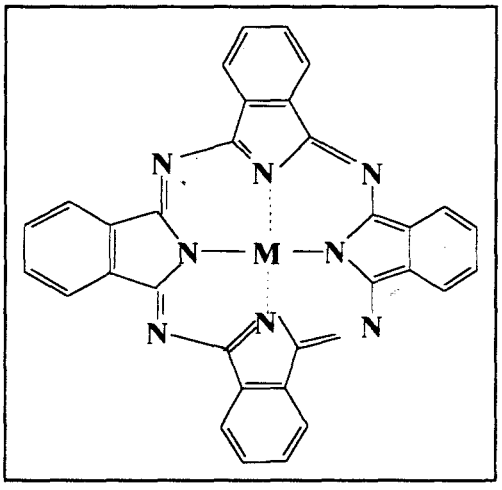

Fig. 1.1 Molecular structure of metallophthalocyanine (MPc).

In 1936, tin diphthalocyanine was synthetised [3] and its structure later confirmed [4,5]. It has two phthalocyanine rings bound to the tin atom. Lanthanide diphthalocyanines, which are synthetic stacked macrocyclic compounds like tin diphthalocyanine, were first reported three decades after the synthesis of tin diphthalocyanine by Kirin et al. [6,7]. These complexes possess two phthalocyanine macrocycles bound to a single metal centre, the lanthanide tervalent ion, Ln(III). The phthalocynaine ring is a dianion, Pc(-2), ($[C_{32} H_{16} N_8]^{-2}$). The lanthanide ion is coordinated to the eight nitrogen atoms.

Lanthanide diphthalocyanine ($LnPc_2$) complexes are a typical class of compounds with π-π^* transitions and they exist in different forms associated with specific colours. The green species is a neutral form and the blue form is the singly reduced species. In the case of lutetium diphthalocyanine, the green form is formulated as $LuPc_2$ or $Pc(-2)Lu^{III}Pc(-1)$, whereas the blue species is denoted as $LuPc_2^-$ or $[Pc(-2)Lu^{III}Pc(-2)]^-$.

The study of lanthanide diphthalocyanine complexes is very attractive due to their electrochromic properties [8-10] and semiconducting behaviours [11-14]. These complexes might be useful in various applications where monophthalocyanines are widely used, such as gas sensors, molecular electronics, photovoltaic and solar cells.

In this thesis, the photocatalytic reactions of metallodiphthalocyanine complexes, Fig. 1.2 are reported.

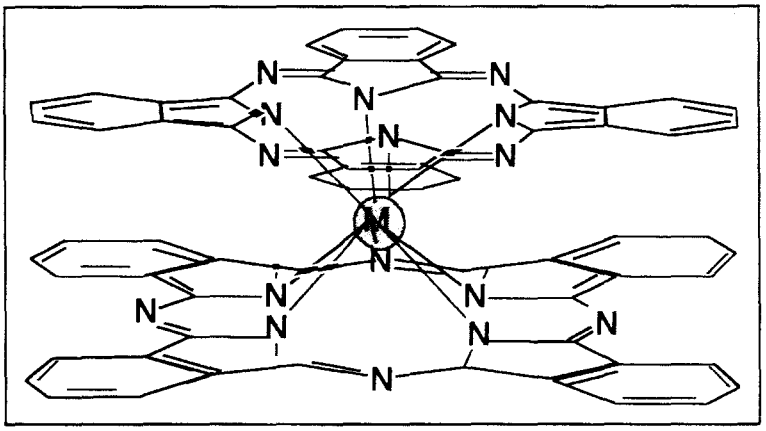

Fig. 1.2 Molecular structure of a metallodiphthalocyanine complex.

Though the electrochemistry aspect of $LnPc_2$ complexes has been well studied [15,16], there are very few studies reported on the photochemistry and photocatalytic properties of these complexes [17]. This work focuses on the study of interactions between lanthanide diphthalocyanine complexes with some pollutants. Thus, this work reports on the photochemical reactions of lutetium, thulium, dysprosium, europium and neodymium diphthalocyanine complexes with sulphur dioxide, pentachlorophenol, thionyl chloride and 4-chlorophenol. Photochemical reactions of tin diphthalocyanine in the presence of sulphur dioxide and in CH_2Cl_2/CH_3CN solvent mixture are also reported. The third aspect is the possible use of lanthanide diphthalocyanine complexes as a cathode in lithium batteries. Thus, photocatalysed interactions of thionyl chloride, $SOCl_2$ with lanthanide diphthalocyanine complexes are also studied. The electrochemistry and spectroelectrochemical studies of these complexes in dimethylformamide (DMF) and dichloromethane are also reported. Tin diphthalocyanine was included because of its similar structure with lanthanide complexes, thus its electrochemical and

spectroelectrochemical behaviours were studied. The photochemical reaction of $SnPc_2$ in the presence of the oxidant CH_2Cl_2 is also reported.

1.2 Nature and structure of diphthalocyanine complexes

Diphthalocyanine complexes are highly stable even at high temperature and are versatile compounds [18]. The physicochemical properties of the rare-earth diphthalocyanines do not show changes in their properties through the whole lanthanide series [19].

Moskalev et al. [20] studied the electrochromic behaviour of lanthanide diphthalocyanines and have observed two forms of lutetium diphthalocyanine; the protonated form $LuHPc_2$ and the ionised form, $LuPc_2^-$. Whereas in the study of the X-ray diffraction of green lutetium diphthalocyanine, De Cian et al. [21] concluded that the green form is a non-protonated , one-electron ligand-oxidized [Pc(-2)LuPc(-1)], species, in which the unpaired electron could be localized on the Pc ring or delocalized over both rings.

These authors also found that metal coordination polyhedron has eightfold symmetry in the green form, (e.g. $LuPc_2$) and it is a slightly distorted square antiprism [22]. The four isoindole nitrogens of phthalocyanine rings are almost coplanar in the green and blue forms. Both phthalocyanine rings are parallel with their dihedral angles being 0.4° in $[Pc(-2)LuPc(-2)]^-$ and 0.2° in green form [Pc(-2)LuPc(-1)].

Nowadays, lutetium diphthalocyanine structures that are accepted are [Pc(-2)LuPc(-2)]$^-$ and [Pc(-2)LuPc(-1)] which are the ionised or blue form and the neutral or green form, respectively. There is great interest in understanding the delocalization of the hole over the rings. Some researchers support the idea that the hole is localised in one ring, hence the neutral form is written as [Pc(-2)Lu Pc(-1)] [21-23], whereas Gasyna et al. [24] defended the proposal that $LuPc_2$ is a delocalized system and might be presented as [$Pc^{-1.5}$ Lu $Pc^{-1.5}$]. On the other hand, it is said that the green form of lanthanide diphthalocyanine complexes is a bicyclic monophthalocyanine complex and not a dimer since lanthanide metal is a trivalent [25]. It is accepted in this work that the hole delocalization concept requires further study.

In the specific case of neutral lutetium diphthalocyanine, [Pc(-2)LuPc(-1)], the lutetium atom lies 1.337 Å away from the first ring and 1.339 Å from the other ring. Thus the distance between the two rings is only 2.676 Å [22]. Whereas, in the molecular geometry study of the blue species, $[LuPc_2]^-$, rings are also parallel and rotated by 45°. The rings are separated by 2.9Å in the blue species, which is slightly higher than the green species (2.68 Å) [26]. On the other hand, transition-metal bis(porphyrinato) complexes, 5, 10, 15, 20-tetraphenylporphyrin zirconium, $Zr(TPP)_2$ and 2,3,7,8,12,13,17,18-octaeyhylporphyrin zirconium, $Zr(OEP)_2$, have shorter distances between substituted rings at 2.54 Å [27].

It has been shown that the structure of lutetium diphthalocyanine exhibits a dissymmetry in the blue species, $[LuPc_2]^-$ contrary to the green species, $LuPc_2$ probably due to the cation-anion packing [22]. Whereas, the green species of unsymmetrical t-butyl-substituted lutetium

diphthalocyanine, exhibited dissymmetry which could affect the delocalization of the unpaired electron present in this molecule [33].

In the structure of lanthanide diphthalocyanines, the bond distance between the central metal and isondole nitrogens vary according each lanthanide. The lutetium-nitrogen bond was found to be 2.383 Å in $[LuPc_2]^-$ and 2.380 Å in $LuPc_2$ [22]. Whereas, in neodymium diphthalocyanine, the eight Nd-N bond distances varied from 2.39Å to 2.49Å [29].

Unlike monomers with D_{4h} symmetry [30], dimers and especially lanthanide diphthalocyanines have D_{4d} symmetry which is associated with spectroscopic properties of these complexes. The study of phthalocyanine complexes is attractive due to their remarkable electronic absorption properties [30,35]. According to Kroenke et al. [5], the D_{4h} symmetry is represented by a cubic structure whereas the D_{4d} symmetry characterises the square antiprismatic.

It has been shown that the electronic structure and the type of chemistry exhibited by rare-earth dipthalocyanines and other diphthalocyanine complexes with similar geometry, such as $SnPc_2$ and UPc_2 depend on their D_{4d} symmetry. [22].

1.3 Preparation of lanthanide diphthalocyanines

Lanthanide diphthalocyanines were first reported by Kirin et al. [6,7] as products of the reaction of a lanthanide acetate with o-phthalonitrile mixed at molar ratio of 1:8 and heated at 280-290°C. The blue and green compounds were separated using electrochromatographic separation on

paper. The green species moved towards the cathode while the blue species moved towards the anode, suggesting that the green species is the neutral form and the blue species is negatively charged.

The blue species of lanthanide diphthalocyanines are prepared using the method reported by Daniels et al.[8]. Thus, the preparation starts by mixing lanthanide acetate trihydrate with 1,2 dicyanobenzene. Then , the mixture is heated at 200°C for 3 hours. After purification on silica column, the blue-greenish lanthanide diphthalocyanine complex is obtained. The yield of chromatographically pure lanthanide diphthalocyanine was very poor.

Pondaven et al. [32] prepared the green species of lutetium diphthalocyanine, $LuPc_2$, by mixing dilithium phthalocyanine and lutetium acetate. The mixture was refluxed for 3 hours in 1-chloronaphthalene. After cooling the mixture, it was poured on a silica column. And after evaporating the solvent, the green powder was obtained.

On the other hand, Collins and Schiffrin [33] reported the preparation of the green species of lutetium diphthalocyanine, $LuPc_2$ using two different methods. The first method consisted of slowly mixing lutetium acetate and 1,2-dicyanobenzene at a molar ratio of 1:8 and heating at 300°C for 3 hours. After cooling the mixture to room temperature, the solid product was washed with acetic anhydride, acetone, and DMF before air drying. The yield was 35% and the $LuPc_2$ was purified by sublimation.

In the second method lutetium acetate and 1,2-dicyanobenzene at molar ratio of 1:25 were refluxed for 2 hours. After cooling, further refluxing and washing in 1-pentanol the green species, $LuPc_2$ was obtained with a yield of 66%. Both of these methods are based on a simple mixture of a lanthanide acetate with 1, 2-dicyanobenzene, and heated at high temperature. Recently, Janczak et al. [25] obtained the blue-violet complex of indium diphthalocyanine, $InPc_2$ in crystalline form. It was prepared from InMg alloy and 1,2- dicyanobenzene in a 1:2 weight proportion, mixed together and pressed into pellets. The pellets were inserted into an evacuated glass ampule and sealed. The ampule was heated at 210°C for 1 day. It yielded blue-violet good quality crystals.

The purity of complexes prepared from the methods discussed above is still questionable. The method developed by Daniels et al.[8], by which the blue form of lanthanide diphthalocyanines was prepared, showed the presence of minor impurities of lanthanide triple decker phthalocyanine and lanthanide monophthalocyanine complex in their mass spectrum. The presence of triple decker phthalocyanine could be explained because similar methods are used in the preparation of rare-earth triple decker phthalocyanines, except the heating time (8 h) is longer than for the dimers [34]. The presence of a triple decker compound was also observed by Guyon and co-workers [35], when they isolated a novel lutetium(III) triple-decker sandwich, a tri(1,2-naphthalocyaninato) lutetium as a by-product in the synthesis of lutetium bis (1,2-naphthalocyanine).

In addition, Clarisse et al. [36] pointed out that time and temperature are the most important factors in the synthesis of lanthanide diphthalocyanines, hence the green species $LuPc_2$ was

obtained as a by- product in the reaction of lutetium acetate with 1,2-dicyanobenzene at 310°C and as the main product of the same reaction at 300°C.

On the other hand, actinide and other diphthalocyanine complexes are obtained according to Equation 1.1 by reacting $Na_2(Pc)$ with MCl_4 in a boiling chloronaphthalene [37]:

$$Na_2Pc \xrightarrow[MCl_4]{\text{1-chloronaphthalene}} MPc_2 \qquad (1.1)$$

Diphthalocyanine complexes are soluble in most common organic solvents. However, lanthanide diphthalocyanines containing aza-crown ether substituents are the only phthalocyanine dimers reported to be soluble in water [38-40].

1.4 Electronic structure of diphthalocyanine complexes

Metallodiphthalocyanines including lanthanide diphthalocyanine complexes possess a D_{4d} molecular symmetry as already discussed above. The molecular orbitals involved in this case, are ring π orbitals. Thus, π-π^* transitions occur both in dimer and monomeric phthalocyanines [30].

The description of the electronic structure of diphthalocyanine complexes corresponds to the mixture of two phthalocyanine ring structures. An overall splitting of the molecular orbitals is observed when passing from monomeric to dimeric phthalocyanines due to the interaction

between both rings [11]. The electronic structure of the monomeric phthalocyanine is characterised by two main transitions Q and B bands, Fig. 1.3.

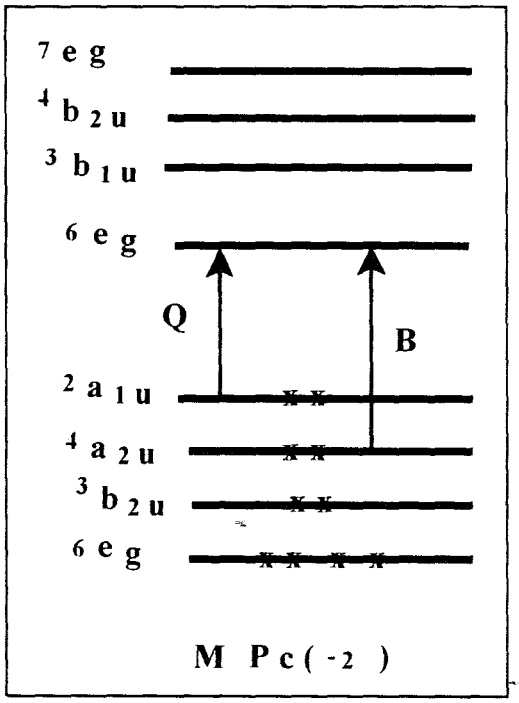

Fig. 1.3 Energy level diagram of monophthalocyanine complex.

When molecular orbitals, $2a_{1u}$ (A) and $2a_{1u}$ (B) of two phthalocyanine rings A and B are mixed, considerable splitting of the energy levels due to the interaction between the rings, resulting in $2a_{2u}$ and $2b_{1u}$, Fig. 1.4 . In the similar way, $4a_{2u}$ (A) and $4a_{2u}$ (B) are mixed, the splitting between these molecular orbitals is very small compared to the splitting of $2a_{1u}$, and results in $4a_{1u}$ and $4b_{2u}$, Fig. 1.4. The Fig. 1.4 (a) shows all possible transitions and the two energy levels, which are the highest occupied molecular orbitals (HOMO) and the lowest unoccupied molecular

orbitals (LUMO) of the ring. In the neutral form of lanthanide diphthalocyanine complexes, $LnPc_2$, the HOMO is replaced by the semi-occupied molecular orbital (SOMO) with an unpaired electron, Fig. 1.4(b) [26].

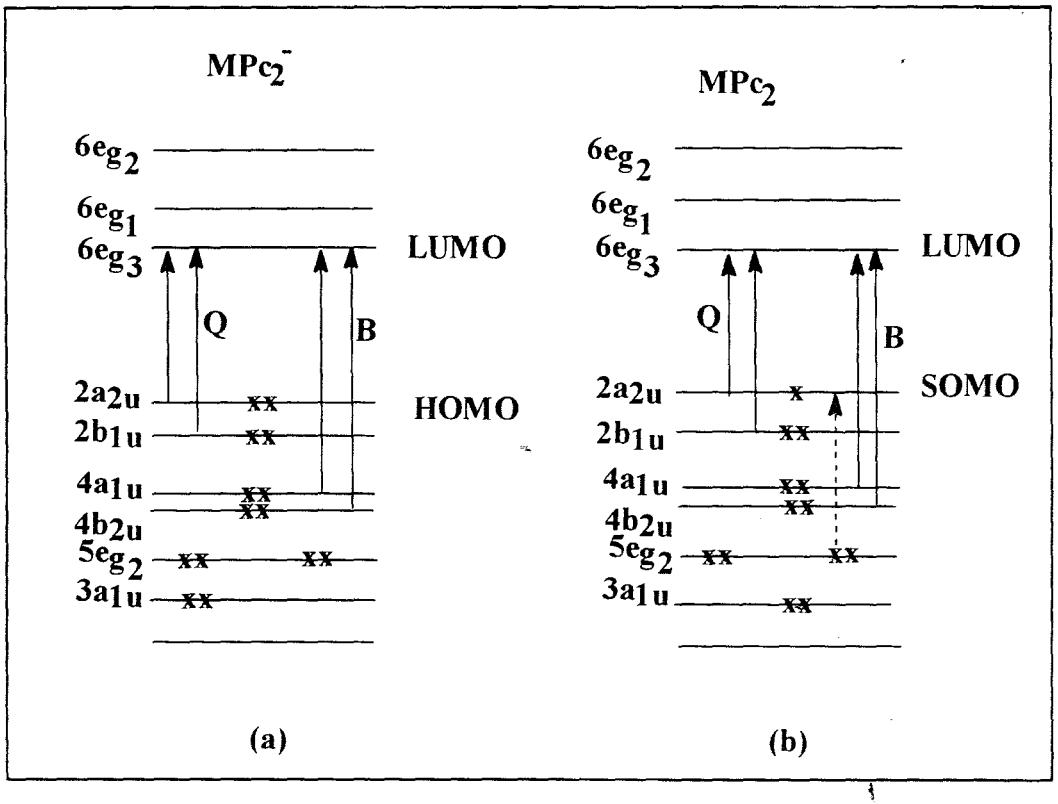

Fig. 1.4 Energy level diagrams for diphthalocyanine complexes. (a) MPc_2^- and (b) MPc_2.

The main electronic transition ($2a_{2u} \rightarrow 6e_g$) corresponds to the electronic absorption in the visible region and known as Q band whereas ($4a_{1u} \rightarrow 6e_g$) transition occurs in the near ultra-violet region and it is known as a Soret or B band [41]. The localized orbitals (Los) of $[LuPc_2]^-$ are destabilized compared to monomeric phthalocyanines and tin diphthalocyanine due to the

negative charge [42]. In Fig. 1.4 (b), the interaction of the $2a_{1u}$ molecular orbitals of individual phthalocyanine rings results in one electron in $2a_{2u}$ (SOMO) [43], due to the intramolecular charge transfer between the two phthalocyanine rings [11]. The transition ($5e_g \rightarrow 2a_{2u}$) characterises the intramolecular charge-transfer which is only observed in the green species of lanthanide diphthalocyanines at 450-470 nm [11], whereas the vibronic allowed transition ($4b_{2u} \rightarrow 2a_{2u}$) absorbs in the near-infrared region at 1494 nm [11,43] for $LuPc_2$.

Using Valence Effective Hamiltonian (VEH) studies, Orti and co-workers [11] presented a comparative study of electronic structure and possible transitions between metal-free phthalocyanine dimer and lutetium diphthalocyanine. VEH calculations predict a larger splitting of 0.83 eV in green species of $LuPc_2$ whereas a small splitting of 0.35 eV was predicted in $(PcH_2)_2$. The large splitting is explained as a result of closer interaction between two phthalocyanine rings in $LuPc_2$.

1.4.1 Formation of ring-reduced and ring-oxidized complexes

In some lanthanide diphthalocyanines and other dipthalocyanine complexes, chemical reactions are controlled by ring interactions [10,44]. Lanthanide diphthalocyanine complexes have a rich redox chemistry centred on the ring [11]. It has been shown that the reduction or oxidation of $[LuPc_2]^-$ results in a series of complexes, each having a unique colour. The complexes range from [Ln Pc(-1)Pc(-1)]$^-$ to [Pc(-3)Ln Pc (-3)]$^{-3}$ [31] (Ln = lanthanide). This wide range of colour changes makes these materials useful for displays devices [45]. On the other hand, the redox

properties of monomers have also been well discussed by Lever et al. [46]. The ring-oxidized and reduced systems were thoroughly reviewed by Stillman [31]. Fig.1.5 shows different energy level diagrams of ring oxidized and reduced of monomeric species.

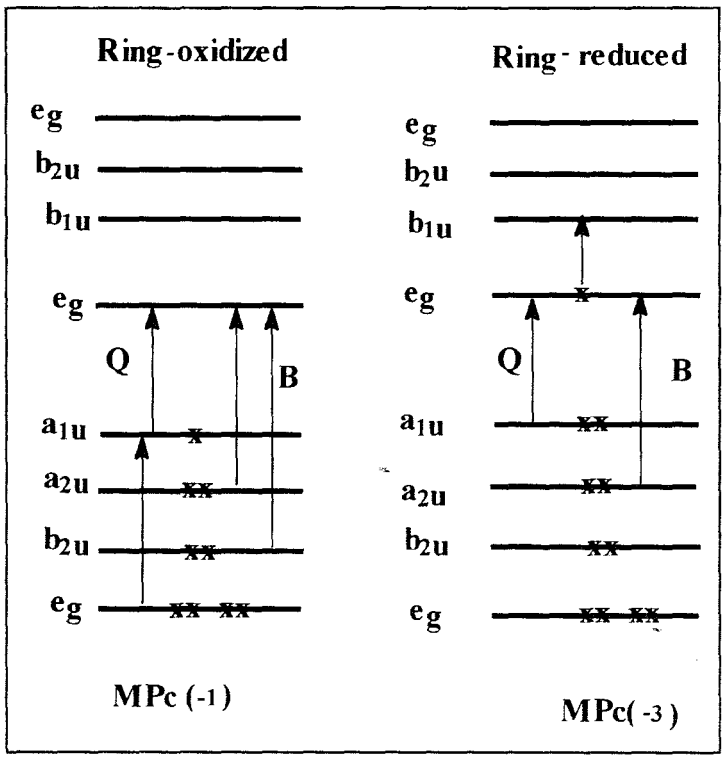

Fig. 1.5 Energy level diagrams of ring-oxidized and ring reduced monomeric phthalocyanine rings [31].

Q and B transitions are due to transitions from the a_{1u} and a_{2u} (or b_{2u}) respectively to e_g level. The ring oxidized MPc(-1) has one transition in the Q band region and two transitions in the Soret region. It also shows an intramolecular charge-transfer to the SOMO which was observed in $LuPc_2$ [11]. This transition is characterized by absorption in the near-infrared region. The ring

reduced complex, MP(-3) exhibits an intramolecular transfer from LUMO to higher energy orbitals.

1.5 Molecular Orbital Calculations of diphthalocyanine complexes

Dimers are formed by adding two monomers, hence, the molecular orbitals (MO)s of dimers are derived from the molecular orbitals (MO)s of two monomers stacking in D_{4d} symmetry [26]. The splitting of these molecular orbitals in the dimer is assigned to the exciton coupling in the phthalocyanine dimer [31,45]. In their study on the cerium and europium bis(octaethylporpohyrinate), Estiú et al. [47] observed that MOs are linear combination of porphyrin or phthalocyanine molecular orbitals, and these MOs are the basis of the eight-orbital model .

Ishikawa and co-workers have presented calculations on electronic states of $[LuPc_2]^-$, $[Sn(Pc)_2]$ and $[(SiPc)_2O]$ by the use of localised orbitals (LO), showing that the excited states of dimers were characterized as a superposition of intraligand and interligand excitations [26]. The calculation of the excited singlet state of $[LuPc_2]^-$ on an LO basis gave three allowed excited states which are $1E_1$, $2E_1$ and $3E_1$. The lowest allowed excited singlet state $1E_1$ mainly consists of the charge resonance configuration while the second allowed excited state, $2E_1$ is predominantly made of the exciton coupling configuration. The third allowed excited state was not discussed. From the calculated excitation energies and intensities, they assigned the absorption band at 714 nm to $1E_1$ whereas the band at 625 nm was attributed to $2E_1$ transition [26].

The coupling interaction (CI) calculations of $LuPc_2^-$ using molecular orbital (MO) theory were done using the same allowed excited states and it is was found that the higher component band $2E_1$ (Q band) had a greater intensity than the lower component $1E_1$ (B band) [26].

Van Cott et al.[43] found two fully allowed transitions in the study of green species, $LuPc_2$, which were attributed to the Q and B bands and one vibrational induced transition which characterises the intramolecular transition ($5\ e_g \rightarrow 2a_{2u}$) as shown in Fig. 1.4(b).

On the other hand, VEH calculation on the [Pc(-2)LuPc(-1)] radical complex predicted two pairs of doubly degenerate transitions (centred at 1.71 and 2.02 eV) [11]. It should be noted that the calculated charge-resonance state is smaller than that of the lowest excited singlet in phthalocyanine dimer [41].

The calculation behind this model is empirical but it gives expected values of absorption bands in spectroscopic studies. Thus the electronic structure of phthalocyanine dimers as well as the energies calculated predict the position of absorption bands in electronic absorption spectra of these complexes.

1.6 Spectroscopic Studies

1.6.1 UV / Visible Absorption Spectra

The study of phthalocyanine complexes became very attractive due to their unique spectral properties. They absorb strongly in the visible region, Fig. 1.6, whereas the structurally similar porphyrins absorb strongly in the near ultra-violet (UV) region [30]. The presence of aza-bridges in phthalocyanine is the reason of the observed strong electronic absorption in the visible region compared to the porphyrins.

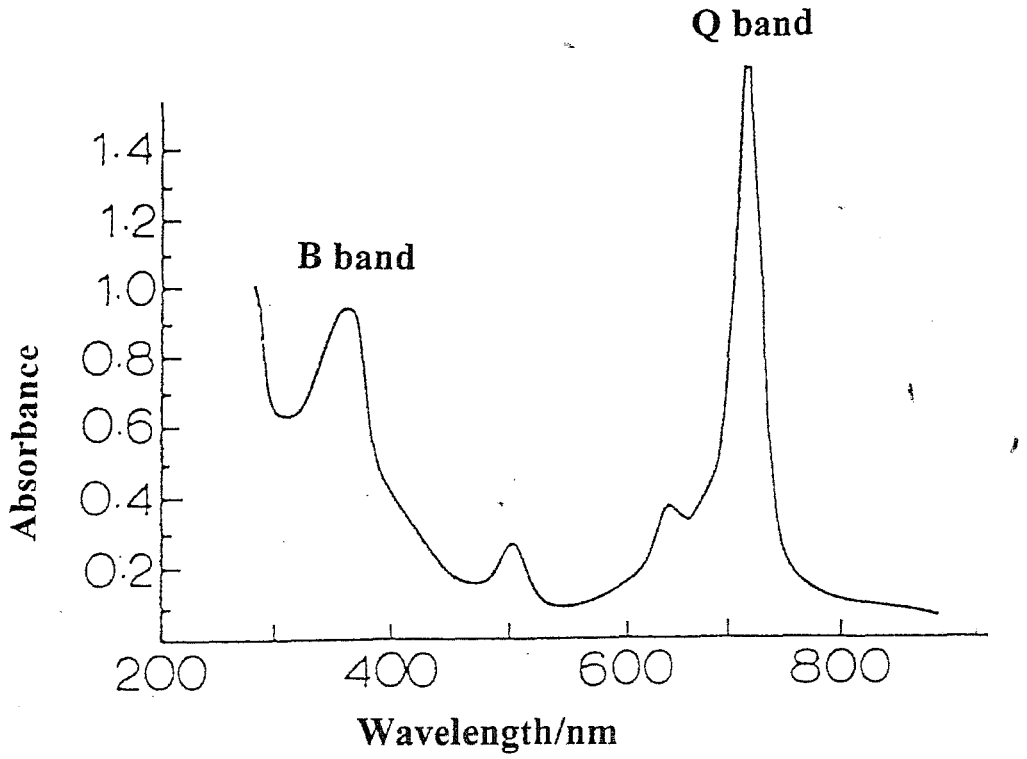

Fig. 1.6 Electronic absorption spectrum of metallophthalocyanine (MPc).

The electronic absorptions of metallophthalocyanine complexes were well reviewed by Nyokong and Stillman [30,31]. In their discussion on the electronic absorption of lanthanide and actinide complexes, they explained that in $LnPc_2$, the oxidation and reduction of the Pc ring give π cationic or anionic species, as well as the product of aggregation of these species into dimers and trimers [30].

The neutral form of lanthanide diphthalocyanine complexes ($LnPc_2$) is characterised by a band around 665 nm, whereas the anionic complex ($[LnPc_2]^-$) exhibits bands near 620 and 700 nm [30]. In the case of the neutral $LnPc_2$, a shoulder observed around 450-470 nm [23,28,32, 48], was attributed to the SOMO to LUMO charge-transfer transition [49].

The splitting observed in the Q band of phthalocyanine dimers is characteristic of these complexes. This splitting is ascribed to the exciton coupling interaction of two phthalocyanine rings [26,41]. The Q band splitting is more extensive in $SnPc_2$ than $LuPc_2^-$, although the later shows a considerable splitting of the Q band and a notable B band accompanied by a shoulder around 417 nm [26]. It has been shown that the Q-band splitting decreases with the increase of the lanthanide ion radius throughout the lanthanide series and characterises the strength of interaction between the two phthalocyanine rings in the complex.[26].

Kirin and co-workers [7] reported on the changes of the Q band absorption wavelength relative to the atomic number of lanthanide element. It was also said that lutetium diphthalocyanine was the most studied complex relative to other lanthanide complexes due to its greater Q- band splitting and high chemical activity [31].

1.6.2 Near Infrared Absorption Spectra

The near infrared absorption characterises transitions within the green $LnPc_2$ complexes containing Pc(-1) ring. Markovitsi and co-workers [49] studied the near infrared absorption spectra of lanthanide diphthalocyanines in dichloromethane and as thin films, they observed that the absorption band maxima shifted to longer wavelengths starting from $LuPc_2$ to $DyPc_2$ [49]. The near infrared (NIR) wavelengths of these neutral lanthanide diphthalocyanine complexes were: $LuPc_2$ (1382 nm), $YbPc_2$ (1386 nm), $TmPc_2$ (1392 nm), and $DyPc_2$ (1404 nm). Whereas, the wavelengths of the same complexes as thin films were shifted to longer wavelengths as follows: $LuPc_2$ at 1423 nm and $TmPc_2$ at 1415 nm.

The same authors concluded that the near infrared absorption does not characterise the interaction between the solvent and the lanthanide diphthalocyanine complexes hence the bands were observed with both solution and solid of $LuPc_2$ at 906nm. The near infrared band was assigned to the intramolecular charge transfer, characterized by the transition $5e_g(\pi) \rightarrowtail 2a_{2u}(\pi)$ [49].

Moreover, in their study on nonlinear optical properties of bis(phthalocyanines), Shirk and co-workers [50] found that the wavelengths of the near IR bands were closer to the results reported by Markovitsi et al. [49]. They also pointed out that the position of these intervalence bands depend effectively on the metal ion [50].

Furthermore, in the study of the absorption spectra of lanthanide bis (octaethylporphyrinates), $Ln(OEP)_2$ in the near infrared region, Buchler et al. [51] observed that the absorption band maxima range from 1135 nm for $Lu(OEP)_2$ to 1480 nm $La(OEP)_2$, which imply that it depends on the lanthanide ion. The energy level of the near infrared absorptions were related to the redox potentials of $Ln(OEP)_2$. It was found that the redox potentials decreased with the increase of the ionic radius of the lanthanide ion, and with the energies of the near infrared bands [44]. Thus, lutetium bis (octaethylporpyrinate) is expected to produce higher oxidation potentials because of the largest electronegativity of lutetium element [49].

The origin of the near infrared absorption is well explained by the electronic structure of these complexes. The near infrared bands only appear in the neutral form of lanthanide diphthalocyanines because they possess one dianion phthalocyanine ring and a phthalocyanine ring containing one electron. According to Markovitsi et al. [49], Pc(-2)Lu Pc(-1) is a system in which Pc(-2) plays a role of an electron donor whereas, Pc(-1) an electron receptor. The electronic structure of these complexes show an intramolecular charge transfer from $5e_g$ to $2a_{2u}$ in the semi-occupied molecular orbital (SOMO). The VEH calculations done by Orti et al.[11] predicted the existence of a near infrared absorption in $LuPc_2$ model at 1494 nm.

1.6.3 Mid-Infrared Spectra

Shurvell and Pinzuti [52] studied thoroughly the infrared (IR) spectra of metal-free phthalocyanine and some metallophthalocyanines. They gave frequencies related to some vibrations in H_2Pc; e.g. N-H vibrations were found at 3290 cm^{-1}, whereas C-H and C-C vibrations were localized around 3000-3100 cm^{-1} and 1952 cm^{-1} respectively. The pyrrole unit vibrations were observed at 1144 cm^{-1} and the band at 720 cm^{-1} is attributed to C-H out of plan bending vibrations [52].

In addition, Kroenke and Kenney [4,5] studied the infrared spectra of the two allotropic forms of tin diphthalocyanines, α and β $SnPc_2$; and they observed that the IR spectra of both forms are quite similar to that of monophthalocyanines except the vibrations observed in 1500 cm^{-1} region.

However, in the study on symmetrically and unsymmetrically substituted $LuPc_2$, the bands at 1452 cm^{-1} and 1323 cm^{-1} have been identified as characteristic of $LuPc_2$ dimeric species [28]. The bands observed between 1530 and 1685 cm^{-1} are attributed to the pyrrole moiety, whereas the bands observed between 1150 and 1050 cm^{-1} were assigned to the benzene rings vibrations. While the two bands at 880 cm^{-1} and 810 cm^{-1} were attributed to the lutetium ion-ligand vibrations [28]. The band at 720 cm^{-1} was assigned to the C-H out of plane bending vibrations as observed by Kroenke and co-worker [4,5].

For substituted diphthalocyanines, many modifications of the infrared spectra may result from the lowering of the symmetry of the molecules. Pondaven et al. [32], observed that in unsymmetrical complexes, the characteristic band of $LuPc_2$ at 1452 cm^{-1} shifted between 1452 and 1472 cm^{-1}.

On the other hand, Gobernardo-Mitre and co-workers [53] studied the vibrational spectra of perchlorinated lutetium diphthalocyanine, $LuPc_2Cl_{32}$ and $LuPc_2Cl_{16}$ and they pointed out that the observed Raman and infrared spectra did not fit the symmetry groups of D_{4d} and D_{4h}, although these complexes have shown some similarities with the unsubstituted $LuPc_2$.

In the study of infrared spectra of unsymmetrical neutral (phthalocyaninato)(tetra-4-pyridylporphyrinato) lanthanide (III) (LnPcTPyP), it was observed that the Eu(Pc)(TPyP) and the Gd (Pc)(TPYP) exhibited a strong band at 1311 cm^{-1} which is characteristic of the phthalocyanine π- radical anion [54], while $[EuPcTPYP]^-$ and $[Gd\ PcTPYP]^-$ exhibited this band at 1328 cm^{-1}, which was assigned to a dianionic phthalocyanine [53].

Infrared is still a powerful technique in the characterization of these complexes as well as the understanding of their structures. Mostly, the new area of far-infrared spectra of metallophthalocyanines [53] could bring numerous contributions to the understanding of the characterization of symmetrical and unsymmetrical metallophthalocyanines.

1.6.4 Electron Spin Resonance (ESR)

Since the nature of the neutral form of lanthanide diphthalocyanine was debatable, ESR spectroscopy was the appropriate technique which could give an insight to this issue. From its discovery, the neutral form was known as a protonated form of lanthanide complex. The acidic hydrogen, served to balance the charge in one of the phthalocyanine ring of these compounds [7,20] but was however not detected using proton NMR [10].

Later, Chang and Marchon [23], characterized the oxidized form of lutetium diphthalocyanine using the magnetic susceptibility and ESR spectroscopy, and showed the existence of an unpaired-electron containing phthalocyanine ring, Pc(-1), with an intense signal at g=2.00. From the ESR spectra the neutral form formulation was established as a non-protonated, $LuPc_2$. They also confirmed that $LuPc_2$ contains Lu^{3+} which is diamagnetic, sandwiched between one dianionic phthalocyanine ring, Pc (-2) and one-electron oxidized Pc(-1) ring [23]. Moreover, De Cian et al.[21], confirmed the existence of the unpaired electron on the phthalocyanine ring in $LuPc_2$ molecule, questioning if this hole-electron was localized in one Pc ring, or was delocalized over both Pc rings.

Buchler and co-workers [55], studied the ESR spectra of cation radicals of bis(octaethylporphyrinato) zirconium (IV) ($[Zr(OEP)(OAC)_2]^+$)and bis(chelate)(octaethyl-porphyrinato) zirconium (IV) complexes $[Zr(OEP)_2]^+$, and showed that these radical cations gave a signal with g=2.00. The localization of a hole-electron was still debatable although ESR line width shows that if the delocalization is greater, it gives a broader ESR line [55].

1.7 Electrochemistry: an overview

1.7.1 Cyclic Voltammetry

In cyclic voltammetry, the diffusion currents of reduction and oxidation are equal for reversible systems, so the same number of electrons is exchanged in both processes. For a given process, the potential, E, varies linearly with log $[(i_d-i)/i]$, where i_d is the diffusion current and i is the cell current. When both oxidation and reduction processes are considered, this relation is extended to a new relationship, $E= f([\log (i_d^a-i)/(i_d^c-i)])$ [56], where i_d^a and i_d^c are the diffusion currents of anodic and cathodic processes respectively. If the reaction is rapidly reversible, the reaction obeys the Nernst Equation [57,58].

$$E = E^0 + \frac{RT}{nF} \ln \frac{C_O}{C_R} \qquad (1.2)$$

E is the cell potential whereas E^0 is the standard cell potential determined at 25° C at 1 atm for 1M solution. R is the gas constant ($R= 8.314$ J $mol^{-1}K^{-1}$), T is the temperature expressed in Kelvin, n is the number of electrons involved in the reaction and F is the Faraday constant ($F= 96500$ C). C_O and C_R are concentrations of oxidized and reduced species for the reaction:

$$R \rightarrow O + e^- \qquad (1.3)$$

The reversible couple of a given complex, e.g. $LuPc_2$ is characterized by an anodic potential E_{pa} and a cathodic potential E_{pc}. The half-wave potential depends on the redox nature of each compound and it is given as follows:

$$E_{1/2} = \frac{E_{pa} + E_{pc}}{2} \qquad (1.4)$$

Whereas the number of electrons transferred at the electrode, n, for a reversible couple can be determined from the following equation [57]:

$$E_p = E_{pa} - E_{pc} = 2.3\frac{RT}{nF} \qquad (1.5)$$

at 25° C, the preceding equation can be written as

$$E_p = \frac{0.059}{n} \qquad (1.6)$$

On the other hand, the peak current of a reversible system can be described by Randles-Sevcik Equation for the forward sweep of the first cycle [59]:

$$i_p = 2.67x10^3 n^{3/2} A D^{1/2} C v^{1/2} \qquad (1.7)$$

Where i_p is the peak current in Amperes; n is the stoichiometric number of electrons in equivalent/mol; A is the electrode area in cm^2; C is the solution concentration given in mol cm^{-3} and v is the scan rate expressed in volts s^{-1}. A plot of current versus the square root of scan rate will be linear using the Equation 1.6 [59].

Cyclic voltammetry (CV) is widely used in the study of the electrochemistry of metallophthalocyanines. In CV, the potential is swept back to and forth between two chosen limits [57,60]. It has been shown that substituted and unsubstituted lanthanide diphthalocyanine complexes have the best performance in reversibility, rapid switching times with little degradation over 10^6 cycles [61]. It has been pointed out that $LuPc_2$ shows a very good reversibility in its whole redox field compared to $SnPc_2$ and $ZrPc_2$ [61].

1.7.2 Redox properties of diphthalocyanine complexes

Redox processes in lanthanide diphthalocyanines occur on the π-orbitals of the conjugate macrocyclic phthalocyanine rings except for the case of cerium diphthalocyanine where the redox properties are controlled by the metal [44,62]. The study on the electrochemistry of metallophthalocyanine complexes in solution and as part of electrodes has shown that redox processes of phthalocyanine complexes may occur in Pc rings or at the central metal depending on some factors such as the nature of: i) substituents on Pc ring, ii) oxidation state of the central metal, iii) the axial ligands and solvents [59,62-66].

The Valence Effective Hamiltonian study of lutetium diphthalocyanines, Orti et al.[11] stated that an oxidation process involves removing an electron from HOMO while a reduction process consists of adding an electron to the LUMO.

In $LuPc_2$, the HOMO-LUMO gap is found to be 0.40 V [15] while in $LuPc_2^-$ the gap is 1.09 V vs the ferrocenium/ ferrocene couple [62]. Komani et al. [16], in their report on the redox potential of a series of lanthanide diphthalocyanine complexes, have shown that the HOMO-LUMO gap changes with the central lanthanide ion and this gap is narrower in $LnPc_2^-$ than in $Ln(OEP)_2$. The HOMO-LUMO gap is a good estimate of the thermal activation energy for the electrical conduction in solid materials [15].

Electrochemical studies of lanthanide diphthalocyanines have attracted a lot of attention from many researchers due to their rich redox properties. Komani et al. [16] have studied thoroughly the electrochemical behaviour of a series of lanthanide diphthalocyanine sandwich complexes in o-dichlorobenzene, and they observed that redox potentials of $[LnPc_2]^-$ vary linearly as function of the ionic radii of tervalent lanthanides. Buchler and Scharbert [44] also observed the same trend from the electrochemical behaviours of $Ln(OEP)_2$ in DMF.

Lanthanide diphthalocyanine complexes show similar electrochemical behaviour apart from the shift in potentials, confirming that phthalocyanine rings are responsible for electrochromic behaviour [67]. The same researchers suspected the formation of an unspecified complex between $LuPc_2$ and oxygen or water during the anodic oxidation of lutetium diphthalocyanine in acidic medium [67]. However, the electrochemical behaviour of $LuPc_2$ in methylene chloride

did not show major modifications, neither water nor oxygen had any influence on redox properties of this complex in organic medium [56]. Similar observations were reported in the study of redox properties of alkyl substituted lutetium diphthalocyanine in CH_2Cl_2 [69].

It has been shown that the electrochemical behaviour of heteroleptic lanthanide porphyrin-phthalocyanine dimers have quasi-reversible redox properties which are also controlled by the rings [69]. The electrochemical behaviour of heteroleptic actinide complexes in which porphyrin and phthalocyanine dianion rings were mixed, showed no significant interaction between these rings, and their electrochemistry was similar to that of individual diporphyrin and diphthalocyanine complexes [70]. The characteristic electrochemical behaviour of diphthalocyanine complexes was also observed with lanthanide bis (ethylsulfanyl)tetraazaporphyrins, $Ln(OESPZ)_2$ in DMF and CH_2Cl_2 [71].

1.7.3 Spectroelectrochemistry of diphthalocyanine complexes

Spectroelectrochemical properties of monophthalocyanines have been widely studied either in solution, as thin films or adsorbed on electrode surfaces [59,64-66,72,73]. The spectroelectrochemical studies of lanthanide diphthalocyanines have mainly been studied with reference to their electrochromic behaviour. Spectroelectrochemistry was used to study redox properties of a series of lanthanide diphthalocyanines, giving the behaviour shown by the Equation 1.8 [49].

$$[\mathbf{LnPc_2}]^{+} + \mathbf{e}^{-} \Leftrightarrow [\mathbf{LnPc_2}]^{0} + \mathbf{e}^{-} \Leftrightarrow [\mathbf{LnPc_2}]^{-} + \mathbf{e}^{-} \Leftrightarrow [\mathbf{LnPc_2}]^{-2} + \mathbf{e}^{-} \Leftrightarrow [\mathbf{LnPc_2}]^{-3} \quad \textbf{(1. 8)}$$

The electronic spectra of $[LnPc_2]^{-}$, $[LnPc_2]^{0}$ and $[LnPc_2]^{+}$ were reported in solution [56,68,], and in solid state [67]. However, in this work, further oxidation to the $[Pc(0)LnPc(-1)]^{2-}$ species is reported.

In addition, the electronic spectra of the oxidized and reduced zirconium diphthalocyanine, $Zr(Pc)_2$ and tin diphthalocyanine, $SnPc_2$ have been reported [10]. Different species of $ZrPc_2$ such as $[ZrPc_2]^{-}$, and $[ZrPc_2]^{+}$ were observed, whereas tin diphthalocyanine only showed $[SnPc_2]^{0}$ and $[SnPc_2]^{+}$ in solid state [10].

1.8 Photochemistry of diphthalocyanine complexes: an overview

1.8.1 General considerations

Photooxidation as well as photoreduction consist of electron excitations and consequently involve the population of the low-lying of triplet state, $^3\pi\pi^*$, followed by an electron transfer to or from a quencher [74-80]. In photoreactions, UV irradiation of monomeric MPc complexes result in a process which originates from the $n\pi^*$ states while the excitations in the Q band result in the population of the low-lying triplet state, $^3\pi\pi^*$, followed by an electron-transfer process between the excited complex and the electron donors or acceptors [17,74,81].

Photochemical properties of metallophthalocyanines are widely studied in part due to their possible use in the photovoltaic cells [82-84] and as photocatalysts [85-87]. And on the other hand, the electron-transfer quenching of the low-lying $^3\pi\pi^*$ states of some metallophthalocyanines have been intensively reported by Ferraudi and co-workers [74-77]. The triplet excited state has longer lifetime compared to the singlet state [74-77], hence the electron transfer process involving the triplet state is favoured.

1.8.2 Photooxidation reactions of diphthalocyanine complexes

Photooxidation reactions of monoporphyrins in alkyl chloride solutions [78] and in frozen solution using alkyl chloride or quinones [79] forms porphyrin ring π-cation radical species. In the study on the photooxidation of ZnPc and RuPc, CoPc and FePc, Nyokong et al.[80] obtained π-cation radical species which resulted through oxidation of the ring in the case of ZnPc, RuPc and CoPc, while in the case of FePc, metal oxidation occurred prior to the ring oxidation.

On the other hand, the photolytic reaction of oxomolybdenum phthalocyanine ($OMO^{V}Pc$) in dichloromethane resulted in a metal based photooxidized MO^{VI} complex [81]. Irradiation of tetraazaporphyrin derivatives in DMF in the presence of air has been reported to result in a photoreaction between the complex and oxygen [88]. The photostability of these complexes depend on the solvents employed [88].

There exist very few reports on the photochemical behaviours of lanthanide double decker phthalocyanines although they show rich redox properties and interesting electronic spectra.

Ricciardi et al. [71] observed that diphthalocyanine complexes are not suitable photosensitizing agents due to their very short lifetime and relative low energy in their low-lying excited states.

Kraut and Ferraudi carried out a comparative study on photochemical properties of tin(IV) diphthalocyanine, $SnPc_2$ and tin (IV) dichlorophthalocyaninate, $SnPcCl_2$ in dichlorobenze [17]. The photolysis of $Sn(Pc)Cl_2$ showed that a phthalocyanine radical was first formed, $[Sn(Pc^{\cdot})Cl_2]^-$ and was converted to a new feature containing Sn(III), $[Sn^{III}(Pc^{0})Cl_2]^-$. Whereas the photolysis of $SnPc_2$ resulted in changes which gave $Sn^{II}(Pc)$ and $Sn^{IV}(Pc)_2^-$ as final products [17].

Photolysis of diphthalocyanine complexes of lanthanum(III), neodymium (III) and yttrium(III) in the presence of benzoquinone resulted in the formation of radical species [48]. The photolysis resulted in a complex containing one Pc ring with an unpaired-electron and a dianionic Pc ring [89]. The ease of photooxidation of dimers increased with decrease in ring-ring distance.

Kasuga et al. [90] also generated stable green $[PcLnPcH]^-$ complexes from the blue complexes, PcLnPcH in the solvent mixture of dichloromethane and acetonitrile. The photoreaction could not generate the radical in the absence of the dichloromethane. In the presence of CH_2Cl_2, the solvent absorption was filtered ($\lambda \geq 320$ nm), to avoid direct photooxidation of dichloromethane. The photooxidation of PcLnPcH by dichloromethane was also facilitated by π-π interactions of the two rings. The mechanism followed could be illustrated in the following way:

$$PcLnPcH + CH_2Cl_2 \xrightarrow{h\nu} [PcLnPcH]^+ + CH_2Cl^{\bullet} + Cl^- \quad (1.9)$$

$$(PcLnPcH) \rightarrow PcLnPc^- + H^+ \quad (1.10)$$

Scheme 1.1

As in any photochemical process, lanthanide diphthalocyanines are expected to populate the low-lying triplet excited state, $^3\pi\pi^*$ [80], before quenching by electron acceptors or donors.

1.8.3 Photoreduction reactions of diphthalocyanine complexes

The photoreduction of monophthalocyanine complexes has been extensively studied [81,87,91-94]. The photoreduction of tin(IV) phthalocyanines, Sn(IV)Pc and Sn(IV)$PcCl_2$ have shown that Sn(IV)Pc was reduced to Sn(IV)Pc(-3) which is a one-electron reduction process whereas the photoreduction of Sn(IV)$PcCl_2$ in the presence of Sn(II)Cl_2 resulted in the formation of $[Sn(IV)Cl_2]^{2-}$ in which two electrons were involved in Pc reduction [81].

In the photoreduction of MgPc(-2) and AlPc(-2)Cl in DMF and in the presence of azaferrocene, Zakrzewski et al.[87] observed a one-electron reduced phthalocyanine ring. Similar behaviour has been observed in the photoreduction of Zn(II) tetrasulphonatophthalocyanine,$[ZnSPc]^{4-}$ to monoanion radical $[ZnSPc]^{5-}$ in the presence of triethanolamine (TEOA) [93]. The formation of a trianionic Pc ring in the photoreductions of tin(IV)phthalocyanine in the presence of sulphur

dioxide [86] and of aluminium(III) sulfonated phthalocyanine, $[AlSPc]^{4-}$ in the presence of benzoquinone [91,92], are examples of ring-reduced phthalocyanines. There have been no reports on the photoreduction of diphthalocyanine complexes.

1.8.4 Solvent effects in photoreactions of metallophthalocyanines

Spectroscopic absorptions, electrochemistry and photochemistry of metallophthalocyanine complexes depend on the solvent [95]. Basic solvents such as DMF and pyridine favour the reduction of metallophthalocyanines either electrochemically [64] or photochemically [80,81]. Whereas the acidic or protonated solvents favour the oxidation of phthalocyanine complexes.

There are two categories of solvent which are protic and aprotic depending on their structure. Aprotic solvents are acceptors of protons whereas protic solvents are proton donors [96]. Both types of solvents can influence reactions rates differently [96].

Frink and co-workers [77] discussed solvent effects in photochemistry and stated that the disappearance of the excited state in metallophthalocyanines depends on the solvent. They also observed that the decay of the excited phthalocyanine does not result in the formation of a radical in aprotic solvents. They also remarked that the redox potentials for oxidation and reduction of phthalocyanines show that radical formation must be slightly exoergonic in protic solvents and endoergonic in aprotic ones [77].

However, Petke et al. [97] observed different behaviours between CH_2Cl_2 and tetrahydrofuran (THF) in the study of the photochemical properties of magnesium porphine-porphine, MgP-P heterodimer although both solvents show nearly identical dipole moments and static dielectrical constants. The photodynamics in CH_2Cl_2 was consistent with the formation of longer-lived singlet charge transfer which decayed by two pathways, while in THF it had a short-lived singlet ($^1\pi,\pi^*$) state.

It has been shown that photobleaching is favoured by solvents which form radicals.[88]. Thus, the photobleaching of unsubstituted zinc phthalocyanine was found to increase in the following order: Pyridine < DMF < toluene < CH_2Cl_2 [88]. On the other hand, the photooxidation of lanthanide diphthalocyanine complexes in methanol-dichloromethane [48] and in acetonitrile-dichloromethane [90] solvent mixtures, needed the presence of CH_2Cl_2 to generate π radicals. Solvent effects in photochemical reactions are sometimes explained by the involvement of the same solvents in the photoreaction as is observed when dichloromethane quenched the photooxidation of monoporphyrins [78,79]. This means that the solvent is also excited to the low-lying triplet state where it exchanged electrons with porphyrins.

1.8.5 Photophysics of diphthalocyanine complexes

Photophysical radiationless transitions start from an excited state and terminate with the return of the molecule to its original state, the ground state [98]. The energy diagram which presents the energy levels and photophysical transitions is known as Jablonski diagram and it is illustrated in the Fig.1. 7. In this diagram, S_0 is the ground state, S_1 and S_2 are both excited singlet states

whereas T_1 and T_2 are the triplet excited states. Fluorescence occurs from the singlet excited state to the ground state while the phosphorescence is observed from the triplet state.

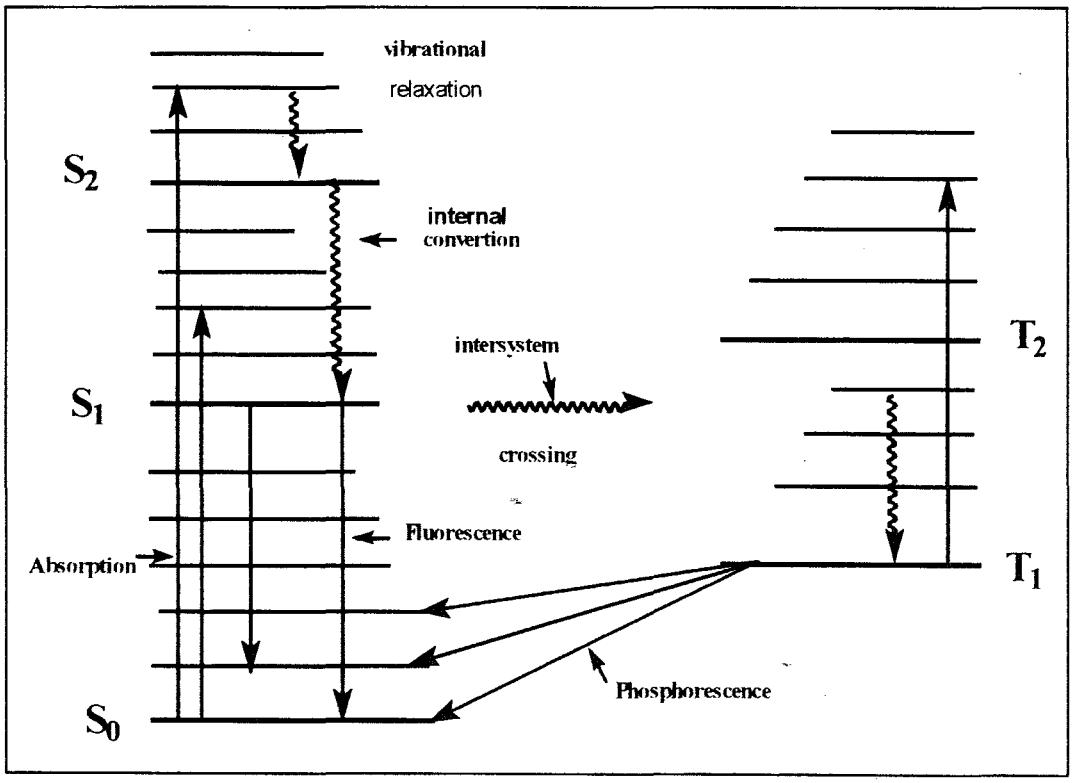

Fig. 1.7 Jablonski diagram

The lack of fluorescence in the stacking face-to-face dimers, could be interpreted as the lack of S_2 and S_1 emission because of large exciton coupling in dimers [99]. In other words, the lack of fluorescence in dimers could be attributed to a rapid relaxation time in the lowest excited singlet state [41]. In such systems, there should be a predominance of singlet-triplet, $S_1 \rightarrow T_n$,

intersystem crossing (isc) transition which is a consequence of a large separation between S_1 and S_0, making $S_1 \rightarrow S_0$ transition less probable [99,100].

Electron paramagnetic resonance (EPR) study on diphthalocyanine complexes shows that the excited state of dimers can be expressed in terms of an exciton state and charge resonance state [101]. The exciton state of the triplet state is characterized by a linear combination of the two locally excited states originally from monomers. Whereas, in the radical of lanthanide diphthalocyanines, the exciton is delocalized over the two rings [101].

Yan and co-worker [102], in the study of photophysics of cerium (IV)porphyrin sandwich complex, pointed out that photophysical behaviour of $Ce(OEP)_2$ shows ring-metal interactions which are absent in lanthanide diporphyrin complexes.

The lowest excited triplet state, T_1 of lanthanide diphthalocyanine complexes has been studied by Yamauchi et al [103] using the time resolved electron paramagnetic resonance technique and they showed that T_1 of $LuPc_2^-$ contained more than half of charge resonance character and the interplanar interactions were larger in lutetium diphthalocyanine compared to yttrium diphthalocyanine due the closeness of rings in $LuPc_2^-$.

1.8.6 Kinetic studies of photochemical processes

Photochemical reactions of diphthalocyanine complexes occur in the low-lying triplet state, $^3\pi\pi^*$ [99]. Diphthalocyanine complexes follow pseudo first-order kinetics [99] and form exciplexes with quenchers [90].

Kinetics of photolysis can be understood from the following scheme, which represents the ground state of lanthanide diphthalocyanine complex represented as A and where Q is the quencher:

$$A \xrightarrow{h\nu} A^* \qquad (1.11)$$

$$A^* + Q \rightarrow \text{Products (slow)} \qquad (1.12)$$

Scheme 1.2

Since these complexes do not fluoresce, the rate constant of the photoreaction corresponds to phosphorescence processes only and are related to quantum yields. Φ as follow:

$$\Phi = \frac{k_p [A^*]}{- I_0} \qquad (1.13)$$

Or

$$\Phi = \frac{k_p}{k_{ic} + k_{isc} + k_p} \qquad (1.14)$$

Where k_p, k_{IC} and k_{ISC} are the rate constants of phosphorescence, and the internal conversion and intercrossing systems respectively. I_0 is the intensity of incident light. The value of k_p can be determined from Equation 1.14 if other parameters are known.

The kinetic feasibility in quantitative mechanistic analyses of photochemical reactions was postulated in the following way: an excited molecule can acquire sufficient activation energy during its lifetime before being quenched [98]. Then, the lifetime of an activated complex is also related with the decay rate constant in the following manner:

$$k_p = \frac{1}{\tau} \qquad (1.15)$$

Where τ is the lifetime. Hence the relationship between the rate constant and the activation energy is expressed by the Arrhenius expression [98]:

$$k_p = A \exp\left(-\frac{E_a}{RT}\right) \qquad (1.16)$$

Where k_p is the decay rate constant, A the constant of activation and E_a is the activation energy. The combination of these two preceding equations give a new relationship between lifetime and energy:

$$\tau = \frac{1}{A \exp\left(-\frac{E_a}{RT}\right)} \qquad (1.17)$$

For the normal kinetics of metallophthalocyanine reactions, let us assume firstly that the amount of quencher is known and is in excess, then the complex follows pseudo first-order kinetics according to the Equation 1.18:

$$\log \frac{[A]}{[A]_0} = -\frac{k\,t}{2.303} \qquad (1.18)$$

The second assumption is that the reaction is second-order kinetics, and when concentrations of both reagents (A and Q) are equal, then the following relationship may be employed:

$$\frac{1}{[A]} - \frac{1}{[A]_0} = k\,t \qquad (1.19)$$

In this case, the value of rate constant could be obtained graphically plotting 1/[A] versus t as in second order kinetics.

In the particular case of reversible reactions of metallophthalocyanines such as:

$$(L)_2\,MPc \underset{k_{-1}}{\overset{k_1}{\leftrightarrow}} (L)MPc + L \qquad (1.20)$$

$$Y + (L)MPc \underset{k_{-2}}{\overset{k_2}{\leftrightarrow}} (L)MPc(Y) \qquad (1.21)$$

Scheme 1.3

In this case,

$$\frac{d\left[(L)_2MPc\right]}{dt} = -k_1\left[(L)_2MPc\right] + k_{-1}\left[(L)MPc\right]\left[L\right] \qquad (1.22)$$

After examination of the steady state approximation where the rate of the formation of intermediate is equal to the rate of its disappearance, the reaction rate is obtained after some mathematical analysis giving the following equation:

$$\text{Rate} = k_{obs}\left[L_2MPc\right] \qquad (1.23)$$

The observed rate constants, k_{obs}, are related to the concentration of the quencher [Y], as follows:

$$k_{obs} = k_f [Y] + k_r \qquad (1.24)$$

Where $k_f = k_1k_2/k_{-1}[L]$ is the rate constant of the forwards reaction while $k_r = k_{-2}$ is the rate constant of the reverse reaction. Thus, the linear plot of observed rate constant, k_{obs} versus the concentration of the quencher gives us the slope which is k_f and the intercept is k_r. In flash irradiation, k_f and k_r are known as the formation and decay rate constants, respectively [17].

Ohno and co-workers [99] observed that the lifetime of dimer phthalocyanines in the triplet state is slightly longer (8.9 ms) than for monomers (6.7 ms) at 77 K and that both exhibit first order decay. Whereas Yamauchi et al.[103] observed shorter lifetime of $LuPc_2^-$ (1.3 μs) in the triplet state compared to YPc_2^- (6.5 μs) and YPc^- (18.6 μs). On the other hand, Frink and co-workers [77] studied the dependence between the lifetime of the excited complex against the concentration of Si(Pc)$(OET)_2$, Al(Pc)Cl and the metal-free phthalocyanine, PcH_2 , in which shorter lifetimes of these complexes were observed at higher concentrations. This observation confirms the reciprocity between the concentration of reactants and the reaction time.

Typical rate constants of fluorescence of any organic compound vary from 10^7 to 10^9 s^{-1} whereas the rate constants in phosphorescence are smaller and vary from 10^{-1} to 10^{-4} s^{-1} [104]. Frink et al. [77] observed first-order rate constants for the decay of $^3\pi\pi^*$ in phthalocyanines varying from 3.5 to 9.8 x 10^{-3} s^{-1}.

The Stern-Volmer analysis of photochemical kinetics postulates that a reaction mechanism which involves a competition between an inherent unimolecular decay of the excited complex and

bimolecular quenching by Q depends on the rate constant of any photoreaction with the quencher [98].

1.8.7 Quantum yields of MPc_2 complexes

The quantum yield, Φ_x of a photochemical reaction is the ratio of number of moles of a given compound x, to the number of moles of photons absorbed, represented as follows:

$$\Phi_x = \frac{d[x]\ dt}{I_0} \qquad (1.25)$$

Where I_0 is the incident light of the energy required for a photoreaction [98]. Quantum yields vary from 0 to 10^6. Quantum yields less than 1 characterize deactivation.

Quantum yields of photochemical reactions could be calculated from Stern-Volmer plots of $1/\Phi$ versus 1/[Q] (where Q is the quencher) presented by the following equation [88]:

$$\frac{1}{\Phi} = \frac{1}{\Phi^0} + \frac{k_d}{\Phi^0 k_f}\frac{1}{[Q]} \qquad (1.26)$$

where k_d is the decay rate constant, k_f is the rate constant of the reaction between a quencher and phthalocyanine complex, and Φ and Φ^0 are quantum yields measured in the presence and absence of the quencher, respectively. The same equation may be used for fluorescence and phosphorescence.

The evaluation of photochemical rate constants could be done from the Stern-Volmer plots of Φ^0/Φ versus the concentration of quencher [q] [98]. The lifetime of a excited complex could also determined from this plot if k_f is known.

The quantum yields determined may provide information on the relative quantum yields for radical formation upon photoirradiation of lanthanide diphthalocyanines in acetonitrile-dichloromethane solvent mixture [90]. It has been shown that the relative quantum yields increase with the decrease of ionic radius of lanthanide (III) ion, hence the π-π interactions of the two ring systems must be stronger in the order of neodymium (III), yttrium (III) and lutetium (III). This might raise the energy level of HOMO orbital of the rings, and thus the oxidation of these complexes becomes easier in this order [90]. On the other hand, the relative quantum yields increase with the increase of the concentration of dichloromethane (quencher) when the concentration of PcNdPcH was kept constant [90]. Gasyna and co-workers [78] observed that the quantum yield was highly influenced by the radius and the nature of the metal involved in the tetraphenylporphyrin complexes, hence CuTPP had a quantum yield less than 10^{-4} while ZnTPP had Φ= 0.16 and MgTPP had Φ= 0.79.

1.8.8 Correlation between electrochemistry and photochemistry of MPc complexes

The relationship between these two areas could be explained by molecular orbital theory. It is said that oxidation either in photochemistry or electrochemistry is a process of removing an electron from HOMO and reduction is adding an electron to the LUMO [11]. Hence it is reasonable to expect a direct connection between experimental redox potentials and HOMO-

LUMO energy on one side, and the relationship between the light-energy conversion with the HOMO-LUMO energy on the other side.

Guyon and co-workers [15] related the HOMO-LUMO gap to the destabilisation of the HOMO and LUMO of H_2(2,3-Nc) (Nc=naphthalocyanine) [15]. Whereas, in photoelectrochemical processes, the conduction type which depends on the charge distribution in the porphyrin or phthalocyanine ligand is directly correlated with the HOMO valence band and LUMO conduction band positions [83]. Photoelectrochemical processes are employed in the photochemical treatments of conductive thin films of trivalent phthalocyanines used in the preparation of photovoltaic cells [85].

Meier et al [82], related both photochemistry and electrochemistry, associating the photoconductivity of zinc phthalocyanine with its chemical structure. They observed that the photoelectric sensitivity of the zinc phthalocyanine increases with the replacement of an octamethoxy group by octano group substituents [84].

Recently, in the description of the photoelectrochemical cells, Wöhrle et al. [105] showed that when a semiconducting material is brought into contact with an electrolyte and the equilibrium is established, the charge carriers in the interface will migrate from the phase of higher potential to the phase of lower potential.

1.9. Aim of the work

Metallophthalocyanines, MPc, are known to be inexpensive catalysts, that could replace platinum and other precious and expensive catalysts, for example in oxygen cathode fuel cells and in other reactions [106]. Phthalocyanine complexes are classified among the most promising class of catalysts because they present some advantages over metal oxides due to their low cost [106]. It has been shown that metallophthalocyanines are also promising as photocatalysts [106].

Although, a number of diphthalocyanine complexes have been synthetised and characterized, their photochemical reactivity has not been extensively studied. Photolysis of lanthanide diphthalocyanine in dichloromethane-acetonitrile solvent mixture [90] and in the presence of p-benzoquinone [48], resulted in ring oxidation of these species.

This work reports on the photocatalytic activities of tin diphthalocyanine, the blue form of neodymium, dysprosium, europium, thulium and lutetium diphtalocyanines. The photolysis of tin diphthalocyanine in CH_2Cl_2/CH_3CN solvent mixture is studied in this thesis. Photooxidation of monophthalocyanines in the presence of alkyl chloride compounds have been thoroughly studied [78-80].

This work presents the photochemical reactions of diphthalocyanine complexes with sulfur dioxide. It is well known that oxidation of sulfur dioxide to sulfur (VI) species is of current industrial and environmental interest. Shin et al. [107] showed that the oxo-bridged tetraphenylporphyrinatoiron(III) binuclear complex, $[(TPP)Fe]_2O$ was converted to the

corresponding sulfato-bridged iron(III) complex, $[(TPP)Fe]_2SO_4$ in the presence of sulfur dioxide and oxygen gas. There was no indication of porphyrin ring modification during the reaction. On the other hand, sulfur dioxide interacted reversibly with tetraphenylporphyrin cobalt(II), [(CoTPP)] to form an adduct, $[Co(TPP)]SO_2$ with no evidence of formation of SO_2^- [108]. Zagal [106] showed electrocatalytic activities of iron phthalocyanine, FePc and cobalt phthalocyanine, CoPc towards electrooxidation of SO_2, in acid-medium, which resulted in the coordination of SO_2 via the sulfur atom to the metal. On the other hand, Nyokong [86] reported on photoassisted electron transfer between SO_2 and tin (IV) phthalocyanines complexes, $SnPc(OH)_2$ and $SnPcCl_2$, and observed that SO_2 was coordinated to the metal during photolysis. This work presents the first study on the photocatalysed interaction between $LnPc_2$ or $SnPc_2$ and SO_2.

In a way of exploiting catalytic activities of diphthalocyanine complexes, we studied the photochemical reactions of lanthanide diphthalocyanine complexes with chlorinated phenols.
It has been shown that the contamination of drinking water and air by chlorinated phenols is an increasing problem for the industrialised world [109]. The detoxification and the elimination of chlorinated phenols in water and air is of interest among scientists. It has been shown that chlorinated phenols are among the top priority pollutants [109,110].

Pentachlorophenol (PCP) is a major industrial chemical and a general biocide used throughout the world. PCP contains many impurities which are more slowly degraded and some of them are more toxic than PCP [111], these include polychlorinated dibenzodioxins (PCDD) and dibenzofurans (PCDF) [112]. Once in the environment, chlorophenols can be transformed into more toxic compounds under the action of biodegradation [112]. Thus, photochemical

dechlorination has been suggested as an alternative method to biodegradation for the decomposition of PCP as in the case of polychlorinated biphenyls (PCB) [113].

Crosby et al. [114] attempted to degrade a highly concentrated solution of PCP in aqueous potassium bromide under irradiation for 46 hours. This resulted mainly in the formation of 3-bromo-2,4,5,6-tetrachlorophenol and 2,4,5,6-tetrachlororesorcinol (47 %) which were later converted to bromo-trichlorodihydroxybenzene (23 %). The use of iron tetrasulphophthalocyanine ($[FeTSPc]^{4-}$), as an enzyme-like catalysis in the presence of hydrogen peroxide for the oxidation of polychlorinated phenols was reported by Meunier and co-workers [115-117]. The oxidation of polychlorinated phenols in the presence of $[FeTSPc]^{4-}$ led to ring cleavage and dechlorination resulting in chloromaleic, chlorofumaric, maleic, and fumaric acids as products. The use of MPc_2 complexes for the photochemical degradation or dechlorination of chlorinated phenols has not been explored. In this work, the photolysis of PCP in the presence of lanthanide diphthalocyanines $[LnPc_2]^{-}$ is studied and a mechanism for the reaction is proposed.

Photodegradation of 4-chlorophenol (4-Cp) has been widely studied in the presence of catalysts such as titanium dioxide (TiO_2) [118] and polyoxometalates (POM) [109,110]. The successful mineralisation of 4-CP to CO_2 was reported in the presence of these catalysts via 4-chlorocatechol (4-CC), hydroquinone (HQ) and benzoquinone(BQ) as intermediates. It is important to note that the degradation was only reached under slurry condition of catalyst [118].

Gerdes et al. [119] observed that the photooxidation of phenol and monochlorophenols depends on the solution pH, hence at pH 7 the photooxidation of phenol in the presence of gallium

tetrasulphophthalocyanine($[GaTSPc]^{4-}$) resulted to p-benzoquinone as the final product. This work reports on the photochemical transformation of 4-chlorophenol in the presence of $LnPc_2^-$.

It is well documented that the lithium-thionyl chloride (Li / $SOCl_2$) battery has a higher energy density than any other electrochemical system known to date [120]. The general cell reaction involves the formation of sulfur, sulfur dioxide and lithium chloride as follows:

$$\mathbf{2\ SOCl_2 + 4\ Li \rightarrow S + SO_2 + 4\ LiCl} \qquad \mathbf{(1.27)}$$

This battery has shown tendency to explode under various conditions causing its discharge and it also corrodes easily due to the presence of intermediates such as S_2Cl_2, SCl_2, SO, SO_2, S_2O and SO_2Cl_2 [121].

Zagal [106] reported that metallophthalocyanines enhanced the rate of the reduction of thionyl chloride in Li / $SOCl_2$ cells, and avoids instant discharge hence these complexes prevent the passivation of the electrode by LiCl formed in the reaction. On the other hand, Lever and Bernstein [121] observed the two-electron reduction of $SOCl_2$ in the presence of cobalt tetraneopentoxy-phthalocyanine (CoTnPc) which resulted in the formation of sulfur and sulfur dioxide. Sulfur monoxide was the only intermediate observed. The two-electron reduction could result in a safer Li / $SOCl_2$ battery eliminating reactive intermediates such as $SOCl^-$ formed when $SOCl_2$ is reduced by one-electron.

This work explores the possible use of lanthanide diphthalocyanine complexes as cathodes in the lithium-thionyl chloride battery. Thus, the photochemical interaction between thionyl chloride and lanthanide diphthalocyanines are studied.

Apart from the study of catalytic properties of metallodiphthalocyanine complexes, the cyclic voltammetry of tin and lanthanide diphthalocyanines were also studied. The electrochemistry of tin diphthalocyanine presents particular interest hence it is examined in this work.

2. Experimental

2.1 Materials

2.1.1 Reagents

Lutetium (III) acetate hydrate, thulium (III) acetate hydrate, dysprosium (III) acetate hydrate, europium (III) acetate hydrate, and neodymium (III) acetate hydrate, are all 99,9% pure reagent, purchased from Aldrich and were used without further purification. These compounds were employed in syntheses of blue forms of neodymium, europium, dysprosium, thulium and lutetium diphthalocyanine complexes (represented as $LnPc_2^-$) which are the main chemicals in this work.

Na_2Pc (Aldrich), SO_2 gas (Messer Griesheim), hydroquinone (May and Baker Ltd) and phenol (BDH chemicals Ltd) were used without further purification. Other chemicals used in this work, 1,2-dicyanobenzene (98%), 4-chlorophenol (99%), 4-chlororesorcinol (99%), 1,4-benzoquinone, 2,4,5-trichlorophenol (99%) and pentachlorophenol (99%) were purchased from Aldrich and used as received. On the other hand, thionyl chloride (Riedel-de Haën) was bubbled with nitrogen for 3 hours before use as recommended [121]. Alumina, Al_2O_3 (Sigma) and the silica gel 60 PF_{254} (Merck) were used for preparative chromatography. Lanthanide and tin diphthalocyanine complexes were synthetised according to procedures discussed later in this work. Ferrocene (BDH) was recrystallized from ethanol before used as an internal standard for cyclic voltammetric studies in non-aqueous solvents.

2.1.2 Solvents

Solvents used such as dichloromethane (Saarchem), benzene (NT laboratory supplies Ltd), methanol, ethanol and acetonitrile from Saarchem were dried with calcium hydride or over P_2O_5 and distilled before use. The DMF (Associated chemical enterprises) was stirred in alumina (Al_2O_3) overnight and distilled [122]. After distillation these solvents were kept in a flask which contained molecular sieves (SAARCHEM,(PTY) Ltd) 3 Å beads approximately 3.2 mm. Dimethylsulfoxide (DMSO-d_6), (98%) (Merck), was used for NMR studies and was used as received. Nitrobenzene (Analar) was distilled under reduced pressure before use. The 1-chloronaphthalene was purchased from Fluka Chemika and was used as received. Millipore water was used for HPLC experiments for the photocatalytical transformation of 4-chlorophenol.

2.1.3 Preparation of electrolytes

2.1.3.1 Tetrabutylammonium perchlorate

Tetrabutylammonium perchlorate, TBAP, was prepared by mixing 50 ml of a hot aqueous solution of 1M tetrabuthylammonium chloride (Sigma) with 50 ml of hot aqueous solution of 1M $NaClO_4$ (BDH, reagent). The resulting mixture was cooled in ice, filtered and washed with ethanol. The crystals obtained were recrystallized from ethanol and used for electrochemical studies. TBAP yielded 85 %.

2.1.3.2 Tetraethylammonium perchlorate

The tetraethylammonium perchlorate, TEAP was prepared by mixing 50 ml of a hot aqueous solution of 1M tetraethylammonium bromide (Sigma) with 50 ml of a hot aqueous solution of 1M $NaClO_4$ (BDH, reagent). The solution obtained was cooled in ice, filtered and washed with cold ethanol. The crystals obtained were recrystallized from ethanol and used as electrolyte for electrochemical experiments in solvents such as CH_2Cl_2 and DMF. TEAP yielded 80 %.

2.1.4 Preparation of chemical actinometers for photochemical studies

2.1.4.1 Preparation of tetrathiocyanato diamine potassium chromate

Tetrathiocyanato (diamine) potassium chromate, $KCr(NH_3)_2(NCS)_4$ was used as chemical actinometer for photochemical studies and prepared according to the procedure reported by Wegner et al. [123]. This compound was prepared by dissolving (5.00g, $1.4x10^{-2}$ moles) the Reinecke's salt commercially available as tetrathiocyanato(diamine)ammoniumchromate monohydrate salt, $NH_4[Cr(NH_3)_2(NCS)_4].H_2O$ (Merck, reagent) in warm (40-50°C) water and followed by the addition of an excess (2.01g, $1.99x\ 10^{-2}$ moles) of solid potassium nitrate, KNO_3. The solution was then cooled and filtered. The product obtained was recrystallized from warm aqueous solution containing 10% of KNO_3, washed with cold water and finally dried over P_2O_5 in the vacuum desiccator to obtain the anhydrous product. The entire preparation was carried out in a dark room using red light and stored in a bottle covered with the alumina foil to avoid decomposition by light.

2.1.4.2 Preparation of potassium trioxalatoferrate

Potassium trioxalatoferrate trihydrate, $K_3Fe(C_2O_4)_3.3H_2O$ was used as chemical actinometer for photochemical studies and was prepared according to the procedure described elsewhere [124]. This compound was prepared by mixing a well stirred solution of 6 g of ferrous ammonium sulphate in 50 ml of warm water (acidified with 1ml of dilute sulphuric acid) with a solution of 5 g oxalic acid dihydrate in 50 ml water. The mixture was heated to boiling and a yellow precipitate of ferrous oxalate was formed. After decanting the clear liquid, the precipitate was added to a warm solution of 5 g of potassium oxalate ($K_2C_2O_4.H_2O$) in water. 20 ml of 20% by volume of hydrogen peroxide was then added to the mixture while keeping the temperature near 40 ° C. The resulting mixture was heated and the precipitate allowed to dissolve by adding 10 ml of 10 % of oxalic acid. The solution was filtered hot and ethanol was added to redissolve the precipitate. The solution was kept in a dark cupboard overnight to crystallise. Finally, the precipitate was washed successively with 1:1 ethanol-water mixture and acetone.

2.2 Instrumentation

The electronic absorption spectra were recorded with a Cary 1E UV-Vis spectrophotometer. Whereas the infra-red spectra (KBr discs) were collected with a Perkin-Elmer Fourier Transform Infrared (FT-IR) spectrometer spectrum 2000. NMR data were collected with Bruker 400 MHz AMX, NMR spectrometer. The product formed upon radiation of pentachlorophenol, PCP, in the presence of lanthanide diphthalocyanine complexes was monitored with the HP 8310 Gas chromatograph fitted with an electron-capture detector and a supelco SPB fused silica capillary

column (15 cm length, 0.53 mm inner diameter and 1.5 μm film thickness). The parameters for gas chromatographic analyses were: carrier N_2 gas at 38.7 cm s^{-1}, injection temperature = 300 °C, and detection temperature =280 °C. High performance liquid chromatography (HPLC) technique was used to monitor the product formation and detection of intermediates during the photocatalytic reaction involving 4-chlorophenol. The Spectra-Physics HPLC apparatus, Spectra Series P100 equipped with an analytical column, μ Bondapak C18 (390 x 3.00 mm) and connected with a UV/Vis detector (set at λ=280 nm) was employed. A Perkin-Elmer 561 chart recorder was connected to the HPLC apparatus. The Jenway 3015 pH-meter was used to monitor the pH changes of aqueous solution of 4-chlorophenol throughout the photolysis. Electrochemical data were collected with the BioAnalytical systems (BAS) model CV -50 W voltammetric analyser and all the electrochemical experiments were carried out under an atmosphere of purified nitrogen. Spectroelectrochemical experiments were carried out with a BAS mode CV-27W voltammetric analyser. Irradiations of samples for photochemical experiments were performed with a tungsten lamp 50 W, while a general electrical quartzline lamp of 220 watts was used for the photocatalytical transformation of 4-Cp.

2.3 Methods

2.3.1 Electrochemical Methods

2.3.1.1 Cyclic voltammetry

For the determination of redox potentials for MPc_2 complexes, a three electrode cell containing solutions of MPc_2 in DMF or CH_2Cl_2 was employed. Nitrogen was bubbled before and throughout the experiment. For CV and differential pulse voltammetry (DPV), in non-aqueous solvents, a platinum disk (1.6 mm diameter) was used as a working electrode, a silver wire coated with silver chloride was used as a quasi-reference electrode, and a platinum wire as an auxiliary electrode. TEAP and TBAP (0.03-0.1 mol dm^{-3}) were used as electrolytes for electrochemical studies in DMF and CH_2Cl_2, respectively. Ferrocene was used as internal standard, hence the potentials were internally referenced to the ferrocenium/ferrocene (Fc^+/Fc) couple. It has been reported that Fc^+/Fc couple has potentials of 0.46 V [66] and 0.47 V [59] versus standard calomel electrode (SCE) in DMF and CH_2Cl_2, respectively. Thus, the potentials determined can be referenced to SCE using the following equations:

$$E_{1/2}(\text{vs } Fc^+/Fc) = E_{1/2}(\text{vs Ag wire}) - E_{1/2}(Fc^+/Fc)(\text{vs Ag wire}) \quad (2.1)$$

$$E_{1/2} \text{ vs SCE} = E_{1/2}(\text{vs } Fc^+/Fc) + E_{1/2}(Fc^+/Fc)\ (\text{vs SCE}) \quad (2.2)$$

2.3.1.2 Bulk electrolysis

For the characterization of MPc_2 species formed following the oxidation or reduction of these complexes, bulk electrolysis was carried using a two-compartment three electrode cell. One compartment contained a solution of MPc_2 ($1x10^{-5}$ mol dm^{-3}), a platinum sheet (1.6x1.4 cm) working electrode and a silver wire coated with silver chloride as pseudo reference. A platinum sheet (1.3x1.1 cm) counter electrode was housed in the other compartment [125]. At the end of the electrolysis of the species of interest, the absorption spectra were recorded with a Cary 1E UV-VIS spectrophotometer. The total charge was used to calculate the number of electrons transferred by means of Faraday 's law:

$$\mathbf{Q = nvFc} \qquad \mathbf{(2.3)}$$

Where

Q = electrical charge, in coulombs (C)

F = Faraday's constant, in coulombs /mole ($C.mol^{-1}$)

n = number of electrons transferred per mole ion

v = volume of the solution in cell (dm^3)

c = concentration of the solution (mol dm^{-3})

2.3.2 Photochemical methods

2.3.2.1 Photocatalytic reactions

2.3.2.1.1 Interactions of diphthalocyanine complexes with CH_2Cl_2 and SO_2

Solutions of $SnPc_2$ or $LnPc_2^-$ in dichloromethane were added to a 1 cm pathlength UV/vis cell (fitted with a stopper) and were degassed. Sulfur dioxide was dissolved in dichloromethane and allowed to equilibrate, and a known volume of the SO_2 solution or acetonitrile (or DMF for studies involving $LnPc_2^-$) was then added to the cell and the solution degassed again. The solutions were then irradiated with a 50 Watt tungsten lamp, a 590 nm filter was used for irradiations into the Q bands region. Changes in the concentration of the $SnPc_2$ with the photolysis time were monitored spectrophotochemically. For the photoreactions involving tin diphthalocyanine and CH_2Cl_2, the amounts of CH_2Cl_2 in the solvent mixture CH_2Cl_2/CH_3CN ranged from 70 to 95 %.

The concentration of SO_2 dissolved in dichloromethane was determined by titration of SO_2 with an excess of iodine 0.05 M I_2 solution according to the following reaction [126]:

$$SO_2 + I_2 + H_2O \rightleftarrows SO_4^{2-} + 2H^+ + 2I^- \qquad (2.4)$$

The unreacted amount of I_2 was determined by titrating the solution with 0.1N of sodium thiosulphate $Na_2S_2O_3$ as follows:

$$I_2 + 2\,S_2O_3^{2-} \rightleftarrows S_4O_6^{2-} + 2\,I^- \qquad (2.5)$$

or

$$2\,S_2O_3^{2-} + I_3^- \rightleftarrows S_4O_6^{2-} + 3\,I^- \qquad (2.6)$$

During the titration, the colourless intermediate $S_2O_3I^-$ was formed by a rapid reversible reaction:

$$S_2O_3^{2-} + I_2 \rightleftarrows S_2O_3I^- + I^- \qquad (2.7)$$

The intermediate reacts with the thiosulphate ion to provide the overall reaction:

$$S_2O_3I^- + S_2O_3^{2-} \rightleftarrows S_4O_6^{2-} + I^- \qquad (2.8)$$

The same intermediate also reacts with iodine ion from a parallel reaction as follows:

$$2\,S_2O_3I^- + I^- \rightleftarrows S_4O_6^{2-} + I_3^- \qquad (2.9)$$

The above reaction explains the reappearance of iodine after the end-point in the titration of very diluted solutions of I_2 by thiosulphate ion.

The concentration of unreacted I_2 was determined as shown in reaction 2.5, the concentration of I_2 involved in the reaction is the difference between the initial concentration of I_2 and the concentration of unreacted I_2. The number of moles and the concentrations of SO_2 were calculated from the stoichiometric relation in the reaction 2.4, once the concentration of I_2 is known. In the

photochemical experiments, solutions of SO_2 with concentrations ranging from $1.0x10^{-5}$ to $1.0x10^{-2}$ mol dm^{-3} were used.

2.3.2.1.2 Interactions of lanthanide diphthalocyanines with PCP

Solutions to be photolysed were contained in a 1cm pathlength UV-vis cell fitted with a stopper. Acetonitrile solutions of $[LnPc_2]^-$ contained in the cell were degassed, then known amounts of PCP dissolved in acetonitrile were added to the cell and the solution deoxygenated. The electronic absorption spectra were recorded before photolysis and periodically during the photolysis with the 50 watt tungsten lamp. Photolysis in the visible region was achieved by using a 590 nm filter to exclude the UV radiation. Extinction coefficients for $Pc(-2)Lu^{III}Pc(-1)$, and $Pc(-2)Dy^{III}Pc(-1)$ were found to be $2x10^5$ and $1.8x10^5$ dm^3 mol^{-1} cm^{-1} [49] respectively, and were used in estimating the concentration of these species in solution. Concentrations of $[LnPc_2]^-$ were in the range $2x\ 10^{-6}$-$1x10^{-5}$ mol dm^{-3}, whereas concentrations of PCP were varied from $4x10^{-5}$ to $5x10^{-4}$ mol dm^{-3}. The light intensity at 600 nm was determined, using Reinecke's salt actinometer to be $1.1\ x10^{-8}$ einstein s^{-1}, as shown below.

Products formed upon irradiation of $[LnPc_2]^-$ species in the presence of PCP were also monitored with HP 8310 gas chromatograph described in section 2.2.

2.3.2.1.3 Photocatalytic transformation of 4-Cp

For the formation of products (or intermediates) and kinetic studies, a glass photoreactor (Fig. 2.1) of 40 ml of capacity was used. The reactor had three ports used for monitoring pH, sampling and introducing oxygen.

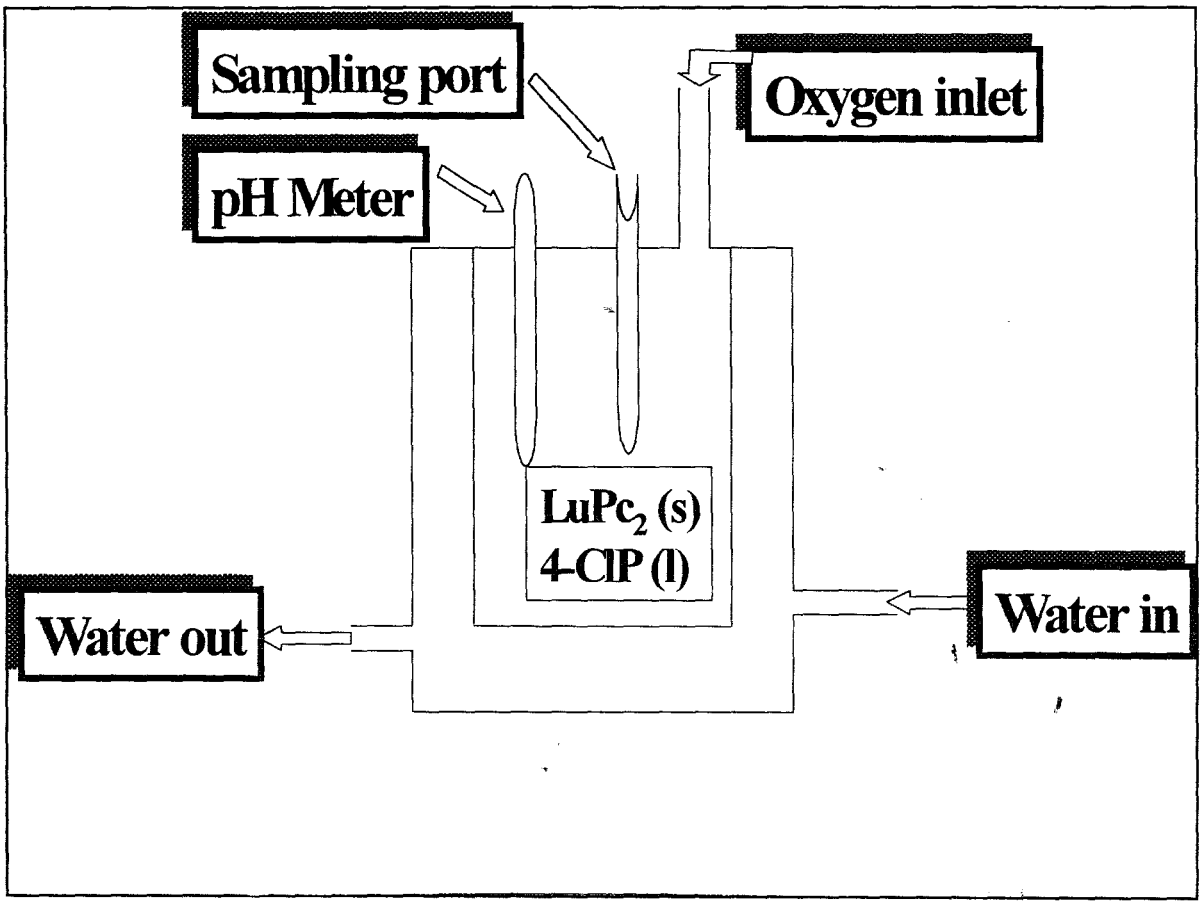

Fig. 2.1 Photoreactor

The reactor was surrounded by a water jacket to keep the contents cool. Aqueous solutions of 4-chlorophenol ($2x10^{-6}$-$1.5x10^{-5}$ mol dm^{-3}) containing known amounts of solid [Pc(-2)Nd^{III} Pc(-2)]$^{-}$ (0.028 mg/ml) were added to the reactor and the solution was saturated with oxygen. The reaction mixture was illuminated with the General Electric Quartzline lamp (220 W), and was stirred using a magnetic stirrer throughout the photolysis. Experiments were performed by using a filter (λ>590 nm) to prevent direct excitation of 4-chlorophenol, whereas some experiments were performed without a filter. After allowing the reaction to proceed for known time, the photolysis was stopped periodically and the sample of the solution was taken for HPLC measurements. The reactor ports were tightly closed during the photolysis. Sampling was done as quick as possible and an amount of 100 µl was taken each time for analyses.

Kinetics studies were performed by monitoring changes in absorbance of 4-chlorophenol by using HPLC technique, using the spectra-Physics HPLC apparatus described in section 2.2. The photolysed solution was filtered to avoid particles of neodymium diphthalocyanine affecting the detector performance. 4-chlorophenol peak was detected within 17 minutes using a mobile phase, comprising a 70:30 mixture of methanol and Millipore water which was flowing at a rate of 1cm ^{3} min^{-1}.

2.3.2.1.4 Interactions between lanthanide diphthalocyanines and $SOCl_2$

Solutions to be photolysed were contained in 1 cm pathlength UV/Visible cell fitted with a stopper. Solutions of the blue, [Pc(-2)Ln^{III}Pc(-2)]$^{-}$, complex dissolved in acetonitrile or a mixture of acetonitrile and DMF were degassed, then known amounts of thionyl chloride in the same

solvent (or solvent mixture) were added to the cell and the solution deoxygenated. The electronic spectra were recorded (Cary 1E spectrophotometer) before photolysis and periodically during the photolysis with a 50 W tungsten lamp. For some experiments photolysis was carried out in the visible region by using a 590 nm filter to exclude the UV radiation. The $Pc(-2)Ln^{III}Pc(-1)$ were also photolysed in the presence of $SOCl_2$ as described for the blue $[Pc(-2)Ln^{III}Pc(-2)]^-$ species. Concentrations of lanthanide diphthalocyanine complexes were in the range of $1x\ 10^{-6}$ to $1x10^{-5}$ mol dm^{-3}, whereas concentrations of thionyl chloride were varied from 1.0×10^{-6} to 0.1 mol dm^{-3} depending on the type of experiment. The light intensity was determined using Reinecke's salt actinometry as described earlier.

2.3.2.2 Determination of light intensity, I_0

2.3.2.2.1 Reinecke's salt Actinometry

This actinometer was used for the determination of I_0 at $\lambda > 600$ nm, where there is strong absorbance by MPc_2 complexes. The light intensity incident on the sample during the irradiation was determined using chemical actinometry with aqueous $KCr(NH_3)_2(NSC)_4$ obtained by dissolving $1.4x10^{-2}$ moles of Reinecke's salt, $(NH_4)Cr(NH_3)_2(NCS)_4.H_2O$ in a warm aqueous solution containing an excess ($1.99x10^{-2}$ moles) of KNO_3 as described in section 2.1.4.

The aqueous solution of potassium salt, $KCr(NH_3)_2(NCS)_4$ shows an absorption maximum at 520 nm. In this work, the solution of 0.050M of potassium salt was used since this concentration allows 99% of the incident radiation to be absorbed in the wavelength region of 600-700 nm

[123]. Diphthalocyanine complexes absorb strongly between 600 and 700 nm, justifying the choice of the $KCr(NH_3)_2(NCS)_4$ as an appropriate chemical actinometer.

When $KCr(NH_3)_2(NCS)_4$ is photolysed, the thiocyanate ion (NCS^-) is released. The NCS^- can be complexed to form iron thiocyanate ($Fe(III)(NCS)_3$) by adding iron nitrate ($Fe(NO_3)_3$) and hypochloric acid to the photolysed solution. The iron thiocyanate complex has an absorption maximum at 450 nm with an extinction coefficient of 4.30×10^3 dm ^{3} mol $^{-1}$ cm $^{-1}$. The absorbance of $Fe(III)(NCS)_3$ at this wavelength gives the concentration of free thiocyanate ion.

The determination of free thiocyanate ion, NCS^- was performed in the following manner: 3ml of aqueous solution of $KCr(NH_3)_2(NCS)_4$ was added to 1cm path length spectrophotometric cell, followed by the photolysis with a 50 W tungsten lamp, a glass filter (590 nm) was used to cut off shorter wavelength radiation.

Afterwards, 1ml of photolysed solution of $KCr(NH_3)_2(NCS)_4$ was diluted with 4 ml of 0.1M $Fe(NO_3)_3.9H_2O$ in 0.5 M $HClO_4$. the resulting solution was photolysed and its absorbance was recorded with time. The increase in absorbance band at 450 nm reflected an increasing concentration of the iron thiocyanate. The changes in absorbance (ΔA) at 450 nm, between the non-photolysed and the photolysed sample are plotted against the photolysis time in seconds (Fig. 2.2) and the slope was determined. The number of moles of NCS^- (per second of irradiation) was calculated as shown in Equation 2.10.

$$\text{Moles of } NSC^- / \text{sec} = \frac{V_1 V_3 \dfrac{\Delta A}{\text{sec}}}{1000\, \varepsilon\, l\, V_2} \qquad (2.10)$$

Where V_1 (ml) is the volume of $KCr(NH_3)_2(NCS)_4$ solution irradiated, V_2 (ml) is the sample of the photolysed solution to be complexed to $Fe(III)(NCS^-)_3$, V_3 (ml) the total volume after dilution of V_2 with 0.1 M $Fe(NO_3)_3.9H_2O$ in 0.5 M $HClO_4$, l is the path length of the spectrophotometric cell, ε is the molar extinction coefficient of the iron thiocyanate complex and ΔA/ sec represents the slope of the plot of ΔA versus the photolysis time. The whole preparation and the mixing of chemical solutions was done in the dark room with red light.

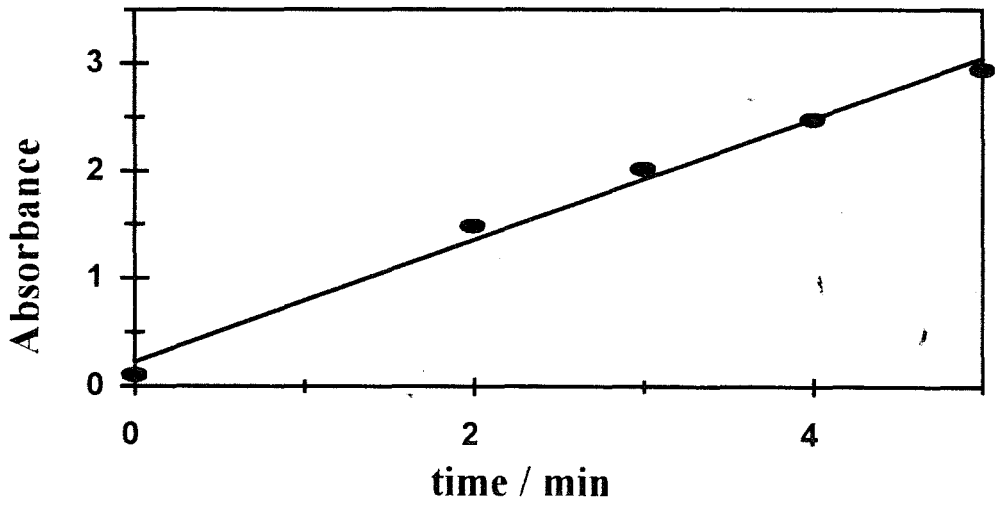

Fig. 2.2 Changes in absorbance of the photolysed iron thiocyanate sample versus time at 450nm.

The number of moles of photoreleased thiocyanate ion divided by the quantum yield given for $KCr(NH_3)_2(NCS)_4$ gives the incident light intensity (I_0) in Einstein per second as follows:

$$I_0/sec = \frac{\text{Moles of } NCS^- \text{ sec}}{\text{Quantum yields of } NCS^-} \qquad (2.11)$$

In our experimental conditions, the light intensity was determined at 600 nm and was found to be $I_0 = 1.1 \times 10^{-8}$ einstein / sec and used for PCP, SO_2 and $SOCl_2$ interactions with diphthalocyanine complexes.

2.3.2.2.2 Ferrioxalate Actinometry

This actinometer was used for the determination of I_0 in the UV region where 4-chlorophenol absorbs. The light intensity of the Quartzline lamp used for the photochemical transformation of 4-chlorophenol in the presence of solid lanthanide diphthalocyanine was determined using ferrioxalate actinometry. For the determination of the light intensity incident on the sample, aqueous solutions of 8.1×10^{-5} mol dm^{-3} $K_3Fe(C_2O_4)_3.3H_2O$ were prepared.

Upon photolysis of $K_3Fe(C_2O_4)_3.3H_2O$, the ferrous ion was released according to the scheme established by Parker and Hatchard [127]. According to these authors, the dissociation of the excited complex occurs as follows:

$$Fe^{2+}(C_2O_4)^- \rightarrow Fe^{2+} + (C_2O_4)^- \quad (2.12)$$

and this is followed by reaction between the oxalate radical with ferric oxalate ion:

$$(C_2O_4)^- + Fe^{3+}(C_2O_4)^{2-} \rightarrow 2CO_2 + Fe^{2+} + (C_2O_4)^{2-} \quad (2.13)$$

$$2\,(C_2O_4)^- \rightarrow 2CO_2 + (C_2O_4)^{2-} \quad (2.14)$$

Under normal conditions, the oxalate radical should be consumed as shown in the Equation 2.13. But, when the solution is exposed to a very high light intensity and low ferrioxalate concentration, the interaction between them is reflected in Equation 2.14.

For the determination of incident light intensity, we consider the slow reaction (Equation 2.13) where the radical reacts with an excess of ferrioxalate ion. The instantaneous decrease in absorbance which occurs during the photolysis corresponds to the dissociation of an initial amount of one ferrioxalate ion and followed by a slow decrease in absorbance as shown in Fig. 2.3.

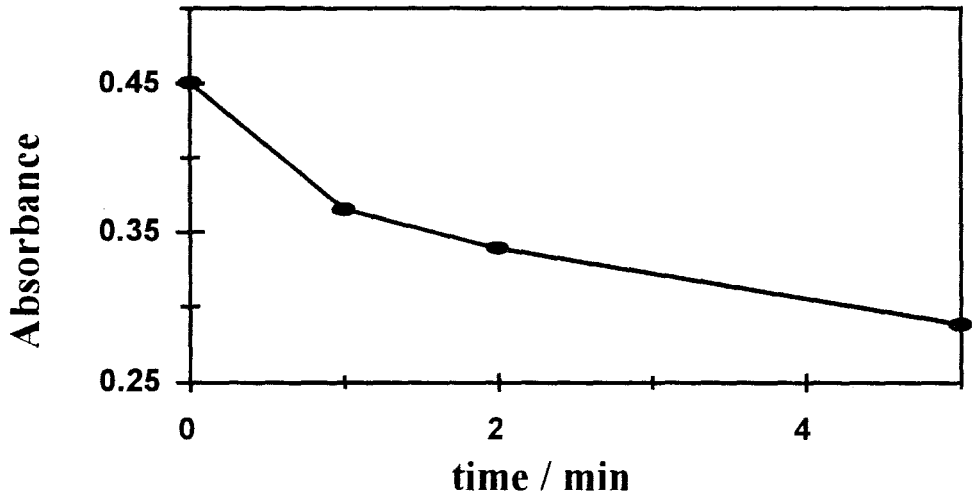

Fig. 2.3 Changes in absorbance during the photolysis of a solution of potassium ferrioxalate.

According to the Equation 2.13, the dissociation of one mole of ferrioxalate ion corresponds to the formation of one mole of ferrous ion. Then, the number of moles of ferrous ion produced is determined according to Equation 2.15 which is similar to Equation 2.10.

$$n_{Fe^{2+}} / sec = \frac{V_1 V_3 \frac{\Delta A}{sec}}{1000 \varepsilon l V_2} \qquad (2.15)$$

The symbols are as described under Equation 2.10.

The number of moles of the photoreleased Fe^{2+} divided by the quantum yield for this species [123] gives the incident light intensity (I_0) in einstein per unit time.

$$I_0 = \frac{n_{Fe^{2+}} \text{ sec}}{\Phi_{Fe^{2+}}} \qquad (2.16)$$

The value of incident light intensity determined at 280 nm where 4-chlorophenol absorbs strongly is equal to 2.0×10^{-7} einstein per second in the 40 ml photoreactor with a quartzline lamp of 220 watts by using unfiltered radiation. For unfiltered radiation in 1 cm UV/vis cell with a 50 W tungsten lamp, I_0 was found to be 2.0×10^{-9} einstein per second. This I_0 value was used for the calculation of quantum yields for the reactions of SO_2 and CH_2Cl_2 using $SnPc_2$ as sensitizer.

2.4 Syntheses

2.4.1 Synthesis of $SnPcCl_2$

The dichloro(phthalocyanato) tin (IV) complex, $SnPcCl_2$ was prepared according to the literature [3-5], by mixing 28 mmol of tin chloride, $SnCl_2$ with 86 mmol of 1,2- dicyanobenzene and added to 15 ml of 1-chloronaphthalene. The solution was then refluxed for 4 hours. The solution was filtered and the solid complex was washed with benzene using Soxhlet extraction, for 24 hours. $SnPcCl_2$ obtained was purified by Soxhlet extraction into 1-chloronaphthalene. The solid obtained was washed with benzene and dried at approximately 100°C. The yield obtained was 51

%. $SnPcCl_2$: IR (KBr disc): ν (Sn-Cl) 295 cm^{-1}. UV/Vis in pyridine: λ_{max} (log ε) = 696 (5.0), 664 (4.2), 626 (4.3), 336 (4.6) nm.

2.4.2 Synthesis of tin diphthalocyanine, $SnPc_2$

Tin diphthalocyanine, $SnPc_2$, was prepared according to the method of Ohno et al. [41]. A well ground mixture of dichloro(phthalocyanato) tin (IV), $SnPcCl_2$ (0.74 g, 1.05 mmol) and Na_2Pc (0.70 g , 1.25 m mol) (Aldrich) in a ratio of 1:1.2 was placed in a dry flask and dried for 3 hours at 110°C. To this flask, 30 ml of 1-chloronaphthalene was added, and the mixture was refluxed for 90 min under nitrogen atmosphere. By vacuum distillation, the 1-chloronaphthalene was separated from the solid. The solid was Soxhlet extracted with benzene. The extracted sample was loaded onto an alumina column (Sigma) and eluted with benzene. The benzene was removed by rotary evaporation, and the $SnPc_2$ crystals were dried at 80°C and yielded 12%. The synthesis of tin diphthalocyanine is summarized by Scheme 2.1.

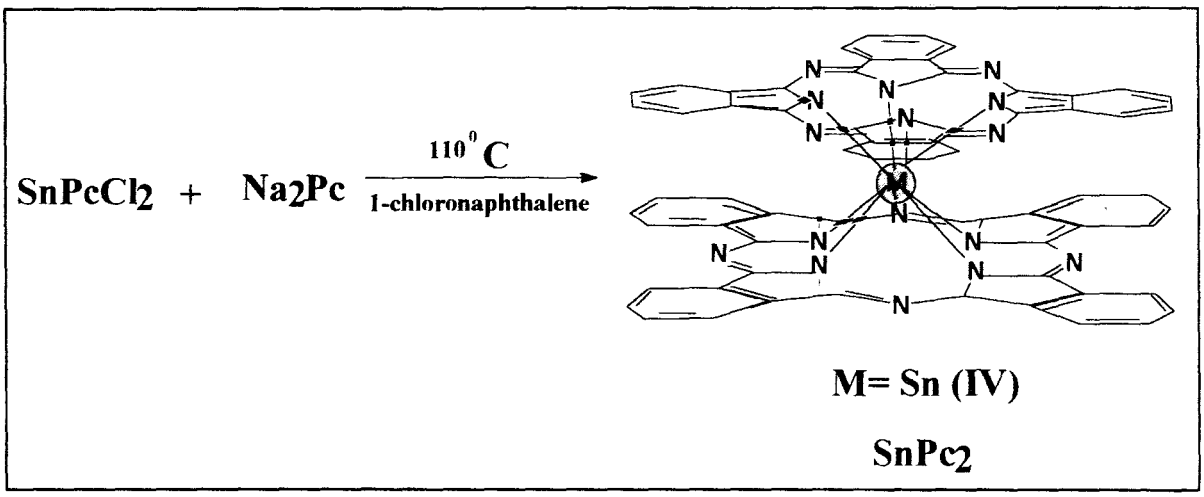

Scheme 2.1

$SnPc_2$: UV/Visible in CH_2Cl_2: λ_{max} (log ε) = 337 (5.08), 568 (4.50), 624 (5.00), 779 (4.60) nm.

2.4.3 Lutetium diphthalocyanine, $LuPc_2$

Lutetium diphthalocyanine was synthetised by the method of Daniels et al.[8], by mixing lutetium acetate, $Lu(Ac)_3 3H_2O$ (Aldrich) (0.2 g, 0.57 mmol) with 1,2- dicyanobenzene (0.65 g, 5.1 mmol) in a mole ratio of 1:9. The mixture was heated at 200°C for 3 hours in crucible with a lid. After cooling the mixture, the solidified mixture was ground to a powder, then Soxhlet extracted with 100 cm^3 of dried DMF for 2 hours. The entire DMF extract was purified using a column of silica (silica gel F_{254}, E. Merck). The column was developed with 20 cm^3 of dried methanol and then the elution continued with DMF. Fractions of 25 cm^3 were collected with the entire blue-

greenish band. A second chromatographic purification was applied to these fractions. After collection, only those fractions in which the ratio A_{624}/A_{312} less than 1.4 were retained. The blue complex, $LuPc_2^-$, was obtained after rotary evaporation. A yield less than 10% was obtained as expected [9]. Other complexes, neodymium, europium, dysprosium and thulium diphthalocyanines were prepared in a similar manner .The synthesis of these complexes is illustrated by Scheme 2.2. When the blue lanthanide diphthalocyanine complexes are dissolved in dichloromethane or chloroform, the colour goes from blue to green. Thus the green lanthanide diphthalocyanine species is formed. The characterization of the lanthanide diphthalocyanine complexes is discussed in the chapter 3.

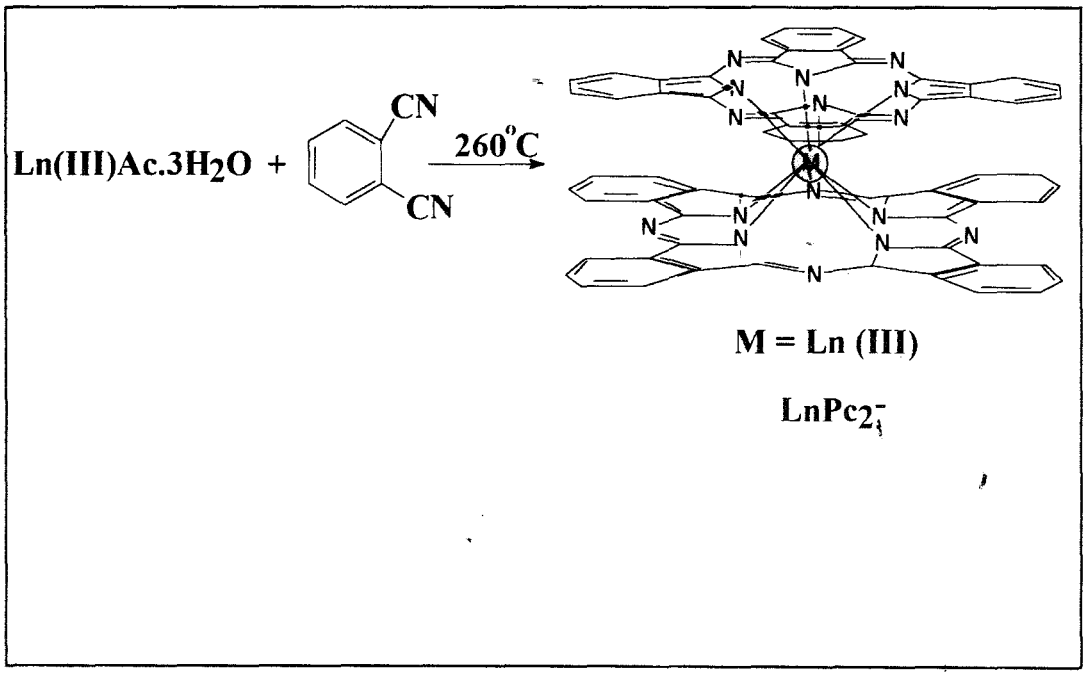

Scheme 2.2

3. Characterization

3.1 General considerations

The blue form of lanthanide diphthalocyanine complexes, $[LnPc_2]^-$ and tin diphthalocyanine, $SnPc_2$ have two dianionic Pc rings, Pc (-2), bound to central lanthanide and tin metal ions, respectively. The two Pc rings are neither perfectly planar nor parallel to one another, but rather parts of each ring system bend away from the other [128] as discussed in the introductory chapter.

Synthetic methods developed for these complexes give very poor yields and their contamination by monomeric and triple decker phthalocyanines have been reported [8,129]. The contamination by unreacted phthalonitrile has also been reported, and both phthalonitrile and diphthalocyanines are eluted simultaneously during column chromatography [32]. On the other hand, Clarisse et al. [36] pointed out that temperature and reaction times are the most important parameters in the synthesis of lanthanide diphthalocyanine complexes, since $LuPc_2$ is obtained as a by-product to the free phthalocyanine (H_2Pc) at 310 ° C and as the main product at 300 ° C.

The characterization of lanthanide and tin diphthalocyanine complexes have been extensively reported using UV/Visible [30,31,41], infra-red [4,5,32], and NMR [28,129] spectroscopies.

3.2 Spectroscopic methods

3.2.1 UV/ Visible Spectroscopy

The electronic spectra of the blue forms of lanthanide and tin diphthalocyanine complexes have a pronounced split Q band structure [9,41]. This splitting is due to the exciton coupling interaction in diphthalocyanine complexes. Increase of intensity of the Soret band [41] is also associated with the exciton coupling.

Thus, blue forms of lanthanide diphthalocyanine complexes absorb strongly in the visible region (Q band) and near-ultraviolet (B or Soret band). These compounds have similar structure and electronic absorption spectra with the bacteriochlorophyll dimeric complexes [44,130,131]. Fig. 3.1 shows the electronic absorption spectra of the blue form of lutetium ($[LuPc_2]^-$) and tin diphthalocyanines ($SnPc_2$). Both electronic spectra show two absorption bands in the visible region and one absorption band in the Soret region in DMF. The splitting of the Q band of tin diphthalocyanine (152 nm) is larger than the one observed in lutetium diphthalocyanine (76nm). This could be explained in terms of higher exciton coupling interaction between phthalocyanine rings of tin diphthalocyanine. The electronic spectra of tin diphthalocyanine obtained is similar to the one reported by Ohno et al. [41]. The electronic spectra of lutetium and other lanthanide diphthalocyanine complexes observed were also reported by Daniels et al. [8,9].

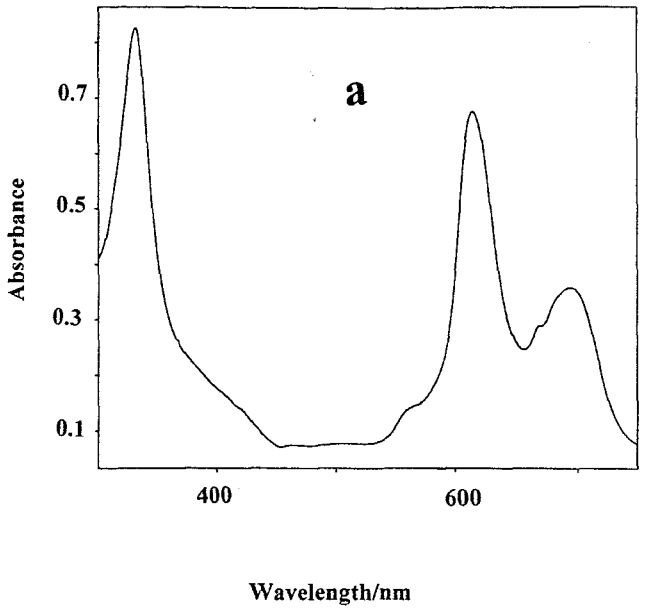

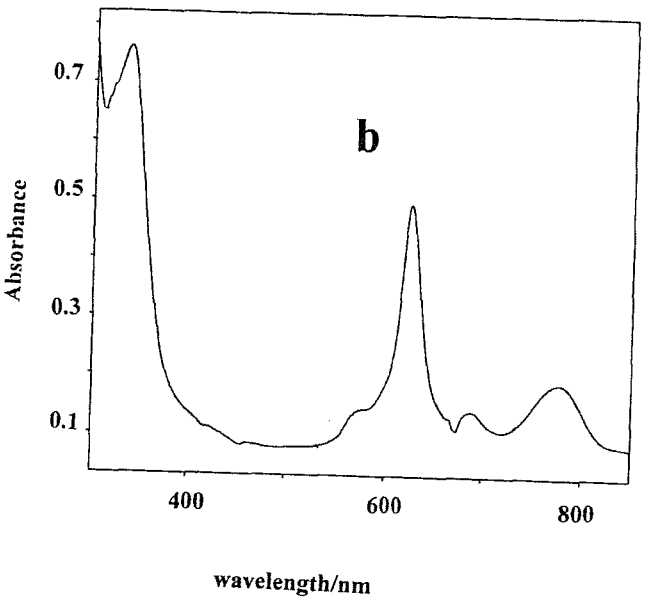

Fig. 3.1 Electronic absorption spectra of [Pc(-2)Lu^{III}Pc(-2)]$^{-}$ (a) and [Pc(-2)Sn ^{IV}Pc(-2)] (b) in DMF.

Table 3.1 gives wavelengths of the electronic absorption bands observed for lanthanide and tin diphthalocyanine complexes in DMF.

Table 3.1 Absorption bands of lanthanide and tin diphthalocyanine complexes in DMF.

Complex	B band (nm)	log (ε)	Q_1 band (nm)	log (ε)	Q_2 band (nm)	log (ε)
$SnPc_2$	334	5.25	625	5.07	777	4.65
$NdPc_2^-$	333	5.22	632	5.18	668	5.01
$EuPc_2^-$	334	5.18	625	5.15	670	4.97
$DyPc_2^-$	333	5.23	620	5.15	669	5.0
$TmPc_2^-$	332	5.27	618	5.16	684	4.9
$LuPc_2^-$	332	5.30	615	5.18	691	5.05

Table 3.1 shows that the Q_1 band of the different lanthanide diphthalocyanine complexes shifts to shorter wavelengths with the decrease of ionic radii of lanthanide metals as observed by Kasuga et al. [34]. Thus, changes in the Q_1 band positions of lanthanide diphthalocyanine complexes show a straight line with the inverse of the tervalent ionic radii [132] of lanthanide metals as illustrated in Fig. 3.2. This relationship is explained by the fact that the distance between Pc rings in a diphthalocyanine complex is shortened by the decrease of the ionic radii of the central metal, resulting to higher π-π interactions. Extinction coefficient of the green species are Pc(-2)Nd(III)Pc(-1), Pc(-2)Dy(III)Pc(-1), Pc(-2)Eu(III)Pc(-1), Pc(-2)Tm(III)Pc(-1) and Pc(-2)Lu(III)Pc(-1), $\varepsilon = 2.0 \times 10^5$, 1.8×10^5, 1.8×10^5, 1.9×10^5 and 2.0×10^5 $dm^3\ mol^{-1}\ cm^{-1}$, respectively [49,67]. Whereas the extinction coefficients of the blue forms [Pc(-2)Nd(III)Pc(-2)]$^-$, [Pc(-2)Dy(III)Pc(-2)]$^-$, [Pc(-2)Eu(III)Pc(-2)]$^-$, [Pc(-2)Tm(III)Pc(-2)]$^-$ and [Pc(-

2)Lu(III)Pc(-2)]$^-$ were found to be 1.5 x10^5, 1.35x10^5, 1.35x10^5, 1.4x10^5 and 1.5 x10^5 dm^3 mol^{-1} cm^{-1}, respectively. The extinction coefficient of $SnPc_2$ (ε = 117000 dm^3 mol^{-1} cm^{-1}) [133] is at same range with the extinction coefficients of blue forms of lanthanide diphthalocyanine.

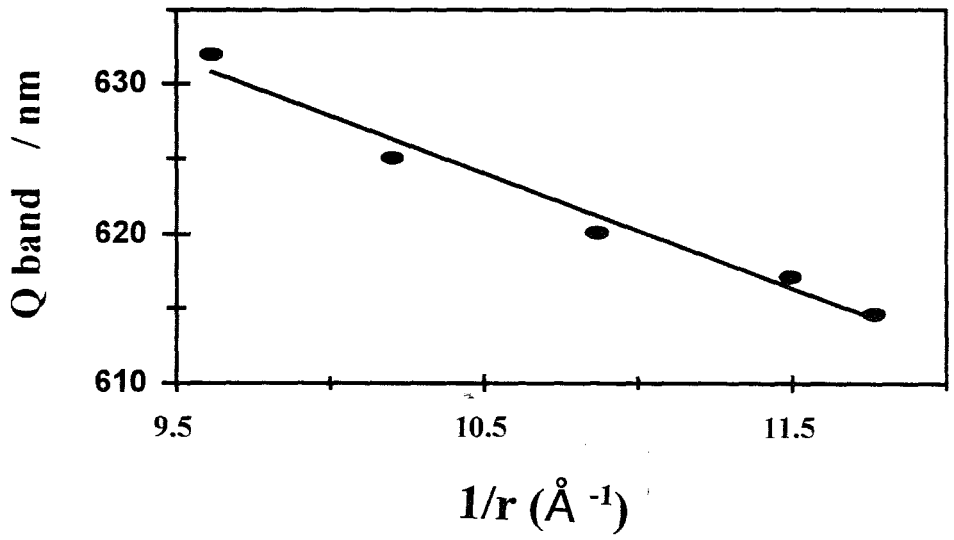

Fig. 3.2 Changes of Q band position with the reciprocal of the ionic radius of lanthanide ion of diphthalocyanine complexes [132].

The splittings of the Q band of the blue form of lanthanide diphthalocyanine complexes showed linear change with the inverse of the cube of the ionic diameters of lanthanide metals [9]. Fig. 3.3 shows the change of Q band splittings with the inverse of the lanthanide ionic diameters cubed. Fig. 3.3 shows that higher exciton coupling is expected for lutetium diphthalocyanine leading to a more reactive nature.

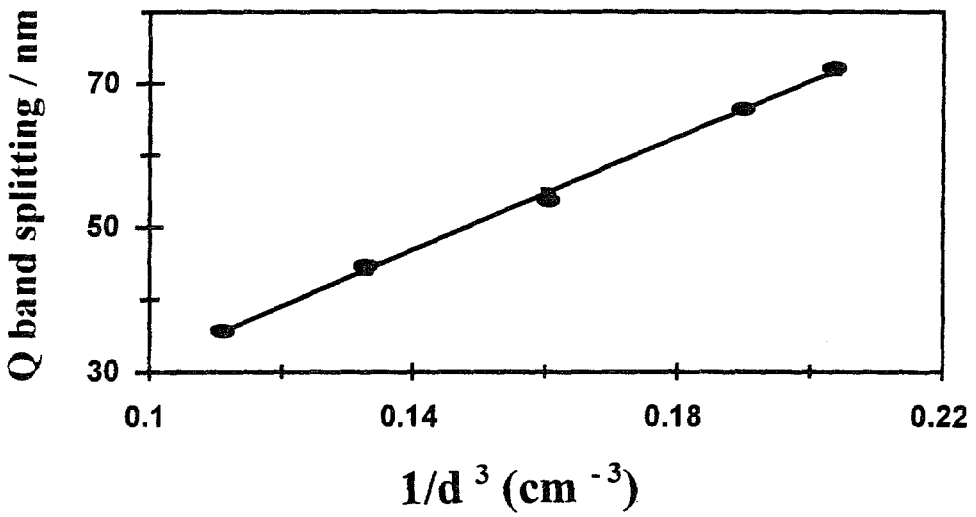

Fig. 3.3 Changes of Q band splittings with the reciprocal of the cubic of lanthanide ion diameter [9].

The Q band splitting was also reported for tin diphthalocyanine, $SnPc_2$ [41,133] and it was attributed to the exciton coupling between two identical phthalocyanine rings. The larger splitting observed in $SnPc_2$ compared to $LuPc_2^-$ and other lanthanide diphthalocyanine complexes confirm the enhancement of π-π interactions in tin diphthalocyanine complex.

All these findings are in keeping with the notion that these complexes contain two identical dianionic phthalocyanine rings, Pc (-2) per complex and bound to the central lanthanide or tin ion. These Pc rings are responsible for chemical and physical properties, while the metal contribution is negligible.

3.2.2 Infrared Spectra

Infrared spectroscopy is mainly used to check the purity of complexes synthetised and possible detection of unwanted compounds. In the study of lanthanide diphthalocyanine complexes, monophthalocyanines and metal-free phthalocyanine, H_2Pc compounds are claimed to be common contaminants [9]. The amount of H_2Pc increased sharply from 2% in $LuPc_2$ to 75% in $NdPc_2$ [36] and it shows a characteristic IR band at 1000-1020 cm^{-1} [32,36].

The infrared spectra of tin and lanthanide diphthalocyanine complexes have been extensively studied [4,5,32, 36]. The infrared (IR) study of Pc_2Sn shows that both α and β forms of the complex are similar to that of monomeric phthalocyanines except the 1500 cm^{-1} region which is more complicated [5,131]. This observation suggests that the rings are not greatly distorted in this unusual compound. On the other hand, the IR studies of lutetium diphthalocyanine confirmed that in the region between 1550 and 1385 cm^{-1}, the pyrrole moiety possesses three absorptions bands, and the band observed at 1452 cm^{-1} was more intense than the two others at 1493 and 1507 cm^{-1} [36]. The band found at 1452 cm^{-1} is considered as a characteristic band of lutetium diphthalocyanine [32].

Fig. 3.4 shows IR spectra of europium diphthalocyanine. Since the infrared spectra of diphthalocyanine complexes show rich vibrational bands in the region of 1700 to 600 cm^{-1}, this study is limited in the region between 2000 to 600 cm^{-1}. The IR spectra obtained are similar to those reported by others [5,32,36,134]. The IR spectra of tin and lanthanide diphthalocyanines

are similar, except in the regions of 1000 to 1300 cm^{-1} and 1380 to 1550 cm^{-1} where $SnPc_2$ showed four bands in each region, whereas $LnPc_2^-$ showed fewer bands in these regions.

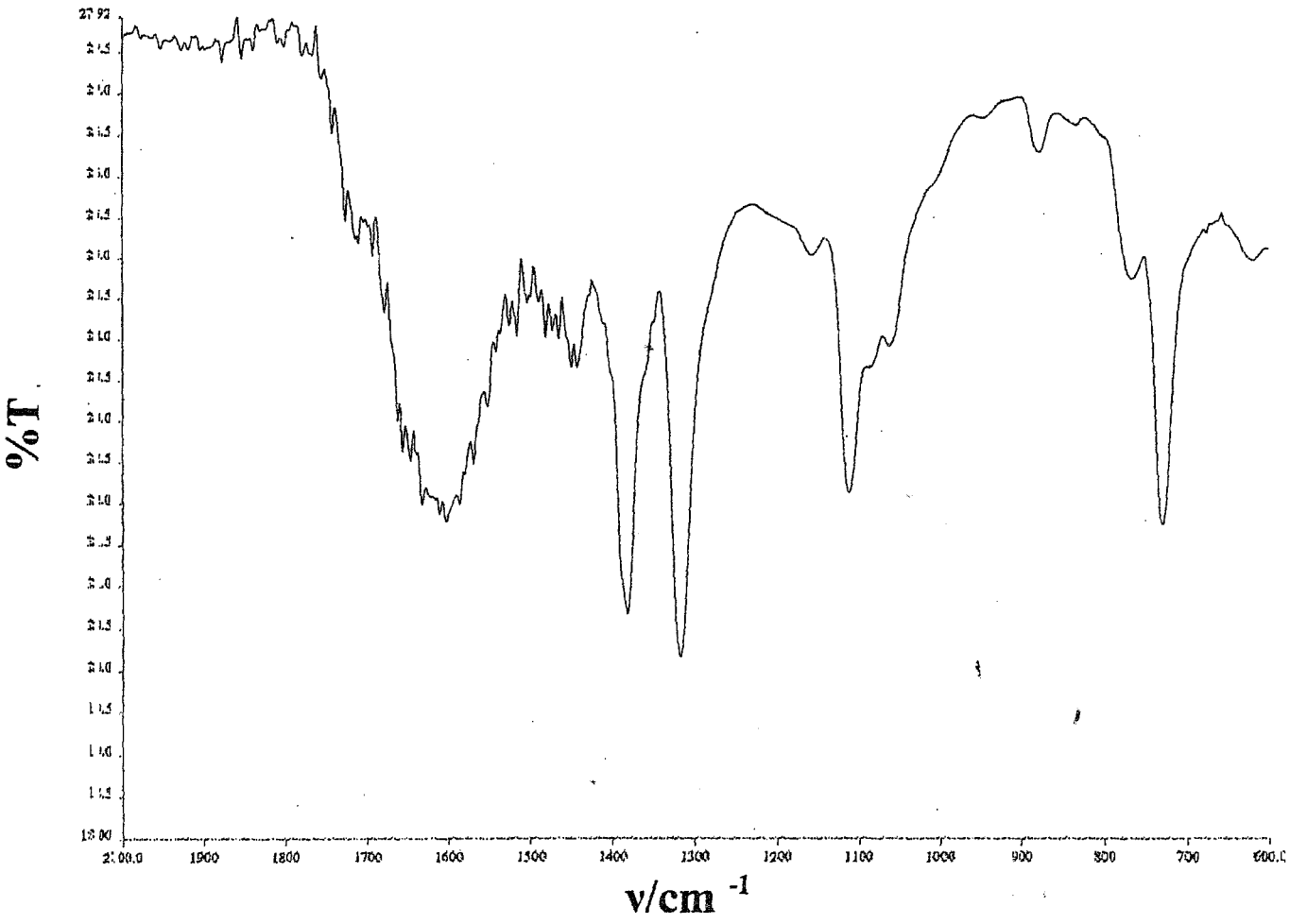

Fig. 3.4 Infrared spectrum of $[Pc(-2)EuPc(-2)]^-$ using KBr discs.

The complications observed in the region of 1550 to 1380 cm^{-1} may confirm that the rings are less distorted in tin diphthalocyanine [5]. The other lanthanide diphthalocyanine complexes have IR spectra similar to that shown for $EuPc_2^-$, although the frequencies of the vibrations change throughout the lanthanide series.

Fig. 3.4 shows an IR band that is typical of the blue form of lanthanide diphthalocyanine complexes, near 1380 cm^{-1}. This band varies from 1379 in $LuPc_2^-$ to 1394 cm^{-1} in $NdPc_2^-$. It is a strong band which has never been observed for the neutral (green) form of lanthanide diphthalocyanine complexes, $LnPc_2$ [28,32,36]. The same band was observed in tin diphthalocyanine with a weak intensity at 1381cm^{-1}. Table 3.2 gives common bands observed in the IR study of tin and lanthanide diphthalocyanine complexes. Some bands presented in the Table 3.2. have been claimed to be characteristic of lanthanide diphthalocyanine complexes [32,36]. These bands have a tendency to shift towards high frequencies from lutetium to neodymium.

The strongest band was observed at 1318 cm^{-1} in blue form lutetium diphthalocyanine. The same band was observed at 1323 cm^{-1} in green species of lutetium diphthalocyanine [32]. In other lanthanide diphthalocyanine complexes, this band has slightly shifted towards lower frequency when going from Lu to Nd diphthalocyanine complexes. The same band was obtained at 1327 cm^{-1} in $SnPc_2$ with similar intensity.

Table 3.2 Common IR bands of tin and lanthanide diphthalocyanine complexes.

Compound	Frequencies (cm^{-1})						
$LuPc_2^-$	734 (s)	834(w)	884(w)	1112(s)	1318 (s)	1379 (s)	1452(m)
$TmPc_2^-$	730 (s)	830 (w)	879 (w)	1110(s)	1318 (s)	1384 (s)	1445 (w)
$EuPc_2^-$	730 (s)	838 (w)	881(w)	1113 (s)	1317 (s)	1383 (s)	1445 (w)
$DyPc_2^-$	724 (m)	832 (w)	886 (w)	1108 (s)	1316 (s)	1385 (s)	1467 (m)
$NdPc_2^-$	727 (s)	838 (w)	876 (m)	1053 (s)	1316 (s)	1394 (m)	1473 (m)
$SnPc_2$	721 (s)	806 (w)	887(m)	1114(s)	1327 (s)	1381 (w)	1469 (w)

w = weak ; m = medium ; s = strong

The band observed at 1112 cm^{-1} in lutetium diphthalocyanine shifts to lower frequency with increase in the size of the central lanthanide ion, with the exception of europium diphthalocyanine. This band was attributed to the vibrations of benzene rings [32].

Below 900 cm^{-1}, two important bands were observed at 884 and 834 cm^{-1} in $LuPc_2^-$ as reported by Pondaven et al. [32] while in $SnPc_2$, these bands are localized at 887 and 806 cm^{-1}. These bands were associated with a possible metal-ligand vibration [36]. On the other hand, Pondaven et al.[32] observed that these bands were affected differently by ring substituents in lutetium diphthalocyanine. Moreover, in this work, it was not possible to draw a possible relationship between these bands and lanthanide parameters. Therefore, these bands are assigned to possible ν C-H vibrations as suggested by Shurvell and Pinzuti [52]. The bands observed below 800 cm^{-1} in tin and lanthanide diphthalocaynine complexes have been attributed to out-of-plane C-H bending vibrations [5], due to the deformation frequencies of the four adjacent hydrogen atoms of ortho-disubstituted aromatics. NH deformation frequencies also occur in this region [135].

From the IR data reported for $SnPc_2$ and $LnPc_2^-$, it can be concluded that tin diphthalocyanine and blue forms of lanthanide diphthalocyanine complexes did not show impurities due to metal-free phthalocyanine.

3.2.3 Nuclear Magnetic Resonance Spectroscopy

Nuclear magnetic resonance (NMR) studies of phthalocyanine complexes are not abundant because of their poor solubilities [129] in most organic solvents and water. On the other hand, NMR studies of lanthanide porphyrins have shown that these complexes are paramagnetic NMR shift reagents [136-138]. NMR studies of lithium, zinc and uranyl phthalocyanines have shown chemical shifts of α and β benzo-protons of these phthalocyanine complexes [139]. NMR studies

of the blue forms of lanthanide diphthalocyanine complexes were thoroughly discussed by Kasuga et al.[129], who observed induced shifts of α and β protons in these complexes.

This work reports on NMR spectrum of blue forms of lanthanide and tin diphthalocyanine complexes with the aim of verifying the presence of an acidic proton claimed elsewhere [9] and checking the purity. Fig. 3.5 shows the NMR spectrum of neodymium diphthalocyanine. According to Kasuga et al. [129], the lower field multiplet is attributed to the α proton of a benzene ring and the higher field to the β proton.

The NMR spectrum of $NdPc_2^-$ shows two bands similar to those reported by Kasuga et al.[129]. Similar behaviour was observed in the NMR spectrum of lutetium and europium diphthalocyanines. The NMR spectrum of thulium, dysprosium and tin diphthalocyanine complexes did not reveal these protons within the range shown in Fig. 3.5. This could be explained by the possible localization of these protons at very high field as observed for samarium diphthalocyanine in which protons were found at 18.67 and 18.34 ppm [129]. The proton-NMR field used in this work was limited at 12 ppm.

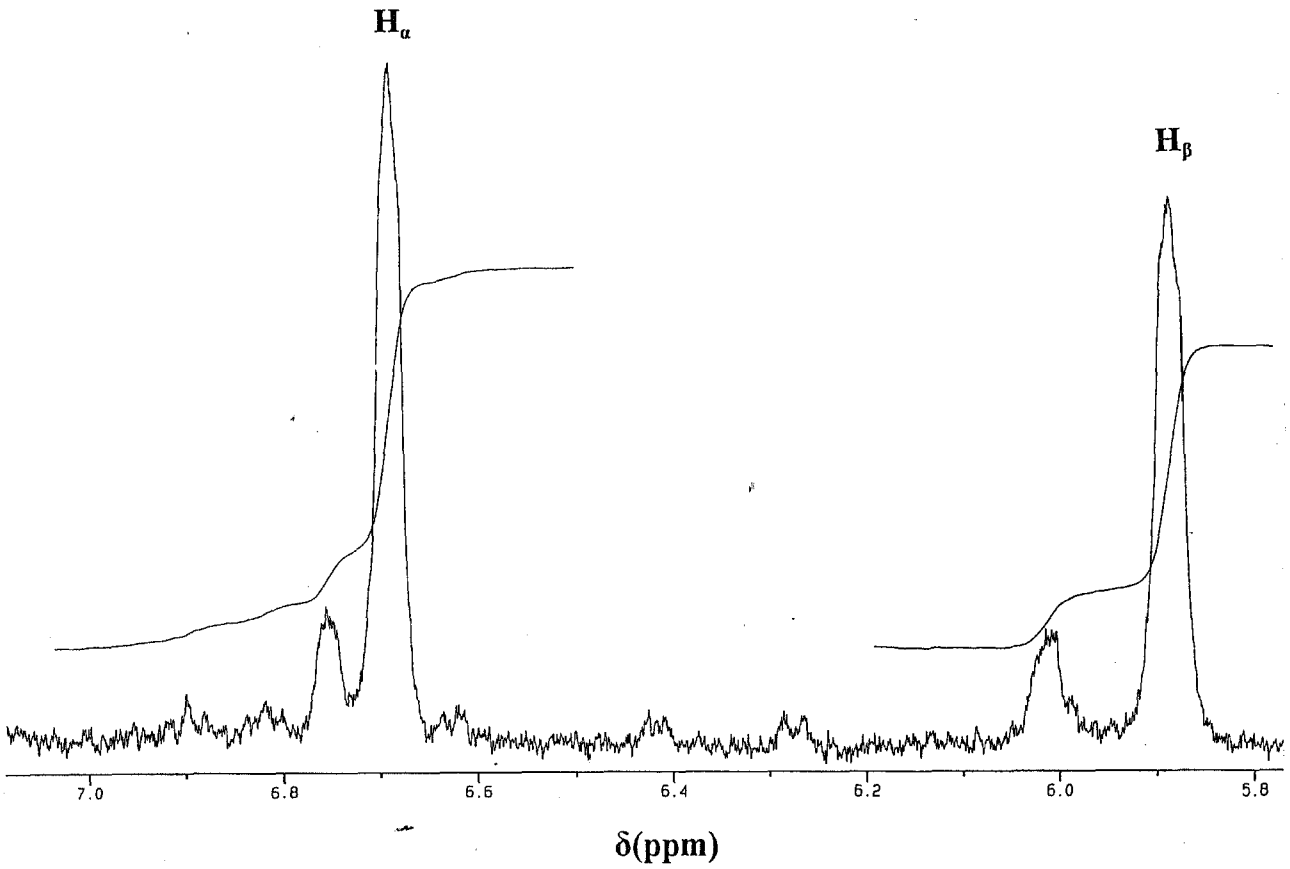

Fig. 3.5 NMR spectrum of neodynium(III) diphthalocyanine in DMSO-d6 at 30 °C.

Table 3.3 gives the positions of α and β benzo-protons observed for some lanthanide diphthalocyanine complexes. From the Table 3.3, it is observed that the two benzo-protons were localized at 6.70 and 5.89 ppm for $NdPc_2^-$ and at 10.80 and 9.00 ppm in $EuPc_2^-$. Kasuga et al. [129] found the same protons at 6.90 and 6.30 ppm for $NdPc_2^-$ and at 10.84 and 9.03 ppm for $EuPc_2^-$, these results are in the same range as reported here, the small changes observed could be associated to the difference of experimental temperature.

Table 3.3 NMR data for lanthanide diphthalocyanine complexes.

Compound	^{1}H-NMR	
	α- proton	β- proton
$LuPc_2^-$	9.05 (16 H)	8.15 (16 H)
$EuPc_2^-$	10.80 (16 H)	9.00 (16 H)
$NdPc_2^-$	6.70 (16 H)	5.89 (16 H)

The induced chemical shifts of α and β protons of these complexes increase in the following order: $NdPc_2^- < LuPc_2^- < EuPc_2^-$. The order of these induced chemical shifts is independent of the size of the lanthanide ions. This fact may imply that the difference in shift induced by various diamagnetic metal ions are small [139].

On the other hand, the ratio α / β calculated for each complex shows that the two multiplets have the same composition as in 1:1 type compound. This observation suggests that both α protons

of the benzene ring are affected equally by shielding consistent with the staggered arrangement of Pc rings in $LuPc_2^-$ and UPc_2 with antiprismatic geometry [129, 140].

All the findings testify the absence of the acidic proton in the blue form of lanthanide diphthalocyanine complexes and support the presence of two identical phthalocyanine rings in these complexes. This study also confirms the lack of influence of lanthanide ion, attributing the chemical shift and activity of these complexes to the π-π interaction controlled by Pc rings.

4. Electrochemistry of metallodiphthalocyanines

4.1 General considerations

The electrochemical studies of phthalocyanine complexes show interesting redox properties with a possibility of up to six successive one electron reductions or oxidations [81]. From the time they were first reported, lanthanide diphthalocyanine complexes have shown electrochromic behaviours [20] and interesting spectroelectrochemical features [19]. These complexes have been seen as potential electrochromic materials for displays devices. Recently, the trend in the electrochemistry of lanthanide diphthalocyanine complexes has been in the understanding of their redox properties either in solution or as thin films [45].

Lanthanide diphthalocyanine complexes and their substituted derivatives show similar electrochemical behaviour in solution. The neutral green species, $LnPc_2$ produced a blue species, $[LnPc_2]^-$ at cathodic potentials, while the orange (red), $[LnPc_2]^-$ species was observed at anodic potentials [56.68]. It has been shown that the transition from one species to an other is accompanied by an electron exchange. The lack of reversibility reported in the case of Ce (IV) bis (octaethylporphyrinato), $Ce(OEP)_2$ [44,62] was attributed to the involvement of an orbital which is primarily metal in character [62].

The electrochemical studies of thin Langmuir-Blodgett films of octakis-substituted lanthanide diphthalocyanine complexes, $(CH_3CH_2CH_2O)_4(CH_3)_3C)_4LnPc_2$ have shown rich redox properties

with good reversibility and stability [141,142]. These compounds show similar electrochromic behaviours with unsubstituted lanthanide diphthalocyanine complexes dissolved in solution.

Previous work on the electrochemistry of lanthanide diphthalocyanine complexes has revealed that their redox properties are essentially controlled by the distance between the two rings linked through π-π interactions [44]. The interaction between Pc rings is correlated with the change of the energy levels of HOMO and LUMO in these complexes which is related with their redox potentials [16].

In the electrochemistry of $LnPc_2$, the energy gap HOMO-LUMO is characterized by the difference between the half-wave potentials of the first oxidation couple and the first reduction couple [15]. This difference, $\Delta E^0_{1,2}$ may define the richness of redox properties, since the compound with narrower gap is electrochemically more active. This potential gap, $\Delta E^0_{1,2}$ is said to be a good estimate for the thermal activation energy for the conduction of electrical charges in solid materials [15]. It is also the energy characterizing the lowest optical absorption band [143]. This potential gap was found to be larger in lanthanide bis (octaethylporphyrin) complexes, $Ln(OEP)_2$ compared to lanthanide diphthalocyanine complexes, $LnPc_2$, hence the nature of the ring affects the redox properties of the compound.

Thin films of $SnPc_2$ have shown electrochromic behaviours which are similar to those of lutetium diphthalocyanine, hence five distinct colours have been observed, which are turquoise, violet, blue, green and red [33]. Since the neutral $SnPc_2$ is turquoise, the green and the red species correspond to the oxidation products resulting in mono, $[SnPc_2]^-$ and di-cation $[SnPc_2]^{2-}$ species.

respectively. Whereas, the blue and violet species are the reduction products and correspond to monoanion, $SnPc_2^-$ and dianion, $SnPc_2^{2-}$ species, respectively. All these colour changes are associated with electron-transfer processes. However, Silver et al. [10] reported difficulties in observing reversible colour changes upon oxidizing $SnPc_2$ films, and this was attributed to the greater polarizing power of the tetravalent metal ion which destabilizes the oxidized rings. Collins et al. [33] observed a considerable degradation of the $SnPc_2$ film at potential around zero (vs Ag/AgCl).

This work reports on the cyclic voltammetric studies of $SnPc_2$ in solution for the first time. Many influences that complicate the study of this compound in solid state are absent in solution [45]. The spectroelectrochemical behaviour of $SnPc_2$ is also presented.

4.2 Electrochemical studies of tin diphthalocyanine complex*

4.2.1 Cyclic voltammetry of tin diphthalocyanine

Fi.g.4.1 shows the cyclic voltammogram (CV) and differential pulse voltammogram (DPV) of $SnPc_2$ in dichloromethane (CH_2Cl_2) containing tetrabutylammonium perchlorate (TBAP). Three quasi-reversible one-electron couples were observed at 0.35 (O_1), -0.56 (R_1) and -0.89 (R_2) V versus the saturated calomel electrode (SCE). The potentials were recorded versus ferrocene as an internal standard and converted to E versus SCE as explained in the experimental section. The

*. The following publication resulted from work presented in this section: N. Nensala and T. Nyokong. Polyhedron. 15 (1996). 867.

cathodic to anodic peak potential separations (ΔE) ranging from 80 to 100 mV were obtained in CH_2Cl_2. A ΔE value of 80 mV was also obtained for the internal standard Fc^-/Fc couple [144], thus confirming that each redox couple represents a one-electron transfer reaction process. The half-wave potentials for $SnPc_2$ in DMF and in CH_2Cl_2 are listed in the Table 4.1. ΔE values were found to range between 60 to 80 mV in DMF.

Oxidation is expected to occur at the ring in $Sn(IV)Pc_2$, since further oxidation of the metal is not likely. Thus, the one-electron oxidation couple located at 0.35 V versus SCE (-0.12 V versus Fc^-/Fc) in CH_2Cl_2 corresponds to the oxidation of one of the phthalocyanine ring in $SnPc_2$, giving the $[Pc(-2)SnPc(-1)]^+$ species. All reported cyclic voltammetry data on lanthanide diphthalocyanine complexes show successive one-electron oxidation or reduction of the ring.

An overall splitting of the molecular orbitals is observed on going from the monomeric to dimeric phthalocyanines due to the interaction between the rings in the dimer [11]. The shorter the ring-ring distance becomes , the less energy is required to oxidize the dimer.

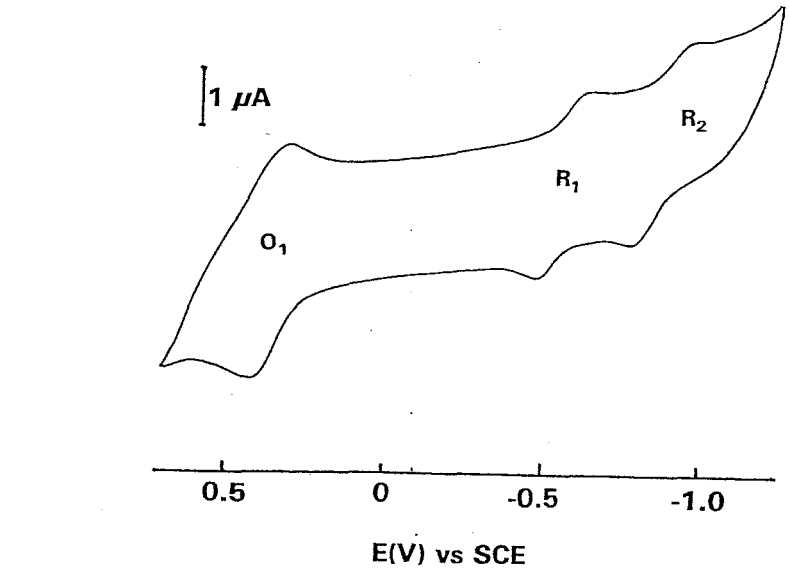

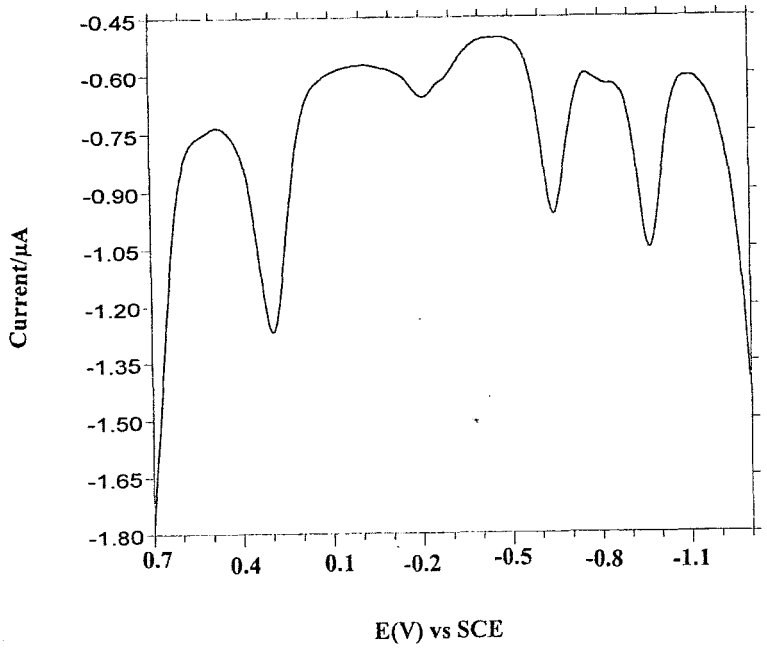

Fig. 4.1. CV and DPV diagrams of $SnPc_2$ in dichloromethane

Table 4.1 Half-wave potentials ($E_{1/2}$) of $SnPc_2$.

Complex	$E_{1/2}$ versus Fc^+ / Fc (V)			$E_{1/2}$ versus SCE (V)		
$SnPc_2$	O_1	R_1	R_2	O_1	R_1	R_2
(DMF / TEAP)	-0.03	-0.90	-1.27	0.43	-0.44	-0.81
$SnPc_2$	O_1	R_1	R_2	O_1	R_1	R_2
(CH_2Cl_2 / TBAP)	-0.12	-1.03	-1.36	0.35	-0.56	-0.89

The first oxidation of $SnPc_2$ occurs at lower potentials ($E_{1/2}$ = -0.12 V versus Fc^+ /Fc) than that of the green form of $LuPc_2$ ($E_{1/2}$ = 0.03 V versus Fc^+/ Fc) [56]. The green form of $LuPc_2$ is the ring oxidized, Pc(-1)LuPc(-2) species, thus the product of oxidation of this species is a di-π-cation species, whereas the oxidation of $SnPc_2$ is the mono-π-cation radical species, [Pc(-2)SnPc(-1)]$^+$. The first oxidation potential of $SnPc_2$ is also lower than those of actinide diphthalocyanine complexes, UPc_2 and $ThPc_2$ ($E_{1/2}$ = 0.75 V versus SCE) [37].

The two one-electron reduction couples observed for $SnPc_2$ in CH_2Cl_2 at -0.56 and - 0.89 V versus SCE are also associated with ring-based processes. The reduction couples are observed at less negative potentials in DMF. The colour changes observed during the reduction of $SnPc_2$ thin films have been associated with the reduction of the rings [10]. The first reduction couple in $SnPc_2$ is thus associated with the Pc(-2)SnPc(-2)/[Pc(-2)SnPc(-3)]$^-$ couple. The magnitude of the gap between the first ring oxidation and the first ring reduction, $\Delta E^0_{1/2}$, is important in predicting spectra in electrochemistry [11]. $\Delta E^0_{1/2}$ values ranging from 1.36 to 1.7 V have been

reported for monomeric phthalocyanine complexes. For example, a $\Delta E^0_{1\,2}$ value of 1.56 V has been observed for the main group phthalocyanines [145] and $\Delta E^0_{1\,2}$ values of 1.69 and 1.36 V has been observed for $(OH)_2Zr^{IV}Pc$ [146] and BrBiPc [147]. The separation between the first ring oxidation and the first ring reduction was found to be 0.91 V for $SnPc_2$ in CH_2Cl_2 and 0.87 V in DMF, a value much lower than the $\Delta E^0_{1\,2}$ values for monophthalocyanines. The low value of $\Delta E^0_{1\,2}$ in $SnPc_2$ is a consequence of the interactions between the rings in diphthalocyanine species. Konami et al. [16] reported the redox potentials of a series of $[Pc(-2)LnPc(-2)]^-$. The $\Delta E^0_{1\,2}$ values in these species ranged from 1.08 V for $[LuPc_2]^-$ to 1.30 V for $[NdPc_2]^-$. These values decreased with the decrease in the ionic radii of the lanthanide ion. The electronic interaction between the π-electrons systems of the phthalocyanine rings is stronger for metals with a small ionic radii. The magnitude of $\Delta E^0_{1\,2}$ decreases with the increase in the interaction between the phthalocyanine rings. It has been shown that the splitting of absorption spectra is higher in $SnPc_2$ than in lutetium diphthalocyanine due to the exciton coupling in the former [41]. The smaller value of $\Delta E^0_{1\,2}$ in $SnPc_2$ as compared with the blue $[Pc(-2)Lu^{III}Pc(-2)]^-$ species may thus be attributed to the exciton coupling interactions in the former. The separation between the first oxidation and the first reduction in substituted and unsubstituted green $Pc(-2)LuPc(-1)$ are very low, ranging from 0.29 to 0.40 V [35]. This is a consequence of the fact the highest occupied molecular orbital (HOMO) is the semi-occupied molecular (SOMO) in these complexes, resulting in lower reduction potentials [15].

The second reduction couple for $SnPc_2$ is observed at - 0.89 V in CH_2Cl_2 and is separated from the first reduction couple by 0.33 V. This separation is within the range observed between ring

reductions in $[LnPc_2]^-$ species [16], thus confirming that the second reduction couple in $SnPc_2$ is due to the formation of the $[Pc(-3)SnPc(-3)]^{2-}$ species.

4.2.2 Spectroelectrochemistry of tin diphthalocyanine

Spectroelectrochemistry provides a useful means of confirming the nature of various redox waves in metallophthalocyanines [65,72]. The electronic spectra have been used successfully to characterize anion and cation radical species in monophthalocyanines [30,31]. The spectroscopic data for the products of the reduction or oxidation of monopthalocyanines is more abundant than for diphthalocyanine complexes [65,66,72,143]. The spectroscopic data reported on diphthalocyanine complexes have contributed extensively on the study of electrochromic behaviours of these complexes [10,56,67,68]. The electronic spectra of lanthanide diphthalocyanine species such as $[Pc(-1)\ Ln\ Pc(-1)]^-$, $[Pc(-2)\ Ln\ Pc(-1)]$, $[Pc(-2)\ Ln\ Pc(-2)]^-$ and $[Pc(-2)\ Ln\ Pc(-3)]^{-2}$ have been reported for several lanthanide complexes [30, 45,56,67,68,142], and actinide diphthalocyanine complexes [37]. Each oxidized and reduced species show a characteristic electronic spectrum which reflects the anionic or cationic electronic structure discussed by Stillman [31].

In this work, the spectra of $SnPc_2$ obtained on the oxidation or reduction of $SnPc_2$ species is compared with the spectra of the oxidized or reduced lanthanide diphthalocyanine complexes. It has been shown before that the spectra of the diphthalocyanines is not significantly affected by changes in the central metal [11].

Compared with the spectra of monophthalocyanines, the spectra of $SnPc_2$ show an extensive splitting of the Q band and an increased intensity of the Soret band, Fig. (4.2.a). The splitting is a result of coupling interaction between the phthalocyanine rings in diphthalocyanines which results in the splitting of molecular orbitals.

Fig. 4.2 shows the absorption spectral changes observed when $SnPc_2$ dissolved in CH_2Cl_2, was oxidized at a potential of 50 mV more positive than the potential of oxidation couple. The original visible region bands at 573, 624, 692 and 779 nm , decrease in intensity and three new bands are formed at 669, 604 and 471 nm with isosbetic points at 691, 643 and 538 nm. The colour of solution goes from blue to green. The 669 nm absorption band is more intense than the original bands. The weaker band at 471 nm is characteristic of the electronic transition into SOMO level [15]. The absorption band in this region is associated with the formation of π-cation radical species in monophthalocyanine [31]. Changes in the Soret band were not as pronounced as those observed in the visible region during the reduction of $SnPc_2$. The Soret absorption band increases in intensity and a new band is formed at 320 nm. In general, the Soret band is not affected significantly by the oxidation or reduction of diphthalocyanine complexes [15]. But, significant shifts in the Soret band are however, observed upon oxidation or reduction of monophthalocyanine species [31].

Van Cott et al. [43] have recently shown that the spectra of Pc(-2)LuPc(-1) is not a simple superposition of the spectra of Pc(-2) and Pc(-1), due to some delocalization of the unpaired electron over the two rings. The final spectra in Fig. 4.2 (b) is typical to the spectra of the green $Pc(-2)Ln^{III}Pc(-1)$ species [31]. The number of moles of electrons transferred during the controlled

potential oxidation of $SnPc_2$ was determined by coloumetry to be unity, confirming the formation of the singly oxidized $[Pc(-2)SnPc(-1)]^-$ species following electrochemical oxidation of $SnPc_2$ in CH_2Cl_2. Silver et al. [10] reported difficulties in obtaining an oxidized form of $SnPc_2$ thin films. It was found in this work that the $[Pc(-2)SnPc(-1)]^-$ species was quite stable in CH_2Cl_2 solutions. This species could be reduced back to the original $SnPc_2$ without loss of intensity. Spectral changes shown in Fig. 4.2 were also observed during the chemical oxidation of $SnPc_2$ dissolved in CH_2Cl_2 with bromine.

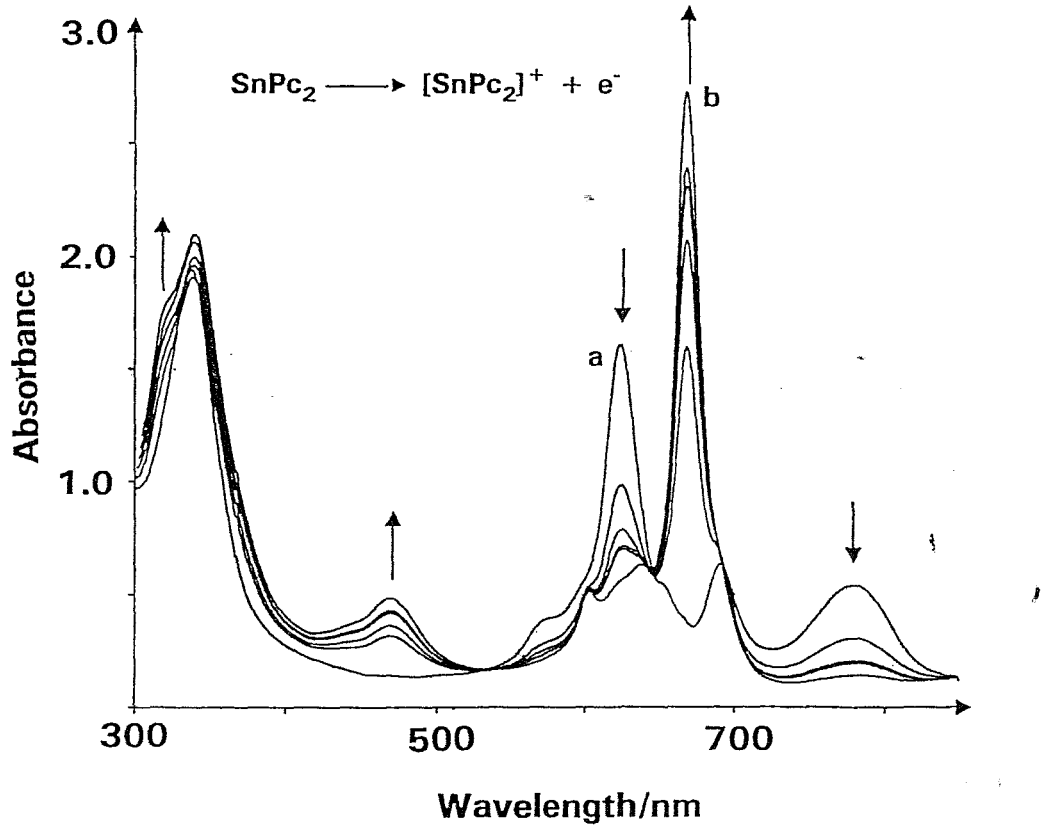

Fig. 4.2 Electronic absorption spectral changes observed during the electrooxidation of [Pc(-2)SnPc(-2)] (a) to [Pc(-2)SnPc(-1)] (b) at 0.4 V versus SCE in CH_2Cl_2 containing TBAP.

The reduction of $SnPc_2$ in DMF-TEAP system at potentials of the first reduction couple resulted in spectral changes shown in Fig. 4.3. The original bands observed at 574, 626, 689 and 777 nm decrease in intensity and three new bands are formed isosbestically at 569, 602 and 667 nm. The isosbestic points are observed at 353, 610, 640 and 735 nm and confirm the existence of only two species in solution. Apart from the small decrease in intensity, the Soret band is un affected by the reduction of $SnPc_2$ as it has been observed before during the reduction of lanthanide naphthalocanines [15]. The colour of the solution changes from blue to purplish-blue following reduction. The band associated with the electronic transition into SOMO level, near 470 nm, is not observed in the spectra of the reduced species.

In monophthalocyanines, the singly reduced MPc (-3) species, is characterized by bands centred near 560 and 640 nm [65, 148]. These bands are weaker than the Q band of the MPc(-2) species. In Fig. 4.3 (b), the two new weak bands observed at 569 and 602 nm are most likely due to the presence of one reduced phthalocyanine ring formed following the reduction of $SnPc_2$. The more intense band at 667 nm in Fig. 4.3 (b) reflects the presence of Pc(-2) ring. The final spectra in Fig. 4.3 (b) is similar to the spectra of the purplish-blue $[Pc(-2)Lu^{III}Pc(-3)]^{2-}$ [23], although the low energy band is less intense for the lutetium diphthalocyanine species. Also the number of moles transferred during the reduction were determined by coloumetry to be unity. Thus, the spectral changes observed in Fig. 4.3 during the electrochemical reduction of $SnPc_2$ at potentials of the first reduction are due to the formation of $[Pc(-2)Sn^{IV}Pc(-3)]^{-}$. Reduction in tin (IV) monophthalocyanines also occurs at the phthalocyanine ring. The spectral changes shown in Fig. 4.3 were also observed on chemical reduction using sodium borohydride, of DMF solutions of $SnPc_2$.

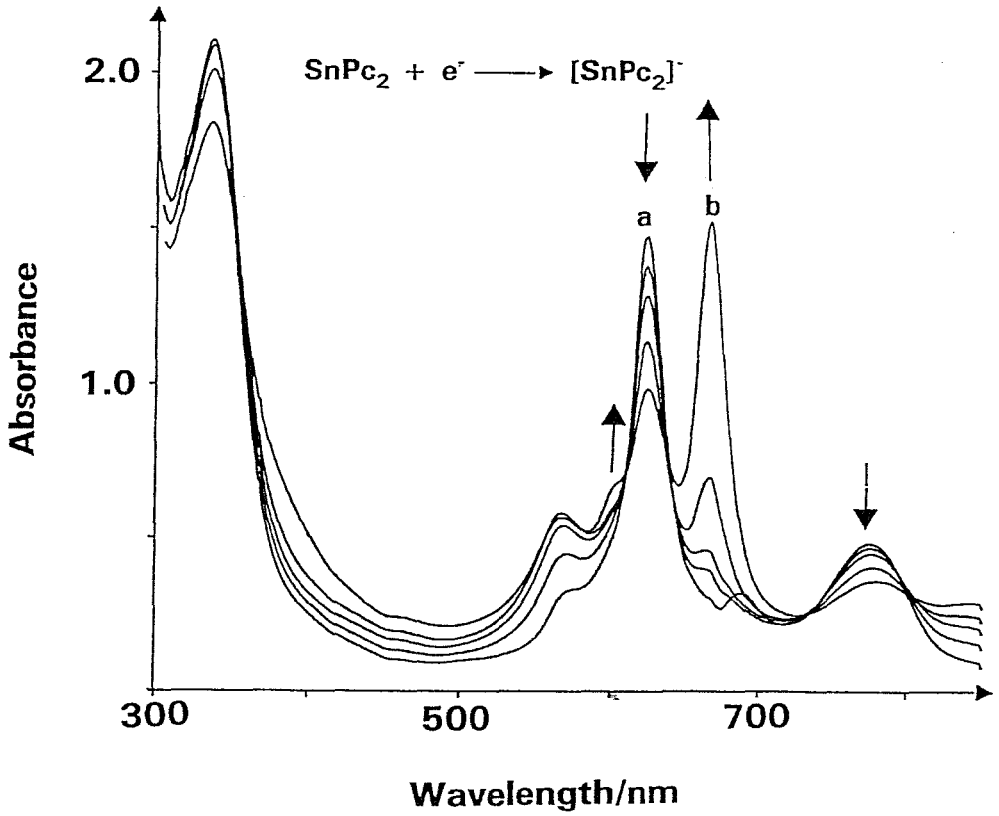

Fig. 4.3 Electronic absorption spectral changes observed during the electroreduction of [Pc(-2)SnPc(-2)] (a) to [Pc(-2)SnPc(-3)]$^{-}$ (b) at -0.6 V versus SCE in CH_2Cl_2 containing TBAP.

Further electrochemical reduction of $SnPc_2$ at potentials of the second reduction couple resulted in spectral changes shown in Fig. 4.4. The main absorption band due to the [Pc(-2)SnPc(-3)]$^{-}$ species at 667 nm decreases in intensity and a new band is formed at 689 nm. The new species formed was quite unstable and was readily oxidized back to the [Pc(-2)SnPc(-3)]$^{-}$ species. Thus the complete conversion of [Pc(-2)Sn Pc(-3)]$^{-}$ species to the new species was not possible under the present experimental conditions and it was not possible to accurately determine the number

of moles of electrons transferred during the reduction at potentials of - 0.90V. The bands associated with the formation of Nc(-3)LuNc(-3)]$^{3-}$ [Nc(-2)= naphthalocyanine dianion] are weak and are located between 600 and 750 nm [15, 67]. The new absorption band observed at 689 nm when $SnPc_2$ is reduced at potentials of the second reduction could thus be due to the formation of the tin (IV) diphthalocyanine dianion. This absorption band is observed near 720 nm in the spectra of [Nc(-3) LuNc(-3)]$^{3-}$. The fact that the bands are observed at different wavelengths in the two complexes is attributed to ring expansion effects in naphthalocyanines, which induce bathochromic shifts in the absorption spectra [35, 149], thus the spectral changes observed in Fig. 4.4 are tentatively assigned to the formation of the [Pc(-3)SnPc(-3)]$^{2-}$ species. This assignment is consistent with the cyclic voltammetry data above.

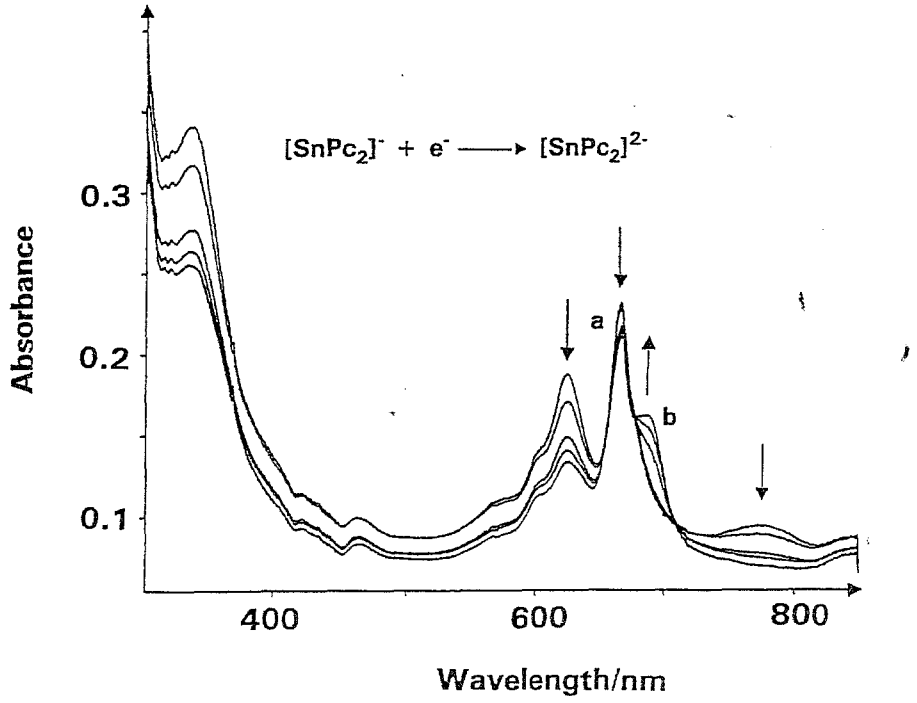

Fig. 4.4 Electronic absorption spectral changes observed during the further electroreduction of [Pc(-2)SnPc(-3)]$^{-}$ to [Pc(-3)SnPc(-3)]$^{2-}$ at -0.90 V vs SCE.

In summary, the oxidation or reduction products of $SnPc_2$ are formed as result of successive one-electron processes as shown in Scheme 4.1.

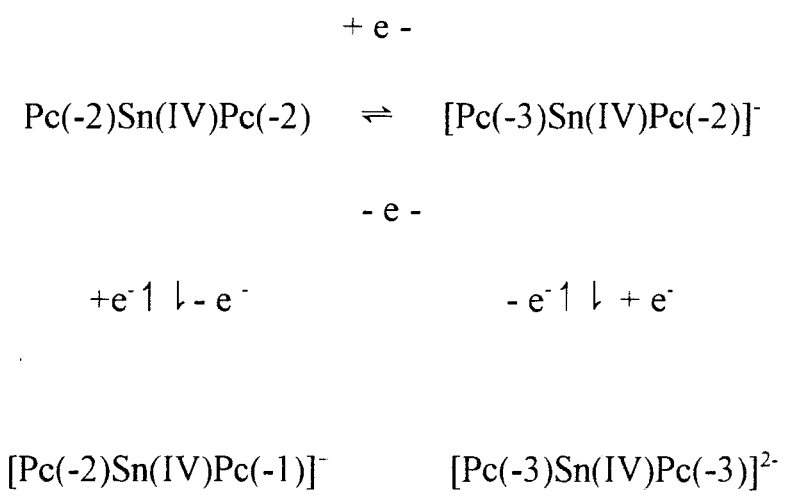

Scheme 4.1

No further oxidation of the $[Pc(-2)SnPc(-1)]^-$ species to $[Pc(-1)SnPc(-1)]^{2-}$ was observed under the present experimental conditions.

The reported electrochromic behaviours of $SnPc_2$ species is due to the electronic transformations shown in Scheme 4.1. The spectra of the oxidized or reduced species are similar to the spectra of the corresponding lanthanide diphthalocyanine complexes.

4.3 Electrochemical studies of lanthanide diphthalocyanine complexes

Even though electrochemical studies of the lanthanide diphthalocyanine complexes have been reported [16], some of the electrooxidation products have not yet been reported. Also in this work, the electrochemical properties are reported in solvents different from those reported in literature. Solvents such as CH_2Cl_2 and DMF are good for photocatalytic studies and it is thus important to study the electrochemistry of lanthanide diphthalocyanine in these solvents. CH_2Cl_2 favours the oxidation whereas DMF favours the reduction.

4.3.1 Cyclic voltammetry of lanthanide diphthalocyanine complexes

Fig. 4.5 shows the cyclic voltammogram and the differential pulse voltammogram of lutetium diphthalocyanine in CH_2Cl_2 containing TBAP. In CH_2Cl_2/ TBAP system, three quasi-reversible redox couples were obtained while in DMF/ TEAP system, four quasi-reversible couples were observed. The cyclic voltammogran of lutetium diphthalocyanine in dichloromethane shows two oxidation couples and one reduction couple. Whereas, in DMF, two oxidation couples and two reduction couples were obtained.

Komani et al.[16] observed four redox couples in the cyclic voltammetry of lanthanide diphthalocyanine complexes in o-dichlorobenzene, except for Pr and Nd diphthalocyanine complexes in which the second oxidation couple was not observed. On the other hand, the cyclic voltammetry of lanthanide bis(octaethylporphyrinate), $Ln(OEP)_2$ in DMF shows only three reversible couples [44].

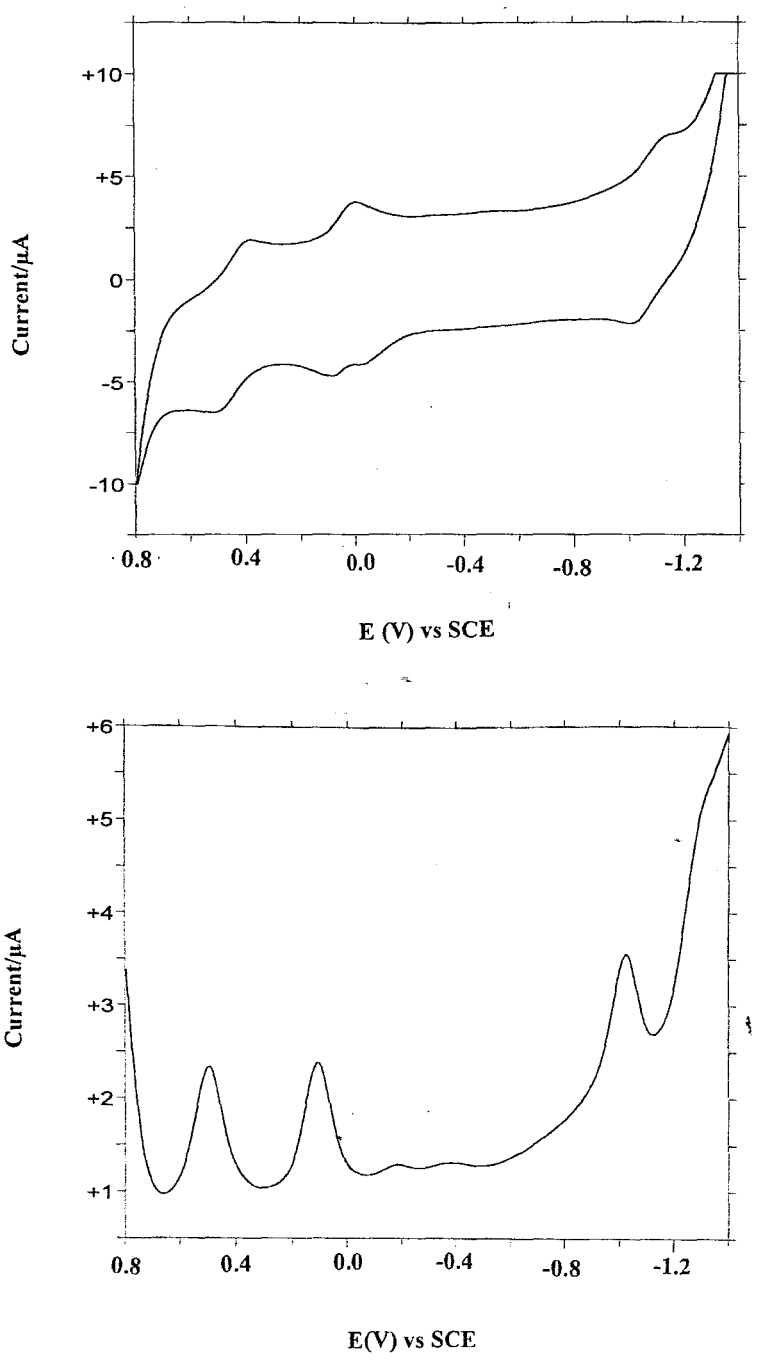

Fig. 4.5 CV and DPV diagrams of $LuPc_2^-$ in CH_2Cl_2 / TBAP system.

Table 4.2 gives the redox potentials of lanthanide diphthalocyanine complexes in CH_2Cl_2 and DMF. From the table, the two oxidation couples observed for $LnPc_2^-$ in CH_2Cl_2 at $E_{1/2}$ = 0.07 V and 0.46 V versus SCE, are in the same range as the oxidation potentials reported for $LnPc_2^-$ in dichlorobenzene ($E_{1/2}$ = 0.094 V and 0.547 V versus SCE) [17]. The differences are attributed to solvent effects. On the other hand, the oxidation couples of lutetium diphthalocyanine occur at lower potentials than the oxidation couples of uranium diphthalocyanine ($E_{1/2}$ = 0.74 V and 1.09 V versus SCE) [40] and Ln $(OEP)_2$ ($E_{1/2}$ = 0.10 V versus SCE) [29].

In general, diphthalocyanine complexes have lower oxidation potentials than the monomeric phthalocyanines. Even the electrochemical generation of the $Ce(OEP)_2^-$, π cation radical occurred at lower oxidation potential than for any monomeric OEP π-cation radical [62]. It is important to note that the first and second oxidation potentials of lanthanide diphthalocyanine complexes increase with the ionic radii of lanthanide metals throughout the lanthanide series [16,44]. Buchler et al. [44] studied the electrochemistry of lanthanide bis (octaethylporphyrinates) in DMF, and observed that reduction potentials decrease with the ionic radii of lanthanide metal while the oxidation potential increase with the ionic radii. On the other hand, Komani et al.[16] observed that oxidation potentials of $[LnPc_2]^-$ increase almost linearly with the increase in ionic radii, whereas the reduction potentials did not show significant change. Similar behaviours have also been observed for heteroleptic double-decker complexes of the type of phthalocyaninato-porphyrinato actinide [70].

Table 4.2 Redox potentials of lanthanide diphthalocyanines.

Complex	$E_{1/2}$ (V) versus Fc^+ / Fc				$E_{1/2}$ (V) versus SCE			
	O_2	O_1	R_1	R_2	O_2	O_1	R_1	R_2
$NdPc_2^-$								
CH_2Cl_2/TBAP	0.49	0.12	-1.14	-	0.49	0.11	-1.15	-
DMF / TEAP	0.61	0.37	-0.88	-1.15	0.43	0.12	-1.06	-1.32
$EuPc_2^-$								
CH_2Cl_2 /TBAP	0.72	0.34	-0.90	-	0.49	0.19	-1.02	-
DMF / TEAP	0.80	0.36	-0.88	-1.05	0.66	0.33	-0.95	-1.23
$DyPc_2^-$								
CH_2Cl_2 / TBAP	0.70	0.31	-0.85	-	0.48	0.13	-1.06	-
DMF / TEAP	0.78	0.53	-0.63	-0.96	0.62	0.25	-0.80	-1.13
$TmPc_2^-$								
CH_2Cl_2 / TBAP	0.64	0.29	-0.87	-	0.47	0.12	-1.05	-
DMF / TEAP	0.76	0.42	-0.74	-0.88	0.64	0.24	-0.92	-1.06
$LuPc_2^-$								
CH_2Cl_2 / TBAP	0.63	0.24	-0.88	-	0.50	0.11	-1.01	-
DMF / TEAP	0.71	0.35	-0.61	-0.75	0.55	0.19	-0.77	-0.91

O_1 = first oxidation couple ; R_1 = first reduction couple; O_2 = second oxidation couple ; R_2 = second reduction couple.

Fig. 4.6 shows the change of redox potentials with ionic radii of lanthanide ions. The oxidation as well as the reduction potentials increased with the ionic radii, in Fig. 4.6 contrary to the literature report for the reduction potentials but confirming the behaviour observed by Komani et al. [16] for the oxidation couples.

From Table 4.2, the difference between the first and second oxidation potential changes slightly from one lanthanide metal to another, from 0.30 to 0.40 V. Whereas, the difference between the first and second reduction potentials showed changes from 0.15 to 0.30 V throughout the lanthanide series. However, the oxidation potentials of $NdPc_2^-$ showed some deviation from the linear relationship shown in Fig. 4.6 possibly due to some irregularities that occur in Nd and earlier lanthanide diphthalocyanine complexes [16].

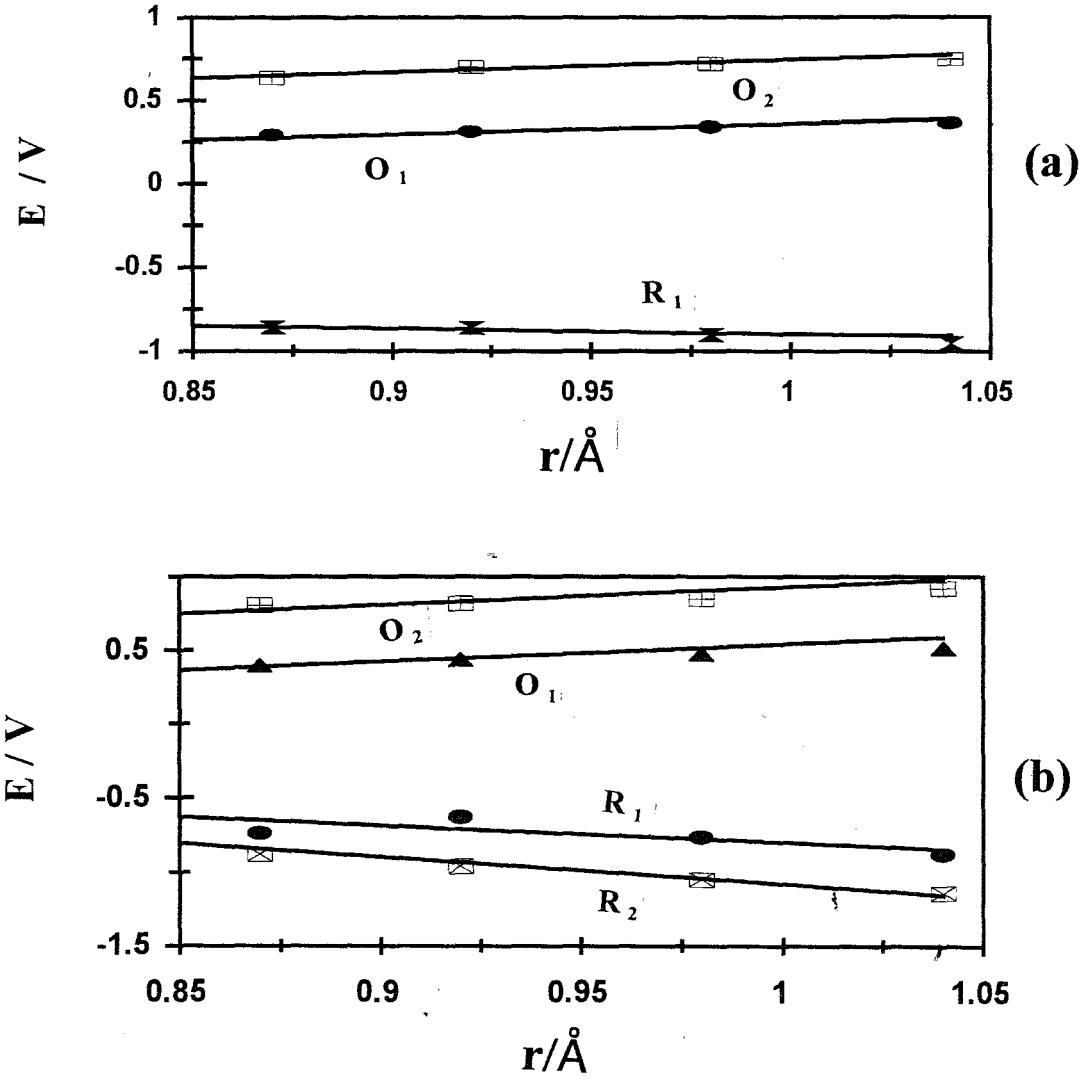

Fig. 4.6. Changes of redox potentials of $[LnPc_2]^-$ with the ionic radii of lanthanide ions in CH_2Cl_2 (a) and DMF (b).

As already discussed the distance between the first oxidation and the first reduction characterises the energy gap HOMO-LUMO [11] or the splitting of molecular orbitals of dimers. From the electrochemical study of the blue forms $[LnPc_2]^-$, it has been shown that the potential gap characterises the interaction between Pc rings [16]. Table 4.3 gives the potential gap between the first oxidation and the first reduction of diphthalocyanine complexes studied. The potential gap $\Delta E^0_{1\,2}$ for $SnPc_2$ is lower than for $LnPc_2^-$ in both solvents. This smaller value of $\Delta E^0_{1\,2}$ for $SnPc_2$ may be attributed to exciton coupling interactions in this complex. The exciton coupling results in the large Q band splitting observed in the electronic spectra of tin diphthalocyanine [41].

Within the lanthanide series, $LuPc_2^-$ has the narrowest potential gap. Having the smallest ionic radius, the lutetium complex exhibits a more attractive electrochemical behaviour due to the strong interaction between the π electron system of Pc rings [16]. The $\Delta E^0_{1\,2}$ values range from 1.12 to 1.26 V in CH_2Cl_2 while in DMF they vary from 1.0 to 1.25 V on going from $LuPc_2^-$ to $NdPc_2^-$. These potential gaps are in the range observed by Komani et al. which are 1.08 and 1.30 V for lutetium and neodymium diphthalocyanine, respectively, [16] in dichlorobenzene.

The potential gaps observed are narrower than the ones reported for $Ln(OEP)_2$ which vary from 1.745 V for $Lu(OEP)_2$ to 1.935 V for $La(OEP)_2$ [44]. This may imply that interactions of Pc rings in $LnPc_2^-$ are stronger than in $Ln(OEP)_2$. On the other hand, potential gaps obtained in this work are less than 1.52 V, the potential gap predicted for dimers [11]. The potential gaps for monomers are near 1.90 V [11].

Table 4.3 Potential gaps, $\Delta E^0_{1\,2}$ of diphthalocyanine complexes.

Complex	$\Delta E^0_{1\,2}$ (V) in CH_2Cl_2	$\Delta E^0_{1\,2}$ (V) in DMF
$NdPc_2^-$	1.26	1.25
$EuPc_2^-$	1.23	1.20
$DyPc_2^-$	1.21	1.17
$TmPc_2^-$	1.16	1.10
$LuPc_2^-$	1.12	1.00
$SnPc_2$	0.91	0.87

Since the potential gap, $\Delta E^0_{1\,2}$ characterises the exciton coupling in dimers which decrease with the ionic radius of lanthanide diphthalocyanine, $\Delta E^0_{1\,2}$ was plotted against the inverse of ionic radii to confirm the relationship between the potential gap and the Q band splitting. Fig. 4.7 illustrates that the $\Delta E^0_{1\,2}$ changes with the inverse of ionic radii throughout the lanthanide series. The variation of potential gaps of diphthalocyanine complexes with the ionic radii of lanthanides shows that redox potentials of diphthalocyanine complexes are related to the ring-ring distance throughout the lanthanide series. The difference in $\Delta E^0_{1\,2}$ in CH_2Cl_2 and DMF could just be explained in terms of the different solubilities of a given lanthanide diphthalocyanine complex in both solvents and the electronegativity of the solvent.

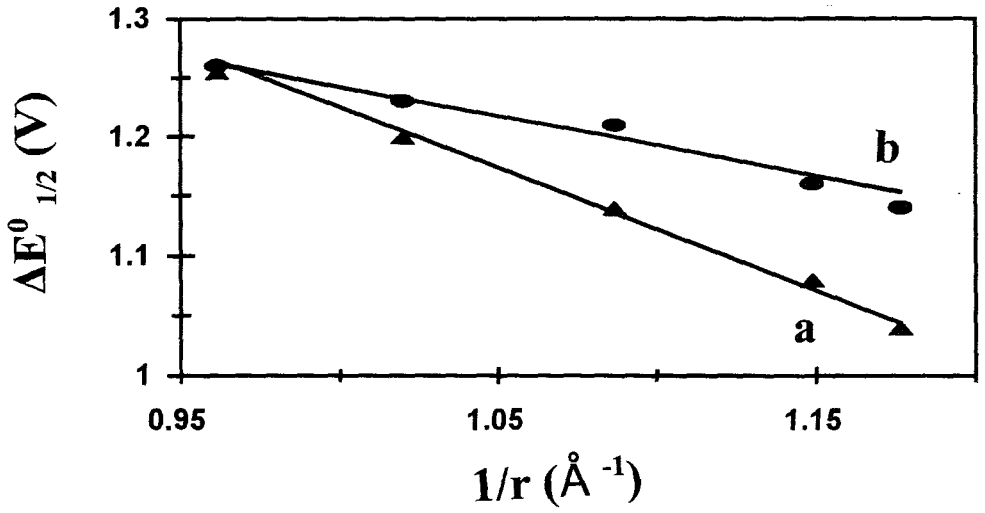

Fig. 4.7 Changes of potential gaps, $\Delta E^0_{1/2}$ versus the inverse of the lanthanide ion radius 1/ r for different lanthanide diphthalocyanine complexes in DMF (a) and CH_2Cl_2 (b).

4.3.2 Spectroelectrochemistry of lanthanide diphthalocyanine complexes

Spectroscopic data for the various oxidation and reduction products of lanthanide diphthalocyanine complexes have been widely reported, due to the good reversibility of their couples compared to $SnPc_2$ and $ZrPc_2$ [61]. Thus, the electronic spectra of $[Pc(-1)LnPc(-1)]^-$, [Pc(-1)LnPc(-2)], $[Pc(-2)\ LnPc(-2)]^-$ and $[Pc(-2)LnPc(-3)]^{2-}$ have been reported for several lanthanide diphthalocyanine complexes [31, 56].

Fig. 4.8 (a) shows the electronic spectrum of the blue form of dysprosium diphthalocyanine, $DyPc_2$ with the characteristic splitting of the Q band due to the exciton coupling interaction. Similar electronic spectra were observed in this work for $SnPc_2$ and for UPc_2 [37].

Fig. 4.8 (b) shows the spectrum of the blue form of dysprosium diphthalocyanine in dichloromethane. The new green ($DyPc_2$) complex was formed instantly when blue form of dysprosium diphthalocyanine was dissolved in dichloromethane. This means that the dichloromethane alone oxidizes spontaneously the blue form of lanthanide diphthalocyanine complexes. It has been reported that photogeneration to green forms of lutetium, neodymium and lanthanum diphthalocyanines was facilitated by the presence of dichloromethane in the solvent mixture of dichloromethane and methanol [90].

When the original blue dysprosium diphthalocyanine was dissolved in dichloromethane, the two absorption bands in the Q band region at 621 and 669 nm disappeared and resulting in a new intense band at 665 nm and a shoulder at 602 nm. In the region of 450-480 nm, a new band was observed at 462 nm, while the B band decreased in intensity and shifted to lower wavelengths. The band observed at 462 nm characterises the intramolecular transition into the SOMO of the radical complex [11]. The electronic spectrum of the new complex is similar to the absorption spectrum of the radical complex, $LuPc_2$ reported by other groups [23,45,56, 68,150].

The dysprosium diphthalocyanine, $DyPc_2$ possesses a dianion Pc(-2) ring and an unpaired-electron Pc ring, Pc(-1) bound to a central lanthanide metal [49]. There is still a lack of information concerning the role played by the nature of the central lanthanide on the structure and

the electrochemical properties of these complexes [150]. The green colour of the new complex and the absorption spectral features confirm that the complex formed is a radical species denoted as Pc(-1)DyPc(-2). Other lanthanide diphthalocyanine complexes used in this work behaved in a similar manner when dissolved in dichloromethane.

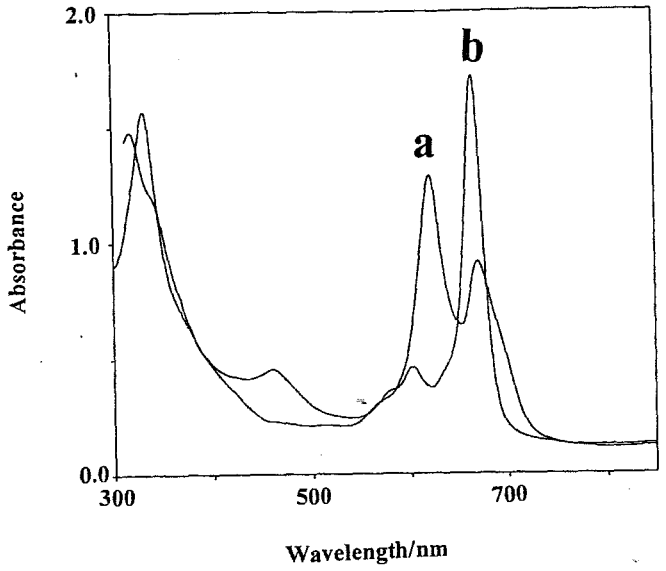

Fig. 4.8 Electronic absorption spectra of $DyPc_2^-$ in DMF (a) and in CH_2Cl_2 (b).

Oxidation of dysprosium diphthalocyanine once in dichloromethane required an anodic potential. Fig. 4.9 shows the electronic spectral changes observed on oxidation of dysprosium diphthalocyanine dissolved in CH_2Cl_2/ TBAP at a potential of 0.4 V. At this potential, the absorption bands of green species at 665 nm and 462 nm disappeared, and two new bands were observed at 710 and 494 nm. Both bands are typical of the π-cation radical species. The electronic spectrum of oxidation product of the green lutetium diphthalocyanine, $LuPc_2$ has been reported and is similar to the one observed in this work as illustrated in Fig. 4.9.b [31,56,142].

It has been shown that the band at 710 nm characterises the presence of dimers of the radical species [31]. The electronic spectra shown in Fig. 4.9 was also observed on chemical oxidation of dysprosium diphthalocyanine, $DyPc_2$ using bromine. During the electrooxidation of $DyPc_2$ in CH_2Cl_2, the colour of the solution changed from green to orange. The orange colour was also observed by Castenada et al. [68]. Bulk electrolysis showed that the formation of $[DyPc_2]^-$ species was accompanied by one-electron transfer. All the findings about the electronic spectra and colour change confirm that the oxidation product obtained is the monocation with two identical Pc rings containing unpaired electrons represented as $[Pc(-1)DyPc(-1)]^-$.

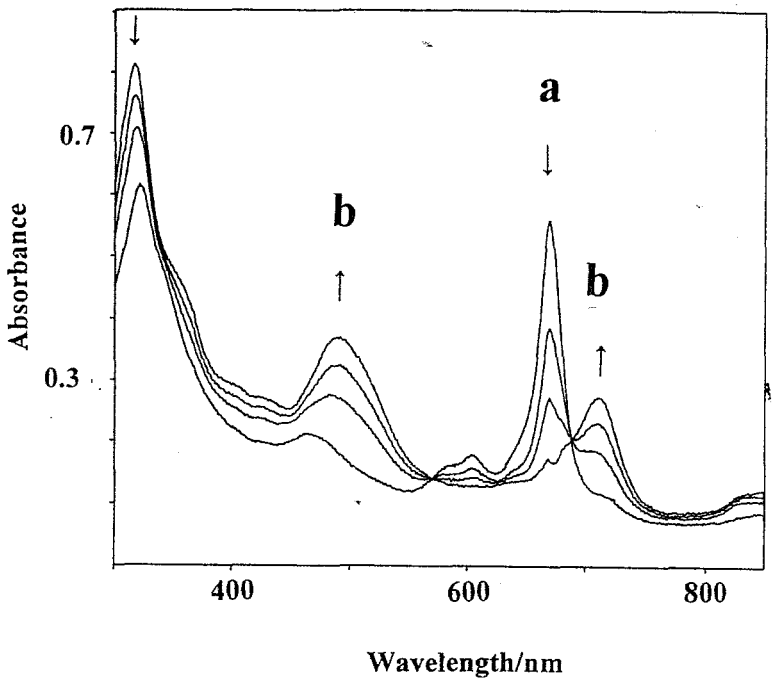

Fig. 4.9 Electronic absorption spectral changes observed during the electrooxidation of Pc(-2)DyPc(-1) (a) to $[Pc(-1)DyPc(-1)]^-$ (b) at potential of 0.4 V in CH_2Cl_2/TBAP system.

Further electrooxidation of $DyPc_2$ in CH_2Cl_2/TBAP (Bu_4NPCl_6) at potential of 0.8 V resulted in a small shift of the band at 710 nm to 720 nm and the disappearance of the band at 494 nm, Fig. 4.10. The new complex obtained was stable for a long period of time and could go back to the orange and then the original green species by lowering the potential to zero. The electronic spectrum of $Lu(2,3\text{-}Nc)_2^{2-}$ has been reported and it is characterized by broad band at 650 nm [15], whereas a single broader band around 720 nm was observed here. The product formed in Fig. 4.10 is associated with the $[DyPc_2]^{2-}$ species. The fact that the bands are observed at different wavelengths in these two complexes could be attributed to the different ring expansion effects [15].

During the electrooxidation of $[DyPc_2]^-$ to $[DyPc_2]^{2-}$, the colour of solution goes from orange to yellow-green. L'her et al. [56] observed the yellow-green species as oxidation product of $LuPc_2$. Bulk electrolysis showed that two electrons were involved in the oxidation process starting from the neutral dysprosium diphthalocyanine, $DyPc_2$ to the species with electronic spectra shown in Fig. 4.10 (b) confirming that the product formed is the $[Pc(0)\ Dy\ Pc(-1)]^{2-}$ species. Other lanthanide diphthalocyanine complexes behaved in the similar manner. Unlike the $[DyPc_2]^-$, the electronic spectrum of $[DyPc_2]^{2-}$ was not observed using bromine as the chemical oxidant.

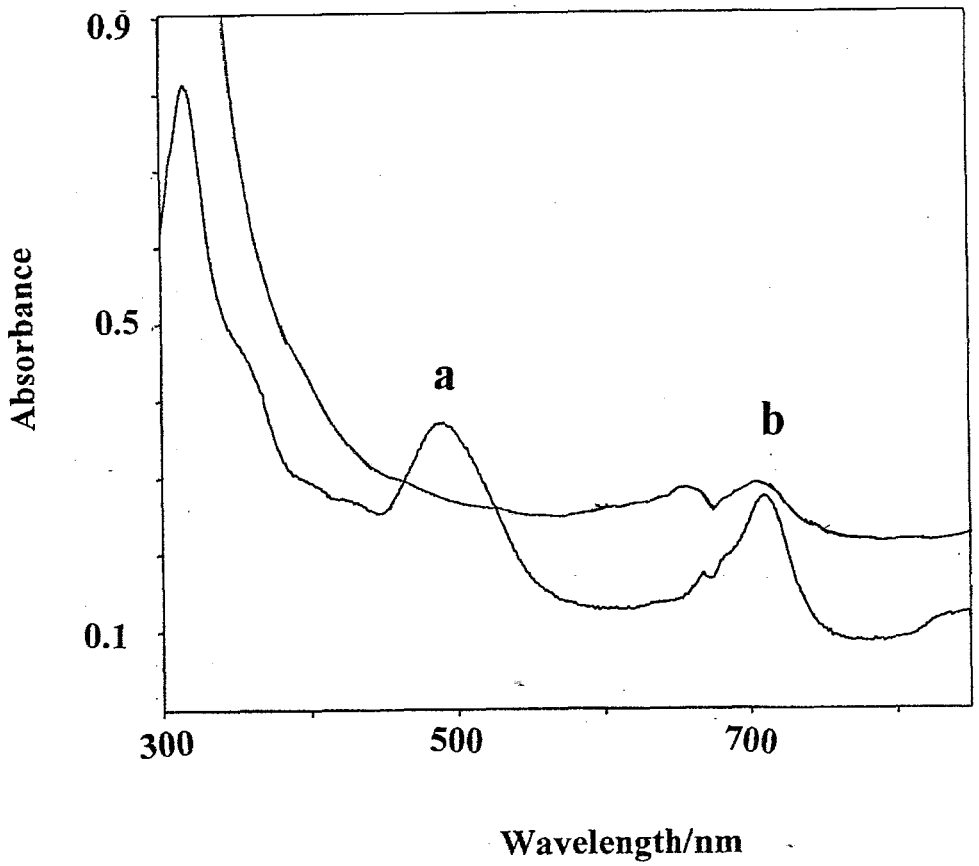

Fig. 4.10 Electronic absorption spectral changes observed during the further electrooxidation of $[Pc(-1)DyPc(-1)]^{-}$ (a) to $[Pc(-1)DyPc(0)]^{2-}$ (b) at 0.8V in CH_2Cl_2/TBAP.

The electroreduction of lanthanide diphthalocyanine complexes in DMF / TEAP solution did not show any change in the electronic spectra of these complexes although two reversible couples were observed in their cyclic voltammetry. But, it has been shown that the reduction of lutetium diphthalocyanine gave a dianionic complex $[Pc(-3)LuPc(-2)]^{2-}$ which is purple coloured [31,142]. The spectroelectrochemical study of lanthanide diphthalocyanine complexes observed in this work can be summarised in Scheme 4.2. It is important to note that colour changes of each

species are associated with electron transfers, and that the transfer of these electrons occur at the Pc rings.

$$\begin{array}{ccc} & \overset{-e^-}{\rightleftharpoons} & \\ Pc(-1)LnPc(-2) & & [Pc(-1)LnPc(-1)]^- \\ & \underset{+e^-}{} & \\ -e^- \downarrow\uparrow +e^- & & +e^- \downarrow\uparrow -e^- \\ [Pc(-2)LnPc(-2)]^- & & [Pc(0)LnPc(-1)]^{2-} \end{array}$$

Scheme 4.2

Table 4.4 gives different colours observed in this work. From this table, it can be seen that the oxidation state of phthalocyanine rings involved in each complex play an important role in the colour changes observed.

Table 4.4 Different colours of diphthalocyanine species.

M^{n-}	Yellow-green	Orange	Green	Blue	Purple
III	$[LnPc_2]^{2-}$	$[LnPc_2]^-$	$LnPc_2$	$[LnPc_2]^-$	$[LnPc_2]^{2-}$ (a)
IV			$[SnPc_2]^-$	$SnPc_2$	$[SnPc_2]^-$
IV(b)			$[ZrPc_2]^-$	$ZrPc_2$	$[ZrPc_2]^-$

(a): [142]

(b): [10].

5. Photochemical reactions of diphthalocyanine complexes

5.1 Photolysis of $SnPc_2$ in the presence of CH_2Cl_2

As discussed in the introduction, alkyl halides are common organic solvents and are also used as efficient anaesthetics. The toxicity of polyhalogenated compounds depends essentially on their metabolism. The one-electron reduction of these polyhalogenated compounds leads to the formation of radicals which are responsible for destruction of the membrane structure in the living cells [152,153].

The fast reduction of these polyhalogenated compounds has been suggested as a possible means of detoxification in living organisms and is also an alternative way of biodehalogenation [154]. For instance, methylene dibromide (CH_2Br_2) and ethylene dibromide (CH_3CHBr_2) have been reduced to methane and ethylene, respectively in the presence of iron (II) deuteroporphyrin. The reactivity of simple alkyl halides vary as follows: RI > RBr > RCl where R is the alkyl radical [154].

The use of visible light for the dehalogenation and the reduction of these alkyl chlorides to alkanes in the presence of porphyrins and phthalocyanines have been discussed [78-80]. The visible-light photooxidation of metalloporphyrins in alkyl chloride solutions containing carbon tetrachloride (CCl_4) and tetrachloroethane (TCE) involves a charge-transfer interaction from the photoexcited porphyrin to CCl_4 or TCE, resulting to the formation of a porphyrin π-cation radical [78]. Generally, the photoreaction can only occur if the alkyl halide exhibits higher oxidation

potential than the porphyrin or phthalocyanine complex [78]. The formation of π-cation porphyrin radical was also observed by the same researchers upon the visible light photolysis of metalloporphyrins in a frozen solution containing CCl_4 and TCE. It was suggested that the lowest singlet excited state is likely to be involved in the electron transfer from the photoexcited porphyrin to the CCl_4 or TCE acceptor, in the same manner as observed at room temperature [79]. In both photochemical reactions at room temperature and in frozen solutions, the mechanisms testify the formation of alkyl radicals which can undergo rapid dimerization reactions or can lead to the formation of alkanes through elimination of chlorides [78,154].

Nyokong and co-workers [80] observed the photooxidation of transition metallophthalocyanines during the visible photolysis of these phthalocyanines in solutions containing carbon tetrabromide, CBr_4 as electron acceptor. The formation of the alkyl radical, $CBr_3^{\cdot}$ followed by its dimerization was then discussed. The main photoproduct was the π-cation radical of phthalocyanines.

From these examples, it is clear that the alkyl halides act as oxidizing agents. The oxidizing power of the alkyl halides have been compared to that of benzoquinones. They both form radicals upon photolysis in the presence of metallophthalocyanines [79,92]. Unlike with benzoquinone, the alkyl halides photooxidize phthalocyanines irreversibly [79].

There is very little information about photochemical properties of diphthalocyanine complexes [48,90], although these complexes show electrochemical, electrochromic, optical and semiconducting behaviour as discussed in the introduction chapter. The photochemical reactions

of lanthanide (III) diphthalocyanine complexes in solutions containing benzoquinone [48] and dichloromethane [90] resulted in the oxidation of lanthanide diphthalocyanines, generating the π-cation radical diphthalocyanine species. This work reports on the photochemical reactions of tin diphthalocyanine, $Sn(IV)Pc_2$ in the solvent mixture containing dichloromethane and acetonitrile. This photoreaction has never been reported before. Laser photolysis studies on tin diphthalocyanine in dichlorobenzene gave $[Sn(IV)Pc]^{2-}$ as one of the transient products [17]. The photochemistry of transition-metal phthalocyanines following ultraviolet irradiation is associated with the population of charge-transfer or nπ* ligand-centered states. The low-lying ^{3} ππ* ligand-centered states are populated by excitations in the Q band region [74-77].

Electronic absorption spectra have been used successfully to monitor changes during the photolysis of metallophthalocyanines in the presence of electron acceptor quenchers [48,78,79,90]. The visible region of the electronic spectra of the neutral Pc(-2)Sn(IV)Pc(-2) species shows an extensive splitting of the Q band when compared to monomeric phthalocyanine complexes as already discussed. Fig. 5.1 shows spectral changes observed when solutions containing $SnPc_2$ in the solvent mixture of dichloromethane and acetonitrile were photolysed with unfiltered radiation from the tungsten lamp. No significant spectral changes were observed when UV radiation was filtered, that is when $\lambda > 590$ nm was employed. The spectral changes in Fig. 5.1 are accompanied by isosbestic points characterizing the presence of two species in solution. The formation of new species is characterised by two new absorption bands at 669 and 470 nm. The electronic spectra of the new species is similar to the absorption spectra of the product of the photolysis of lanthanide diphthalocyanine complexes in the solvent mixture containing dichloromethane and acetonitrile [90]. It has been shown that the appearance of the band at 470

nm is associated to the formation of a radical species of diphthalocyanine complexes [48,90], and characterises the intramolecular transition into the SOMO level [11]. On the other hand, the band at 669 nm was also observed by Kasuga et al. [48,90] and it represents a dianion phthalocyanine ring. Thus, the product formed upon photolysis of a solution containing $SnPc_2$ in the solvent mixture of dichloromethane and acetonitrile is a radical tin diphthalocyanine species, [Pc(-2)Sn(IV)Pc(-1)]$^{\cdot}$.

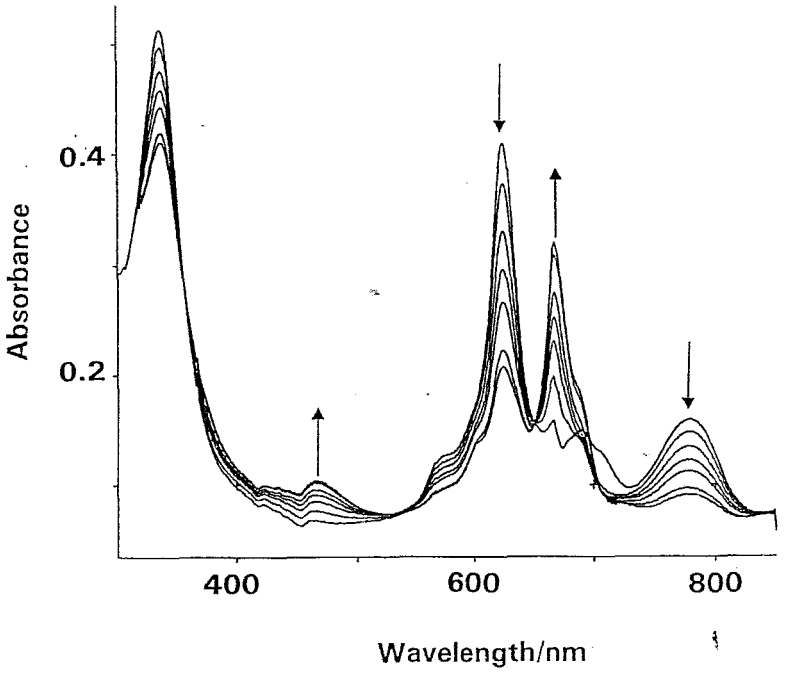

Fig. 5.1 Electronic absorption spectral changes observed during the photolysis of a solution containing 3.5 x10 $^{-6}$ mol dm $^{-3}$ of $SnPc_2$ in the solvent mixture containing 90% of CH_2Cl_2 and 10 % CH_3CN.

Apart from the two absorption bands associated with the formation of [Pc(-2)Sn(IV)Pc(-1)]$^{\cdot}$, the electronic spectra observed following photolysis showed a shoulder at 691 nm. Photolysis (λ_{exc} = 640 nm) of $SnPc_2$ in chlorobenzene by Kraut et al [17], showed a band at 694 nm which was

assigned to the presence of monophthalocyanine product, $[Sn(IV)Pc]^{2-}$. In this work, the new absorption band at 691 nm was also attributed to the parallel formation of Sn(IV) monophthalocyanine product. The slight difference in the position of this band can be associated with some differences in the solvent.

It is important to note that in the absence of dichloromethane, the π-cation $[Pc(-2)SnPc(-1)]^{-}$ radical was not generated. It is most likely that the role of acetonitrile as a polar solvent was to stabilize the excited states [97]. Solutions of $SnPc_2$ in dichloromethane and in the absence of acetonitrile were photolysed with unfiltered radiation from the 50 Watt tungsten lamp, spectral changes shown in Fig. 5.2 were observed. Three new bands were observed at 470, 669 and 691 nm as observed in Fig. 5.1, showing the formation of $[Pc(-2)Sn(IV)Pc(-1)]^{-}$. However, the band at 691 nm was more enhanced in the absence of CH_3CN, showing that the Sn(IV) monophthalocyanine species is more enhanced under these conditions. This observation confirms that dichloromethane acts as a quencher whereas acetonitrile simply stabilizes the excited states. The $[Pc(-2)Sn(IV)Pc(-1)]^{-}$ species was not formed unless dichloromethane was in excess in the acetonitrile/dichloromethane solvent mixture.

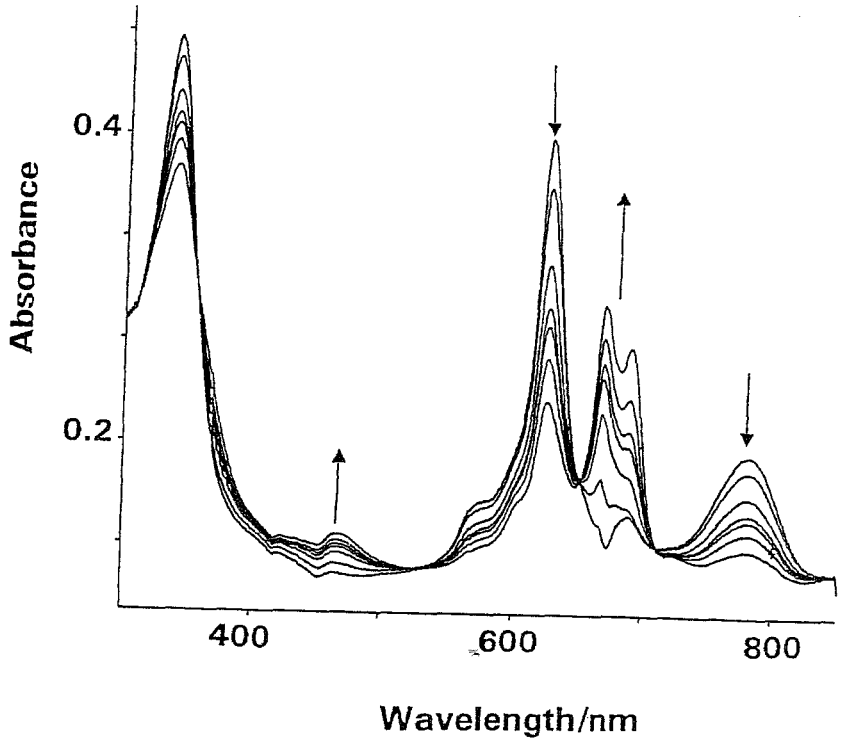

Fig. 5.2 Absorption spectral changes observed during the photolysis of a solution of 4.3 x 10^{-6} mol dm^{-3} of $SnPc_2$ in dichloromethane after 120 minutes.

5.1.1 Kinetic studies for the photolysis of $SnPc_2$ in the presence of CH_2Cl_2

Absorption spectra have been used successfully to study kinetic behaviour of chemical and photochemical reactions. Photolysis of $SnPc_2$ in the solvent mixture of dichloromethane and acetonitrile were followed by monitoring the disappearance of the absorption band of the neutral species, $SnPc_2$ at 624 nm. In this study, the concentration of $SnPc_2$ was kept constant in all experiments while the concentration of CH_2Cl_2 was in excess and was varied from 70 % to 95 % by volume of the solvent mixture (10.82 to 14.69 mol dm^{-3}). A 3ml (1cm pathlength)

spectrophotometric cell was used. Fig. 5.3 shows the changes in absorbance with time when a solution containing $5x10^{-5}$ mol dm^{-3} $SnPc_2$ in a mixture of CH_2Cl_2 and CH_3CN (90:10) was photolysed. The concentration of CH_2Cl_2 was in excess hence pseudo-first order conditions were assumed.

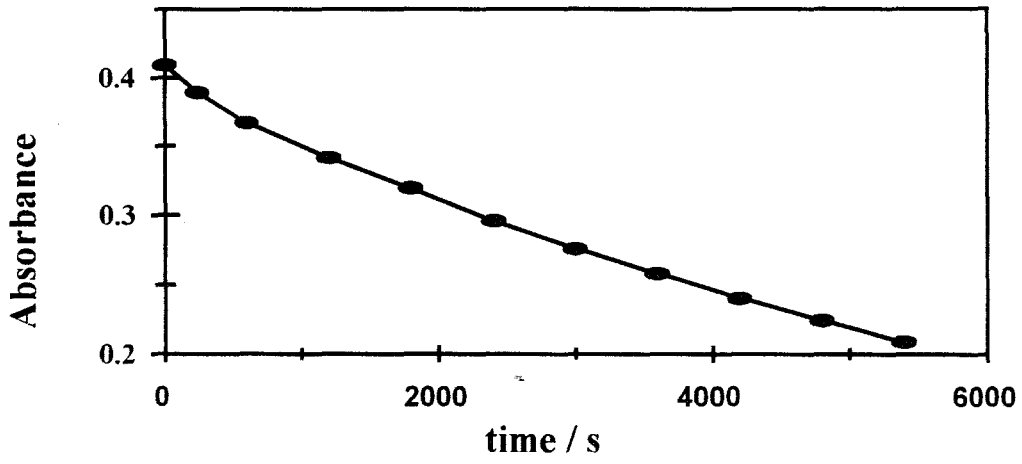

Fig. 5.3 Changes of Pc(-2)Sn(IV)Pc(-2) absorbance at 624 nm with the photolysis time during the photolysis of $5x10^{-5}$ mol dm^{-3} of $SnPc_2$ in the solvent mixture containing 90 % CH_2Cl_2 and 10 % CH_3CN.

Under these conditions the rate law observed as follows:

$$\frac{-d([Pc(-2)Sn(IV)Pc(-2)])}{dt} = k_{obs}[Pc(-2)Sn(IV)Pc(-2)] \qquad (5.1)$$

Where k_{obs} is the rate constant observed for the disappearance of $SnPc_2$ at a given concentration of CH_2Cl_2. The plot of the Log (A_t-A_∞) (where A_t is absorbance at time t and A_∞ is the absorbance at infinity) versus time for 80 % of the disappearance of $SnPc_2$, is linear showing that the photolysis of $SnPc_2$ in the solvent mixture containing dichloromethane and acetonitrile follows a first order in $SnPc_2$. (Fig. 5.4).

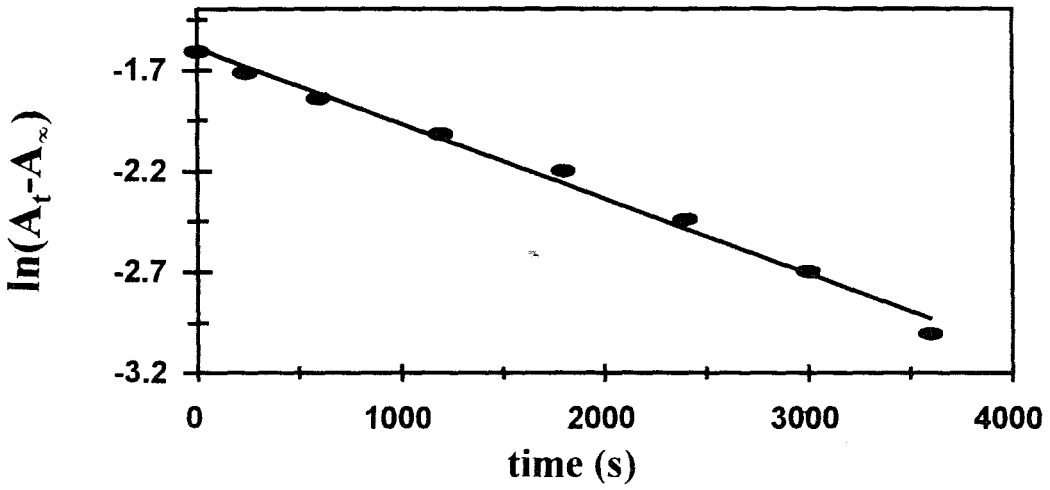

Fig. 5.4 Plot of Ln(A_t-A_∞) versus time for the visible photolysis of $SnPc_2$ in the solvent mixture containing 90 % CH_2Cl_2 and 10 % CH_3CN.

Kasuga et al. [48], also observed pseudo-first order kinetics during the photolysis of lanthanide diphthalocyanine complexes in the presence of p-benzoquinone. The slopes of the plots exemplified by Fig. 5.4 gave the observed rate constants, k_{obs}, which increased with the increase

of the volume (or concentration) of dichloromethane in the solvent mixture, and obey the following relationship [155]:

$$k_{obs} = k_f [CH_2Cl_2] + k_r \qquad (5.2)$$

where k_f is the rate constant of formation of $[SnPc_2]^-$ and is obtained from the slope of the k_{obs} versus the concentration of CH_2Cl_2 plot, whereas k_r is the rate constant for the reverse reaction regeneration of $SnPc_2$, and it is determined as the intercept of the plot. Fig. 5.5 shows the plot of k_{obs} versus the concentration of CH_2Cl_2. A straight line obtained in this plot confirms the involvement of CH_2Cl_2 in the photooxidation of $SnPc_2$. k_f was determined to be $4.7 \pm 0.16 \times 10^{-5}$ mol $^{-1}$ dm ^{3} s $^{-1}$. Fig. 5.4 also confirms that the interaction between photoexcited $SnPc_2$ and CH_2Cl_2 is first order in CH_2Cl_2.

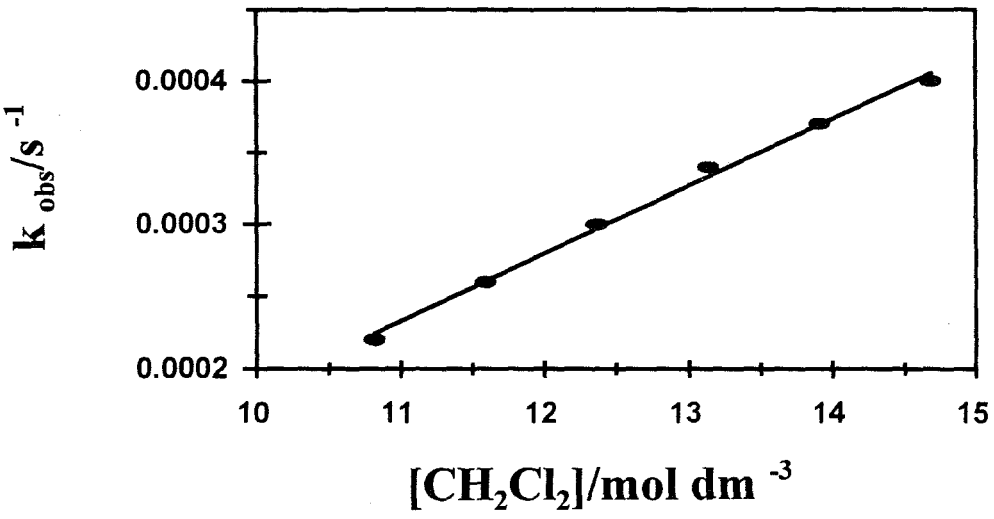

Fig. 5.5 Plot of k_{obs} versus $[CH_2Cl_2]$ for the photolysis of $SnPc_2$ in the CH_2Cl_2/ CH_3CN solvent mixture.

5.1.2 Determination of quantum yields for the photoreaction of $SnPc_2$ with CH_2Cl_2

The relative quantum yields determined in the photolysis of lanthanide diphthalocyanine complexes in the presence of dichloromethane increased with the increase of the concentrations of CH_2Cl_2 [90]. In this work, the quantum yields for the photolysis of $SnPc_2$ in the presence of CH_2Cl_2 also increased with the increase of CH_2Cl_2 concentrations according to the following relationship [88, 158]:

$$\frac{1}{\Phi} = \frac{1}{\Phi^0} + \frac{k_d}{\Phi^0 k_f} \frac{1}{[CH_2Cl_2]} \qquad (5.3)$$

Where k_f is the rate constant of formation and k_d is the decay rate constant. The value of $1/\Phi^0$ is obtained from the intercept from the Stern-Volmer plot ($1/\Phi$ versus $1/[CH_2Cl_2]$), Fig. 5.6. Φ^0 is the limiting quantum yield. The Stern-Volmer plot confirms that CH_2Cl_2 was used as a quencher in this particular reaction.

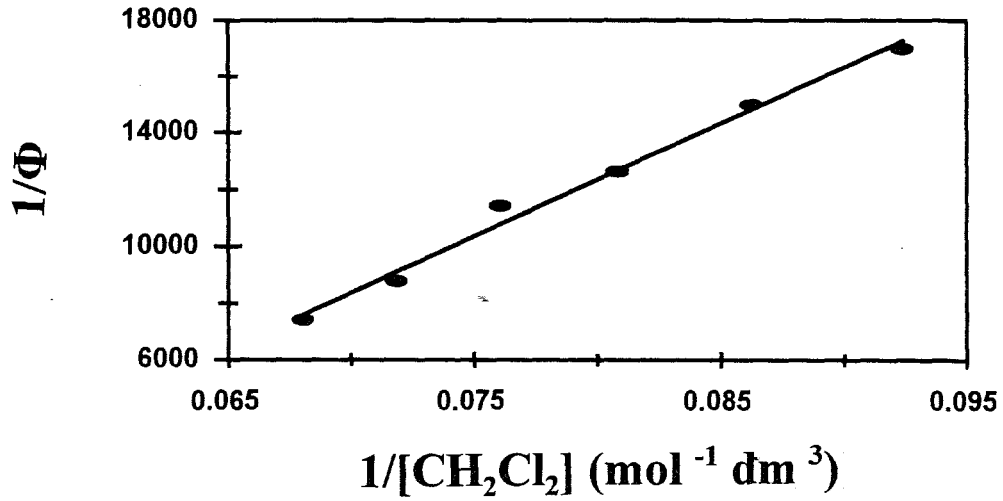

Fig. 5.6 Plot of $1/\Phi$ versus $1/[CH_2Cl_2]$ for the photolysis of $SnPc_2$ in the CH_2Cl_2/ CH_3CN solvent mixture.

The ratio k_d/k_f is called the β-value [158]:

$$\beta = \frac{k_d}{k_f} \qquad (5.4)$$

β is the decay constant of the complex in a particular solvent and is a solvent dependent for a certain quencher [158]. Similar values of β are very unlikely to be obtained for redox reactions or electron transfer reactions from an excited state [158]. In this case, the β-value of $SnPc_2$ in the CH_2Cl_2/CH_3CN solvent mixture was found to be negative (- 20.4). The β-values found in the literature are in the range of 3×10^{-5} to 1×10^{-4} [158] when electron-transfer exchanges from excited states were not involved.

However, the quantum yields of disappearance of $SnPc_2$ obtained are very low compared to those reported for the photolysis of lanthanide diphthalocyanine complexes in the solvent mixture containing dichloromethane and acetonitrile [90]. In this work the quantum yields obtained are in the order of 10^{-4}.

Despite the fact that both reactions are controlled by the phthalocyanine rings and that the electrochemistry of diphthalocyanine complexes shows that there is a stronger interaction between the Pc rings in $SnPc_2$, the high quantum yields for $LuPc_2^-$ can be associated with their anionic nature. It is also important to note that quantum yield may vary due to differences in the conditions of photolysis.

5.1.3 Mechanism of photooxidation of $SnPc_2$ in the presence of CH_2Cl_2

Photolysis of $SnPc_2$ in the presence of CH_2Cl_2 is assumed to occur in the triplet excited state of $SnPc_2$ as observed by Kasuga et al. [48,90] for the photolysis of $LnPc_2$ in CH_2Cl_2. The formation of radical species, $[Pc(-2)Sn(IV)Pc(-1)]^-$ shows that the photolysis is consistent with one-electron

transfer process. The linear Stern-Volmer plot confirmed that CH_2Cl_2 acts as a quencher in the photoreaction.

In general, irradiation of metallophthalocyanine dimers, $(MPc)_2$, at wavelengths of the Q band produce low-lying $^3\pi\pi^*$ states, but irradiation in the Soret region generally populates $^*n\pi$ states and induces photoredox reactions of the type described in the following Scheme [156]:

$$(M(II)Pc)_2 \xrightarrow{hv} [M(I)Pc(-2)]^- + [M(III)Pc(-2)]^+ \quad (5.5)$$

OR

$$(M(II)Pc)_2 \xrightarrow{hv} [M(II)Pc(-3)]^- + [M(II)Pc(-1)]^+ \quad (5.6)$$

Scheme 5.1

The mechanism of the photooxidation of $SnPc_2$ could be based on the assumption that an electron was transferred from the photoexcited state $n\pi^*$ $SnPc_2$ to the acceptor CH_2Cl_2. CH_2Cl_2 exhibits a higher oxidation potential of 1.35 V (versus SCE) [157] compared to [Pc(-2)Sn(IV)Pc(-2)] with an oxidation potential of 0.35 V (versus SCE in CH_2Cl_2/TBAP system in this work), which means that the thermodynamic requirement for the photooxidation of [Pc(-2)Sn(IV)Pc(-2)] by CH_2Cl_2 is fulfilled [78-80].

In comparison with the lanthanide bisphthalocyanines [90], the photolysis of $SnPc_2$ in CH_2Cl_2/CH_3CN mixture may be represented as follows:

$$[Pc(-2)Sn(IV)Pc(-2)] \overset{h\nu}{\rightleftarrows} *[Pc(-2)Sn(IV)Pc(-2)] \quad (5.7)$$

$$*[Pc(-2)Sn(IV)Pc(-2)] + CH_2Cl_2 \overset{kq}{\rightarrow} [Pc(-2)Sn(IV)Pc(-1)]^+ + CH_2Cl^{\cdot} + Cl^- \quad (5.8)$$

Scheme 5.2

The $CH_2Cl^{\cdot}$ radical undergoes rapid dimerization reactions, resulting in the formation of alkane derivatives through the elimination of chloride [78].

5.2 Photolysis of diphthalocyanines in the presence of SO_2

Sulfur dioxide is a pollutant which is found in photochemical smog with a concentration of 20 pphm (1 pphm represents a concentration of $4x10^{-10}$ mol dm^{-3}) [159]. It has been shown that atmospheric pollution in the east and mid-west of USA, as well as in Europe involves higher concentrations of SO_2, and as reducing agent, it leads to the formation of sulfuric acid causing economic damage by corrosive action on structural stone and metals [159]. Thus, the oxidation of SO_2 to sulfur (VI) species is of current industrial and environmental interests. The coordination of sulfur dioxide to metalloporphyrins, followed by an electron transfer reactions provids a useful method for converting harmful sulfur dioxide to their less harmful analogues

[108,160,161]. The dinuclear μ-peroxo(tetraphenyl porphyrinato) iron (III), (TPP)Fe-O-O-Fe(TPP), species reacted with SO_2 in the presence of molecular oxygen to give μ-sulphato iron (III) complex, $[(TPP)Fe]_2 SO_4$ [160]. In the similar way, the mononuclear peroxo iron (III) complex, $(TPP)FeO_2$ and the peroxotitanium(IV) complex, $(TPP)TiO_2$ gave $(TPP)FeSO_4$ and $(TPP)TiSO_4$, respectively in the presence of SO_2 [160].

In addition, Zagal [106] showed that iron(II) (FePc) and cobalt(II) (CoPc) phthalocyanines, exhibited catalytic activities towards the oxidation of SO_2 in acid medium. Moreover, Nyokong [86] reported the photochemical interaction between tin phthalocyanine, $Sn(IV)Pc(L)_2$ and SO_2. It was shown that the photoexcited $^3\pi\pi^*$ Sn(IV)Pc species interacted with SO_2, followed by an electron transfer from the photoexcited complex to the electron acceptor, SO_2.

5.2.1 Photolysis of $SnPc_2$ in the presence of SO_2*

The electronic absorption spectra have been used successfully to monitor the formation of the product during the irradiation of metal diphthalocyanine complexes in the presence of quenchers [48,90] and allowed the characterization of various anionic and cationic species of these complexes [31,45]. The electronic spectrum of the neutral species of tin diphthalocyanine, Pc(-2)Sn(IV)Pc(-2) is well characterised as reported in its earlier photolysis in the presence of CH_2Cl_2.

---

*. The following publication resulted from work presented in this section: N. Nensala, A. Nzimande and T. Nyokong. J. Photochem. Photobiol. A: Chem., 98 (1996), 129.

When solutions of $SnPc_2$ in dichloromethane containing SO_2 were irradiated with unfiltered radiation, the electronic absorption spectra of the original $SnPc_2$ showed changes in the Q band region illustrated in the Fig. 5.7. The original bands located at 573, 624, 692 and 779 nm decreased in intensity and three new bands were formed isosbestically at 470, 603, and 669 nm. An additional band at 691 nm formed as a shoulder. The isosbestic points are clearly observed at 352, 532, 646 and 707 nm and characterise the presence of two species only in solution. In addition, the colour of the solution goes from blue to green.

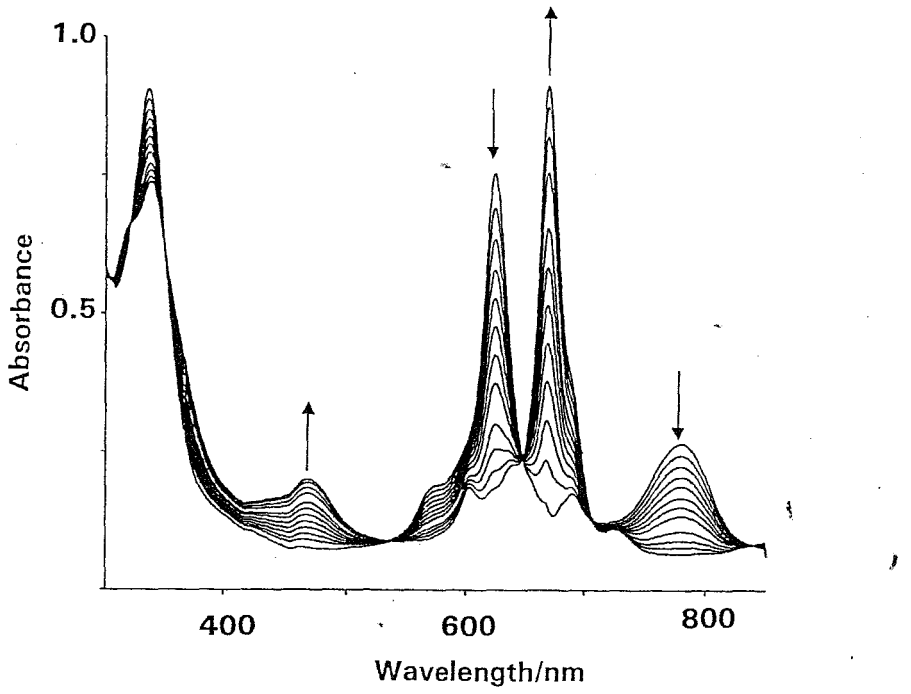

Fig. 5.7 Electronic absorption spectral changes of [Pc(-2)Sn(IV)Pc(-2)] upon photolysis in the presence of SO_2, with unfiltered light from a tungsten lamp. $[SnPc_2] = 6.5x10^{-6}$ and $[SO_2]= 6x10^{-3}$ mol dm^{-3}

The electronic absorption spectra which resulted from the photolysis of [Pc(-2)Sn(IV)Pc(-2)] in the presence of SO_2 look similar to the electronic absorption spectra observed during the photolysis of this complex in the solvent mixture of dichloromethane and acetonitrile. On the other hand, similar electronic absorption spectra were also reported during the photolysis of lanthanide diphthalocyanine complexes in a solution containing p-benzoquinone [48]. As discussed in Section 5.1 for the photolysis of $SnPc_2$ in the presence of CH_2Cl_2, the band at 470 nm is characteristic of radical species and the band at 669 nm characterises a dianion Pc ring. The shoulder observed at 691 nm is consistent with the presence of monomeric product, $[Sn^{IV}Pc]^{2-}$ [17]. The green colour of the double decker phthalocyanine complexes is characteristic of the neutral form in which one Pc ring has an unpaired-electron [23,45]. From these findings, the product formed upon photolysis of [Pc(-2)Sn(IV)Pc(-2)] in the presence of SO_2 is the radical species, $[Pc(-2)Sn(IV)Pc(-1)]^{\cdot}$, as was also the case with photolysis in CH_2Cl_2 in the absence of SO_2.

When solutions of $SnPc_2$ in dichloromethane and containing SO_2 were photolysed with filtered radiation ($\lambda > 590$ nm), the Q band region of $SnPc_2$ showed changes which differ from the absorption spectra with unfiltered radiation, Fig. 5.8. There is very little decrease of the bands due to the original $SnPc_2$ and small bands developed at 669 and 691 nm. There was more enhancement of the band at 691 nm indicating the predominance of the monomeric tin phthalocyanine, $[Sn^{IV}Pc]^{2-}$ in solution.[17], and suggesting that the monomeric species is formed as a result of visible radiation of $SnPc_2$ species. The band at 470 nm previously assigned to the radical species did not develop in this case. Thus, unfiltered radiation is necessary for the photolysis.

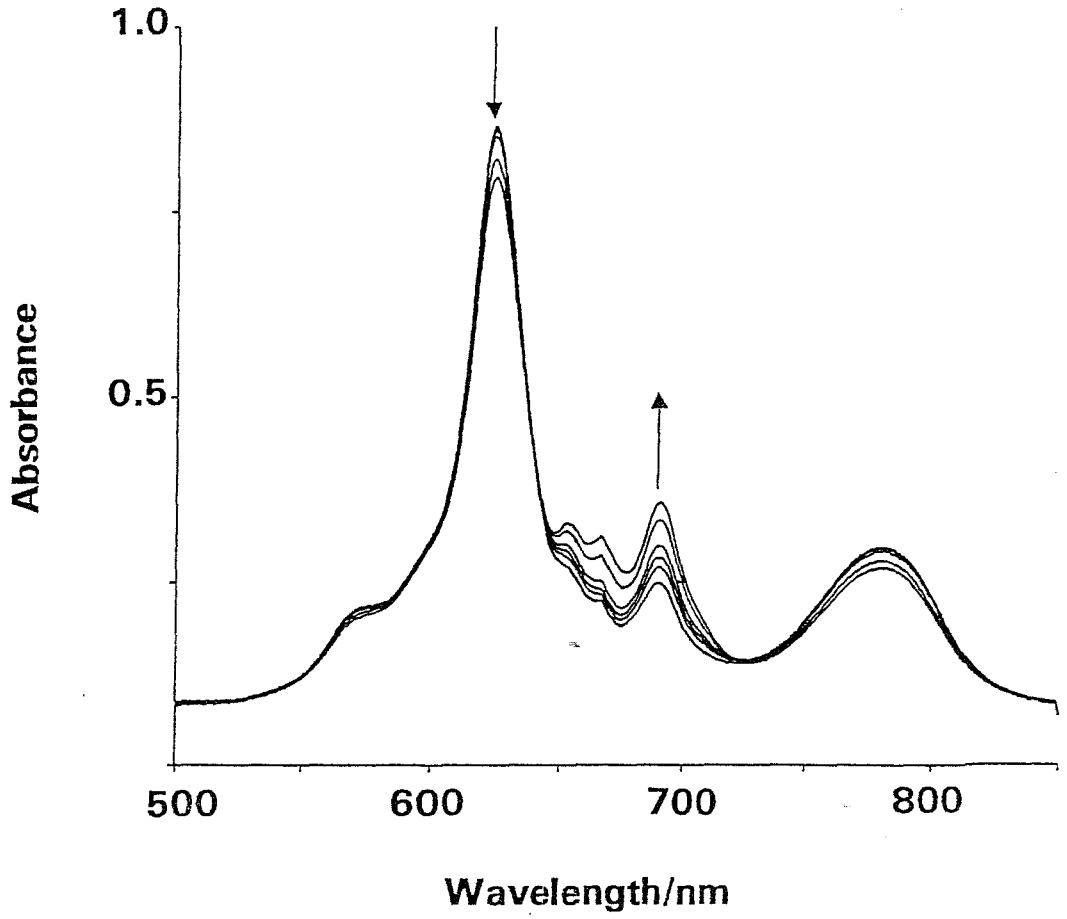

Fig. 5.8 Electronic absorption spectral changes observed during the photolysis of $SnPc_2$ in dichloromethane containing SO_2, with irradiation light of $\lambda > 590$ nm. $[SnPc_2] = 6x10^{-6}$ $[SO_2] = 8x\ 10^{-3}$ mol dm $^{-3}$

Under the present experimental conditions, it cannot be ruled out that the possibility of CH_2Cl_2 being also excited by the ultra-violet radiation. However, earlier studies showed that the oxidized species was formed from the lanthanide bisphthalocyanine complexes on photolysis at wavelengths that were high enough to exclude the possibility of exciting CH_2Cl_2 [90].

Similar experiments using unfiltered radiation were performed in nitrobenzene and in chlorobenzene/methanol solvent mixture. In all these solvents, the formation of the radical species [Pc(-2)Sn (IV)Pc(-1)] $^{-}$ was observed when unfiltered radiation was used.

5.2.1.1 Kinetic studies of the photoreaction of $SnPc_2$ with SO_2

Kinetic studies of the visible photolysis of $SnPc_2$ in dichloromethane containing SO_2 were performed by monitoring the absorption spectral changes for the disappearance of $SnPc_2$ at 624 nm, with the photolysis time. Fig. 5.9 shows the changes in absorbance with time during the photolysis of $SnPc_2$ in the presence of SO_2. The concentration of $SnPc_2$ was kept constant at 6.51×10^{-6} mol dm $^{-3}$ while the concentration of SO_2 was varied from 1.13×10^{-3} to 5.67×10^{-3} mol dm $^{-3}$ and was in excess compared to $SnPc_2$ concentration, giving pseudo first order conditions.

$$\frac{-\,d\,([Pc(-2)Sn(IV)Pc(-2)])}{d\,t} = k_{obs}\,[\,Pc(-2)Sn(IV)Pc(-2)] \qquad (5.9)$$

The plot of ln (A_t-A_∞) versus time showed a straight line, thus confirming that the interaction between photoexcited $SnPc_2$ and SO_2 is first order in $SnPc_2$, Fig. 5.10. The slopes of the plot of ln(A_t -A_∞) gave k_{obs}.

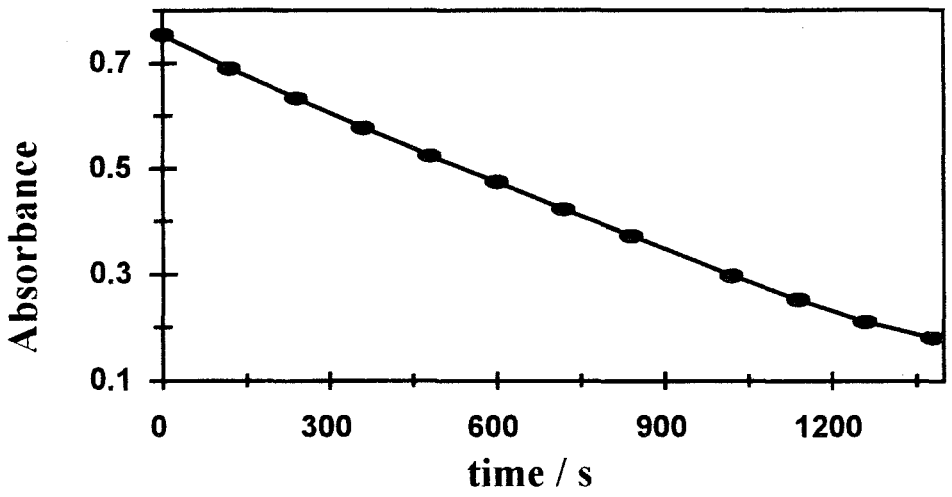

Fig. 5.9 Changes of the absorbance of [Pc(-2)SnPc(-2)] at 624 nm with time following photolysis of $SnPc_2$ in dichloromethane containing SO_2. $[SnPc_2] = 6.51 \times 10^{-6}$ and $[SO_2] = 6 \times 10^{-3}$ mol dm $^{-3}$.

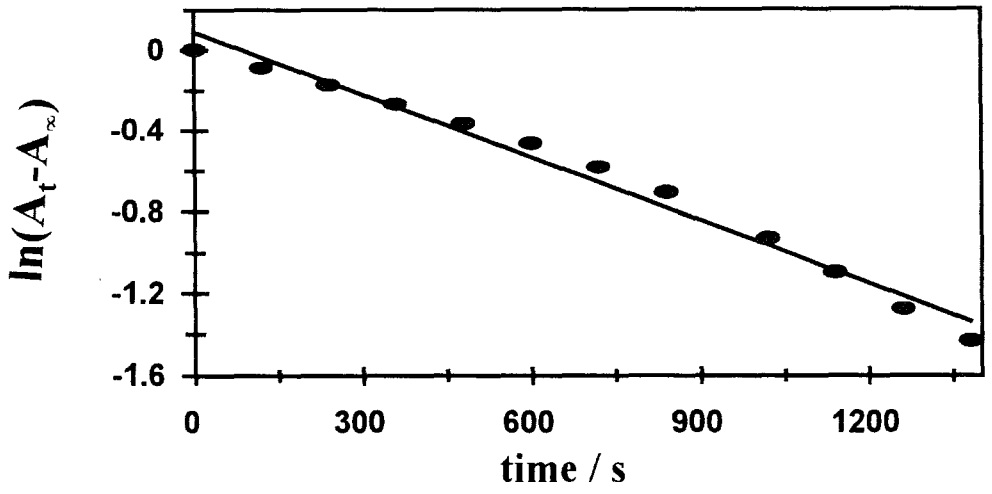

Fig. 5.10 Plot of Log (A_t-A_∞) versus time for the photolysis of a solution 6.5 x10 $^{-6}$ mol dm $^{-3}$ $SnPc_2$ in dichloromethane containing 6x10 $^{-3}$ mol dm $^{-3}$ SO_2.

It has been shown that the observed rate constants of the photolysis of lanthanide diphthalocyanine complexes in the presence of p-benzoquinone and CH_2Cl_2 increased with the increase of the concentrations of these oxidants [48,90]. The photolysis of $SnPc_2$ discussed above in solvent mixture containing dichloromethane and acetonitrile also showed that the observed rate constants increased with the increase of the concentrations of CH_2Cl_2. Moreover, the observed rate constants obtained in the photooxidation of $SnPc_2$ in the presence of SO_2 are higher than the observed rate constants during the photolysis of $SnPc_2$ in CH_2Cl_2 and in absence of SO_2, although the quencher CH_2Cl_2 was used in higher concentration compared to SO_2. This fact could be explained in terms of the different reactivities of SO_2 and CH_2Cl_2, suggesting that SO_2 is more efficient quencher of the excited $SnPc_2$ * than CH_2Cl_2.

The observed rate constants are related with the concentration of a quencher according to the Equation 5.10:

$$\mathbf{k}_{obs} = \mathbf{k}_f [\mathbf{SO_2}] + \mathbf{k}_d \qquad \textbf{(5.10)}$$

Fig. 5.11 shows the plot of observed rate constants, k_{obs} versus the concentration of SO_2. The linearity of the plot confirms that SO_2 was involved as a quencher in the photolysis of $SnPc_2$ and that the rates of photoreaction depend directly on the concentration of SO_2. Thus, the reaction is first order in terms of SO_2 .

The slope of the plot gave the rate constant of formation of [$SnPc_2$], $k_f = 0.1577 \pm 0.0052$ mol $^{-1}$ dm ^{3} s^{-1} and the rate constant of the reverse reaction is $k_r = 2.2 \pm 1.9 \times 10^{-5}$ s $^{-1}$ was obtained from the intercept of the plot.

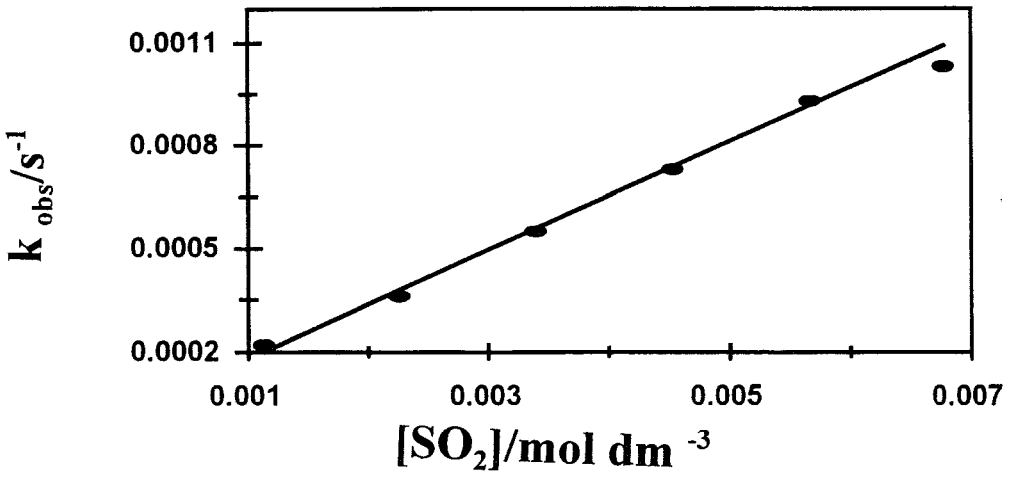

Fig. 5.11 Plot of k_{obs} versus concentrations of SO_2 for the photolysis of $SnPc_2$ in dichloromethane containing SO_2.

5.2.1.2 Determination of quantum yields of photolysis of $SnPc_2$ in the presence of SO_2

The quantum yields of disappearance of $SnPc_2$ following visible photolysis in the presence of SO_2 were determined in the similar way as for CH_2Cl_2. Kasuga et al. [90] observed that quantum yields were increasing with the increase of the concentration of quencher CH_2Cl_2. In the photolysis of $SnPc_2$ in the presence of CH_2Cl_2 discussed in section 5.1.2, the quantum yields also increased with the increase of the concentration of CH_2Cl_2. Quantum yields and concentration of SO_2 are related by Equation 5.11 [158]:

$$\frac{1}{\Phi} = \frac{1}{\Phi^0} + \frac{k_d}{\Phi^0 k_f} \frac{1}{[SO_2]} \qquad (5.11)$$

The symbols for this equation are defined for Equation 5.3. The decay constant, β (Equation 5.4) for $SnPc_2$ in dichloromethane was found to be 3.232 which is far higher than those values found in the literature. But, in this case, β is meaningless.

Fig. 5.12 shows a Stern-Volmer plot for the interaction of SO_2 with photoexcited $SnPc_2$. The linearity of the plot supports the idea that SO_2 is a quencher in the photoreaction. The quantum yield values for the photolysis of $SnPc_2$ in the presence of SO_2 are higher ($2.8x10^{-4}$- $1x10^{-3}$) than when $SnPc_2$ was photolysed in CH_2Cl_2 ($5.9x10^{-5}$ - $1.4x\ 10^{-4}$), and in absence of SO_2.

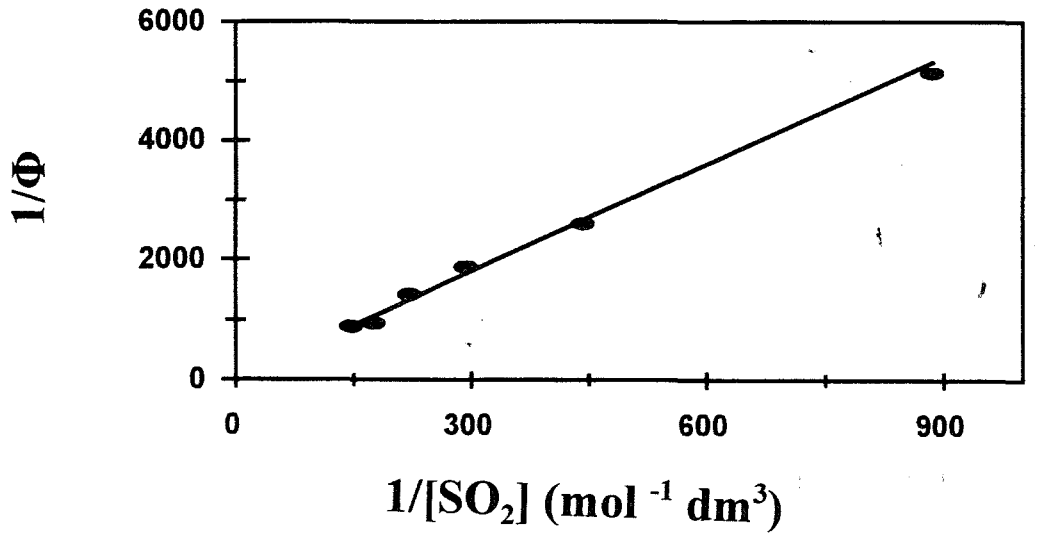

Fig. 5.12 - Plot of 1/ Φ versus 1/ $[SO_2]$ for the photolysis of $SnPc_2$ in dichloromethane containing SO_2.

It is possible that both CH_2Cl_2 and SO_2 quench the excited $SnPc_2$ species and form both the one-electron oxidized, $[Pc(-1)Sn(IV)Pc(-2)]^-$ complex and monomeric MPc species to a varying extent. Irradiation with unfiltered radiation shows that the one-electron oxidized product is favoured by SO_2. The increase of quantum yield with SO_2 concentration, Fig. 5.12, shows that SO_2 quenches the excited state when solutions of Pc_2Sn are photolysed in CH_2Cl_2 in the presence of SO_2. This implies that SO_2 is a better one-electron quencher of the excited state of the Pc_2Sn species than CH_2Cl_2. SO_2 has a relatively high electron affinity, and it is generally even better than O_2 as an electron acceptor [108, 162]. It is thus reasonable to assume that SO_2 will be a better electron transfer quencher than dichloromethane.

However, the quantum yields obtained in the photolysis of $SnPc_2$ in the presence of SO_2 are slightly smaller than the quantum yields reported in the photoinduced radical formation of lanthanide diphthalocyanine complexes photolysed in a solvent mixture of dichloromethane and acetonitrile [90]. The quantum yields of the photolysis of $SnPc_2$ in dichloromethane containing SO_2 were in the order of 10^{-4}, while for the photolysis of lanthanide diphthalocyanine complexes in the solvent mixture of CH_2Cl_2 / CH_3CN, the quantum yields varied from 0.51 to 1.00 [90]. The differences could be due to different lamps used by Kasuga et al..

5.2.1.3 Mechanism of the photolysis of $SnPc_2$ in the presence of SO_2

As discussed in section 5.1.3, irradiation of phthalocyanine dimers , $(MPc)_2$ in the Soret region generally induces photoreactions of the types described in Scheme 5.1. Since UV radiation was not filtered for this particular reaction, it is likely that $n\pi^*$ excited sates are involved. The

mechanism of the visible photolysis of $SnPc_2$ in dichloromethane containing SO_2 can be understood by assuming that the first step of the photolysis is expected to be the photoexcitation of $SnPc_2$ species and then followed by the interaction of the photoexcited $n\pi^*$ $SnPc_2$ species with the SO_2 molecule with subsequent electron transfer from the photoexcited complex to SO_2 as follows:

$$[Pc(-2)Sn(IV)PC\text{-}2)] \overset{hv}{\rightleftarrows} *[Pc(-2)Sn(IV)Pc(-2)] \quad (5.12)$$

$$*[Pc(-2)Sn(IV)Pc(-2] + SO_2 \overset{k_q}{\rightarrow} [Pc(-2)Sn(IV)Pc(-1)]^+ + SO_2^- \quad (5.13)$$

Scheme 5.3

Photochemistry associated with the population of charge transfer , $n\pi^*$, states by ultra-violet irradiation of monomeric MPc complexes results in reactions that are mediated by hydrogen abstraction [156].

5.2.2 Photolysis of lanthanide diphthalocyanine complexes in the presence of SO_2*

When solutions of $[Pc(-2)Dy(III)Pc(-2)]^-$ in the solvent mixture of DMF / CH_2Cl_2 containing SO_2 was irradiated with filtered light (λ> 590 nm), the absorption spectra showed in Fig. 5.13 were observed The original absorption bands due to the $[Pc(-2)DyPc(-2)]^-$ complex, located at 613 and 688 nm decreased in intensity, and new bands developed at 657 and 459 nm. The spectral changes occurred with isosbestic points at 346, 550, 643 and 674 nm. These isosbestic points testify the existence of only two species in solution.

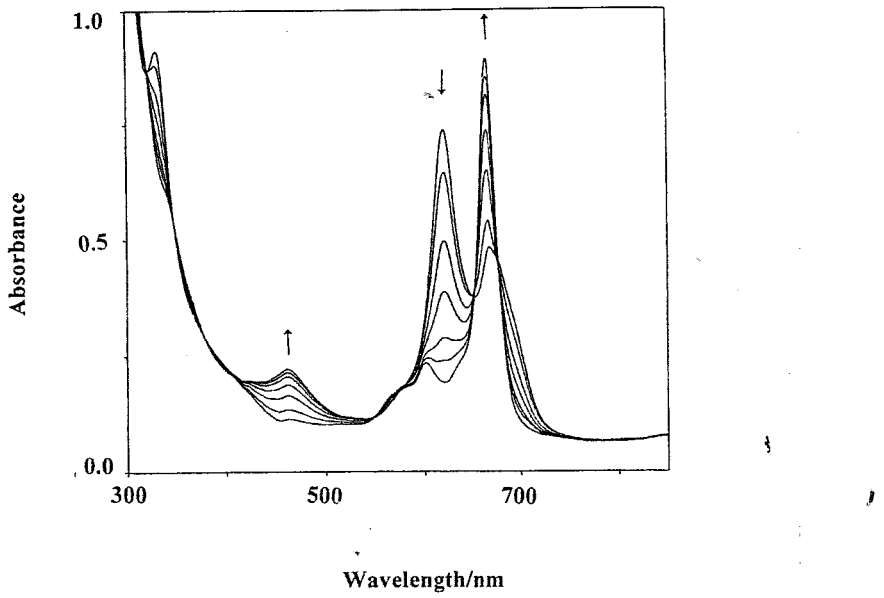

Fig. 5.13 Absorption spectral changes observed during the photolysis of $[DyPc_2]^-$ in DMF /CH_2Cl_2 containing SO_2. $[DyPc_2]_o^- = 5x10^{-6}$ $[SO_2] = 6x10^{-3}$ mol dm^{-3}.

*. The following publication resulted from the work presented in this section: N. Nensala and T. Nyokong. Polyhedron. 16 (1997) 2971.

Similar spectral changes were observed for the photolysis of [Pc(-2)Lu(III)Pc(-2)]$^-$ and [Pc(-2)Nd(III)Pc(-2)]$^-$ in the presence of SO_2. The colour of the solution changed from blue to green. When solutions of [Pc(-2)Lu(III)Pc(-2)]$^-$, [Pc(-2)Dy(III)Pc(-2)]$^-$ and [Pc(-2)Nd(III)Pc(-2)]$^-$ were photolysed in the absence of SO_2, no spectral changes were observed.

Previous studies have shown that photolysis (at $\lambda > 320$ nm) of lanthanide diphthalocyanine complexes in the CH_2Cl_2 / CH_3CN solvent mixture [90] and in the presence of benzoquinone [48] resulted in the formation of radical species with an absorption spectra similar to that observed in Fig. 5.13. Similar absorption spectra were also observed for the photolysis of [Pc(-2)Sn(IV)Pc(-2)] in the CH_2Cl_2 /CH_3CN solvent mixture and in the presence of SO_2 discussed earlier in this work.

The spectral changes observed in Fig. 5.13 are typical of the formation of the green Pc(-2)LuPc(-1) or [Pc(-2)SnPc(-1)]$^-$ species as discussed above for $SnPc_2$ and hence are assigned to the formation of the green species, [Pc(-2)Dy(III)Pc(-1)], as a result of one-electron oxidation of [Pc(-2)Dy(III)Pc(-2)]$^-$. The new species obtained was a stable radical hence it could be reduced back to the blue species by using sodium borohydride.

The difference between photolysis of [Pc(-2)Sn(IV)Pc(-2)] and [Pc(-2)Ln(III)Pc(-2)]$^-$ in the presence of SO_2 is that for $LnPc_2^-$ species, the formation of monophthalocyanine product was not observed, and due to the anionic nature of $[LnPc_2]^-$, its photooxidation in the presence of SO_2 occurred more readily than for the $SnPc_2$ species as shown by the values of the observed rate constants discussed below.

The formation of the green species, [Pc(-2)Ln(III)Pc(-1)] in the presence of SO_2 is attributed to the photoredox processes that occur following the excitation of $[Pc(-2)Ln(III)Pc(-2)]^-$ species which transfers one-electron to SO_2.

5.2.2.1 Kinetic studies of the photolysis of lanthanide diphthalocynines in the presence of SO_2

The kinetic studies on the interaction between lanthanide diphthalocyanine complexes with SO_2 helps to elucidate the reaction mechanism. Kinetic data for the reaction of $[Pc(-2)Ln(III)Pc(-2)]^-$ with SO_2 were collected by keeping the concentration of the former constant, and varying the concentrations of SO_2. The kinetics were determined by monitoring the disappearance of the peak due to the starting $LnPc_2^-$ complexes. Fig. 5.14 shows the changes in absorbance with the photolysis time for $[Pc(-2)NdPc(-2)]^-$.

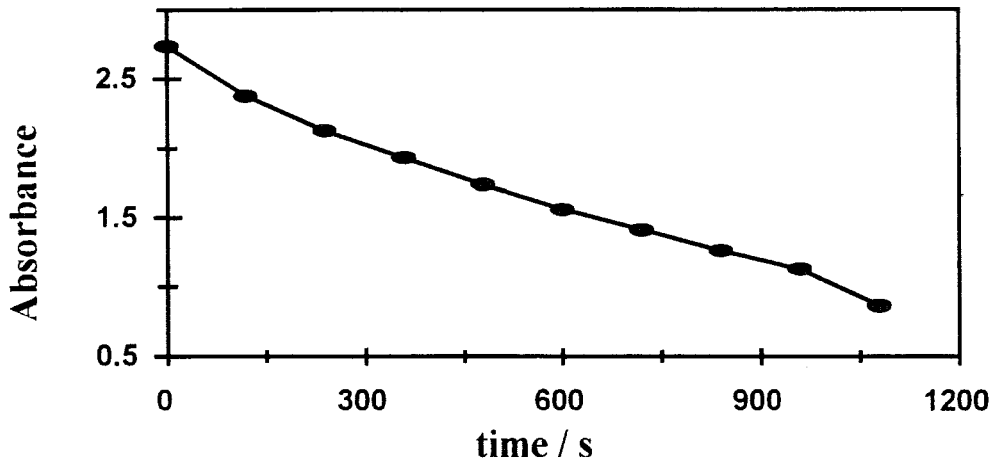

Fig. 5.14 Changes of absorbance of $[Pc(-2)NdPc(-2)]^-$ at 625 nm with time following photolysis of $NdPc_2^-$ in the presence of SO_2. $[NdPc_2]^- = 1.8 \times 10^{-5}$ $[SO_2] = 1.6 \times 10^{-2}$ mol dm^{-3}.

The plot of ln (A_t - A_∞) versus time (Fig. 5.15) was linear for at least 80 % completion, implying that the reaction is pseudo first-order in respect to the concentration of $[Pc(-2)Ln(III)Pc(-2)]^-$ as follows:

$$\frac{-d\left(\left[Pc(-2)Ln(III)Pc(-2)\right]^-\right)}{dt} = k_{obs}\left[\left[Pc(-2)Ln(III)Pc(-2)\right]^-\right] \qquad (5.14)$$

A_t and A_∞ represent the absorbance at time t and infinity, respectively.

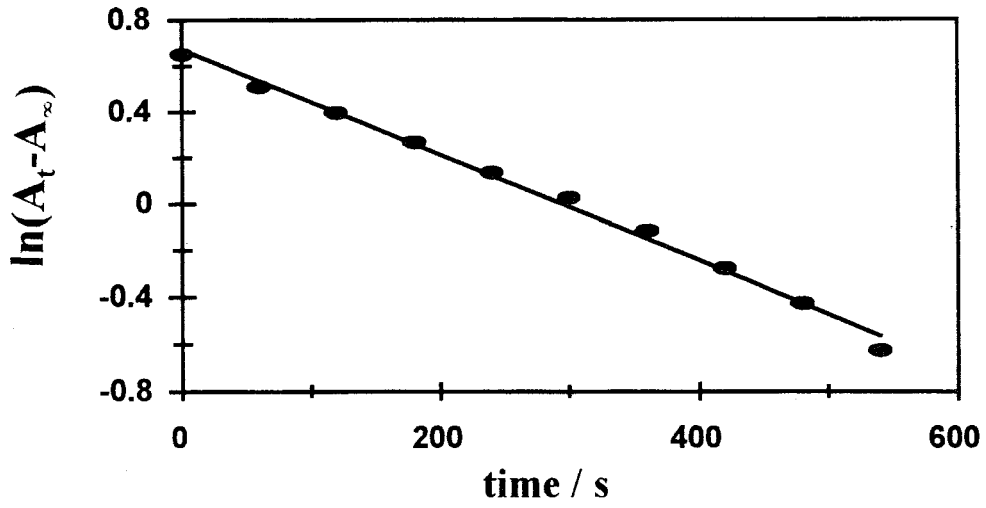

Fig. 5.15 Changes of $\ln(A_t - A_\infty)$ versus time for the photolysis of a solution of $[Pc(-2)NdPc(-2)]^-$ in the presence of SO_2. $[NdPc_2^-] = 1.8 \times 10^{-5}$ $[SO_2] = 3.2 \times 10^{-2}$ mol dm^{-3}.

The observed rate constants are related with SO_2 concentration as in Equation 5.10. The plot of observed rate constants versus SO_2 concentration was linear. The linearity of the plot of k_{obs} versus $[SO_2]$ (Fig. 5.16) shows that the reaction is first-order with respect to the concentration of SO_2, and also confirms the involvement of SO_2 in the reaction. The relative slopes of the plots for the photolysis of $[LnPc_2]^-$ in the presence of SO_2 are listed in the Table 5.1. The slopes give k_f.

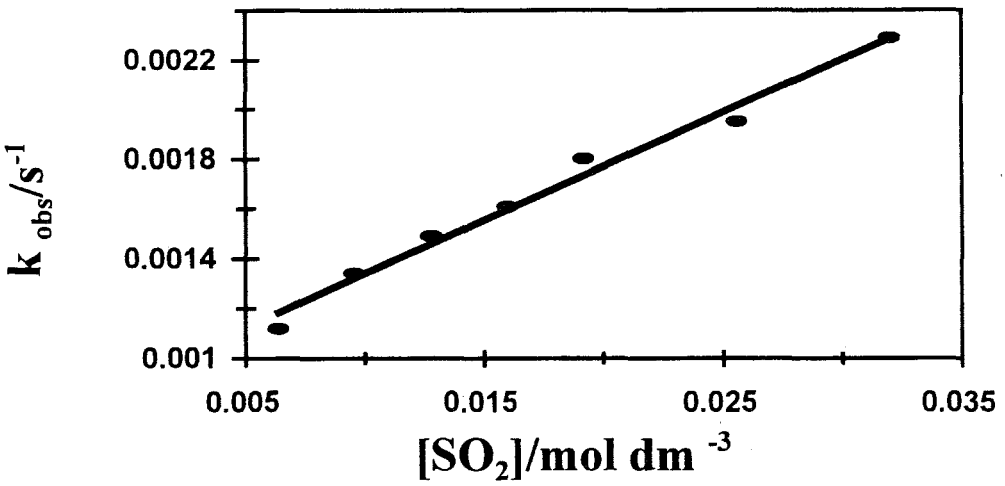

Fig. 5.16 Plot of k_{obs} versus $[SO_2]$ for the photolysis of $NdPc_2^-$ in the presence of SO_2.

Table 5.1 Slopes of the plots of k_{obs} versus $[SO_2]$ of different lanthanide diphthalocyanines.

Complex	Slope (k_f) / $mol^{-1}\ dm^3\ s^{-1}$
$[Pc(-2)NdPc(-2)]^-$	0.043± 0.0019
$[Pc(-2)DyPc(-2)]^-$	0.41± 0.028
$[Pc(-2)LuPc(-2)]^-$	2.568± 0.176

Table 5.1 shows that the values of slopes increase with the decrease of the ionic radius of the lanthanide ion. The observation of a higher slope for the photosensitization reactions involving $[Pc(-2)Lu(III)Pc(-2)]^-$ implies that this species is better photosensitizer for the reactions involving

SO_2 than the other two complexes. In other words, when the ring-ring interaction is stronger the photosensitization effects are higher hence the rate constant of formation (k_f) increases in the order $[Pc(-2)NdPc(-2)]^-$ to $[Pc(-2)DyPc(-2)]^-$ and $[Pc(-2)LuPc(-2)]^-$.

5.2.2.2 Quantum yields of the photolysis of lanthanide diphthalocyanines in the presence of SO_2

It has been shown that relative quantum yield increases linearly with the increase in the concentration of the quencher [90]. The Stern-Volmer plot of $1/\Phi$ versus $1/[SO_2]$ gave a straight line as shown in Fig. 5.17. The straight line confirms the involvement of SO_2 in the photoreaction that means that the excited states of lanthanide diphthalocyanine complexes were quenched by SO_2.

Previous studies on the photolysis of lanthanide diphthalocyanine complexes in the presence of CH_2Cl_2 and benzoquinone showed that the relative quantum yield increases with the decreasing ionic radius of lanthanide (III) ion [90]. Table 5.2. shows the variation of Φ with the nature of the $LnPc_2^-$ species studied in this work.

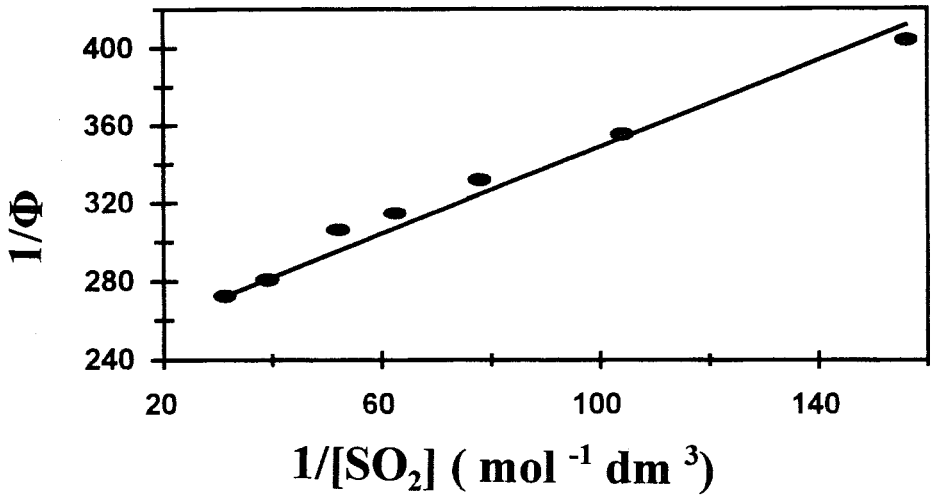

Fig. 5.17 Plot of 1/Φ versus 1/ [SO_2] for the photolysis of $NdPc_2^-$ in the presence of SO_2.

Table 5.2. Quantum yields of photolysis of lanthanide diphthalocyanine complexes in the presence of SO_2.

Complex	[SO_2] x 10^3 (mol dm^{-3})	$10^2 \Phi_{LnPc2}$ (quanta)
[Pc(-2)NdPc(-2)]$^-$	6.4	0.248
[Pc(-2)DyPc(-2)]$^-$	6.4	3.75
[Pc(-2)LuPc(-2)]$^-$	0.067	2.11

Comparing the complexes, [Pc(-2)NdPc(-2)]$^-$ and [Pc(-2)DyPc(-2)]$^-$ photolysed in solutions containing equal concentrations of SO_2, [Pc(-2)DyPc(-2)]$^-$ gave a quantum yield ten times higher than [Pc(-2)NdPc(-2)]$^-$. But, with a SO_2 concentration hundred times lower than that used in the

photolysis of other two lanthanide diphthalocyanine complexes, [Pc(-2)LuPc(-2)]$^-$ gave a quantum yield of the same order of magnitude as [Pc(-2)DyPc(-2)]$^-$ and ten times higher than [Pc(-2)NdPc(-2)]$^-$. Lutetium diphthalocyanine is expected to give higher quantum yields, due to the smaller ionic radius of lutetium ion, compared to the other ions.

The values of slopes of the Stern-Volmer plot give an insight on the reactivity of the lanthanide diphthalocyanine complexes used. Table 5.3 shows the changes of these slopes within lanthanide diphthalocyanine complexes. The species, [Pc(-2)LuPc(-2)]$^-$ shows a very low slope, implying shorter singlet lifetime since the ratio between the intercept ($1/\Phi^0$) and the slope ($k_d/\Phi^0 k_f$) from the Equation 5.11, is directly related to the lifetime [98], Equation 5.15. Evidently, [Pc(-2)LuPc(-2)]$^-$ has a higher photosensitization activity than the two other complexes in the presence of SO_2.

$$\frac{k_f}{k_d} = k_q \tau \qquad (5.15)$$

where k_q is the quenching rate constant and τ is the lifetime. As discussed for the photolysis of $SnPc_2$ in the presence of SO_2, the decay constant (β) is given by the ratio of rate constants, Equation 5.4. For $LnPc_2^-$ complexes in DMF/CH_2Cl_2 solvent mixture, β was found to be -0.21, -0.03 and 0.0001 for $NdPc_2^-$, $DyPc_2^-$ and $LuPc_2^-$ respectively. For these reactions where electron transfer from the excited state is involved, these β-values are meaningless [158].

Table 5.3 confirms that the oxidation of lanthanide diphthalocyanine complexes in solutions containing SO_2 becomes easier in order of $[Pc(-2)NdPc(-2)]^-$, $[Pc(-2)DyPc(-2)]^-$ and $[Pc(-2)LuPc(-2)]^-$ in agreement with the decrease of the ionic radius of lanthanide ions [90].

Table 5.3 Slopes of Stern -Volmer Plot for the photolysis of lanthanide diphthalocyanines in the presence of SO_2.

Complex	Slope (k_d $k_f \Phi^0$) (quanta $^{-1}$)
$[Pc(-2)NdPc(-2)]^-$	0.284 ± 0.0105
$[Pc(-2)DyPc(-2)]^-$	0.0197 ± 0.00013
$[Pc(-2)LuPc(-2)]^-$	0.000184 ± 0.0000032

5.2.2.3 Mechanism of the photolysis of lanthanide diphthalocyanines in the presence of SO_2

For photolysis in the visible region (filtered radiation with $\lambda > 590$ nm), it is expected that the $^3\pi\pi^*$ excited states of $LnPc_2^-$ are populated. Thus, the mechanism of the photoreaction consists of an electron transfer from the triplet excited state complex, $^3\pi\pi^*$ $LnPc_2^-$ to the quencher SO_2, according to Scheme 5.4.

$$[LnPc_2]^- \xrightarrow{hv} (^1\pi\text{-}\pi^*)\,[LnPc_2]^- \xrightarrow{isc} (^3\pi\text{-}\pi^*)\,[LnPc_2]^- \qquad (5.16)$$

$$(^3\pi\text{-}\pi^*)\,[LnPc_2]^- + SO_2 \rightarrow SO_2^- + LnPc_2 \qquad (5.17)$$

Scheme 5.4

In $SnPc_2$ $n\pi^*$ states are involved whereas in $LnPc_2^-$ quenching occurs from $^3\pi\pi^*$ states. The differences between $SnPc_2$ and $LnPc_2^-$, following excitations with visible light can be explained since $SnPc_2$ induces little mixing between the electronic clouds of the two macrocycles and the appearance of a broad band at λ = 777 nm suggests that there is a significant charge transfer interactions [17]. This fact is supported by the crystallographic data of $SnPc_2$ which show that the α pyrrole carbon atoms of the two rings interact weakly causing the slight distortion from the equilateral antiprism [128]. It has been shown that photochemistry associated with charge transfer or $n\pi^*$ excited states are populated with ultraviolet radiation [77]. The lowest-lying triplet $^3\pi\pi^*$ excited states observed in $LnPc_2^-$ complexes, populated by excitations in the Q band, $\lambda > 590$ nm, does not show the type of reactivity presented by $SnPc_2$ where photolysis at $\lambda > 590$ nm gave no evidence of the formation of $[SnPc_2]^-$ species, whereas UV photolysis gave $[SnPc_2]^-$. In $LnPc_2^-$, visible photolysis results in photooxidation to $LnPc_2$.

From an experimental point of view, reactions of SO_2 with $LnPc_2^-$ showed higher quantum yields (100 times higher for $LuPc_2^-$) compared to the reaction of $SnPc_2$ in the presence of SO_2. The

drawback of the reaction of $SnPc_2$ with SO_2 is that the formation of monophthalocyanine product, $[Sn^{IV}Pc]^{2-}$ as a by-product of the $[SnPc_2]^-$ species, while for reactions of SO_2 with $[LnPc_2]^-$ the only product obtained is the $[Pc(-2)LnPc(-1)]^-$ species.

5.3 Photochemical interaction between pentachlorophenol and lanthanide diphthalocyanines*

5.3.1 Environmental chemistry of pentachlorophenol

As discussed in the introduction chapter, polychlorinated phenols are widely used as insecticides, pesticides, germicides, antiseptic and disinfectants [111, 163]. They are also used for the preservation of wood and leather. In particular, pentachlorophenol (PCP) is a major industrial chemical used for many purposes such as in painting, glue and outdoor textiles [111, 163].

Polychlorinated phenols are common environmental pollutants because of their high toxicity, which increases with the increase of the number of halogen atoms in the molecule. PCP residues have been detected in food, water and human urine at very low concentration levels.

The toxicity of pentachlorophenol creates more concern because apart from the high number of chlorine atoms, PCP samples contain impurities such as polychlorinated dibenzo dioxins (PCDD) and dibenzofurans (PCDF) which are more toxic than PCP [112]. Chlorophenols are readily susceptible to breakdown through biological processes, the products of the degradation are more resistant and stable in environment [111].

*. The following publications resulted from work presented in this section: 1) N. Nensala and T. Nyokong, Polyhedron, 16 (1997) 2791. 2) T. Nyokong and N. Nensala, Science, Technology & Development, 15 (1997), 199.

The biodegradation of PCP is very slow and can only occur by a reductive dechlorination or by oxidative pathways [117]. The use of catalysts which are environment friendly could speed up the dechlorination or the complete degradation of PCP.

There are several reports on the purification of water containing chlorophenols by ultra violet photolysis [111, 164, 165]. The products of such irradiations have been found to be more toxic than the parent complexes [164]. Photosensitized dechlorination of chlorophenols has been suggested as an alternative method for the reduction of the toxicity of these complexes [113, 165, 166]. There have been reports on the oxidation or reduction of chlorophenols in the presence of photosensitizers [165,166]. Mainly dimeric products were formed by riboflavin-sensitized photooxidation of dichlorophenol [165], whereas reductive dechlorination of pentachlorophenol (PCP) was observed in the presence of carbazole photosensitizer [166].

The use of tetrasulphonated phthalocyanine complexes of Fe and Mn for hydrogen peroxide oxidation of chlorinated phenols have been reported by Meunier et al [115-117]. Homogenous catalysis using $[FeTsPc]^{+}$ and $[MnTsPC]^{+}$ resulted in the oxidation of trichlorophenol (TCP) and the formation of chloromaleic, chlorofumaric, maleic and fumaric acids [117] as products. Whereas, the catalytic oxidation of (U-^{14}C)-TCP by hydrogen peroxide, supported by $[FeTsPc]^{+}$ resulted to its complete mineralization to $^{14}CO_2$ [167]. The oxidation of PCP by $KHSO_5$ or H_2O_2 supported by $[FeTsPc]^{+}$ resulted in the formation of dichloromaleic anhydride as the only oxidative cleavage product of PCP and tetrachlorobenzoquinone (TCBQ) was the only intermediate observed [117].

The use of MPc complexes as photosensitizers for the photodegradation of PCP has not been explored. Though, metallodiphthalocyanine complexes, MPc_2 have been studied extensively for their possible application in electrochromism and other applications [45], their use as photosensitizers has received less attention.

5.3.2 Photochemical reactions between lanthanide diphthalocyanines and PCP

As already discussed, for the lanthanide diphthalocyanine complexes, the one-electron oxidation of the blue form, $[Pc(-2)Ln^{III}Pc(-2)]^-$ gives the green species $[Pc(-2)Ln^{III}Pc(-1)]$ which is characterized by a strong absorption band in the Q band region near 670 nm and a weaker band around 450- 470 nm attributed to the unpaired-electron of the phthalocyanine ring [23]. The one-electron oxidation of the green species leads to the formation of orange (red) species with an unpaired-electron in each Pc ring as $[Pc(-1)Ln^{III}Pc(-1)]^-$ [45,56].

Fig. 5.18 shows spectral changes observed during the photolysis with a filter ($\lambda > 590$ nm) of a solution of $[Pc(-2)Dy^{III}Pc(-2)]^-$ containing PCP. The reaction did not occur when the solution was kept in the dark. Before photolysis, the absorption spectra of the solution showed characteristic bands of blue form lanthanide diphthalocyanines in the Q band region. After photolysis, the original Q band at 620 nm decreased in the intensity and a new band was observed at 666 nm and a weaker band appeared at 460 nm. The colour of the solution changed from blue to green. The formation of the new species was accompanied by isosbestic points at 347, 378, 548, 650 and 678 nm. Indeed, the new absorption spectrum is similar to that observed during the visible photolysis of lanthanide diphthalocyanine complexes in the CH_2Cl_2/CH_3CN solvent

mixture [90] and in the presence of p-benzoquinone [48] and also similar to spectra obtained for the interactions of $SnPc_2$ and $LnPc_2^-$ in CH_2Cl_2/CH_3CN solvent mixture and SO_2 in sections 5.1 and 5.2. Thus, the absorption spectrum resulting from the photolysis of $[Pc(-2)Dy^{III}Pc(-2)]^-$ in the presence of PCP, is typical of the green species $[Pc(-2)Dy^{III}Pc(-1)]$. Similar spectral changes were also observed without using the filter.

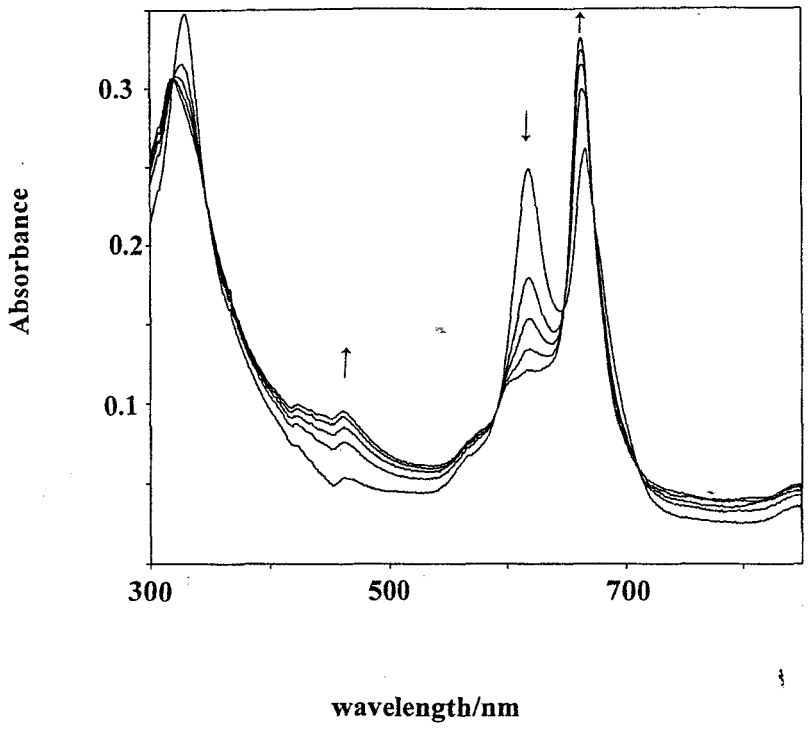

Fig. 5.18 Absorption spectral changes observed during the photolysis of a solution of $[Pc(-2)Dy^{III}pc(-2)]^-$ in acetonitrile containing PCP. $[DyPc_2]^- = 1.8 \times 10^{-6}$ and [PCP] = 2.7×10^{-4} mol dm^{-3}.

Also similar absorption spectral changes were observed during the photolysis of a solution of $[Pc(-2)Lu^{III}Pc(-2)]^-$ containing PCP. In this case lower concentrations of PCP were used, since the reaction was too fast to be accurately measured if concentrations of PCP used were similar

to those used for $DyPc_2^-$, thus $[Pc(-2)Lu^{III}Pc(-2)]^-$ seems to have higher reactivity than $[Pc(-2)Dy^{III}Pc(-2)]^-$.

5.3.3 UV absorption studies of transformation of PCP

Pentachlorophenol and less chlorinated phenols absorb strongly in the UV region. Hence, the absorption spectra have been used successfully in the analysis of PCP even at very low concentrations [111]. The absorption bands of PCP are located at 291 and 302 nm.

Fig. 5.19 shows the spectral changes observed for PCP during the photolysis (using filtered radiation) of a solution of $[Pc(-2)Dy^{III}Pc(-2)]^-$ in acetonitrile and containing PCP. During the photolysis, the Soret band at 330 nm due to the lanthanide diphthalocyanines decreased slightly in intensity, and the absorption band due to PCP at 302 nm increased in intensity, similar absorption spectral changes of PCP were observed by Nowakowska et al. [166] when carbazole was used as a photosensitizer for the dechlorination of PCP. These researchers attributed the increase of the absorption band at 302 nm to the formation of tetrachlorophenols. It is then believed that the increase of the intensity of the band at 302 nm, in the presence of $[Pc(-2)Dy^{III}Pc(-2)]^-$ or $[Pc(-2)Lu^{III}Pc(-2)]^-$ is due to the formation of tetrachlorophenol, following the photoreduction of PCP.

The absorption spectral changes observed during a prolonged photolysis of solution containing PCP and $[DyPc_2]^-$ resulted to the decrease in intensity of the absorption band at 302 nm, and new band was formed at 289 nm. This new band is in the range for the absorption spectra of 2,4,5-

trichlorophenol in acetonitrile. Thus, the prolonged photolysis of PCP in acetonitrile and in the presence of $[Pc(-2)Dy^{III}Pc(-2)]^-$ resulted in further dechlorination of the benzene ring, leading to the formation of trichlorophenols. Similar spectral changes were observed when unfiltered radiation was employed. The spectral changes attributed to the dechlorination of PCP were not observed on photolysis of PCP in the absence of the MPc_2 complexes, hence confirming the involvement of the latter in the photochemical reaction. The spectral changes observed in Fig. 5.18 may thus be attributed to the electron transfer from the photoexcited $^*[Pc(-2)Dy(III)Pc(-2)]^-$ species to PCP.

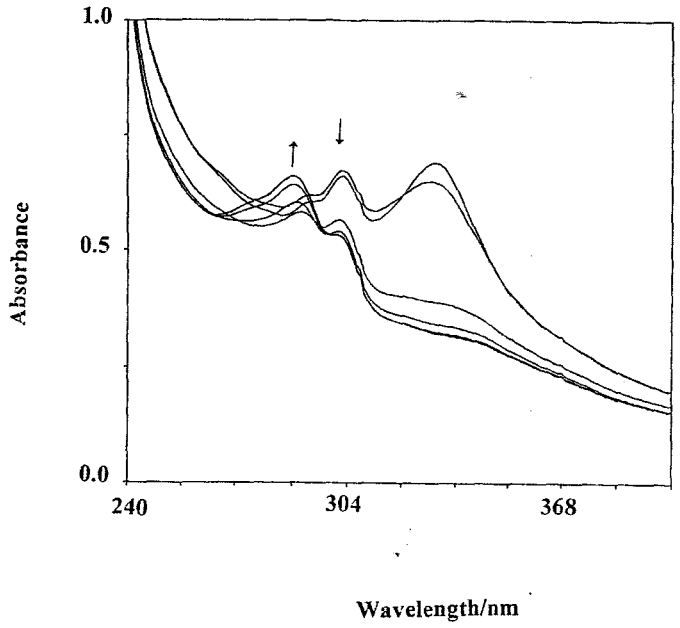

Fig. 5.19 Electronic absorption spectral changes observed during prolonged visible photolysis of solution containing PCP and $[DyPc_2]^-$ in acetonitrile. Concentrations of $DyPc_2^-$ and PCP are 1.8×10^{-6} and 2.7×10^{-4} mol dm^{-3}, respectively.

Although, a number of substances interfere with PCP measurements by gas chromatography, including chloronaphthalene, chlorinated biphenyls and pesticides [111], gas-chromatography (GC) has been used reliably for the characterization of the products of oxidation [117] and reduction [113,167] of PCP and their derivatives.

Photochemical reactions between PCP and lanthanide diphthalocyanine complexes were followed with a gas chromatograph, equipped with an electron capture detector, as described in the experimental section. Fig. 5.20 shows GC traces before and after a prolonged irradiation of the solution containing $[Pc(-2)Lu^{III}Pc(-2)]^{-}$ and PCP in acetonitrile. New peaks with shorter retention times were observed after photolysis. This observation is characteristic of the formation of chlorophenols containing fewer chlorine substituents and this is a clear evidence for the dechlorination of PCP [113]. Fig. 5.20 (b) and (c) show that the retention times in both GC traces coincided with the retention time of trichlorophenol, giving evidence of the formation of trichlorophenol as the final product of the photoreduction of PCP in the presence of $[LuPc_2]^{-}$. Similar GC traces were observed when PCP was photolysed in the presence of $[DyPc_2]^{-}$. The presence of small amounts of chlorophenols with less chlorine substituents than PCP before photolysis, Fig 5. 20 (a) is not surprising since commercial PCP is usually contaminated with tri- and tetra-chlorophenols [113].

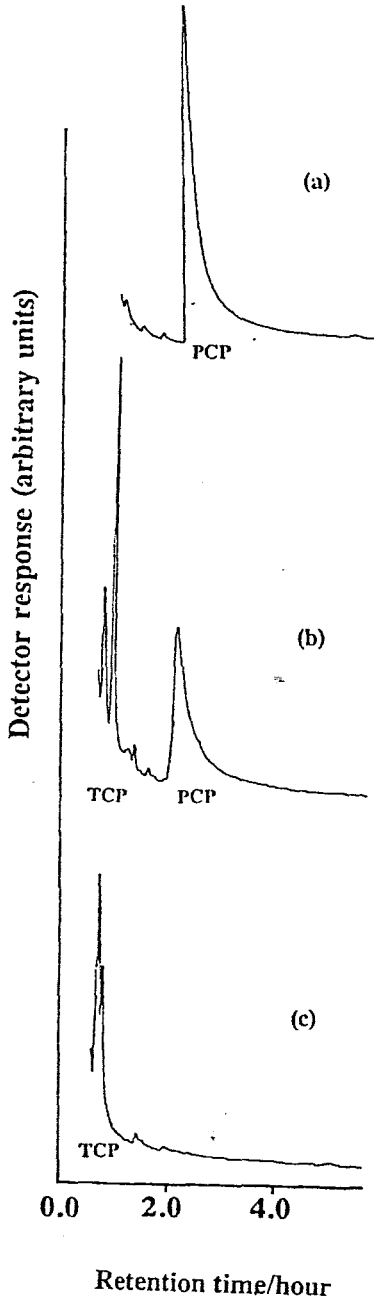

Fig. 5.20 Gas chromatography traces for (a) before photolysis (o h) and b) after (11 h) photolysis of solution containing $[LuPc_2]^-$ and PCP in CH_3CN. (c) GC trace for 2,4,5-trichlorophenol. GC traces due to acetonitrile solvent have been left out.

5.3.4 Kinetic studies of the visible photolysis of lanthanide diphthalocyannes in the presence of pentachlorophenol

Kinetic data were collected by keeping the concentration of the [Pc(-2)Dy(III)Pc(-2)]$^-$ or [Pc(-2)Lu(III)Pc(-2)]$^-$ species constant at 5 x 10^{-6} mol dm^{-3} and varying the concentration of PCP, then photolysing the solutions. The formation of the green form was monitored spectrophotometrically at 666 nm.

$$\frac{d([Pc(-2)LnPc(-1)])}{dt} = k_{obs}[Pc(-2)LnPc(-1)] \qquad (5.18)$$

Typical changes in absorbance of the green species of lanthanide diphthalocyanines with the photolysis time are shown in Fig. 5.21. In Fig. 5.22, the plot of the $\ln(A_\infty - A_t)$ versus time were linear up to 80 % of completion in both diphthalocyanine complexes, showing the pseudo first-order kinetics of these complexes according to Equation 5.18. The slopes of these plots gave the observed rate constant, k_{obs}, and plots of k_{obs} versus the concentration of PCP were also linear, Fig. 5.23, confirming a first order dependence of the photolysis reaction on PCP.

$$k_{obs} = k_f[PCP] + k_r \qquad (5.19)$$

were k_f and k_r are the rate constants of the formation and reverse reactions, respectively.

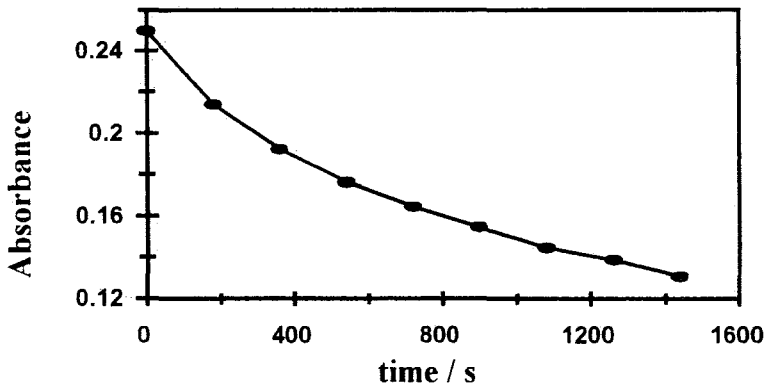

Fig. 5.21 Changes in absorbance of Pc(-2)Dy^{III}Pc(-1) species with time during the photolysis of a solution containing [Pc(-2)Dy^{III}Pc(-2)]$^-$ and PCP in acetonitrile. Concentrations of [DyPc$_2$]$^-$ and PCP are 1.8x10^{-6} and 2.7x10^{-4} mol dm^{-3}, respectively.

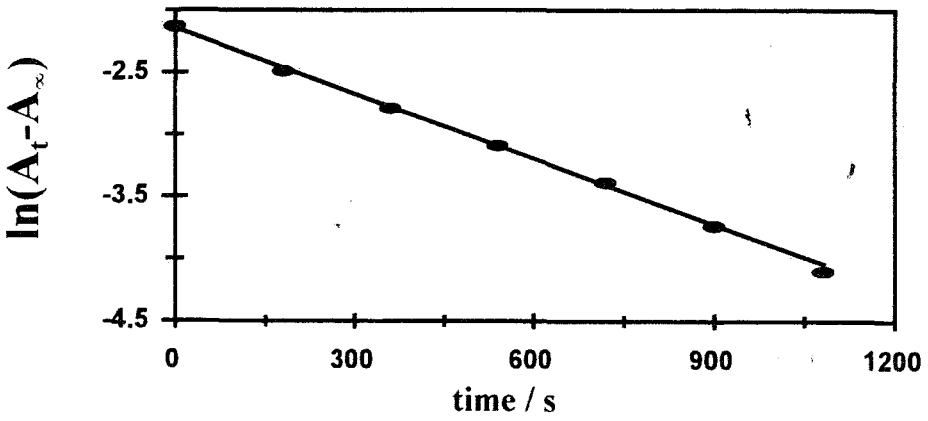

Fig. 5.22 Plot of ln(A$_\infty$ - A$_t$) versus time for the photolysis of a 1.8x10^{-6} mol dm^{-3} solution of DyPc$_2^-$ in the presence of 2.7x10^{-4} mol dm^{-3} PCP.

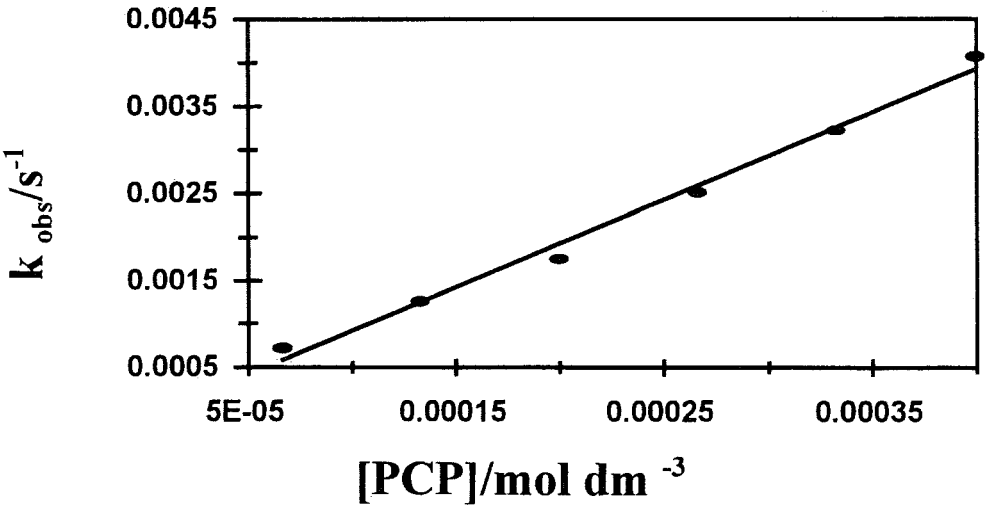

Fig. 5.23 Plot of k_{obs} versus PCP concentration for the photolysis of $[DyPc_2]^-$ in the presence of PCP in acetonitrile.

A comparative study between the two lanthanide diphthalocyanine complexes shows that the photolysis of $[Pc(-2)Lu^{III}Pc(-2)]^-$ in the presence of PCP had higher apparent rate constant of formation, k_f (slope of the plot of k_{obs} versus [PCP]) than for the photolysis of $[Pc(-2)Dy^{III}Pc(-2)]^-$. The value $k_f = 18284 \pm 1110$ mol $^{-1}$ dm ^{3} s^{-1} for the photolysis of $[Pc(-2)Lu^{III}Pc(-2)]^-$ and $k_f = 11.84 \pm 0.37$ mol $^{-1}$ dm ^{3} s^{-1} for $[Pc(-2)Dy^{III}Pc(-2)]^-$ confirm that the former is a better photosensitizer than the latter for the photolysis in the presence of PCP. This observation is supported by the fact that, although the lower concentrations of PCP were used in the photolysis of $[LuPc_2]^-$, their observed rate constants are ten times higher than the observed rate constants in the photolysis of $[DyPc_2]^-$.

5.3.5 Quantum yield studies for the photolysis of lanthanide diphthalocyanines in the presence of PCP

The quantum yields of the formation of the green species for the photoreactions between the excited $LnPc_2^-$ and PCP are related to the concentration of PCP according the Equation 5.20 [88, 158] which is similar to that used for SO_2 reactions (Equation 5.11).

$$\frac{1}{\Phi} = \frac{1}{\Phi^0} + \frac{k_d}{\Phi^0 k_f} \frac{1}{[PCP]} \qquad (5.20)$$

In Fig. 5.24, the Stern-Volmer plot (the inverse of the quantum yields versus the inverse of PCP concentration) is linear showing that PCP does quench the excited $(^3\pi\text{-}\pi^*)LnPc_2^-$ species. The quantum yields obtained for the photosensitized dechlorination of PCP by $[Pc_2Dy]^-$ and $[Pc_2Lu]^-$ were 1.2×10^{-4} and 9.1×10^{-4}, respectively, for a PCP concentration of 4×10^{-4} mol dm^{-3}. The slightly higher quantum yields for the photolysis reactions involving $[Pc_2Lu]^-$ complex may be explained in terms of the relative ease of oxidation of the $[Pc_2Lu]^-$ complexes, compared to $[Pc_2Dy]^-$. Although electrode potentials of the excited $^*[Pc_2Ln]^-$ may differ from the ground state reduction potentials, the relative magnitudes of these ground state reduction potentials may give an approximation of the relative ease of oxidation of the excited states. Factors such as the relative lifetimes and quantum yields of the excited states of the Pc_2M species will also determine the reactivity of the excited states.

The photosensitisation strength of lanthanide diphthalocyanines can be understood in term of the value of the slope of the Stern-Volmer plot. The complex with the smaller slope is expected to have higher photosensitisation. The slopes ($k_d/\Phi^0 k_f$) of the Stern-Volmer plot were 1.44x10 $^{-4}$ and 1.28 quanta for $[LuPc_2]^-$ and $[DyPc_2]^-$, respectively. Thus confirming that $LuPc_2^-$ is a better catalyst since the slope which is directly related to the lifetime (Equation 5.17) is smaller than for $DyPc_2^-$. The values of decay constants, β, were found to be 1.7 x 10 $^{-7}$ and 5.0 x10 $^{-4}$ for $LuPc_2^-$ and $DyPc_2^-$, respectively in acetonitrile. These β-values are meaningless since the reaction consists of electron transfer from the excited state [158].

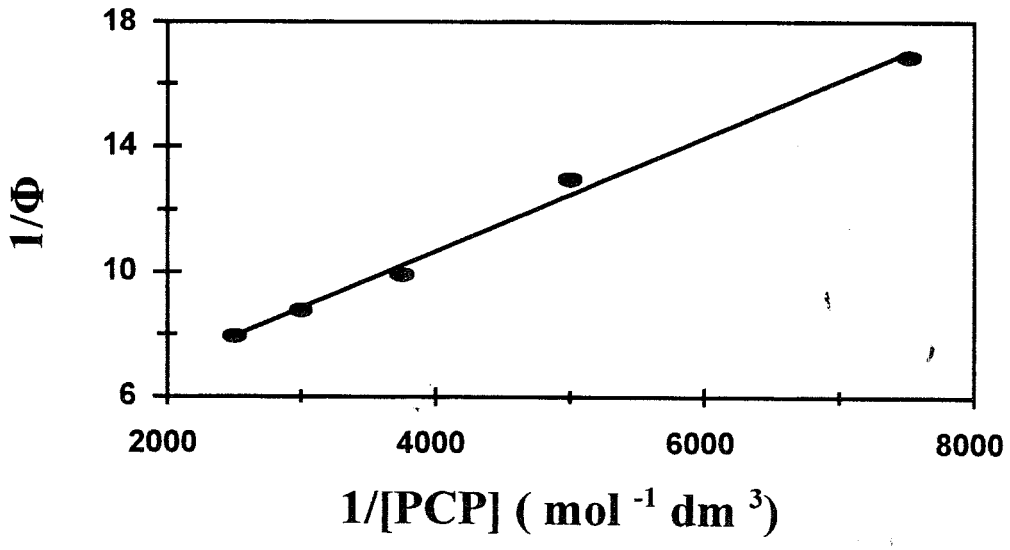

Fig. 5.24 Plot of 1/ Φ versus 1 / [PCP] for the photolysis of $DyPc_2^-$ in the presence of PCP in acetonitrile.

5.3.6 Mechanism of the photolysis of lanthanide diphthalocyanine in the presence of PCP

In comparison with the photosensitization reactions of $SnPc_2$, it is suggested that the $(^3\pi\pi^*)[Pc_2Ln]^-$ state is formed by excitation in the visible region, and that this state may then be quenched by PCP or other electron donors or acceptors. Thus, the mechanism for the dechlorination of PCP may be represented by Scheme 5.5. The first step is the excitation of the $[LnPc_2]^-$ species to the excited singlet state followed by intersystem crossing (isc) to the triplet state. The excited $(^3\pi\pi^*)[LnPc_2]^-$ then transfers an electron to PCP with the formation of PCP^- radical anion which then abstracts hydrogen ions from the media, followed by dechlorination and the formation of tetra- and tri-chlorophenols.

$$[LnPc_2]^- \xrightarrow{h\nu} (^1\pi - \pi^*)[LnPc_2]^- \xrightarrow{isc} (^3\pi - \pi^*)[LnPc_2]^- \qquad (5.21)$$

$$(^3\pi - \pi^*)\ [LnPc_2]^- + PCP \rightarrow LnPc_2 + PCP^- \qquad (5.22)$$

$$PCP^- \rightarrow \text{trichlorophenol and tetrachlorophenol} \qquad (5.23)$$

Scheme 5.5

Earlier work gave spectroscopic evidence for the formation of small quantities of monomeric Sn(IV)Pc species on photolysis of Pc_2Sn in the presence of SO_2. This was evidenced by the occurrence of a weak band to the low energy side of the spectra of the $SnPc_2$ species. There was no evidence of formation of species other than the $LnPc_2$ on photolysis of the $[LnPc_2]^-$ species in the presence of PCP. Monomeric lanthanide phthalocyanine have not been characterized.

5.4 Phototransformation of 4-chlorophenol in the presence of solid $NdPc_2$

5.4.1 Enviromental effects of 4-chlorophenol

As discussed earlier, chlorophenols are a class of molecules which are toxic and commonly spread out throughout the environment from the industrial plants and by current methods of water treatments involving the use of chlorine [168]. Phenols and halogenated phenols are common contaminants in water, toxic to aquatic life and impart tastes and odours to the drinking water even at very low levels [169]. Although, the toxicity of mono-chlorophenols is lower compared to polychlorinated phenols [111], the former are found to be more soluble in water than the latter, hence they exhibit more toxicity in the drinking water [170].

Urgent measures for the development of new methods to clean-up the environment in the industrial world are needed. The degradation of chlorophenol compounds has been possible via chemical, photochemical and biological processes [171]. The photocatalytic degradation of 4-chlorophenol has been extensively studied [168-173], 4-chlorophenol has been claimed to be a common pollutant because it is cheap, easily analysed, water soluble, photochemically inactive and non-volatile [172]. The use of photocatalysts with semiconductor behaviour such as TiO_2 in the elimination of organic pollutants using near UV-light [174-179] has been an important process for the purification of water. The use of TiO_2 and others as heterogenous catalysts for the degradation of 4-chlorophenol is an area of growing interest.

Photocatalytic mineralization of 4-chlorophenol to CO_2 and HCl using UV and near visible light in the presence of TiO_2 [118,171-173, 180], and polyoxometalates [109,110] has been reported. The degradation of 4-chlorophenol by anodic oxidation was also reported [181]. $LuPc_2$ is an intrinsic molecular semiconductor [13, 14] with room temperature conductivity of $6x10^{-5}$ Ω^{-1} cm^{-1}. Based on this observation, $LuPc_2$ species are possible semiconductor catalysts and they are employed in this work for the transformation of 4-Cp.

5.4.2 Photolysis of 4-chlorophenol using visible radiation in the presence of solid $NdPc_2$

5.4.2.1 HPLC and pH results

Photocatalytic transformation of 4-Cp using filtered radiation ($\lambda > 590$ nm)was carried out in the presence of $NdPc_2$ as photosensitizer. This reaction is of particular importance since diphthalocyanine complexes absorb strongly in the visible region. It is also believed that in this region, the creation of the electron-hole pair should be favoured and the photocatalytic activity of the catalyst should be enhanced. In this study, the glass filter prevents the direct excitation of water and 4-Cp by preventing the UV irradiation, while running water cools the system and cuts off near IR radiation [109].

Gerdes et al. [119] showed that at pH 7, the photo-oxidation of monochlorophenols in the presence of MPc photosensitizers occurred more slowly and resulted in the formation of p-benzoquinone, while at pH 13, carbon dioxide and maleic acid were detected as the main photoproducts. Durand et al. [168] showed that the yields of the photoproducts of the photolysis

of aqueous 4-chlorophenol depend on the pH, concentration of 4-chlorophenol and the presence of molecular oxygen. In many reports, benzoquinone was quoted as the main photoproduct of the oxidation of 4-Cp in oxygenated saturated solutions [112, 168, 182]. Hydroquinone (HQ) and 4-chlorocatecol (4-CC) have been claimed to be the main intermediates of the photocatalytic degradation of 4-Cp in the presence of TiO_2 semiconductor [118, 171, 172, 180]. On the other hand, 4-CC was quoted as the main product resulting from the photocatalytic transformation of 4-chlorophenol in the presence of ZnO photocatalyst [170]. Fig. 5.25 shows the HPLC traces resulting from the indirect photolysis of an aqueous solution of 4-Cp in the presence of $NdPc_2^-$ photocatalyst and saturated with oxygen.

Peaks characteristic to HQ (VI) and BQ (V) were observed upon photolysis of a solution containing 4-Cp and $NdPc_2^-$ using visible light. The peak labelled III could not be accurately identified. 4-chlorocatechol has been observed as one of the products of photocatalytic degradation of 4-Cp by some researchers [172]. The degradation of 4-Cp (peak I) is more enhanced and faster than in the photolysis with unfiltered radiation, discussed below. It is important to note that in the absence of $NdPc_2^-$ using filtered radiation, 4-CP showed negligible changes in HPLC. In the presence of $NdPc_2^-$, the degradation of 4-Cp showed a fewer number of intermediates with filtered light than with unfiltered radiation. This is important since fewer intermediates may reduce the toxicity of the photocatalysis products. The presence of oxygen is very important, since in its absence it was shown before that 4-chlorophenol was not converted to benzoquinone, thus the presence of oxygen influences the yield of photoproducts [168]. Molecular oxygen acts an electron scavenger, and prevents the recombination of electrons in the

conduction band with the holes (h^+) of the valence band when catalysts with semiconductor behaviour are employed [109, 169]. The peaks have been labelled to match Fig. 5.28 below.

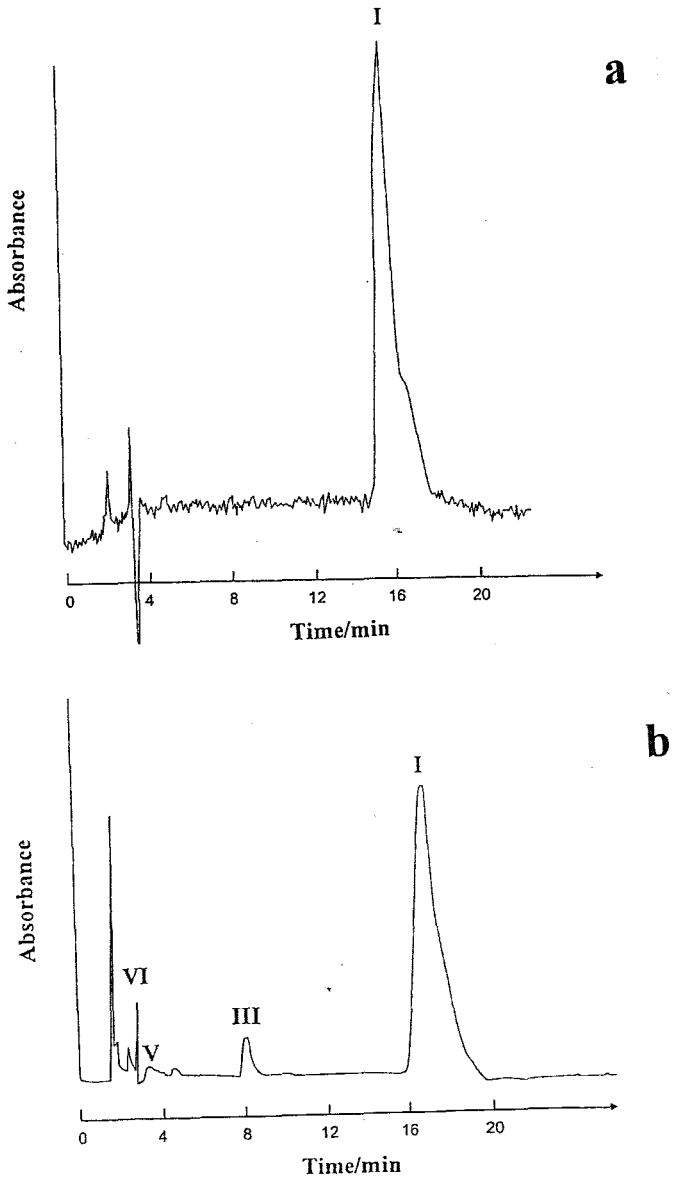

Fig. 5.25 HPLC chromatogram of 5x10 $^{-6}$ mol dm $^{-3}$ 4-Cp oxygenated solution containing 0.025 mg/ml of $NdPc_2^-$ in water before (a) and after 5 minutes of photolysis with filtered radiation ($\lambda > 590$ nm) (b).

It has been shown that photochemical reactions of 4-chlorophenol depend on the pH [168]. At neutral and acid values of pH, the flash photolysis of an aqueous 4-chlorophenol resulted mainly in the formation 1,4-benzoquinone, while at alkaline pH, benzoquinone was not the main product. Mills et al. [172] also observed that the photocatalytic degradation of 4-Cp is sensitive to pH. At pH of 2, the pH of solution did not change throughout the photolysis, while when a solution of a pH of 5.5-6.0 was used, the pH dropped as the irradiation proceeded.

The visible photolysis of an aqueous solution of $5x10^{-6}$ mol dm^{-3} containing 0.0465 mg / ml of $NdPc_2^-$ showed initial increase of pH from 6.5 to 6.70 and followed by the decrease of pH to 6.4 after 150 minutes, Fig. 5.26. Thus, the slow pH drop contrary to the observation during the photocatalytic degradation of 4-Cp under TiO_2, suggests that HCl was not formed under the present experimental conditions.

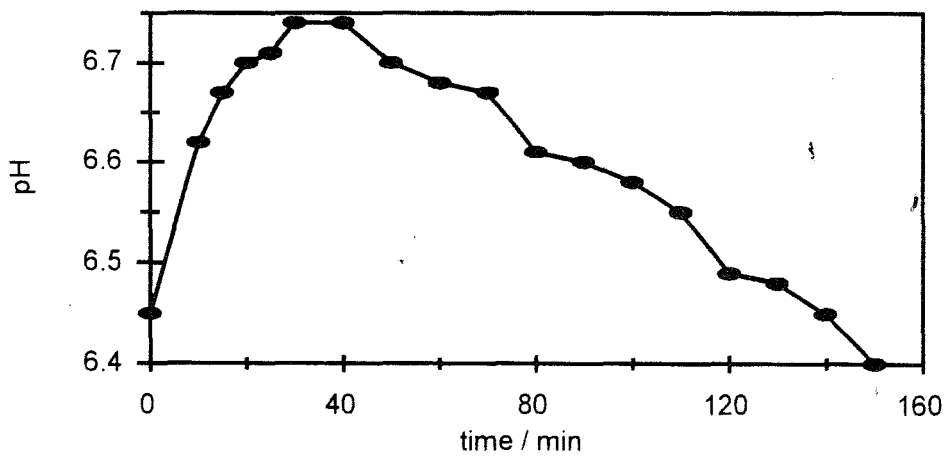

Fig. 5.26 pH changes observed during the visible photolysis of a solution of $5x10^{-6}$ mol dm^{-3} containing 0.0465 mg/ml of $NdPc_2^-$ and saturated with oxygen.

5.4.2.2 kinetic studies of visible photolysis of 4-Cp under $NdPc_2^-$

The photocatalytic transformation of 4-Cp is characterized by several consecutive reaction steps, and consequently by complex kinetics. The visible photolysis is accompanied by a high percent of recovery of 4-Cp species. Óshea et al. [177] also observed a high percent of recovery of phenols in the dark, and they assigned this fact to dark adsorption of the phenols onto TiO_2 surface. Gerdes et al. [119] showed that the visible photolysis of 4-Cp in the presence of metallo-tetrasulphophthalocyanine complexes was also accompanied by a strong retardation of the kinetics due to the inhibition of the photosensitizers by intermediates and products. From an experimental point of view, it may be added that the retardation was associated with the high level of competition between 4-Cp and photoproducts for the surface of the catalyst. The visible photolysis of 4-Cp in the presence of $NdPc_2^-$ showed a degradation of 4-Cp, however this was followed by regeneration of 4-Cp. The strong retardation of kinetics did not allow the study of the kinetics following the degradation of 4-Cp. Table 5.4 summarizes the results obtained after 300 s of irradiation of different concentrations of 4-chlorophenol over 0.025 mg / ml of $NdPc_2^-$ photocatalyst. The rate of degradation of 4-Cp was calculated as the ratio of difference of HPLC peak height with time (300 s).

From the Table 5.4, the rate of degradation of 4-Cp increases with the increase in concentration of 4-Cp. At high concentrations of 4-Cp, the reaction rate is relatively constant, hence the reaction order tends to zero. In heterogenous catalysis, the reaction rate at the surface of the catalyst is related to the concentration of the reactant covering the surface according to the Langmuir-Hinshelwood (L-H) kinetic model [171, 178], Equation 5.24.

Table 5.4 Results obtained from the visible photolysis of 4-Cp over $NdPc_2$

10^5 [4-Cp]/ M	10^8 Rate/ H s^{-1}	% degradation
0.5	0.527	31.5
0.75	1.02	41
1	1.34	40.3
1.25	1.35	32.4
1.5	1.363	27.3

* H : relates peak height to the concentration.

$$\frac{1}{\text{Rate}} = \frac{1}{k_a} + \frac{1}{k_a K C_0} \qquad (5.24)$$

Where k_a is the apparent reaction rate constant and K is the adsorption coefficient, and C_0 corresponds to the initial concentration of 4-Cp in this case.

Thus, the plot of initial reaction rate (Rate $^{-1}$) versus the reciprocal of the initial concentration of 4-Cp (C_0^{-1}) was found to be linear with a non-zero intercept, Fig. 5.27. The results presented in Fig. 5.27 confirm that the L-H kinetic model is appropriate for the kinetic treatment since the plot is linear, and the reaction occurred on the surface of the photocatalyst. From the plot of Rate $^{-1}$ versus C_0^{-1}, k_a was determined to be equal to 2.4×10^{-8} H s^{-1} from the intercept, and the adsorption coefficient was found to be $K = 1 \times 10^5$ mol $^{-1}$ dm ^{3}, from the slope.

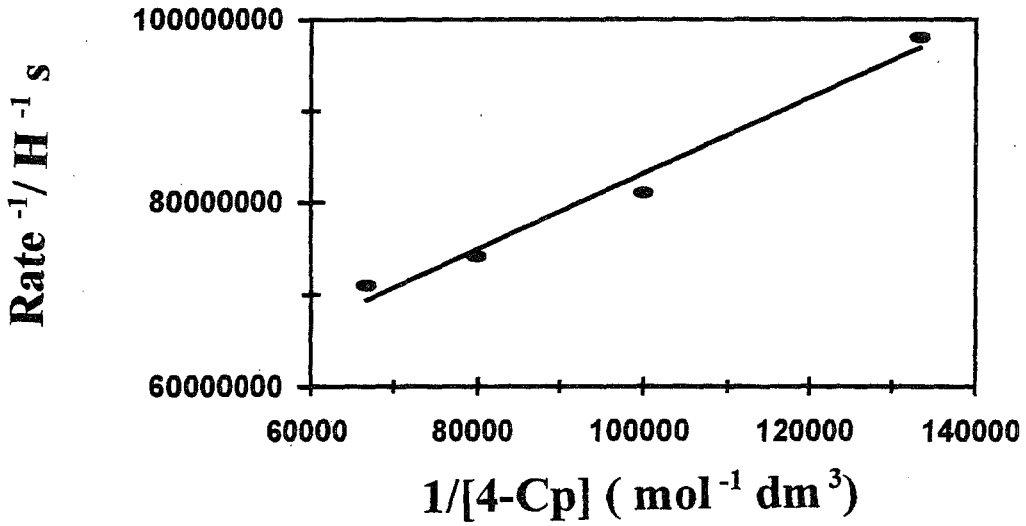

Fig. 5.27 Plot of Rate $^{-1}$ versus C_0 $^{-1}$ for the photocatalytic transformation of 4-Cp over solid $NdPc_2$.

A high percent of degradation is expected at low concentrations of 4-Cp, but a stronger recovery of 4-Cp at these concentrations is observed. The maximum percent of 4-Cp degradation is observed in the first few minutes of irradiation. At high concentrations of 4-Cp, there is evidently a low percent of degradation.

5.4. 2.3 Reaction mechanism for phototransformation of 4-chlorophenol in the visible region

The possible mechanism of the photolysis of 4-Cp using filtered radiation is shown in Scheme 5.7 and the reactions involved during the photocatalytic transformation of 4-chlorophenol in the

presence of $NdPc_2^-$ are shown in this Scheme. For filtered radiation , 4-Cp is not directly affected by the radiation, since the photolysis occurred in the visible region. Irradiation of catalysts with semiconductor properties such as $NdPc_2^-$ generates electrons ($\bar{e}$) and holes (h^-) as shown in the Equation 5.25 of Scheme 5.6 [110, 178]. Once the electrons and holes are produced, the electron scavenging action of molecular oxygen prevents the recombination of the electron-hole pairs.

The formation of reactive hydroxyl radicals produced by the reaction between the photogenerated hole, h^- and the surface adsorbed OH^- (ads) or H_2O and O_2 are known to be the primary oxidizing agents for the photomineralization of organic pollutants over semiconductor catalysts such as TiO_2 [118, 178] and polyoxometalates (POM) [109,110]. In the similar way, it is proposed here that hydroxy radicals are formed in the presence of $LnPc_2(\bar{e} + h^-)$ as shown in the Equation 5.26. In previous reports on the photocatalytic degradation of 4-Cp, the hydroxyl radicals forced the displacement of the halogen [178] and attacked several functional groups of the phenols [181]. The carbon-chloride cleavage was also observed for the photocatalytic degradation of 4-chlorophenol in the presence of POM [109, 110].

By similar analogy, the reaction illustrated in Equation 5.27 shows possible intermediates formed by the reaction between 4-chlorophenol and hydroxyl radical. Spectroscopic and HPLC results discussed above provide proof of the formation of some of the products formed in the Equation 5.27. The benzoquinone is formed from hydroquinone in the presence of oxygen.

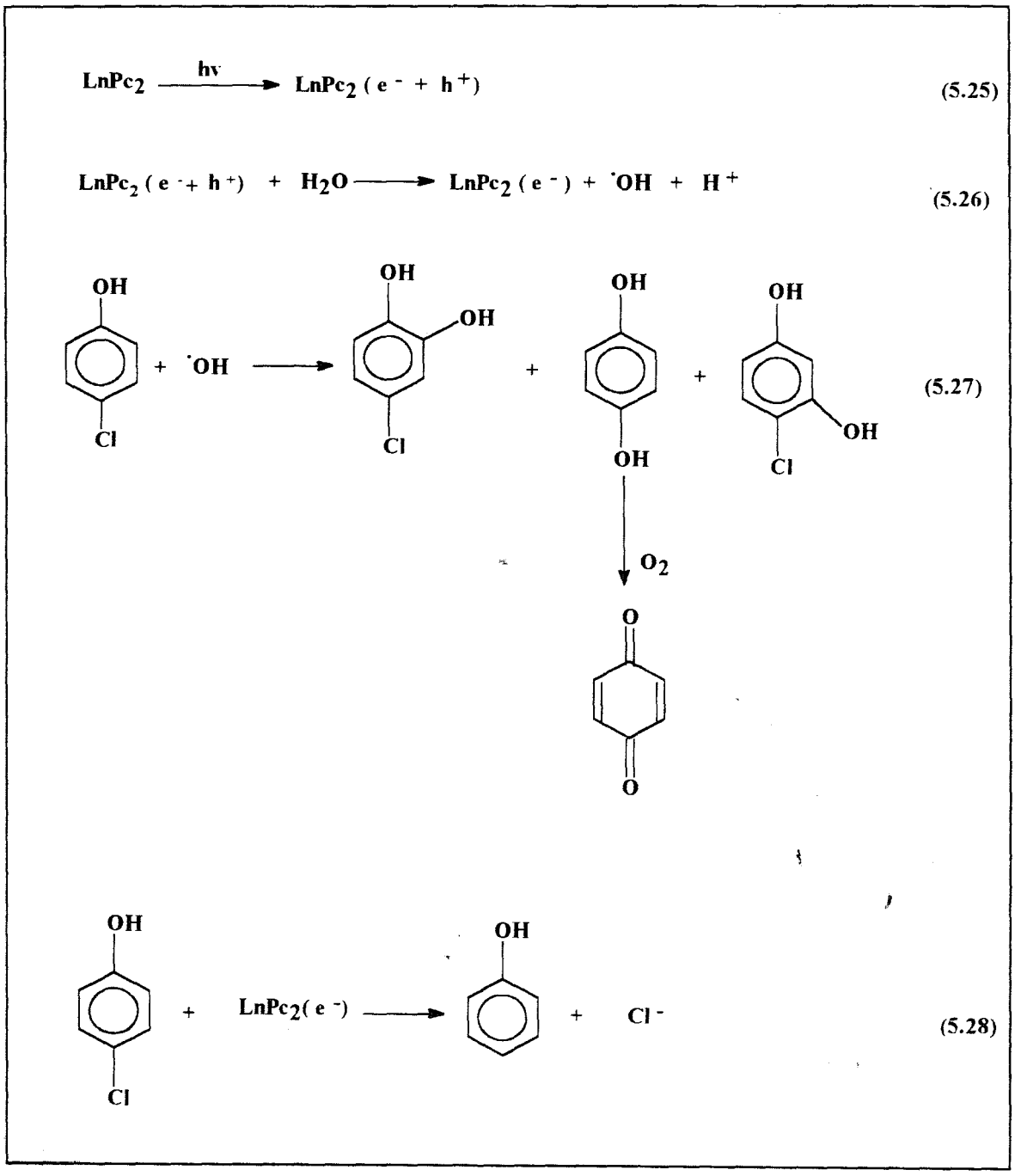
LnPc2 hv LnPc2 (e - + h +)
(5.25)
LnPc2 (e - + h +) + H2O LnPc2 (e -) + OH + H +
(5.26)
OH
Cl
+ OH
OH
OH
Cl
+
OH
OH
+
OH
OH
Cl
(5.27)
O2
O
O
OH
Cl
+ LnPc2(e -)
OH
+ Cl -
(5.28)

Scheme 5.6

The Equation 5.27 shows also the formation of 4-chlororesorcinol and 4-chlorocatechol as observed in the HPLC chromatogram reported by Mills et al. [172]. Direct reaction of $LuPc_2$ ($\bar{e}$ + h^+) with 4-Cp could proceed to a lower extent and give phenol as shown in the Equation 5.28.

The use of lanthanide diphthalocyanines as photocatalysts for the phototransformation of 4-Cp presented less intermediates than the direct photochemical reaction of 4-Cp as reported elsewhere [183].

5.4.3 Photolysis of 4-chlorophenol with unfiltered radiation in the presence of $LnPc_2$

Chlorophenols absorb strongly in the UV region, thus electronic spectra may be used in monitoring photochemical transformation of 4-chlorophenol in water. Lanthanide diphthalocyanines are used in solid state, and since they are insoluble in water, they are not expected to affect the absorption spectra of 4-chlorophenol. It is difficult to evaluate the extent of transformation of 4-Cp from the UV spectra, since the absorption bands are very broad and also 4-Cp and the possible photoproducts 4-CC and HQ absorb at the same wavelength range [170,172]. Thus, HPLC has been used successfully in following the transformation of 4-Cp and the formation of resulting intermediates and products [118,171,172, 180]. HPLC is thus used in this work to follow the photodegradation of 4-Cp.

5.4.3.1 HPLC studies of the photolysis of 4-Cp in the presence of $LnPc_2^-$

Fig. 5.28 shows the HPLC trace of an aqueous solution containing $1.2x10^{-5}$ mol dm^{-3} 4-Cp and 0.035 mg/ml of solid $[Pc(-2)Nd^{III}Pc(-2)]^-$, saturated with oxygen before and after 120 minutes of irradiation. The HPLC analysis revealed different compounds such as: 4-chlorophenol, hydroquinone, benzoquinone, phenol, and 4-chlororesorcinol. The peaks labelled as I, II, IV, V, VI in Fig. 5.28 are respectively due to 4-chlorophenol, 4-chlororesorcinol, phenol, benzoquinone and hydroquinone. By analogy with the literature, the peak labelled III may be assigned to 4-CC as discussed with photolysis using visible radiation. The 4-CC was not easily available, hence its HPLC trace could not be recorded.

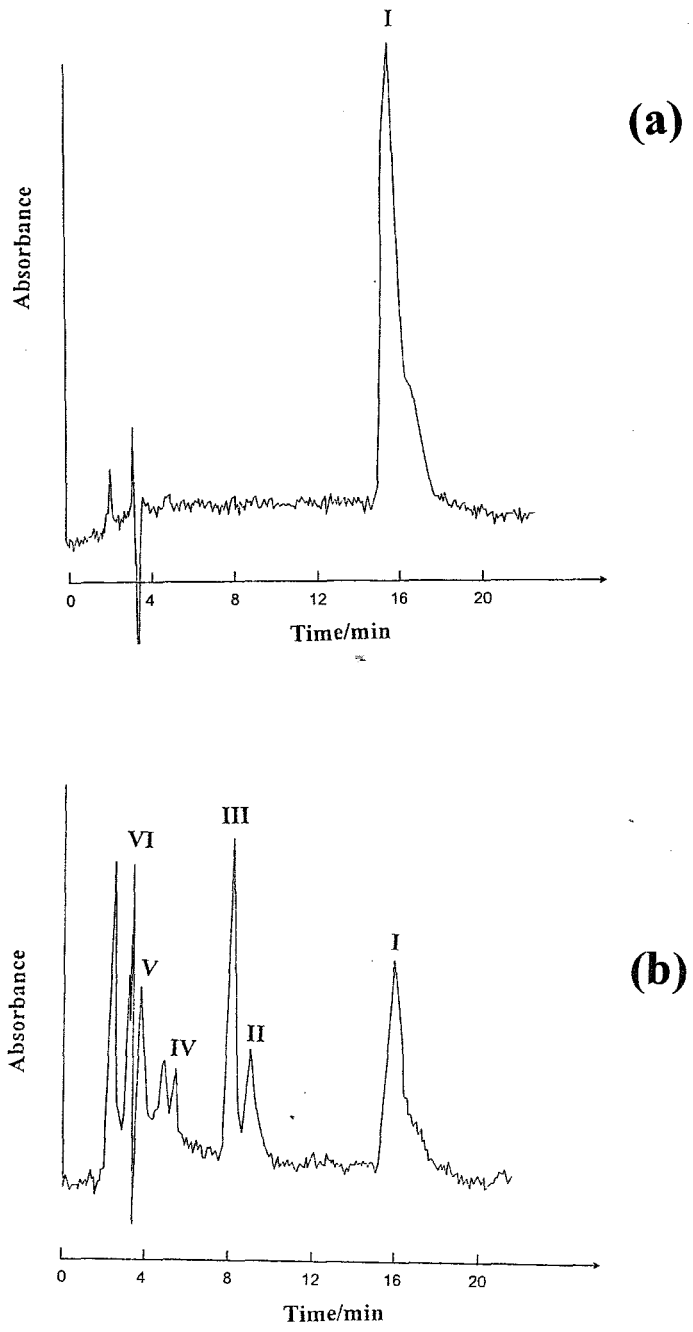

Fig. 5.28 HPLC chromatogram of 1.2×10^{-5} mol dm^{-3} 4-Cp oxygenated solution containing 0.035 mg/ml of $NdPc_2$ in water before (a) and after 120 min of irradiation (b).

From the HPLC results, it was found out that the consumption of 4-chlorophenol was up to 35% after an irradiation period of 120-180 minutes.

5.4.3.2 kinetic studies of the photocatalytic transformation of 4-chlorophenol

The L-H kinetic model has been successfully used to describe the photocatalytic transformation of 4-chlorophenol in the presence of photocalaysts in solid state [109, 118, 171-173, 180]. This kinetic model is known to be good for the description of the solid-gas reaction. The extrapolation of this model to solid-liquid has shown successful results [118,171-173,180,184]. Al-Sayyed et al. [183], employed the L-H kinetic model for the kinetic studies of 4-Cp disappearance under UV illumination in the presence of semiconductor catalysts TiO_2, ZrO_2 and MoO_3.

The L-H kinetic model establishes whether the degradation takes place in the adsorbed state in which 4-chlorophenol is supposed to adsorb to the photocatalyst, or whether semiconductor catalysts provide active species which initiate the reaction[185]. In this model, an adsorption equilibrium is assumed at all times, and the reaction rate is assumed to be much less than the rate of adsorption or desorption [184]. Thus, if a single reactant is decomposed, the process could be assumed as unimolecular or bimolecular depending on the number of product molecules formed per reactant or whether or not the product is absorbed. Two extreme condition should be taken on account [171]: i) both the reactant and solvent compete for the same active sites; ii) both the reactant and solvent are absorbed on the surface without competing for the same active sites.

If the system follows this model, the reaction should be first-order at sufficiently low values of C_0 (where C_0 is the initial concentration) and as C_0 increases, the reaction order gradually drops until it becomes zero order [185]. Thus, at very low concentration of the reactant, the reaction is first-order as follows, Equation 5.29.

$$\ln \frac{C_0}{C} = k' t \qquad (5.29)$$

Where k' is the apparent first-order rate constant and C is the concentration of the substrate at time t.

In this work, the kinetic studies were carried out following the degradation of 4-chlorophenol by HPLC. The degradation of 4-chlorophenol was monitored with the photolysis time as illustrated in Fig. 5.29, which shows that the concentration of 4-chlorophenol (proportional to the height of HPLC peak) decreased with the irradiation time. The plot of ln C (where C is proportional to the height of HPLC peak) versus the irradiation time for the transformation of 4-chlorophenol in the presence of solid of [Pc(-2)Nd^{III}Pc(-2)]$^-$ gave a straight line, Fig. 5.30. The slopes of the plot in Fig. 5.30 gave the apparent first-order rate constant k'.

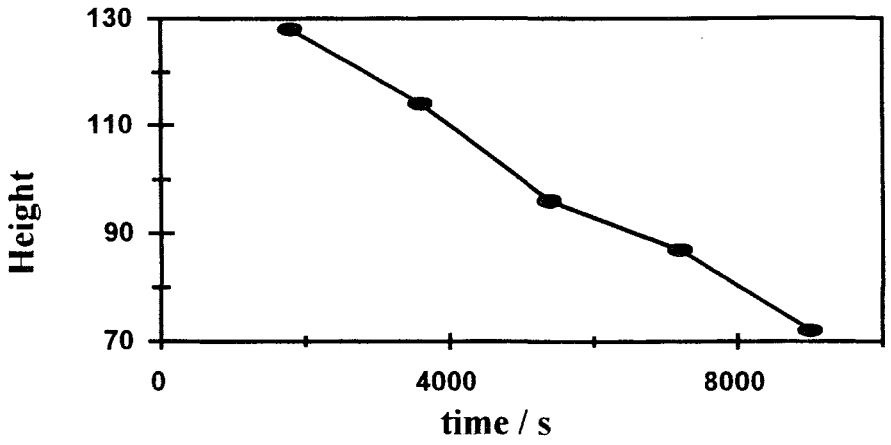

Fig. 5.29 Changes of HPLC peak height observed during the photolysis of an aqueous solution of 3.0×10^{-6} mol dm^{-3} 4-Cp containing 0.035 mg/l of solid $[NdPc_2]^-$ and saturated with oxygen.

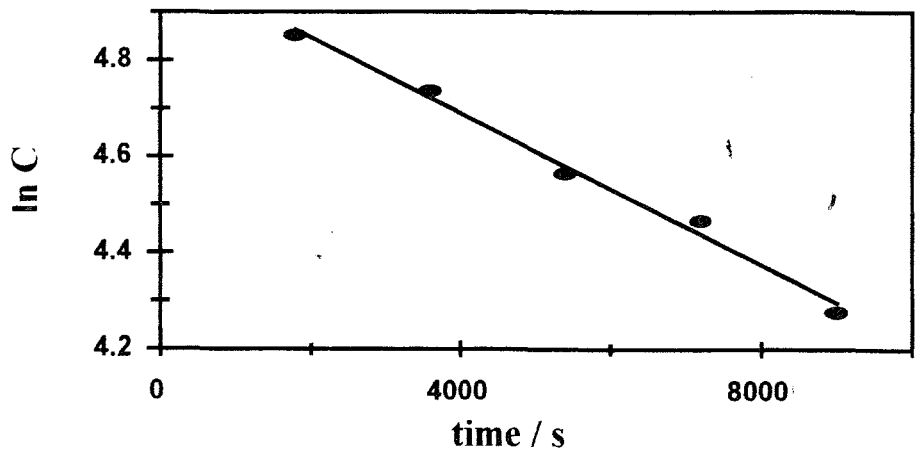

Fig. 5.30 Plot of ln C versus time for the photolysis of 3.0×10^{-6} mol dm^{-3}solution of 4-Cp containing 0.035mg/ml of $NdPc_2^-$ and saturated with oxygen.

5.4.3.2.1 Effect of 4-chlorophenol concentration on the kinetics of reaction

The effect of initial concentrations of 4-chlorophenol ($1\text{-}15 \times 10^{-6}$ mol dm^{-3}) on the photocatalytic transformation of 4-chlorophenol in the reactor shows that the values of apparent first-order rate constants decreased with the increase in the concentration of 4-Cp as shown in Table 5.5. A similar observation was also reported in the photocatalytic degradation of chlorinated phenol over TiO_2 [171]. The rate of transformation of 4-Cp is slower at higher concentration of this compound.

Table 5.5 Apparent first-order rate constants k′ for the photocatalytic transformation of 4-Cp.

10^{6} [4-Cp]$_0$ (mol dm^{-3})	10^{5} k′ (s^{-1})
1.0	7.9 ± 0.42
3.0	7.8 ± 0.35
5.0	7.6 ± 0.55
7.5	6.8 ± 0.48
10.0	6.4 ± 0.52

The plot of the reciprocal of the initial reaction rate (Rate $^{-1}$) against the reciprocal of the initial concentration of 4-Cp (C_0^{-1}) was found linear with a non-zero intercept, Fig. 5.31. The results obtained in Fig. 5.31 confirm that the Langmuir-Hinshelwood kinetic model is appropriate for the kinetic treatment since the plot is linear, and the reaction occurred on the surface of the

photocalysts. From the plot of Rate $^{-1}$ versus C_0^{-1}, k_a was determined to be equal to 2.16x10 $^{-2}$ H s $^{-1}$ and the adsorption coefficient was determined as K= 45.66 mol $^{-1}$ dm ^{3}, from the slope. The high value of adsorption constant K may imply that coverages of the large $NdPc_2^-$ surface by 4-Cp are attained [183]. The possibilities of significant photoadsorption or the involvement of the reaction steps occurring in the double layer could not be ruled out [183].

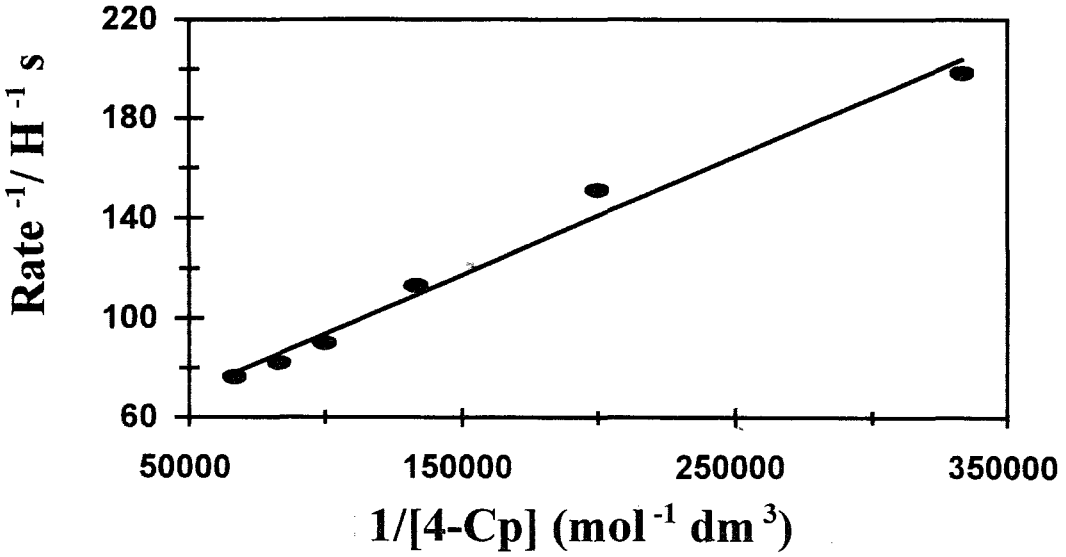

Fig. 5.31 Plot of Rate $^{-1}$ versus C_0^{-1} for the transformation of 4-Cp over solid $NdPc_2^-$ using unfiltered radiation.

The possible mechanism for the transformation of 4-Cp described in Scheme 5.6 with visible photolysis is also valid with UV radiation. The mechanism of 4-Cp photocatalytic degradation in the presence of TiO_2 using UV radiation shows that the formation of OH-monochlorophenol adducts has been suggested as photoproducts of the oxidation of 4-Cp by hydroxyl radicals [183].

Although this work confirms further transformation of 4-Cp to 4-CC and HQ, $LnPc_2^-$ may not be good catalysts for the mineralization of 4-Cp. This study is useful in exploring the catalytic properties of $LnPc_2$ complexes.

The quantum yields for the consumption of 4-Cp were determined using the following equation [158]:

$$\Phi = -\frac{(C_t - C_0)\, V_R}{I_0\, t} \qquad (5.30)$$

Where C_0 and C_t are the 4-Cp concentrations prior to and after irradiation, respectively, V_R is the reaction volume (in this case 40 ml), t is the irradiation time per cycle and the light intensity I_0 was found to be 2.0×10^{-7} einstein/sec. HPLC peak height were correlated with the initial concentrations of solutions.

Table 5.6 gives the quantum yields determined for each $[NdPc_2]^-$ loading for the photolysis of 4-Cp. The quantum yields of disappearance of 4-Cp were higher at lower $[NdPc_2]^-$ loading. This fact was also observed by others [118] and was attributed to a greater portion of photons which have shorter wavelengths and are more energetic being absorbed. The quantum yields varied from 0.0018 to 0.009 whereas those reported for the photocatalytic degradation of 4-Cp over TiO_2 varied from 0.009 to 0.013 [118, 180, 183] and those observed for the photooxidation of organic impurities in water using TiO_2 with a maximum quantum yield of 0.022 [175]. Since different experimental conditions were employed, these data could not be compared to others.

Table 5.6 Quantum yields observed at different $[NdPc_2]^-$ loadings during the direct photolysis of 4-Cp.

$[NdPc_2]^-$ loading (mg/ml)	$10^2\ \Phi$
0.028	0.9
0.044	0.85
0.051	0.62
0.062	0.22
0.122	0.18

5.5 Photolysis of lanthanide diphthalocyanines in the presence of thionyl chloride*

As discussed in chapter 1, batteries based on lithium-thionyl chloride (Li-$SOCl_2$) are receiving attention due to their high current densities. The reduction mechanism of $SOCl_2$ has been the subject of considerable research [120,121,186-189] since reactive intermediates resulting from the one-electron reduction of $SOCl_2$ cause spontaneous exothermic reactions leading to cell discharge [121]. The cathodic reaction of the Li-$SOCl_2$ cell is:

$$2SOCl_2 + 4\bar{e} \rightarrow S + SO_2 + 4Cl^- \qquad (5.31)$$

The formation of sulphur and sulphur dioxide as final products has been confirmed by electrochemical and spectroscopic methods [187, 189]. Intermediate species such as SO and S_2O have been reported [121, 189]. The $SOCl_2$ reduction mechanism is sometimes complicated by the reaction between $SOCl_2$ and the electrolytes [190]. Possible aggregation of $SOCl_2$ may also further complicate the mechanism for its reduction.

The Li/$SOCl_2$ battery however can be explosive. Explosions during storage or exposure to the environment of a partly discharged cell have been attributed to unstable intermediates from the $SOCl_2$ reduction [191]. Another disadvantage of the Li/$SOCl_2$ battery is the polarization of the Li anode associated with the prolonged storage of the batteries. It has been suggested that this

*. The following publication resulted from work presented in this section: N. Nensala and T. Nyokong , Polyhedron. 17 (1998). 3467

polarization is caused by a passive film of LiCl formed on the lithium anode. The LiCl film also adds to the complexity of the reduction mechanism of $SOCl_2$.

Two-electron reduction of $SOCl_2$ was observed by Venkatasetty [120] and was attributed to the formation of donor-acceptor complexes between $SOCl_2$ and aprotic solvents such as acetonitrile and DMF. The two-electron reduction of $SOCl_2$ was also observed when a carbon cathode was coated with tetra neopentoxyphthalocyanine, CoTnPc [121,186]. The CoTnPc firstly formed an adduct with $SOCl_2$ followed by the electron transfer. Reduction of $SOCl_2$ was found to be difficult at high concentrations of $SOCl_2$, due to its aggregation in organic solvents including DMSO, DMF and propylene carbonate [187].

It has been shown that the modification of the carbon cathode of the Li/$SOCl_2$ battery with metallophthalocyanine MPc(-2), complexes improves the cell voltage and the lifetime of the battery [106]. The MPc complexes also prevent passivation of the electrode by LiCl. CoPc and FePc complexes showed catalytic activities towards the reduction of $SOCl_2$ [106]. This work reports on the use of $LnPc_2$ as photocatalysts towards the reduction of $SOCl_2$.

5.5.1 Interactions of [Pc(-2)LnPc(-2)]$^-$ with $SOCl_2$

5.5.1.1 Photolysis of [Pc(-2)LnPc(-2)]$^-$ in the presence of $SOCl_2$

The interaction between the blue form of lanthanide diphthalocyanine complexes and $SOCl_2$ was concentration dependent. At $SOCl_2$ concentrations higher than 1×10^{-4} mol dm^{-3}, spontaneous

oxidation of [Pc(-2)LnPc(-2)]$^-$ to [Pc(-2)LnPc(-1)] species occurred. At concentrations of $SOCl_2$ less than $1x10^{-4}$ mol dm $^{-3}$, no noticeable reactions were observed. When a solution containing $4.5x10^{-5}$ mol dm^{-3} of $SOCl_2$ and $1x10^{-6}$ mol dm $^{-3}$ [Pc(-2)Eu^{III}Pc(-2)]$^-$ in acetonitrile was photolysed with filtered radiation ($\lambda > 590$ nm) from a tungsten lamp, the spectral changes are shown in Fig. 5.32. Similar spectral changes were observed when DMF or DMF-acetonitrile were used.

Fig. 5.32(a) shows the spectrum of [Pc(-2)EuPc(-2)]$^-$ before the addition of $SOCl_2$. This spectrum is typical of the blue [Pc(-2)LnPc(-2)]$^-$ species and shows a relatively intense absorption band at 623 nm and a weaker band at 667 nm. The spectrum observed on addition of $SOCl_2$, prior to photolysis, was similar to the spectrum shown in Fig. 5.32(a). There was no shift in the Q band region. Shifting in the spectra of the MPc complexes on addition of $SOCl_2$ has been attributed to the formation of an adduct between $SOCl_2$ and the MPc species [121]. When a solution containing $SOCl_2$ 4.5 x 10^{-5} mol dm $^{-3}$ and [Pc(-2)EuPc(-2)]$^-$ was photolysed, the 623 nm band decreased in intensity and the low energy band increased in intensity, Fig. 5.32. The new spectra was formed with a clear isosbestic point at 593 nm showing that only two species are involved. The colour of the solution changed from blue to green. The spectra at the end of photolysis, Fig. 5.32(b), is typical of the spectra of the Pc(-2)LnPc(-1) species [31], with a characteristic weak band near 460 nm associated with electronic transition into the semi-occupied molecular orbital (SOMO) of the phthalocyanine ring.

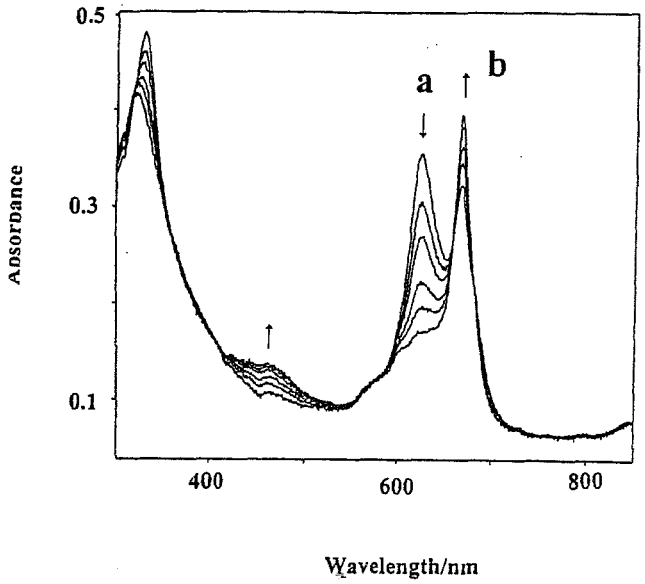

Fig. 5.32. Spectral changes observed during the photolysis of a solution containing 4.5×10^{-5} mol dm^{-3} of $SOCl_2$ and 1×10^{-6} mol dm^{-3} $[Pc(-2)Eu^{III}Pc(-2)]^-$ in acetonitrile.

Similarly, photolysis of the $[Pc(-2)NdPc(-2)]^-$, $[Pc(-2)TmPc(-2)]^-$ and $[Pc(-2)LuPc(-2)]^-$ species in the presence of $SOCl_2$ gave spectra due to the corresponding green Pc(-2)NdPc(-1), Pc(-2)TmPc(-1) and Pc(-2)LuPc(-1), respectively. The $[Pc(-2)NdPc(-2)]^-$, $[Pc(-2)TmPc(-2)]^-$ and $[Pc(-2)LuPc(-2)]^-$ species were found to have low solubility in acetonitrile, hence the photochemical reactions of these complexes were carried out in DMF or a mixture of DMF and acetonitrile. The oxidation of the $[Pc(-2)LnPc(-2)]^-$ species was reversible since the green species could be reduced back to the starting blue species by reducing agents such as sodium borohydride. Spectral changes shown in Fig. 5.32 were observed even when unfiltered radiation was employed. Without photolysis, no changes in the spectra were observed at these low concentrations of $SOCl_2$.

At low concentrations (< 3 x 10^{-4} mol dm^{-3}), the spectra of $SOCl_2$ consists of a single absorption band near 220 nm in acetonitrile. The observation of a single absorption band at 220 nm confirmed that $SOCl_2$ was not aggregated at these low concentrations. Since concentrations lower than 1 x 10^{-4} mol dm^{-3} were employed for the photolysis studies (Fig. 5.32) it is assumed that $SOCl_2$ is not aggregated under our conditions. There is a possibility of the photodecomposition of $SOCl_2$ when unfiltered radiation is used. Photolysis of 4 x 10^{-5} mol dm^{-3} of $SOCl_2$, in the absence of the lanthanide diphthalocyanine complexes, and using unfiltered radiation resulted in no absorption spectral changes of $SOCl_2$, hence suggesting that $SOCl_2$ does not photodecompose under these conditions. Also, no spectral changes were observed when the $[Pc(-2)LnPc(-2)]^-$ species was photolysed in acetonitrile, in the absence of $SOCl_2$. No noticeable spectral changes were observed, without photolysis, for the solutions containing $SOCl_2$ and $[Pc(-2)LnPc(-2)]^-$ at the concentrations used in Fig. 5.32.

It has been shown before that $SOCl_2$ rapidly (within seconds) oxidizes cobalt(I) tetraneopentoxyphthalocyanine ($[Co^{I}TnPc(-2)]^-$) by a two-electron transfer process to form the $[Co^{III}TnPc(-2)]^-$ species [3]. Whereas the two-electron oxidation of $Co^{II}TnPc(-2)$ by $SOCl_2$ occurred relatively more slowly with the formation of a $[Co^{III}TnPc(-1)]^{2-}$ species [121]. One-electron oxidation of $[Co^{III}TnPc(-2)]^-$ to $[Co^{III}TnPc(-1)]^{2-}$ by $SOCl_2$ occurred very slowly. As mentioned above, oxidation of the $[Pc(-2)LnPc(-2)]^-$ species by $SOCl_2$ was concentration dependent. When concentrations of $SOCl_2$ greater than 1 x 10^{-4} mol dm^{-3} were employed for $[Pc(-2)LnPc(-2)]^-$ concentrations in the range 1 x 10^{-6} to 1 x 10^{-5} mol dm^{-3}, oxidation of the later occurred immediately without photolysis. As the concentration of the $SOCl_2$ decreased, the extent of the oxidation of the $[Pc(-2)LnPc(-2)]^-$ decreased and at very low concentrations of $SOCl_2$ (<

1 x 10^{-4} mol dm^{-3}), no noticeable oxidation of [Pc(-2)LnPc(-2)]$^-$ was observed spectroscopically, without photolysis of the solution. The actual concentration of $SOCl_2$ needed for oxidation of the [Pc(-2)LnPc(-2)]$^-$ species without need for photolysis depended on the central lanthanide metal ion. The ease of oxidation of lanthanide diphthalocyanine species increase across the series [16]. Thus, [Pc(-2)LuPc(-2)]$^-$ is more readily oxidized, followed by [Pc(-2)TmPc(-2)]$^-$, then [Pc(-2)EuPc(-2)]$^-$, with [Pc(-2)NdPc(-2)]$^-$ being the least readily oxidized. Considering the same concentrations of the lanthanide diphthalocyanine species, the [Pc(-2)LuPc(-2)]$^-$ species required lower concentration of the $SOCl_2$ species to initiate one-electron oxidation (without photolysis) to the green, Pc(-2)LnPc(-1), complex than the rest of the [Pc(-2)LnPc(-2)]$^-$ complexes.

As shown by Equation 5.31, SO_2 and S are the expected final products for the four electron reduction of $SOCl_2$. Since only one electron was transferred to $SOCl_2$ from the [Pc(-2)LnPc(-2)]$^-$ species, it is unlikely that S or SO_2 are formed during the photolysis reactions shown in Fig. 5.32. Spectra due to the $SOCl_2$ species is located in the ultraviolet region and hence it is masked by the Soret band absorption of the [Pc(-2)LnPc(-2)]$^-$ species, it was thus not possible to monitor changes in the spectra of $SOCl_2$ during photolysis. The species formed by the one-electron transfer reaction occurring between $SOCl_2$ and the [Pc(-2)LnPc(-2)]$^-$ species is most likely the reactive intermediate, $SOCl^{\cdot}$, Equation 5.32:

$$\mathbf{SOCl_2 + e^- \rightarrow SOCl^{\bullet} + Cl^-} \qquad \textbf{(5.32)}$$

The $SOCl^{\cdot}$ radical is not good for the safe operation of the $Li/SOCl_2$ battery since the radical is known to dimerize and decompose into hazardous intermediates [121, 192]. In the presence of metallophthalocyanine complexes, the $SOCl^{\cdot}$ radical can undergo a further one-electron reduction, leading to safer reduction products. Attempts to photoinduce the transfer of the second electron from the green, Pc(-2)LnPc(-1) species formed following the photolysis of solutions containing $SOCl_2$ and $[Pc(-2)LnPc(-2)]^-$ in acetonitrile or DMF, at low concentrations of $SOCl_2$, were unsuccessful. There was no spectroscopic evidence for the formation of the red, $[Pc(-1)LnPc(-1)]^-$, species expected to be formed by one-electron oxidation of Pc(-2)LnPc(-1). As will be discussed below, one-electron oxidation of the green Pc(-2)LnPc(-1) species to the red $[Pc(-1)LnPc(-1)]^-$ occurred in dichloromethane on photolysis in the presence of low concentrations of $SOCl_2$.

5.5 1.2 Kinetic studies of the interaction between $[Pc(-2)LnPc(-2)]^-$ and $SOCl_2$

Kinetic data for the photolysis of $[Pc(-2)LnPc(-2)]^-$ species in the presence of $SOCl_2$ were collected by keeping the concentration of the former constant at 1×10^{-6} mol dm^{-3} and varying the concentration of the latter, then photolysing the solution. Since concentrations of the $SOCl_2$ were larger than those of the lanthanide diphthalocyanines by a factor of at least 20, pseudo first order conditions were assumed. The formation of [Pc(-2)LnPc(-1)] species was followed by monitoring the decrease in absorbance of the Q band at 623 nm. The decrease of this band represents the disappearance of $[Pc(-2)LnPc(-2)]^-$ with the photolysis time as shown in Fig. 5.33. In Fig. 5.34, plots of $\ln(A_t - A_\infty)$ versus time were linear for at least 80% completion, confirming a first order

dependence of the photocatalytic reaction on lanthanide diphthalocyanines. A_t and A_∞ represent the absorbances at time t and infinity, respectively.

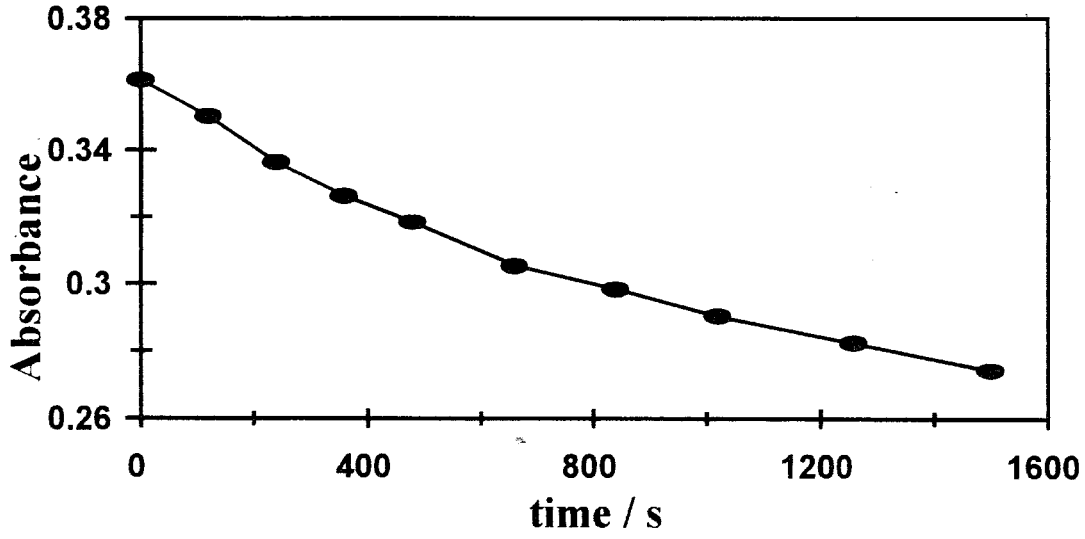

Fig. 5.33 Changes in absorbance for the band at 623 nm following photolysis of a solution containing $SOCl_2$ and $EuPc_2^-$ in acetonitrile. Concentrations of $SOCl_2$ and $[Pc(-2)EuPc(-2)]^-$ are $2.2x10^{-5}$ and $1x10^{-6}$ mol dm^{-3}, respectively.

The slopes of the plots $\ln(A_t-A_\infty)$ versus time gave the observed rate constants, k_{obs} which is proportional to $SOCl_2$ concentration as follows:

$$k_{obs} = k_f[SOCl_2] + k_r \qquad (5.33)$$

The symbols of this equation are explained in Sections 5.2 and 5.3.

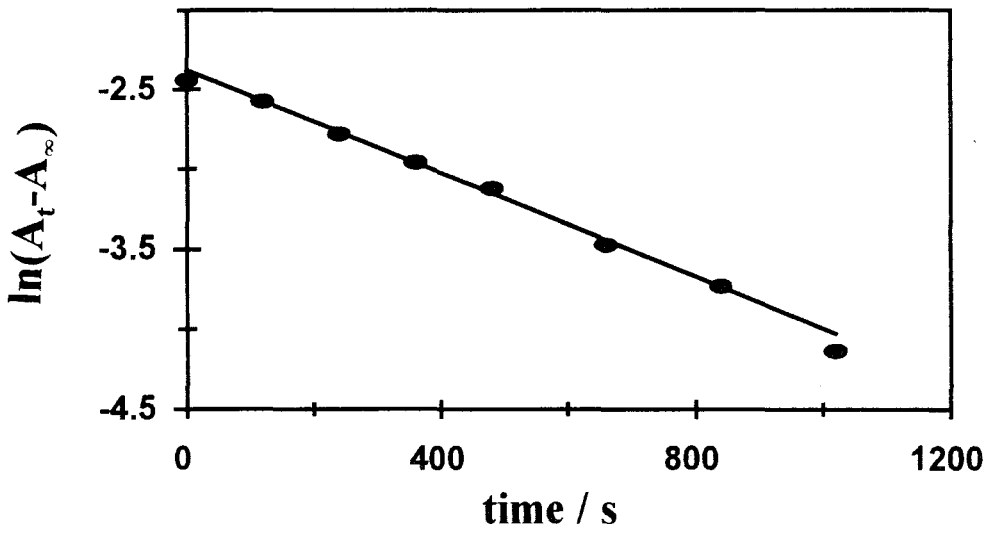

Fig. 5.34 Plot of $\ln(A_t-A_\infty)$ versus time for the photolysis of a solution containing 2.2×10^{-5} mol dm^{-3} of $SOCl_2$ and 1×10^{-6} mol dm^{-3} of $EuPc_2^-$ in acetonitrile.

The plots of k_{obs} versus the concentration of $SOCl_2$ were linear as shown if Fig. 5.35 for the [Pc(-2)EuPc(-2)]$^-$ species, confirming a first order dependence of the reaction on $SOCl_2$. The slopes of the plots k_{obs} versus time are known as k_f and were found to be 5.4 ± 0.12 for $EuPc_2^-$ in acetonitrile and $k_f = 92.6 \pm 2.8$ for $TmPc_2^-$ in DMF. Photocatalytic studies of $LnPc_2^-$ in the presence of SO_2 and PCP discussed in this work show that, the photosensitization strength increases with the decrease of the lanthanide ion radius. Although, the two complexes were studied in different solvents because of lower solubilities of most $LnPc_2^-$ in acetonitrile, the magnitude of k_f shows that $TmPc_2^-$ is better photosensitizer than $EuPc_2^-$.

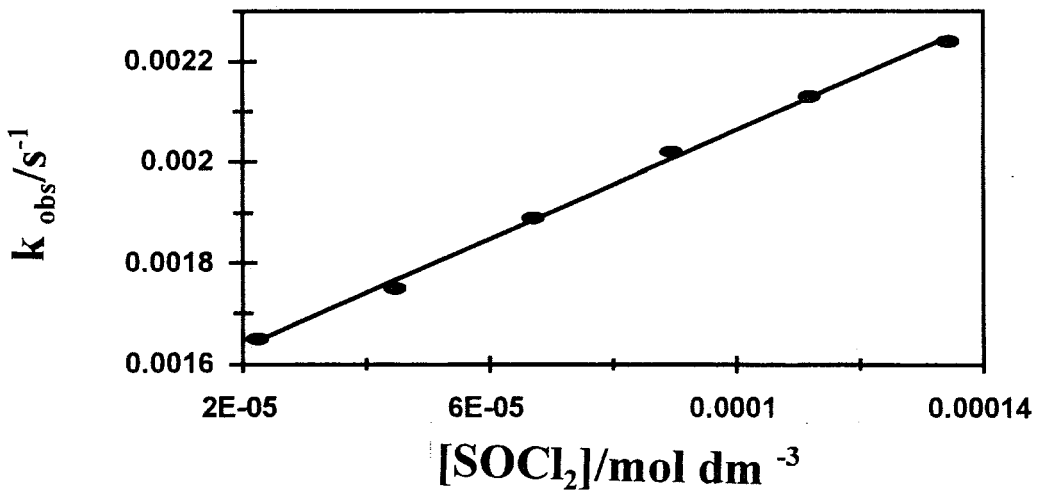

Fig. 5.35 Plot of k_{obs} versus $[SOCl_2]$ for the photolysis of $EuPc_2^-$ in the presence of $SOCl_2$ in acetonitrile.

5.5.1.3 Quantum yield studies for the interaction between $[Pc(-2)LnPc(-2)]^-$ and $SOCl_2$

The relative quantum yields for the quenching of $^*[Pc(-2)LnPc(-2)]^-$ with $SOCl_2$ are of the same order of magnitude of 10^{-4} to 10^{-3} as the quantum yields reported for the quenching of these species by pentachlorophenol and SO_2. The quantum yields of disappearance of $[Pc(-2)LnPc(-2)]^-$ are related to the concentration of $SOCl_2$ according to the Equation 5.34:

$$\frac{1}{\Phi} = \frac{1}{\Phi^0} + \frac{k_d}{\Phi^0 k_f} \frac{1}{[SOCl_2]} \qquad (5.34)$$

The inverse of the quantum yields for the reaction between $SOCl_2$ and the $^*[Pc(-2)LnPc(-2)]^-$ species were plotted versus the inverse of $SOCl_2$ concentration, Fig. 5.36 for $[Pc(-2)EuPc(-2)]^-$, giving linear Stern-Volmer plots and hence showing that $SOCl_2$ is a quencher for the photoexcited $^*[Pc(-2)LnPc(-2)]^-$ species.

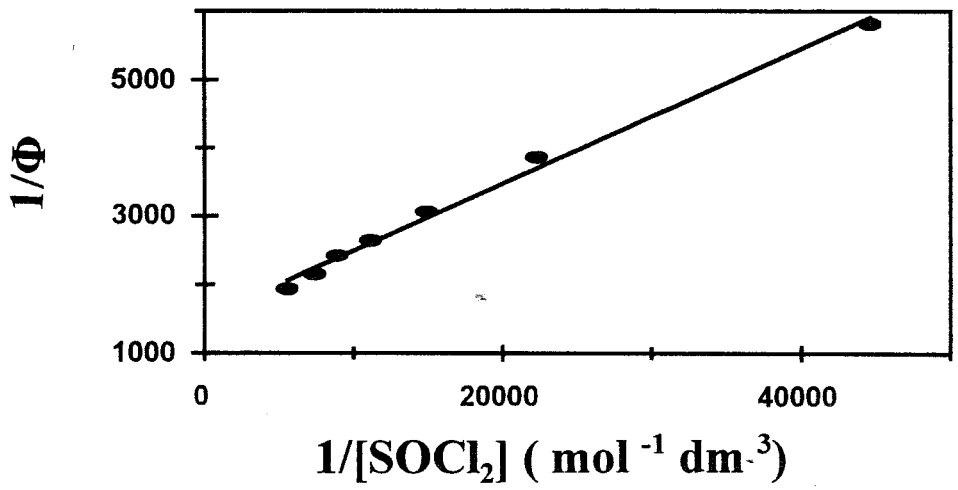

Fig. 5.36 Plot of 1/ Φ versus 1/ $[SOCl_2]$ for the photolysis of $[Pc(-2)EuPc(-2)]^-$ in the presence of $SOCl_2$ in acetonitrile.

5.5.1.4 Mechanism of the reaction between $[Pc(-2)lnPc(-2)]^-$ and $SOCl_2$

As it has been discussed before and in comparison with $SnPc_2$, it is expected that the triplet states of the lanthanide diphthalocyanine species are populated by photolysis of these complexes in the visible region. The $^3\pi\pi^*$ excited states may then be quenched by the reaction with $SOCl_2$, Equations 5.35 and 5.36:

$$\left[Pc(-2)LnPc(-2)\right]^{-} \xrightarrow{h\nu} {}^{*}\left[Pc(-2)LnPc(-2)\right]^{-} \quad (5.35)$$

$${}^{*}\left[Pc(-2)LnPc(-2)\right]^{-} + SOCl_2 \rightarrow SOCl^{\bullet} + Cl^{-} + Pc(-2)LnPc(-1) \quad (5.36)$$

Scheme 5.7

5.5.2 Interaction between Pc(-2)LnPc(-1) and $SOCl_2$

5.5.2.1 Photolysis of Pc(-2)LnP(-1) in the presence of $SOCl_2$

When a solid [Pc(-2)LnPc(-2)]$^{-}$ species was dissolved in dichloromethane, the green species [Pc(-2)LnPc(-1)] was formed instantly. It is important to determine the role of the solvent in the photolytic studies involving the Pc(-2)LnPc(-1) species and $SOCl_2$. Similar studies are reported above for $SnPc_2$ and CH_2Cl_2. When solution of Pc(-2)LnPc(-1) in CH_2Cl_2 were photolysed in the absence of $SOCl_2$, no significant spectral changes were observed, hence showing that CH_2Cl_2 does not act as a quencher of the photoexcited *[Pc(-2)LnPc(-1)] species. The interaction between Pc(-2)LnPc(-1) and $SOCl_2$ was also concentration dependent, with no significant spectral changes observed without photolysis for concentrations of $SOCl_2$ less than 10^{-5} mol dm^{-3}, for Pc(-2)LnPc(-1) concentrations ranging from 1 x 10^{-6} to 1 x 10^{-5} mol dm^{-3}.

Photolysis of a solution containing Pc(-2)LnPc(-1) and 2 x 10^{-5} mol dm^{-3} $SOCl_2$ in CH_2Cl_2 resulted in the spectral changes shown in Fig. 5.37. There was a decrease in the intensity of the Q band at 622 nm and the formation of a new weaker band at lower energies, 696 nm. The band

near 464 nm due to the transition into the SOMO shifted to 475 nm. The new spectra was formed with clear isosbestic points at 346, 375, 557 and 681 nm. The solution turned from green to red. The spectral changes and the corresponding colour changes are typical of the formation of the $[Pc(-1)LnPc(-1)]^-$ species [8,31]. The formation of the $[Pc(-1)LnPc(-1)]^-$ species was reversible. At concentrations larger than 10^{-4} mol dm^{-3}, oxidation of the Pc(-2)LnPc(-1) species to $[Pc(-1)LnPc(-1)]^-$ by $SOCl_2$ occurred without the need for photolysis. The one-electron oxidation of Pc(-2)LnPc(-1) suggests that the reduction of $SOCl_2$ under these circumstances again involves the formation of the same species ($SOCl^-$) as was formed by the photolysis of $[Pc(-2)LnPc(-2)]^-$ in the presence of thionyl chloride.

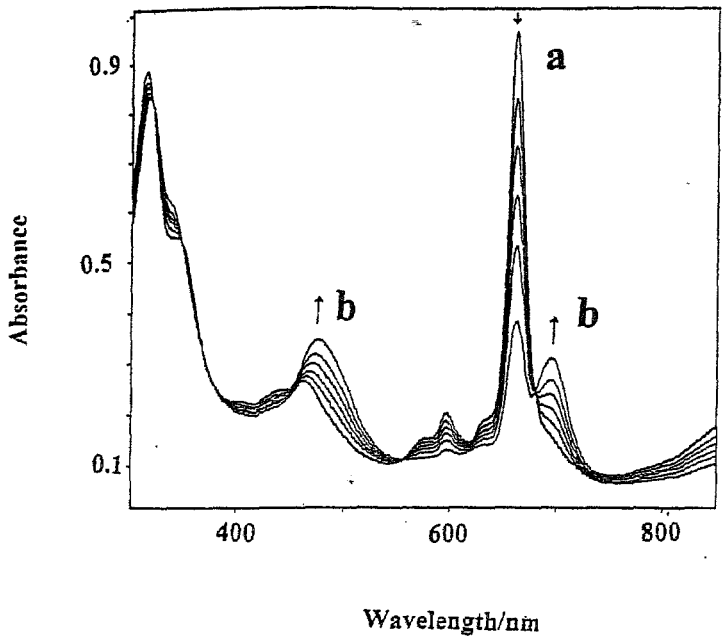

Fig. 5.37 Spectral changes observed during the photolysis of CH_2Cl_2 solution of [Pc(-2)TmPc(-1) in the presence of $2x10^{-5}$ mol dm^{-3} of $SOCl_2$, using filtered radiation from tungsten lamp. a) Spectra of Pc(-2)TmPc(-1) before addition of $SOCl_2$ and b) Spectra afer 30 minutes of photolysis.

5.5.2.2 Kinetic studies of the photochemical reaction between Pc(-2)LnPc(-1) and $SOCl_2$

The formation of the red species [Pc(-1)LnPc(-1)]$^-$ from the [Pc(-2)LnPc(-1)] species was followed by monitoring the decrease in absorbance of the green species at 666 nm. Fig. 5.38 shows the decrease of the peak at 666 nm, characterising the disappearance of [Pc(-2)LnPc(-1)] species with the photolysis time.

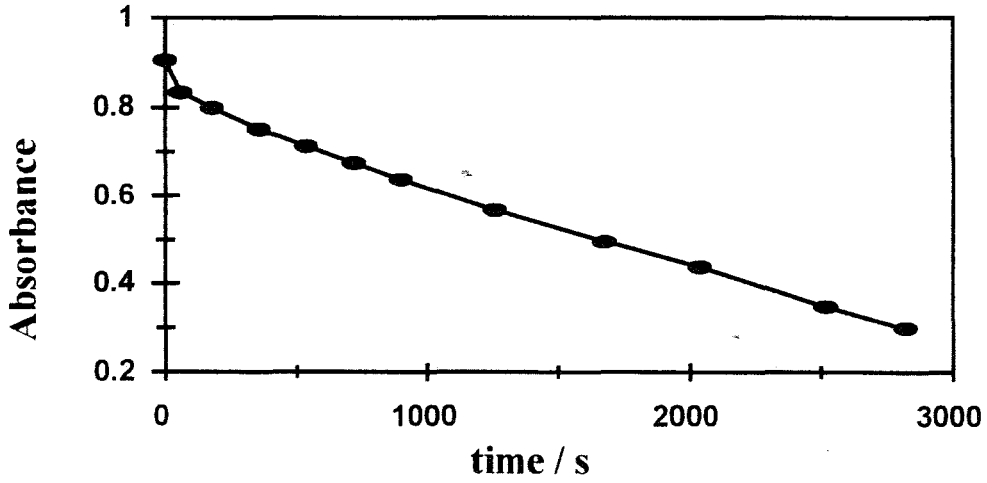

Fig. 5.38 Changes in absorbance of [Pc(-2)TmPc(-1)] at 666 nm following photolysis of CH_2Cl_2 solution of $TmPc_2$ in the presence of 1.74×10^{-5} mol dm^{-3} $SOCl_2$.

Plots of $\ln(A_t - A_\infty)$ versus time were linear at least to 80% completion. Fig. 5.39 confirms the first order dependence of the photocatalytic reaction on [Pc(-2)LnPc(-1)] species. The slopes of the plots shown in Fig. 5.39 gave the observed rate constant, k_{obs}.

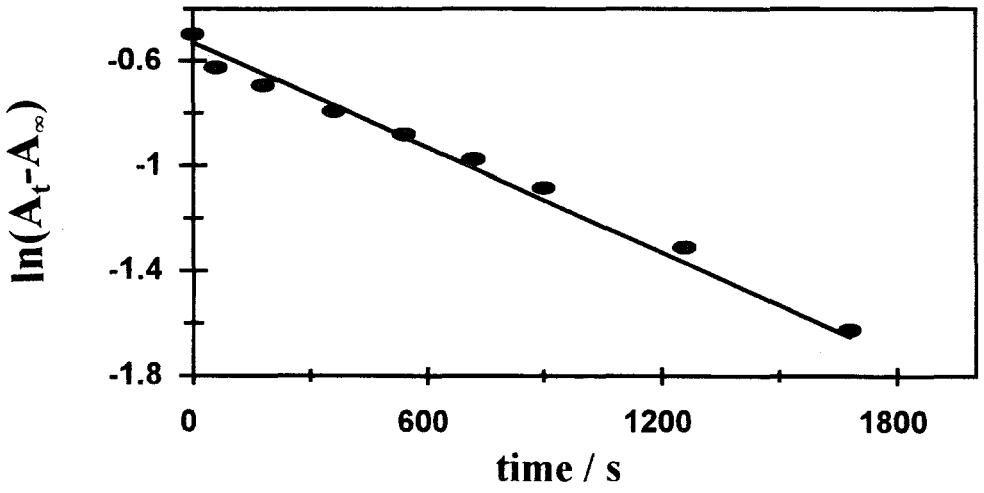

Fig. 5.39 Plot of $\ln(A_t-A_\infty)$ versus time for the photolysis of Pc(-2)TmPc(-1) in the presence of 1.74×10^{-5} mol dm^{-3} of $SOCl_2$ in dichloromethane.

Plots k_{obs} versus concentrations of $SOCl_2$ were found to be linear as shown in Fig. 5.40, confirming the first-order dependence of the reaction on $SOCl_2$. For the reaction between lanthanide diphthalocyanine complexes, $LnPc_2$ and $SOCl_2$, k_f are shown in Table 5.7.

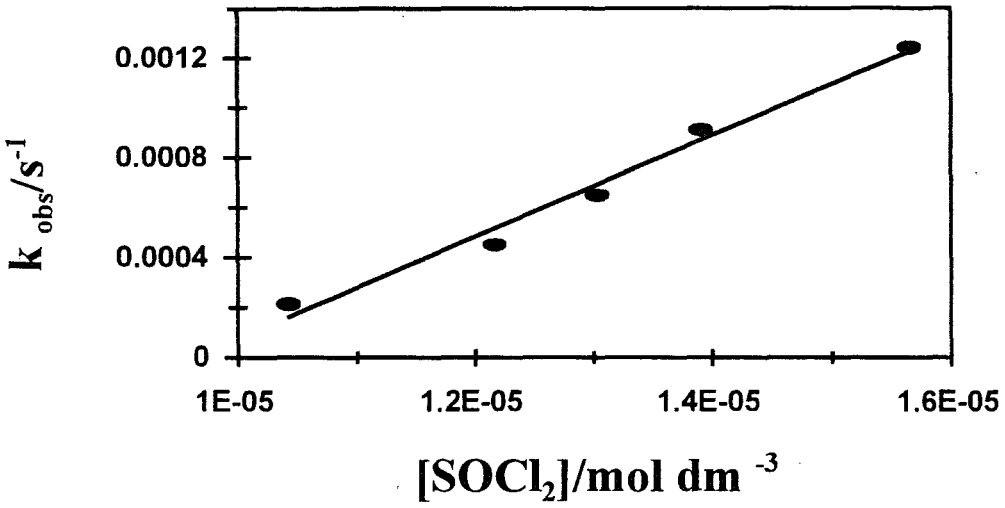

Fig. 5.40 Plot of k_{obs} versus $[SOCl_2]$ for the photolysis of CH_2Cl_2 solutions of Pc(-2)NdPc(-1) in the presence of $SOCl_2$.

Table 5.7 Values of rate constants of formation k_f of different lanthanide diphthalocyanines resulted from their photolysis in the presence of $SOCl_2$ in dichloromethane.

Complex	Slope (k_f) (mol^{-1} dm^3 s^{-1})
Pc(-2)Nd^{III}Pc(-1)	4.883 ± 0.06
Pc(-2)Eu^{III}Pc(-1)	31.509 ± 0.7
Pc(-2)Tm^{III}Pc(-1)	203.210 ± 15.5
Pc(-2)Lu^{III}Pc(-1)	784.700 ± 36

The values of the slopes (k_f) obtained increase with the decrease of the radius of the lanthanide ion. Thus, Pc(-2)LuP(-1) has higher rate constant for the formation of [Pc(-1)LuPc(-1)] $^-$ in the presence of $SOCl_2$ than other lanthanide diphthalocyanines. This implies that the oxidation of Pc(-2)LuPc(-1) in the presence of $SOCl_2$ is easier than other lanthanide diphthalocaynines, hence the complex Pc(-2)LuPc(-1) is better sensitizer of this reaction than others. This suggests that the sensitization power increase with the strength of the π-π interactions in Pc rings in the similar manner as the ease oxidation of these complexes [16].

5.5.2.3 Quantum yield studies of the photolysis of Pc(-2)LnPc(-1) in the presence of $SOCl_2$

Quantum yields for the disappearance of Pc(-2)LnPc(-1) in the reaction between the excited (^{3}π-π*)$LnPc_2$ and $SOCl_2$ were determined in a similar manner as for the interaction between [Pc(-2)LnPc(-2)] $^-$ species with $SOCl_2$. Fig. 5.41 shows a typical Stern-Volmer plot observed in this study. The linear Stern-Volmer plot shows that the $SOCl_2$ does quench the excited (^{3}π-π*) Pc(-2)LnPc(-1) species. Quantum yield values were of the order of 10^{-3} for the Lu^{III} and Tm^{III} complexes and of the order of 10^{-4} for the Nd^{III} and Eu^{III} complexes. Unexpectedly, Stern-Volmer plot in Fig. 5.41 gave a zero- intercept. The reasons of some such behaviours are unknown to us.

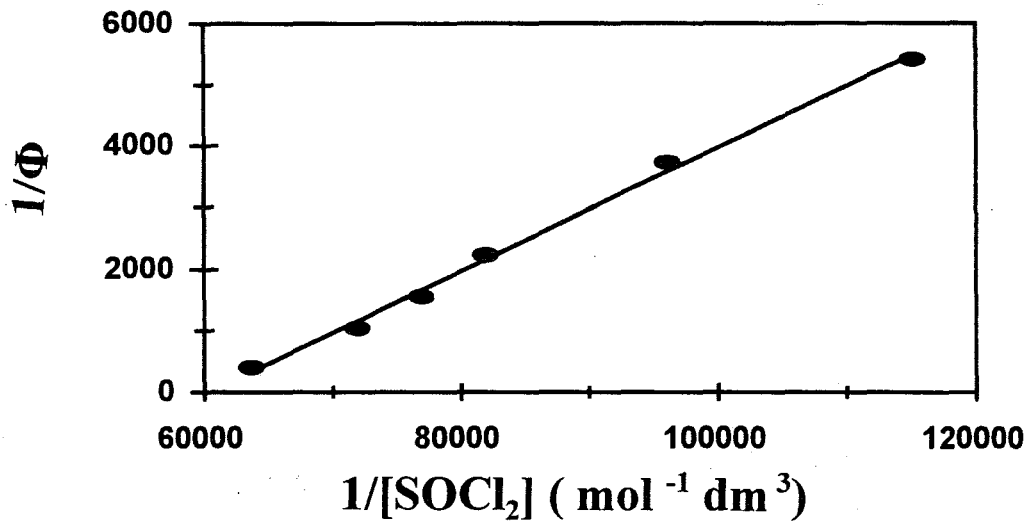

Fig. 5.41 Plot of 1 / Φ versus 1/ [$SOCl_2$] for the photolysis of CH_2Cl_2 solutions of Pc(-2)NdPc(-1) in the presence of $SOCl_2$.

5.5.2.4 Mechanism of the photoreaction between Pc(-2)LnPc(-1) and $SOCl_2$

Kinetic results and quantum yield studies confirm that the photoexcited complex, ($^3\pi$-π^*) Pc(-2)LnPc(-1) transferred an electron to $SOCl_2$. The one-electron oxidation of Pc(-2)lnPc(-1) suggests that the reduction of $SOCl_2$ under these circumstances again involves the formation of the same radical ($SOCl^{\cdot}$) as was formed by the photolysis of [Pc(-2)LnPc(-2)] $^{\cdot}$ in the presence of thionyl chloride. It is thus suggested that the photolysis of Pc(-2)LnPc(-1) in the presence of $SOCl_2$ occurs according to the following equations:

$$Pc(-2)LnPc(-1) \xrightarrow{h\nu} {}^{*}[Pc(-2)LnPc(-1)] \quad (5.37)$$

$${}^{*}[Pc(-2)LnPc(-1)] + SOCl_2 \rightarrow SOCl^{\bullet} + Cl^{-} + [Pc(-1)LnPc(-1)]^{+} \quad (5.38)$$

Scheme 5.8

5.5.3 Interactions of [Pc(-2)LnPc(-2)]$^{-}$ with more highly concentrated $SOCl_2$

When $SOCl_2$ concentrations higher than 10^{-2} mol dm $^{-3}$ were reacted with [Pc(-2)LnPc(-1)] species, the reaction occurred instantly to the formation of [Pc(-1)LnPc(-1)]$^{-}$ species. Typical absorption spectral changes when large concentration of $SOCl_2$ ($\sim 10^{-2}$ mol dm $^{-3}$) were added to acetonitrile solution containing 1×10^{-6} mol dm $^{-3}$ of [Pc(-2)LnPc(-2)]$^{-}$ are illustrated in Fig. 5.42. The spectral changes were observed without photolysis. The solution went directly from blue to red, hence confirming the formation of the [Pc(-1)LnPc(-1)]$^{-}$, species, Fig. 5.42. The two-electron reduction was reversible and the red species could be reduced in a stepwise manner to the green, Pc(-2)LnPc(-1), and finally to the blue, [Pc(-2)LnPc(-2)]$^{-}$, in the presence of reducing agents. The most likely product formed by the two- electron reduction of $SOCl_2$ is the SO species, following the reaction :

$$[Pc(-2)LnPc(-2)]^{-} + SOCl_2 \rightarrow [Pc(-1)LnPc(-1)]^{+} + SO + 2\,Cl^{-} \quad (5.39)$$

This is a more favourable reaction since SO may be less harmful than $SOCl^{\bullet}$ formed by one-electron reduction.

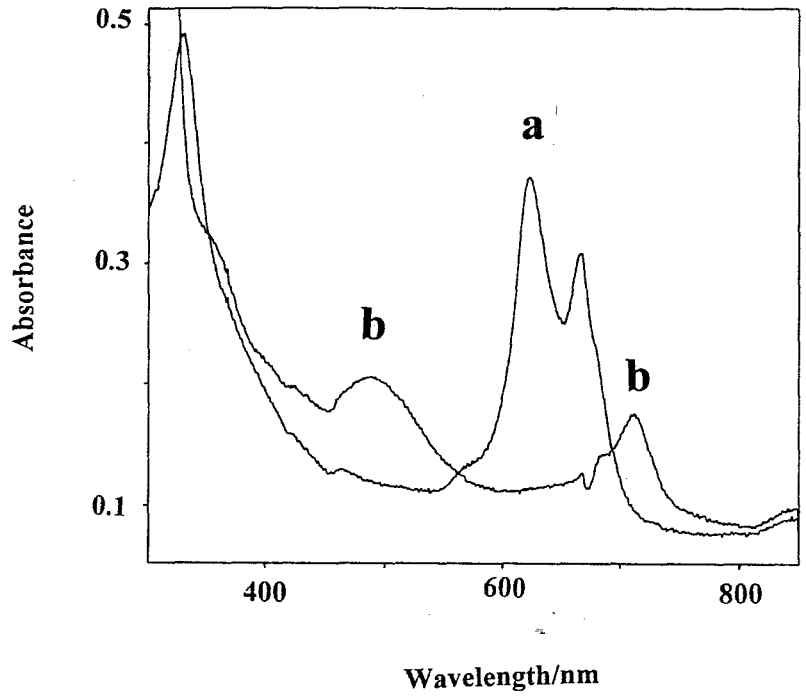

Fig. 5.42 Spectral changes observed by adding 10^{-2} mol dm^{-3} of $SOCl_2$ to acetonitrile solution of [Pc(-2)EuPc(-2)]$^{-}$. a) before addition of $SOCl_2$ and b)after addition.

6. CONCLUSION AND FUTURE WORK

This work has shown that the redox properties of $SnPc_2$ are similar to those of $LnPc_2^-$ species, and that the electronic spectra of oxidized and reduced species are similar to the electronic spectra of the lanthanide diphthalocyanine complexes [45, 56].

Although there are numerous reports on the electrochemistry and spectrolectrochemistry of lanthanide diphthalocyanine complexes [45, 56, 67], this work reports for the first time on the electronic spectra of $[Pc(-1)Ln^{III}Pc(0)]^{2-}$ species.

Phthalocyanines and porphyrins are attractive candidates for the design of photocatalysts since they are highly coloured, exhibit varied redox activity and are chemically stable. However, phthalocyanines have an advantage over porphyrins in that they absorb strongly in the visible and near infrared regions, and are more resistant to ring degradation [193]. This work exploited the catalytic activity of diphthalocyanine complexes. The examples presented in this work show that one-step and multi-step electron transfer reactions occur in catalysis.

The photolysis of [Pc(-2)SnPc(-2)] in the CH_2Cl_2/CH_3CN solvent mixture using unfiltered light leads to the oxidation of this complex to $[Pc(-2)SnPc(-1)]^-$ species, following the electron transfer process from the photoexcited complex, $n\pi^*$ [Pc(-2)SnPc(-2)] to electron acceptor CH_2Cl_2. Consequently, the quencher CH_2Cl_2 is reduced to the radical $CH_2Cl^{\cdot}$ which undergoes rapid dimerization or converted to alkanes in the proton-donor solvents [78, 79]. The mechanism describing these transformations is presented in this work, as referenced in Scheme 5.2. The

weak mixing between orbitals of the two Pc rings of $SnPc_2$ impedes this complex to be oxidized with filtered radiation. The quantum yields obtained are in the order of 10^{-4} which are very low compared to those reported for the photolysis of lanthanide diphthalocyanines in the same solvent mixture [90]. The kinetic data described in the this work showed the catalytic activity of [Pc(-2)SnPc(-2)] towards the dechlorination of methylene chloride. The occurrence of this reaction is justified since the oxidant CH_2Cl_2 has higher oxidation potential than $SnPc_2$. The photocatalytic activity exhibited by $SnPc_2$ towards reduction of CH_2Cl_2 provides a lowering of the toxicity of halogenated compounds in the environment.

This work also reports on the photocatalytic activity of $SnPc_2$ in the photoreduction of SO_2 in solution using unfiltered light. The photolysis of [Pc(-2)SnPc(-2)] in the presence of SO_2, resulted to the oxidation of [Pc(-2)SnPc(-2)] to $[Pc(-2)SnPc(-1)]^-$ species. The one-electron oxidation process is preceded by the excitation of the complex to excited state, $n\pi^*$ [Pc(-2)SnPc(-2)], before transferring an electron to SO_2, which is then reduced to SO_2^-. The formation of $[Pc(-2)SnPc(-1)]^-$ is confirmed from the changes of the electronic spectrum. Detailed mechanistic information is presented in this work in Scheme 5.3. The quantum yields obtained for the photoreduction of SO_2 are low but slightly higher than those obtained in the presence of CH_2Cl_2 alone.

The photocatalytic activities of the blue forms of lanthanide diphthalocaynine complexes, $LnPc_2^-$ are also discussed. The photolysis of blue forms of neodymium, dysprosium and lutetium diphthalocyanines in the presence of SO_2 occur in the similar manner to that for tin diphthalocyanine. Thus, the photolysis of lanthanide diphthalocyanine complexes, [Pc(-2)NdPc(-

2)]$^-$, [Pc(-2)DyPc(-2)]$^-$ and [Pc(-2)LuPc(-2)]$^-$ in the presence of SO_2 using filtered and unfiltered light leads the oxidation of these complexes to [Pc(-2)NdPc(-1)], [Pc(-2)DyPc(-1)] and [Pc(-2)LuPc(-1)], respectively. The electron transfer process is preceded by the excitation of these complexes to the triplet excited state. The mechanism associated to these reactions is shown in Scheme 5.4.

The photosensitization ability is directly related to the magnitude of the ionic radius of lanthanide ions, hence the kinetic data revealed that [Pc(-2)LuPc(-2)]$^-$ is better photosensitizer than the other two $LnPc_2^-$ complexes.

This work also shows that the photolysis of diphthalocyanine complexes [Pc(-2)DyPc(-2)]$^-$ and [Pc(-2)LuPc(-2)]$^-$ in the presence of pentachlorophenol results in the oxidation of these complexes to Pc(-2)DyPc(-1) and Pc(-2)LuPc(-1), respectively. The reductive dechlorination of pentachlorophenol is evidenced by the formation of tetra- and trichlorophenols. There was no evidence of the degradation of the benzene ring of the phthalocyanine (Pc), following photolysis. The electron transfer between lanthanide diphthalocyanines and pentachlorophenol is preceded by the population of the excited triplet state, $^3\pi$-π [Pc(-2)LnPc(-2)]$^-$. Kinetic studies showed that [Pc(-2)LuPc(-2)]$^-$ is a better photosensitizer than [Pc(-2)DyPc(-2)]$^-$. The mechanistic details are shown in Scheme 5.5. The dechlorination of polychlorinated phenol is of environmental importance since it considerably reduces the toxicity of these species. However, the final product formed by the photolysis process described in this work using $LnPc_2^-$ photocatalysts is trichlorophenol which is still relatively toxic. Thus, there is a need for further studies into dechlorination and complete mineralization of PCP. The photochemical method described in this

work for the dechlorination of PCP is a step forward for the degradation of this compound. Pentachlorophenol is a common contaminant of the air, and it is found in small amounts in water.

Even though, the toxicity of 4-chlorophenol and other monochlorophenols is very low compared to the polychlorinated phenols, their high solubility in drinking water place them among the most hazardous compounds to human beings. The mineralization of 4-chlorophenol in aqueous solutions in the presence of catalysts TiO_2, polyoxometalates and MPc have been reported.

The photolysis of neutral aqueous solutions of 4-chlorophenol in the presence of neodymium diphthalocyanine using visible light resulted in the formation of hydroquinone, benzoquinone and 4-chlorocatechol as photoproducts. The drawback of visible photolysis of 4-Cp is the high percent of recovery of 4-Cp, suggesting that there is a little adsorption of 4-chlorophenol on the surface of $NdPc_2$ [177]. The recovery observed for 4-Cp could also be due to the inhibition of 4-Cp by the reaction intermediates. The photocatalytic transformation of 4-chlorophenol in the presence of lanthanide diphthalocyanines using visible light is of great importance, since these complexes absorb strongly in the visible region where most of the solar radiation is used. However, the catalytic activities of $LnPc_2$ using visible light resulted in less intermediates than when unfiltered radiation was used. 4-chlororesorcinol was not observed under these conditions.

Mechanistic details describing the photocatalytic transformation of 4-Cp in the presence of MPc_2 are presented in Scheme 5.6. The photochemical method described in this work for the degradation of 4-Cp using MPc_2 photocatalysts is of great importance because of its potential application in the removal of halogenated hydrocarbons from water on exposure to solar radiation.

This method is also useful for the development of a solar reactor and possibly may be a step forward for the replacement of TiO_2 catalyst in many industrial plants, since TiO_2 absorbs mainly in the UV region which contains only 4% of the solar radiation.

Moreover, the photochemical interaction between lanthanide diphthalocyanine complexes and $SOCl_2$ described in this work, enables us to understand the redox process expected for the possible use of MPc_2 as a cathode in the Li-$SOCl_2$ battery. The photolysis of diphthalocyanine complexes $[Pc(-2)NdPc(-2)]^-$, $[Pc(-2)EuPc(-2)]^-$, $[Pc(-2)TmPc(-2)]^-$ and $[Pc(-2)LuPc(-2)]^-$ in the presence of low concentrations of $SOCl_2$ results in the one-electron oxidation of these complexes to Pc(-2)NdPc(-1), Pc(-2)EuPc(-1) and Pc(-2)LuPc(-1) species, respectively, whereas, the oxidant $SOCl_2$ is reduced to radical $SOCl^{\cdot}$ as the main product. The electron transfer process is preceded by the population of the triplet excited state, $^3\pi$-π^* $[Pc(-2)LnPc(-2)]^-$ which transfers the electron to $SOCl_2$. The mechanism detailing the formation of Pc(-2)LnPc(-1) species is described in Scheme 5.7.

The reaction of blue forms of $[Pc(-2)\ LnPc(-2)]^-$ species with large concentrations of $SOCl_2$ leads instantly to the two-electron oxidation of the $[Pc(-2)LnPc(-2)]^-$ species to $[Pc(-1)LnPc(-1)]^-$. The two-electron reduction of $SOCl_2$ could result in a safer battery, since it eliminates the formation of reactive intermediates responsible for the instant discharge of the battery. The ability of lanthanide diphthalocyanine complexes, $LnPc_2^-$ to photoassist the two-electron reduction of $SOCl_2$ place them as suitable cathodes for safer Li-$SOCl_2$ battery.

The photolysis of green species of lanthanide diphthalocyanine complexes, Pc(-2)LnPc(-1) in the presence of $SOCl_2$ results in one-electron oxidation of these complexes to $[Pc(-1)LnPc(-1)]^+$ species, implying the reduction of $SOCl_2$ to $SOCl^{\cdot}$ radical, following the electron transfer from the triplet excited sate complex, $^3\pi$-π^* Pc(-2)LnPc(-1) to $SOCl_2$. Mechanistic details are given in Scheme 5.8. There was no evidence of further oxidation even when large concentrations of $SOCl_2$ were used. Though the one-electron reduction of $SOCl_2$ results in the formation of an unstable radical and gives many reactive intermediates, this work is useful for the elucidation of the mechanism of the reduction of $SOCl_2$ in the battery.

Unlike most monophthalocyanine complexes, the photocatlytic reactions discussed in this work were controlled by the phthalocyanine rings of the dimers. The ring-ring interaction is stronger in lutetium diphthalocyanine because of the shorter ring-ring distance. This fact implies higher catalytic activity of the complex. These interactions vary throughout the lanthanide series from neodymium to lutetium diphthalocyanine complexes.

This work constitutes a step forward for the study of the chemical interactions of the $LnPc_2$ complexes with some common pollutants such as CO, NO_2, CO_2, and other oxidizing gases. For further studies, the exploration of the electrocatalytic activity of these compounds could be very useful.

7. REFERENCES

1 Ö. Bekaroğlu, *Appl. Organomet. Chem.*, 10 (1996), 605.

2 C.C. Leznoff and A.B.P. Lever, *in Phthalocyanines: properties and applications*, edited by C.C. Leznoff and A.B.P. Lever, VCH, Vol.4, 1993.

3 P. Barrett, C. Dent, and P. Linstead, *J. Chem. Soc.*, (1936), 1719.

4 W.J. Kroenke and M.E. Kenney, *Inorg. Chem.*, 3 (1964), 251.

5 .J. Kroenke and M.E. Kenney, *Inorg. Chem.*, 3 (1964), 696.

6 I.S. Kirin, P.N. Moskalev and Yu. A. Makashev, *Russ. J. Inorg. Chem.*, 10 (1965), 1065.

7. I. S. Kirin, P.N. Moskalev and Yu. A. Makashev, *Russ. J. Inorg. Chem.*, 12 (19967), 369.

8. R. B. Daniels, G.L. Payne and J. Peterson, *J. Coord. Chem.*, 28 (1993), 23.

9. R.B. Daniels, J. Peterson, W.C. Porter and Q.D. Wilson, *J. Coord. Chem.*, 30 (1993), 357.

10. J. Silver, P.J. Lukes, P.H. Hey and J.M. Őconor, *Polyhedron*, 8 (1989), 1631.

11. E. Orti, J. L. Bredas and C. Clarisse, *J. Phys. Chem.*, 92 (1990), 1228.

12. P. Turek, P. Petit, J.J. André, J. Simon, R. Even, B. Boudjema, G. Guillard and M. Maitrot, *J. Am. Chem. Soc.*, 109 (1987), 5119.

13. T. Toupance, P. Bassoul, L. Mineau, and J. Simon, *J. Phys. Chem.*, 100 (1996), 11704.

14. J. J. André, K.- Holczer, P. Petit, M.T. Riou, C. Clarisse, R. Even, M. Fourmigue and J. Simon, *Chemical Physics Letters*, 115 (1997), 65.

15. F. Guyon, A. Pondaven, P. Guenot and M. L'Her, *Inorg. Chem.*, 33 (1994), 4787.

16. K. Konami, M. Matano, N. Kobayashi, and T. Osa, *Chem. Phys. Lett.*, 165(1990), 397.

17. B. Kraut and G. Ferraudi, *Inorg. Chim. Acta,* 149 (1988), 273.

18. G. Dela Torre, P. Vásquez, F. Agulló- Lopez, and T. Torres, *J. Mat. Chem.*, 8 (1998), 1671.

19. L.G. Tomilova, E.V. Chernykh, N.T. Ioffe, and E.A. Luk'yanets, *Russ. J. Gen.Chem.*, 53 (1983), 2339.

20. P.N. Moskalev and I.S. Kirin, *Russ. J. Phys. Chem.*, 46 (1972), 1019.

21. A. De Cian, M. Moussavi, J. Fischer and R. Weiss, *Inorg. Chem.*, 24 (1985), 3162.

22. M. Moussavi, A. De Cian, J. Fischer, and R. Weiss, *Inorg. Chem.*, 27 (1988), 1287.

23. A.T. Chang and J. C. Marchon, *Inorg. Chim. Acta*, 53 (1981), L241.

24. Z. Gasyna, P.N. Schatz and M.E. Boyle, *J. Phys. Chem.*, 99 (1995), 10159.

25. J. Janczak, R. Kubiak, and A. Jezierski, *Inorg. Chem.*, 34 (1995), 3505.

26. N. Ishikawa, O. Ohno, Y. Kaizu and H. Kobayashi, *J. Phys. Chem.*, 96 (1992), 8832.

27. K. Kim, W.S. Lee, H.J. Kim, S.H. Cho, G.S. Girolami, P.A.Gorlin and K. S. Suslick, *Inorg. Chem.*, 30 (1991), 2652.

28. A. Pondaven, y. Cozien and M. L'her, *New J. Chem.*, 15 (1991), 515.

29. K. Kasuga, M. tsutsi, R.C. Petterson, K. Tatsumi, N. Van Opdenbosch, G. Pepe, E.F.Meyer, Jr., *J. Am. Chem. Soc.*, 102 (1980), 4836.

30. M.J. Stillman nad T. Nyokong, *in phthalocyanines: Properties and applications*, C.C. Leznoff and A.B.P. Lever (eds), Vol.1, VCH, 1989.

31. M. J. Stillman, *in Phthalocyanines: properties and applications*, C.C. Leznoff and A.B.P.Lever (eds), VCH, Vol.3, 1993.

32. A. Pondaven, Y. Cozien, and M. L'her, *New J. Chem.*, 16 (1992), 711.

33. G.C.S. Collins and D.J. Schiffrin, *J. Electroanal. Chem.*, 139 (1982), 335.

34. K. Kasuga, M. Ando, H. Morimoto, and M. Isa, *Chem. Lett.*, (1986), 1095.

35. F. Guyon, A. Pondaven, and M. L'her, *J. Chem. Soc., Chem. Commun.*, (1994), 1125.

36. C.Clarisse and M.T. Riou, *Inorg. Chim. Acta*, 130 (1987),139.

37. K.M. Kadish, G. Moninot, Y. Hu, D. Dubois, A. Ibnlfassi, J.-M. Barbe and R. Guillard, *J. Am. Chem. Soc.*, 115 (1993), 8153.

38. E. Musluoğlu, V. Ahsen, A. Gül, and Ö. Bekâroğlu, *Chem. Ber.*, 124 (1991), 2531.

39. A. Gürek, V. Ahsen, A. Gül, and Ö. Bekâroğlu, *J. Chem. Soc., Dalton Trans.*, (1991), 3367.

40. M. Koçak, A. Cihan, A. Okur, and Ö. Bekâroğlu, *J. Chem. Soc., Chem. Commun.*, (1991), 577.

41. O. Ohno, N. Ishikawa, H. Matsuzawa, Y. Kaizu and H. Kobayashi, *J. Phys. Chem.*, 93 (1989), 1713.

42. N. Ishikawa and Y. Kaizu, *J. Phys. Chem.*, 100 (1996), 8722.

43. T.C. Van Cott, Z. Gasyna, P.N. Schaltz and M.E. Boyle, *J. Phys. Chem.*, 99 (1995), 4820.

44. J.W. Buchner and B. Scharbert, *J. Am. Chem. Soc.*, 110 (1988), 4272.

45. M.M. Nicholson, *in Phthalocyanines: properties and applications*, C.C. Leznoff and A.B.P.Lever (eds.), VCH, Vol.3, 1993.

46. A.B.P. Lever, E.R. Milaeva and G. Speier, *in Phthalocyanines: properties and applications*, C.C. Leznoff and A.B.P. Lever (eds), VCH, Vol.3,1993.

47. G.L. Estiú, N. Rösch and M.C. Zerner, *J. Phys. Chem.*, 99 (1995), 13819.

48. K. Kasuga, M. Ando, and H. Morimoto, *Inorg. Chim. Acta*, 112 (1986), 99.

49. D. Markovitsi, T.-H. Tran-Hi, R. Even and J. Simon, *Chem. Phys. Lett.*, 137 (1987),107.

50. J.S. Shirk, J.R. Lindle, F.J. Bartoli and M.E. Boyle, *J. Phys. Chem.*, 96 (1992), 5847.

51. J.W. Buchler, K. Elsässer, M.K.Botulinski, B. Scharbert and T. Tansil, *J. Am.Chem. Soc.*, Symp. Ser., 321 (1986), 94.

52. H.F. Shurvell and L. Pinzuti, *Canadian J. Chem.*, 44 (1996), 125.

53. I. Gobernardo-Mitre, B. Klassen, R. Aroca, and J.A. Desaja, *J. Raman Spectroscopy*, 24 (1993), 903.

54. J. Jiang, T.C.W. Mak, and D.K. Ng, *Chem. Ber.*, 129 (1996), 933.

55. J. W. Buchler, M. Eberle, P. Hammerschmitt, J. Hüttermann, and R. Kappl, *Chem. Ber.*, 126 (1993), 2169.

56. M. L'her, Y. Cozien and J. Courtot-Coupez, *J. Electroanal. Chem.*, 157 (1983),183.

57. A.J. Bard and L.R. Faulkner, *in Electrochemical methods: fundamentals and applications*, John Wiley, 1 st edition, (1980),

58. I.. Rubistein, *in Physical Electrochemistry: principle, methods and applications*, Marcel dekker, 1 st edition, (1995).

59. T. Nyokong, *Polyhedron*, 12 (1993), 375

60. P.A. Christen and A. Hammett, *in Techniques and Mechanism in Electrochemistry*, Chapman and Hall, 1 st edition, (1994).

61. A. Capobianchi, A.M. Paoletti, G. Pennesi, G. Rossi and S. Panero, *Synthetic Metals*, 75 (1995), 37.

62. R.J. Donohoe, J.K. Duchowski and D.F. Bocian, *J. Am. Chem. Soc.*, 110 (1988), 6119.

63. J.L. Kahl, L.R. Faulkner, K. Dwarakanath, and H. Tachikawa, *J. Am. Chem. Soc.*, 108 (1986), 5434.

64. T. Nyokong, *Synthetic Metals*, 66 (1994), 107.

65. T. Nyokong, *J. Chem. Soc. Dalton Trans.*, (1994), 1359.

66. M. Sekota and T. Nyokong, *Polyhedron*, 15 (1996), 2908.

67. M. M'sadak, J. Roncali and F. Garnier, *J. Electroanal. Chem.*, 189 (1989), 99.

68. F. Castenada, C. Piechoki, V. Plichon, J. Simon and J. Vaxiviere, *Electrochim. Acta*, 31(1986), 89.

69. G. A. Spyroulias, A.G. Coutsolelo, D. Montauzon and R. Poilblanc, *J. Coord. Chem.*, 39(1996), 89.

70. R. Guillard, J.M. Barbe, A. Ibnlfassi, A. Zrineh, V.A. Adamian and K.M. Kadish, *Inorg. Chem.*, 34(1995), 1472.

71. G. Ricciardi, S. Belviso, F. Lelj and S. Ristori, *J. Porphyrins phthalocyanines*, 2 (1998), 177.

72. S-I. Mho, B. Ortiz, S. M. Park, D. Ingersoll and N. Doddapaneni, *J. Electrochem. Soc.*, 142 (1995), 1436.

73. D. Wöhrle, D. Schlettwein, G. Schnurpfeil, G.Schneider, E. Karman, T.Yoshida, and Y. Kaneko, *Polymers for advanced technologies*, 6 (1995), 118.

74. D.R. Prasad and G. Ferraudi, *J. Phys. Chem.*, 86 (1982), 4037.

75. D.R. Prasad and G. Ferraudi, *J. Phys. Chem.*, 87 (1983), 1672.

76. G. Ferraudi and J. Granifo, *J. Phys. Chem.*, 89 (1985), 1206.

77. M. E. Frink, D. K. Geiger and G.J. Ferraudi, *J. Phys. Chem.*, 90 (1986), 1924.

78. Z. Gasyna, W. R. Browett and M.J. Stillman, *Inorg. Chem.*, 23 (1984), 382.

79. Z. Gasyna, W.R. Browett and M. J. Stillman , *Inorg. Chem.*, 24 (1985), 2440.

80. T. Nyokong, Z. Gasyna and M. J. Stillman, *J. Am. Chem. Soc., Symp. Ser.* 321 (1986), 309.

81. T. Nyokong, *Polyhedron*, 13 (1994), 2067.

82. H. Meier, W. Albrecht, D. Wöhrle, and A. Jahn, *J. Phys. Chem.*, 90 (1986), 6349.

83. T.J. Klofta, J. Danziger, P. Lee, J. Pankow, K.W. Nebesny, and N.R. armstrong, *J. Phys.* Chem., 91(1987), 5646.

84. T.J. Klofta, T.D. Sims, J.W. Pankow, J. Danziger, K.W. Nebesny, and N.R.Armstrong, *J. Phys. Chem.*, 91 (1987), 56451.

85. E.A. Malinka, G. L. Kamalov, s.V. Vodzinski, V.I. Melnik, Z.I. Zhilima, *J. Photochem.Photobiol.; A: Chem.*, 90 (1995), 153.

86. T. Nyokong, *J. Chem. Soc.; Chem. Commun.*, (1994), 1983.

87. J. Zakrzewski, and C. Giannotti, *Inorg. Chim. Acta*, 232 (1995), 63.

88. G. Schnurpfeil, A. K. Sobbi, W. Spiller, H. Kliesch and D. Wöhrle, *J. Porphyrins Phthalocyanines*, 1 (1997), 159.

89. H. Sugimoto, T. Higashi, and m. Mori, *J. Chem. Soc., Chem. Commun.*, (1983), 622.

90. K. Kasuga, H. Morimoto and M. Ando, *Inorg. Chem.* 25 (1986), 2478.

91. A. Harriman, G. Porter, M. C. Richoux, *J. Chem. Soc., Faraday Trans.2*, 77(1981), 1175.

92. J. R. Darwent, I. McCubin, and D. Phillips, *J. Chem. Soc.Faraday Trans.2*, 78 (1982), 347.

93. Y. Nishimura, Y. Kaneko, T. Arai, H. Sukaragi, K. Tokumaru, M. Kiten, S. Yamamura and D. Matsunaga, *Chem. Lett.*, (1990), 1935.

94. Y. Kaneko, Y. Nishimura, T. Arai, H. Sukaragi, K. Tokumaru, and D. Matsunga, *J. Photochem. Photobiol.; A: Chem.*, 89 (1995), 37.

95. T. Nyokong, *Polyhedron*, 13 (1994), 215.

96. N. Nensala, *Licenciate thesis*, Luanda, 1989.

97. J.D. Petke, and G.M. Maggiora, *J. Am. Chem. Soc., Symp. Ser.* 321 (1986), 20.

98. N. J. Turro, *in Modern molecular photochemistry*, Benjamin and Cumming, 1 st edition, (1978).

99. O. Ohno, Y. Kaizu, and H. Koyabashi, *J. Phys. Chem.*, 82 (1985), 1779.

100. B. T. Lim, S. Okajima, A.K. Chandra, and E.C. Lin, *J. Chem. Phys.*, 77 (1982), 3902

101. K. Ishii, Y. Ohba, M. Iwaizumi and S. Yamauchi, *J. Phys. Chem.*, 100 (1996), 3839.

102. X. Yan, and D. Holten, *J. Phys. Chem.*, 92 (1988), 409.

103. S. Yamauchi, H. Konami, K. Akiyama, M. Hatano and Iwaizumi, *Molecular Physics*, 83(1994), 335.

104. D.O. Cowan and R.L. Drisko, *in Elements of organic photochemistry*, Plenum Press, 1 st edition, (1976).

105. D. Wöhrle, L. Kreienhoop, and D. Schlettwein, *in Phthalocyanines: properties and applications*, C.c. Leznoff and A.B.P. Lever (eds), VCH, Vol.4, 1996.

106. J. H. Zagal, *Coord. Chem. Rev.*, 119 (1992), 89.

107. K. Shin and H.M. Goff, *J. Chem. Soc. Chem. Commun.*, (1990), 461.

108. B.B. Wayland and D. Mohajer, *J. Chem. Soc. Chem. Commun.* (1972), 776.

109 A. Mylonas and E. Papaconstantinou, *J. Photochem. Photobiol. A: Chem.*, 94 (1996), 77.

110 A. Mylonas and E. Papaconstantinou, *Polyhedron*, 15 (1996), 3211.

111. D.G. Crosby, K.I. Beynon, P.A. Greve, F. Korte, G.G. Still and J.W. Vonk, *Pure and Appl. Chem.*, 53 (1981), 1051

112. Yu.I.Skurlatov, L.S. Ernestova, E.V. Vichutinskaya, D.P. Samsonov, I.V. Semenova, I.Ya.Rod'ko, V.O. skvidky, R.I.Pervunina and T.J.Kemp, *J. Photochem. Photobiol., A: Chem.*, 107(1997), 207.

113. M. Nowakowska, E. Sustar and J.E.Guillet, *J. Am. Chem. Soc.*, 113 (1991), 253.

114. D.G. Crosby and A.S. Wong, *Chemosphere*, 5 (1976), 327.

115. A. Sorokin and B. Meunier, *J. Chem. Soc., Chem. Commun.*, (1994), 1799.

116. A. Sorokin, J.L. Séris, and B. Meunier, *Science*, 28 (1995), 1163.

117. A. Sorokin and B. Meunier, *Chem. Eur.J.*, 2 (1996), 1308.

118. U. Stafford, K.A. Gray and P.V. Kamat, *Catalysis*, 167 (1997), 25.

119. R.Gerdes, D. Wöhrle, W. Spiller, G. Schneider, G. Schnurpfeil and G. Schurlt-Ekloff, *J. Photochem. Photobiol. A: Chem.*, 111 (1997), 65.

120. H.V. Venkatasetty, *J. Electrochem. Soc.*, 127 (1980), 2531.

121. P.A. Bernstein and A.B.P. Lever, *Inorg. Chem.*, 29 (1990), 608.

122. D.D. Perrin and W.L.F. Armarego, *Purification of laboratory chemicals*, Pergamon Press, 3rd edition, 1988.

123. E.E. Wegner and A.W. Admson, *J. Am. Chem. Soc.*, 88 (1966), 394.

124. G. Marr and B. W. Rocket, *in Practical Inorganic Chemistry*, Van Nostrand Reinhold, 1 st edition, (1972).

125 A.I. Vogel, *Textbook of quantitative chemical analysis*, longman, 5th edition,1989.

126. A.S. Hinman and P. Wiebe, *Anal. Chem.*, 67 (1995), 694.

127. C.A. Parker and C.G. Hatchard, *J. Phys. Chem.*, 63 (1959), 22.

128. W.A. Bennett, D.E. Broberg and N.C. Baenziger, *Inorg. Chem.*, 12 (1973), 930.

129. K. Kasuga and M. Tsutui, *J. Coord. Chem.*, 10 (1980), 263.

130. I. Fujita, J. Fajer, C.-K. Chang, C.-B. Wang, M.A. Bergkamp and T.L.Netzel, *J. Phys. Chem.*, 86 (1982), 3754.

131. J. Fajer, I. Fujita, A. Foreman, L.K. Hanson, G.W. Graig, D.A. Goff, L.A. Kehres and K.M. Smith, *J. Am. Chem. Soc.*, 105 (1983), 3837.

132. T. Moeller, J.C. Bailar, Jr., J. Kleinberg, C.O. Guss, M.E. Castellion and C. Metz, *in Chemistry with inorganic qualitative analysis*, international edition, 3rd edition, (1989).

133. C. Ercolani, A.M. Paoletti, G. Pennesi and G. Rossi, *J. Chem. Soc. Dalton Trans.* (1990), 1971.

134. A. Copianchi, C. Ercolani, A.M.. Paoletti, G. Pennesi, G. Rossi, A. Chiesi-Villa and C. Rizolli, *Inorg. Chem.*, 32 (1993), 4605.

135. J. H. Sharp and M. Lardon, *J. Phys. Chem.*, 72 (1968), 3230.

136. C.P. Wong, R.F. Venteicher and W.De W. Horrocks, Jr.,. *J. Am. Chem Soc.*, 96 (1974), 7149.

137. W. De W. Horrocks, Jr. and C.-P. Wong, *J. Am.. Chem. Soc.*, 98 (1976), 7157.

138. W. De W. Horrocks, Jr. and E.G. Hove, *J. Am. Chem. Soc.*, 100 (1978), 4386

139. T.J. Marks and D.R. Stojakovic, *J. Am. Chem. Soc.*, 100 (1978), 1695.

140. G.S. Girolami, S.N. Milan and K.S. Suslick, *Inorg. Chem.*, 26 (1987), 344.

141. Y.Liu, K. Shigehara and A. Yamada, *Thin solid films*, 179 (1989), 303.

142. M.T. Riou and C. Clarisse, *J. Electroanal. Chem.*, 249 (1988), 181.

143. R. Even , J. Simon and D. Markovitsi, *Chem. Phys. lett.*, 156 (1989), 609.

144. R.R. Gagné, C.A. Kōval and G.C. Lisensky, *Inorg. Chem.*, 19 (1980), 2855.

145. A. B. P. Lever, S. Licocia, K. Magnell, P.C. Minor and B.S. Ramaswamy, *ACS Symp. Ser.*, 201 (1982), 237.

146. J. Simon and J. J. André, *Molecular semi-conductors*, Springer Verlapg, Berlin, (1985).

147 H. Isago and Y. Kagaya , *Bull. Chem. Soc. Jpn.*, 67 (1994), 3212.

148. A.B.P. Lever, M.R. Hempstead, C.C. Leznoff, W. Liu, M. Melnik, W.A. Nevin and P. Seymour, *Pure and Appl. Chem.*, 58 (1986), 1467.

149. N. kobayashi, S. Nakajima and T. Osa, *Inorg. Chim. Acta*, 210 (1993), 131.

150. M. M´sadak, J. Roncali and F. Garnier, *J. Chim. Phys.*, 83 (1985), 211.

151. P.C. Minor, M. Gouterman and A.B.P. Lever, *Inorg. Chem.*, 24 (1985), 1894.

152. D. Brault, C. Bizet, P. Morliere, M. Rouge, E.J. Land, R. Santus and J. Swallow, *J. Am. Chem. Soc.*, 102 (1980), 1015.

153. D. Brault and P. Neta, *J. Am. Chem. Soc.*, 103 (1981), 2705.

154. R.S Wade and C.E. Castro, *J. Am. Chem. Soc.*, 95 (1973), 226.

155. Mikio Hoshino, *Inorg. Chem.*, 25 (1986), 2476.

156. G. Ferraudi, *in Phthalocyanines: Properties and applications*, A. B. P. Lever and C. C. Leznoff (eds), Vol. I, VCH, New York, 1989.

157. A. Weissberger and B.W. Rossiter, *in Physical methods of chemistry*, John Wiley and sons, Vol. I, Pg.75, 1971.

158. W. Spiller, H. Kliesch, D. Wöhrle, S. Hackbarth, B. Röder and G. Schnurpfeil, *J. Porphyrins and Phthalocyanines*, 2 (1998), 145.

159. D. R. Arnold, N. C. Baird, J. R. Bolton, J.C.D. Brand, P.W.M. Jacobs, P. de Mayo, W. R. Ware, *in Photochemistry: An introduction*, Academic Press, (1974), 1 st edition.

160 . A. R. Miksztal and J.S. Valentine, *Inorg. Chem.*, 23 (1984), 3548.

161. W. R. Scheidt, Y. J. Lee, and M. G. Finnegan, *Inorg. Chem.*, 27 (1988), 4725.

162. R. N. Scott, D. F. Shriwer and L. Vaska, *J. Am. Chem. Soc.*, 90 (1968), 1079.

163. P. Bannasch, *Monographs on the evaluation of carcinogenic risks to humans: polychlorinated dibenzo-para-dioxins and polychlorinated dibenzofurans*, Vol.69, IARC (eds), Lyon, 1997.

164. S. Vollmuth, A. Zajc and R. Niessner, *Environ. Sci. Technol.*, 28 (1994), 1145.

165. J. R. Plimmer, and V. I. Klingebiel, *Science*, 174 (1971), 407.

166. M. Nowakowaska and K. Szczubialka, *J. Photochem. Photobiol. A:Chem.*, 91(1995), 81.

167. A. Sorokin, S. De Suzzoni-Dezard, D. Poullain, J.-P. Nöel and B. Meunier, J. *Am. Chem. Soc.*, 118 (1996), 7410.

168. A.-P. Durand, R.G. Brown, D. Worrall, and F. Wilkinson, *J. Photochem. Photobiol. A:Chem.*, 96 (1996), 35.

169. J. Sýkora, M. Pado, M. Tatarko and M. Izakovič, *J. Photochem. Photobiol. A: Chem.*, 110 (1997), 167.

170. T. Sehili, P. Boule and J. Lemaire, *J.Photochem. Photobiol. A: Chem.*, 50 (1989), 117.

171. H. Al-Ekabi and N. Serpone, *J. Phys. Chem.*, 92 (1988), 5726.

172. A. Mills, S. Morris and R. Davies, *J. Photochem. Photobiol., A: Chem.*, 70 (1993), 183.

173. A. Mills and S. Morris, *J. Photochem. Photobiol. A: Chem.*, 71(1993), 75.

174. R. W. Matthews, *J. Chem. Soc., Faraday Trans. I*, 80 (1984), 457.

175. R. W. Matthews, *J. Phys. Chem.*, 91 (1987), 3328.

176. H.-I. Joschek and S. I. Miller, *J. Am. Chem. Soc.*, 88 (1966), 3269.

177. K. E. Óshea and C. €ardona, *J. Org. Chem.*, 59 (1994), 5005.

178. T. Nguyen and D. F. Ollis, *J. Phys. Chem.*, 88 (1984), 3386.

179. Y. Ohko and A. Fujima, *J. Phys. Chem. B*, 102 91998), 1724.

180. U. Stafford, K.A. Gray and P.V. Kamat, *J. Phys. Chem.*, 98 (1994), 6343.

181. E. Brillas and R. Sauleda, *J. Electrochem. Soc.*, 145 (1997), 65.

182. K. Lang, D.W. Wagnerová and J. Brodilová, *J. Photochem. Photobiol. A: Chem.*, 72 (1993), 9.

183. G. Al-Sayed, J.-C. D'Oliveira and P. Pichat, *J. Photochem. Photobiol. A: Chem.*, 58 (1991), 99.

184. T. T. Y. Wei and C. C. Wan, *J.Photochem. Photobiol. A: Chem.*, 69 (1992), 241.

185. C. N. Satterfield, *in Heterogenous catalysis in practice*, Mc Graw-Hill, 1980.

186. P. A. Bernstein and A.B.P. Lever, *Inorg. Chem.*, 34 (1995), 933.

187. B.-S. Kim and S.-M. Park, *J. Phys. Chem.*, 99 (1995), 9918.

188. E. S. Takenchi, H. Gran, M. Palazzo, R. A. Leising and S. M. Davis, *J. Electrochem. Soc.*, 144 (1997), 1944.

189. B.-S. Kim and S.-M. Park, *J. Electrochem. Soc.*, 142 (1995), 34.

190. M. Kovač, S. Milićev, A. Kovač and S. Pejovnik, *J. Electrochem. Soc.*, 142 (1995), 1390.

191. W. L. Bowdeb, and A. N. Dey, *J. Electrochem. Soc.*, 127 (1980), 1419.

192. P. Vasudevan, N. Phougat and A. K. Shukla, *Appl. Organomet. Chem.*, 10 (1996), 591.

193. A.B.P. Lever, B.S. Ramaswamy, S.A. Kandil and D. V. Stynes, *Inorg. Chim. Acta*, 51 (1981), 169.

APPENDIX 1

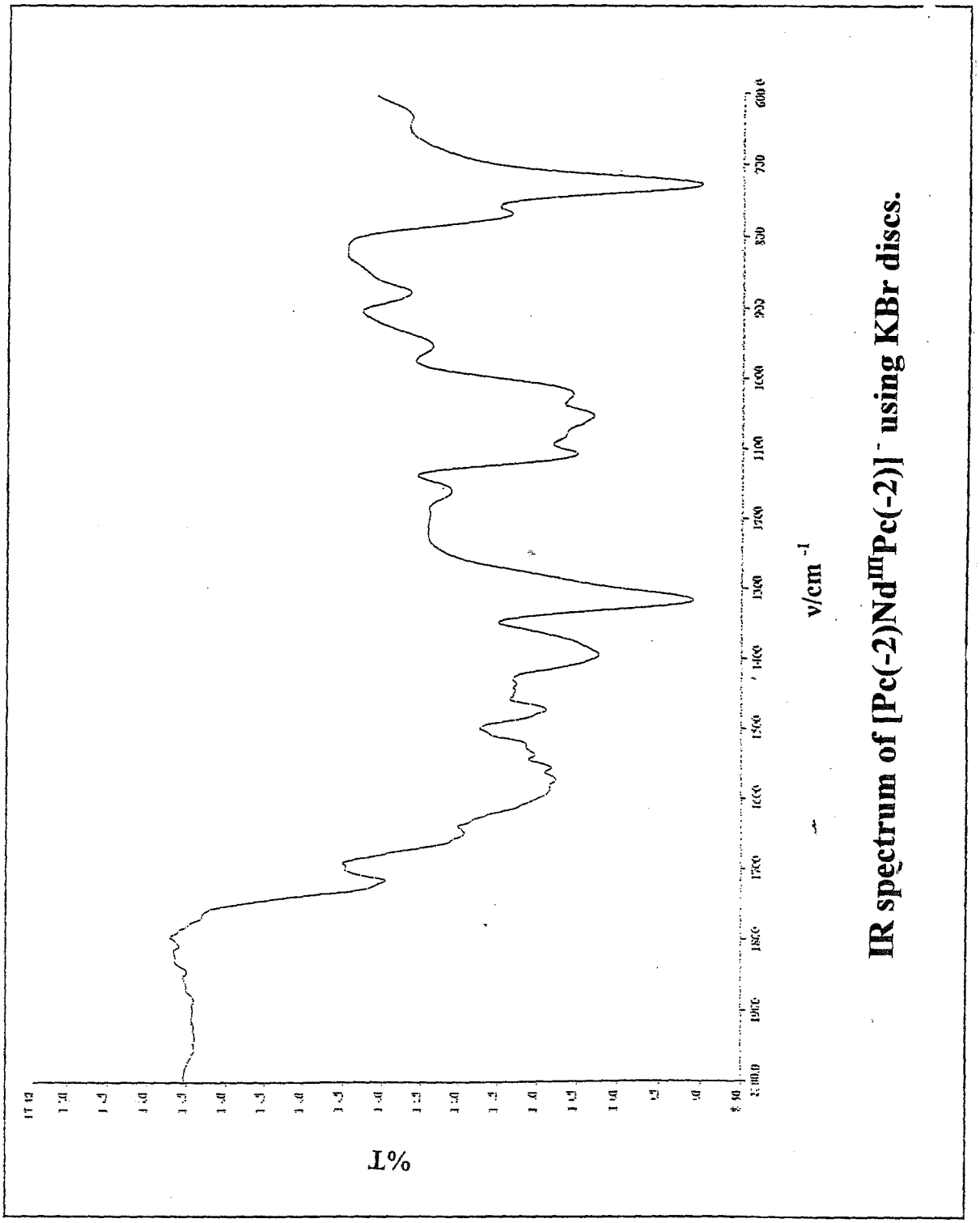

IR spectrum of $[Pc(-2)Nd^{III}Pc(-2)]^-$ using KBr discs.

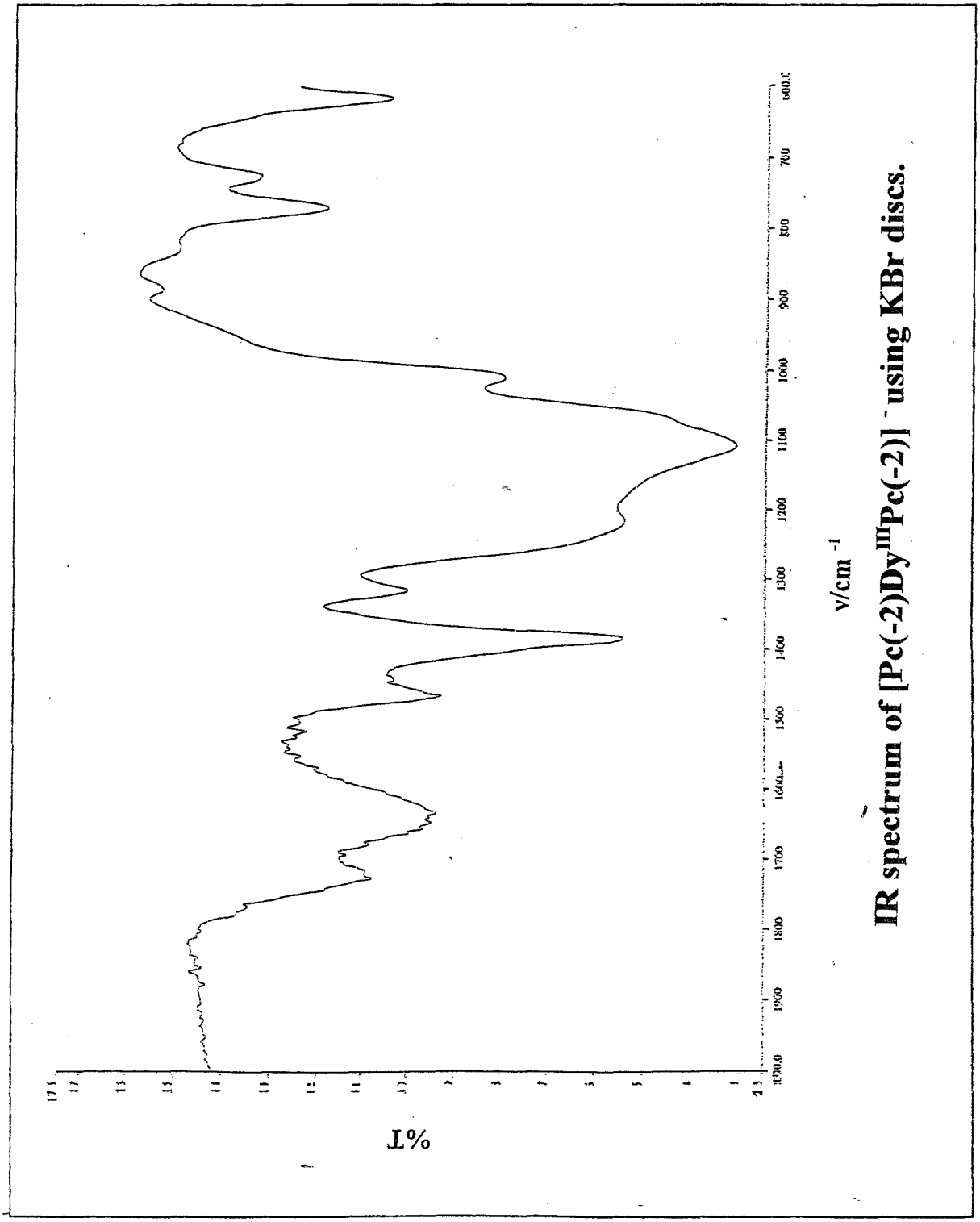

IR spectrum of [Pc(-2)Dy^{III}Pc(-2)] using KBr discs.

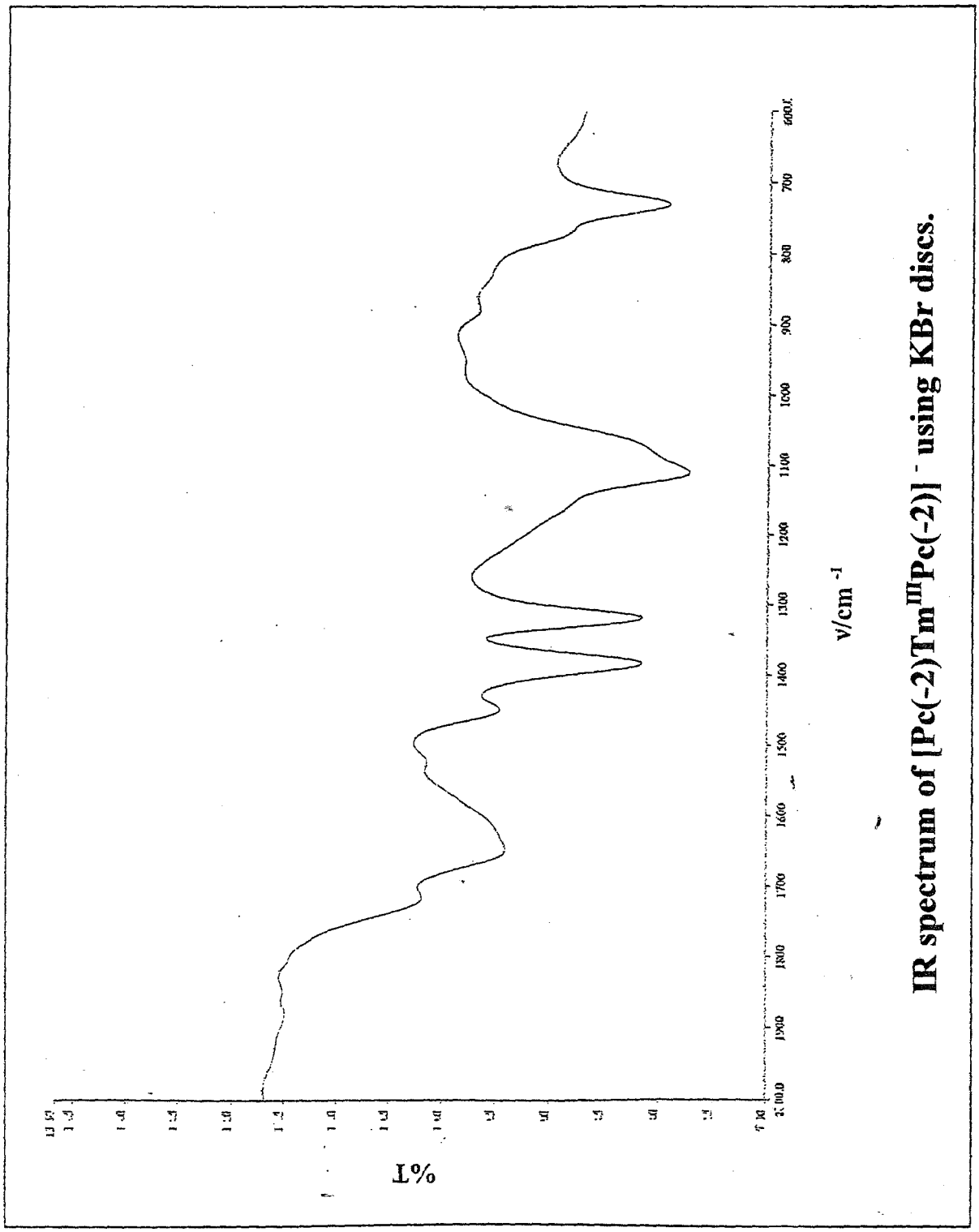

IR spectrum of [Pc(-2)Tm^{III}Pc(-2)] - using KBr discs.

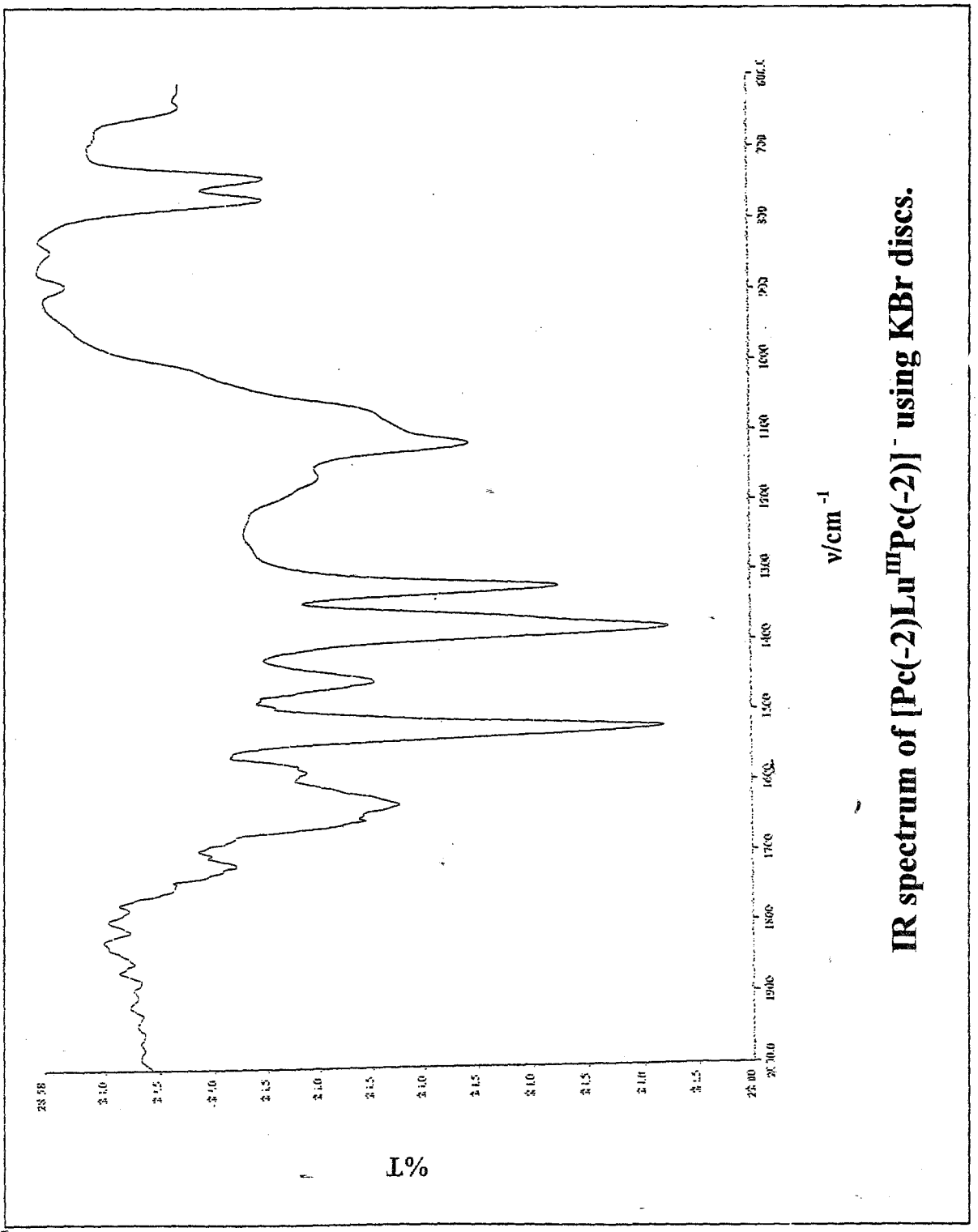

IR spectrum of $[Pc(-2)Lu^{III}Pc(-2)]^-$ using KBr discs.

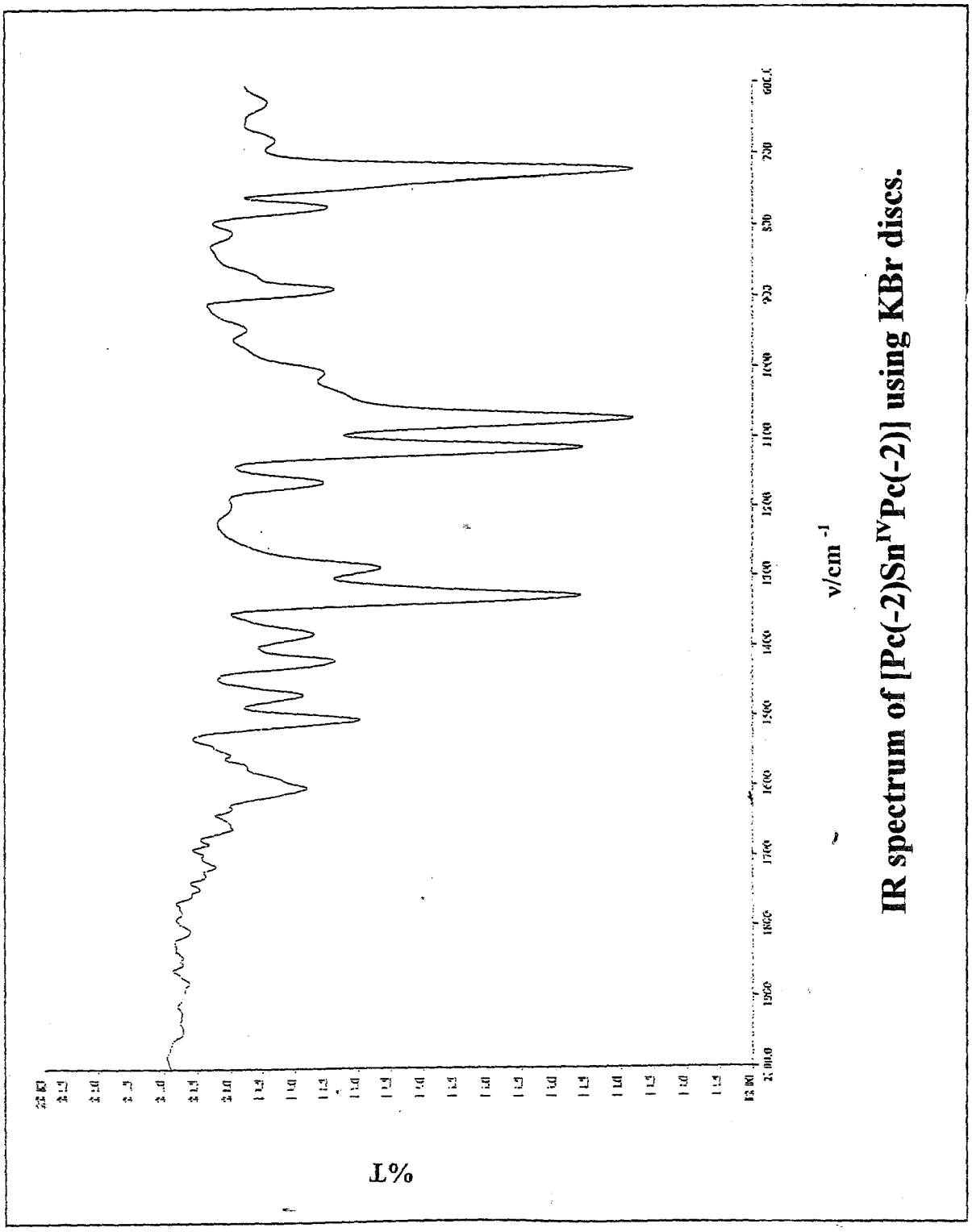

IR spectrum of [Pc(-2)Sn^{IV}Pc(-2)] using KBr discs.